TECHNISCHE UNIVERSITÄT MÜNCHEN

Wissenschaftszentrum Weihenstephan für Ernährung, Landnutzung und Umwelt

Lehrstuhl für Entwicklungsgenetik

The Role of Neddylation in Adipocyte Biology, Obesity and Metabolism

Corinna Anita Bauder

Vollständiger Abdruck der von der Fakultät Wissenschaftszentrum Weihenstephan für Ernährung, Landnutzung und Umwelt der Technischen Universität München zur Erlangung des akademischen Grades eines

Doktors der Naturwissenschaften

genehmigten Dissertation.

Vorsitzender:	Prof. Dr. Johann J. Hauner
Prüfer der Dissertation:	1. Prof. Dr. Wolfgang Wurst
	2. Priv.-Doz. Mathias Schmidt, Ph.D.

Die Dissertation wurde am 19.11.2018 bei der Technischen Universität München eingereicht und durch die Fakultät Wissenschaftszentrum Weihenstephan für Ernährung, Landnutzung und Umwelt am 06.03.2019 angenommen.

Table of Contents

Summary

Pathophysiological conditions, like obesity or lipodystrophy, contribute to adipose tissue dysregulation leading to associated metabolic disorders, such as type 2 diabetes and cardiovascular diseases, which are major public health and economic burdens worldwide. Thus, delineating the mechanisms regulating adipocyte development and function is a pivotal and global research task.

Post-translational protein modifications are well-established key players in adipocyte development. Neddylation is one type of post-translational signaling operating by covalent tagging of a ubiquitin-like protein Nedd8 (neural precursor cell-expressed, developmentally downregulated gene 8) to substrate proteins. Nedd8 conjugation has an important role in cell cycle progression and cancer, regulation of cell signaling and developmental programming processes. However, in contrast to other post-translational protein modifications, the role of neddylation in adipocyte biology remained largely unknown.

The present study revealed that neddylation plays critical roles in controlling adipogenesis and adipocyte function. It acts as a physiological regulatory pathway controlling obesity and metabolism *in vivo*. The increase in neddylation during adipogenesis in cell cultures and during obesity in mice, highlight the relevance of neddylation in adipocyte biology. We found that neddylation of the key transcriptional regulatory protein C/EBPβ (CCAAT/enhancer-binding protein β) promotes its transcriptional activity by controlling the binding to its cognate DNA consensus sites. Thereby, C/EBPβ neddylation regulates the expression of the adipocyte master genes, C/EBPα and PPARγ, and consequently the induction of adipocyte-specific metabolic genes required for the development and function of fat cells.

By using two different mouse models, we gained insight in the biological relevance of Nedd8 in obesity and metabolism. Adipose tissue-specific ablation of the neddylation pathway in mice (*Nae1Adipo*CreER^{T2} KO) prevents and reduces high fat diet-induced obesity by decreasing food intake and adipose tissue mass. However, it manifests many features of the human disorder lipodystrophy, resulting in dysfunctional adipose tissue, hepatic steatosis, glucose intolerance, impaired metabolic flexibility and altered adipokine secretion. In contrast, in a second mouse model, peripheral neddylation blockade by chronic subcutaneous administration of the neddylation inhibitor MLN4924 ameliorates high fat diet-induced obesity and metabolic dysfunction. This mouse model offers a platform upon which we have unraveled the more complex interplay of neddylation in different tissues. Global neddylation inhibition reduces adiposity by stimulating perirenal BAT thermogenesis and

restoring WAT physiology, making this mouse model particularly interesting from a clinical perspective.

Taken together, this study unraveled the potent impact of neddylation on adipocyte identity and survival, obesity and metabolism. Moreover, it suggests that global neddylation inhibition induces a profound adipose tissue remodeling particularly in response to nutritional stress, revealing this posttranslational modification as a potential therapeutic target in the treatment of adiposity and obesity-related metabolic disorders.

Zusammenfassung

Stoffwechselkrankheiten wie Adipositas oder Lipodystrophie führen häufig zu metabolischen Erkrankungen wie Typ 2 Diabetes oder kardiovaskulären Komplikationen. Deshalb stellen diese Stoffwechselerkrankungen weltweit eine erhebliche Bedrohung für die Gesundheit sowie eine starke ökonomische Belastung dar. Die Aufklärung von Mechanismen, welche die Entwicklung und Funktion von Adipozyten kontrollieren, ist daher von bedeutendem wissenschaftlichem Interesse.

Posttranslationale Proteinmodifikationen spielen eine wichtige regulatorische Rolle bei der Entwicklung von Adipozyten. Neddylierung ist eine Art der posttranslationalen Proteinmodifikation, bei der das Ubiquitin-ähnliche Protein Nedd8 (neural precursor cell-expressed, developmentally downregulated gene 8) kovalent an Zielproteine gebunden wird. Die Modifikation von Proteinen durch Nedd8 spielt unter anderem in der Zellzyklusprogression und in der Pathogenese von Krebserkrankungen, in der Regulation von zellulären Signalwegen und in Prozessen, welche die Embryonalentwicklung kontrollieren eine wichtige Rolle. Die Bedeutung der Neddylierung für die Funktion und Entwicklung von Adipozyten ist allerdings noch weitgehend unerforscht.

Die vorliegende Studie zeigt, dass Neddylierung eine wichtige Rolle in der Kontrolle der Differenzierung und Funktion von Adipozyten spielt. Zudem wurde gezeigt, dass Neddylierung von physiologischer Relevanz hinsichtlich der Kontrolle von Adipositas und Metabolismus ist. Die gesteigerte Neddylierung während der Adipozytendifferenzierung in Zellkulturen und als Folge von Adipositas in Mäusen unterstreicht die wichtige Bedeutung von dieser posttranslationalen Modifikation in der Adipozytenbiologie. Es konnte gezeigt werden, dass die Neddylierung des wichtigen Transkriptionsfaktors C/EBPβ (CCAAT/enhancer-binding protein β) dessen transkriptionelle Aktivität steigert, indem es die Kapazität an seine Zielstrukturen auf der DNA zu binden, erhöht. Auf diese Weise kontrolliert die Neddylierung von C/EBPβ die Expression der Transkriptionsfaktoren C/EBPα und PPARγ und somit die Expression der metabolischen Gene, die für die Differenzierung und Funktion von Fettzellen benötigt werden.

Mit Hilfe zweier Mausmodelle konnten wir Einblicke in die biologische Relevanz von Nedd8 in Adipositas und Metabolismus *in vivo* gewinnen. Die Ablation des Nedd8-Signalwegs im Fettgewebe von Mäusen (*Nae1Adipo*CreER^{T2} KO) verhindert und mindert durch fettreiche Kost hervorgerufene Fettleibigkeit. Dies wird durch die Reduktion der Nahrungsaufnahme und Fettgewebsmasse bewirkt. Jedoch weisen diese KO Mäuse viele Charakteristiken der

humanen Stoffwechselerkrankung Lipodystrophie auf, die zu einem dysfunktionellen Fettgewebe, Lebersteatose, Glukoseintoleranz, gestörter metabolischen Flexibilität und einer geänderten Sekretion von Adipokinen führt. In einem zweiten Mausmodell, verbessert die periphere Blockade des Nedd8 Signalwegs durch die chronische Gabe des Neddylierungsinhibitors MLN4924 die durch fettreiche Kost hervorgerufene Fettleibigkeit und damit assoziierte metabolische Störungen. Dieses Mausmodell bietet die Möglichkeit das komplexe Zusammenspiel von Neddylierung in den einzelnen Geweben zu untersuchen. Globale Inhibition des Nedd8 Signalwegs vermindert Adipositas durch die Stimulation von Thermogenese in braunem perirenalem Fettgewebe und der Wiederherstellung der physiologischen Funktion des weißen Fettgewebes. Dementsprechend ist dieses Mausmodell aus klinischer Perspektive sehr interessant.

Zusammengefasst demonstrierten die vorliegenden Untersuchungen den starken Einfluss der Neddylierung auf die Identität und das Überleben von Adipozyten, sowie auf Adipositas und Metabolismus. Außerdem zeigten sie den Effekt von globaler Blockade des Nedd8 Signalwegs auf die Re-Modulierung des Fettgewebes, insbesondere nach Gabe fettreicher Kost. Somit ist diese posttranslationale Modifikation ein potentieller therapeutischer Angriffspunkt bei der Behandlung von Fettleibigkeit und deren assoziierten metabolischen Folgeerkrankungen.

1. Introduction

1.1 Adipose tissue

Adipose tissue (AT) consists of mature adipocytes, preadipocytes, small blood vessels, nerve tissue, fibroblasts, endothelial cells and immune cells. In mammals, two principal types of AT exist, white (WAT) and brown (BAT). Historically, the study of WAT has centered around its principal function in controlling energy homeostasis via the storage and release of lipids in response to systemic nutritional and metabolic needs. However, WAT plays multiple roles in metabolic and inflammatory responses via the production of several adipocyte-derived factors (Kershaw and Flier, 2004). BAT, present in small amounts in adult humans, possesses a unique uncoupling protein (UCP1) which enables the dissipation of energy through the production of heat and the oxidation of lipids and glucose. BAT is associated with significant improvements in glucose and lipid homeostasis (Cannon and Nedergaard, 2004). An exceptional amount of research interest has been accompanied by the discovery of beige fat characterized as discrete areas of UCP1-containing cells dispersed within WAT controlling energy expenditure and metabolic homeostasis (Wang and Seale, 2016).

In this section I examine the prominent AT depots, highlight some of their most distinctive features and review the dynamic role of AT in organ crosstalk controlling metabolic homeostasis.

1.1.1 Distinct types and locations

Adipose tissue types

Two different types of AT exist: WAT and BAT. White adipocytes contain large unilocular lipid droplets (Rosen and Spiegelman, 2014), organelles in which excess energy can be stored in form of triglycerides (TG) (Welte, 2015). In contrast, brown adipocytes are composed of numerous lipid droplets and contain a high quantity of mitochondria, which are responsible for the brown color (Harms and Seale, 2013). Thus, this tissue is a highly oxidative tissue that generates heat via non-shivering thermogenesis (Cannon and Nedergaard, 2004). Until recent years it was supposed that BAT is not present in human adults but only in newborns, which allows them to maintain body temperature without shivering (Betz and Enerback, 2015). However, fluorodeoxyglucose positron emission tomography (PET) analysis revealed that metabolic active regions, which are able to uptake high levels of glucose, are present in healthy human subjects (Cypess et al., 2009; van Marken Lichtenbelt et al., 2009; Virtanen et

al., 2009). Furthermore, in addition to classical brown adipocytes, a brown-fat-like gene expression program can be induced in WAT by various factors, including chronic cold exposure, β-adrenergic stimulation, exercise, PPARγ ligands, tissue injury and cancer cachexia. This process referred to as browning results in beige adipocytes in which the energy expenditure is enhanced to a similar extend as in BAT through thermogenesis (Wang and Seale, 2016). The characteristics of white, beige and brown adipocytes are highlighted in Figure 1.

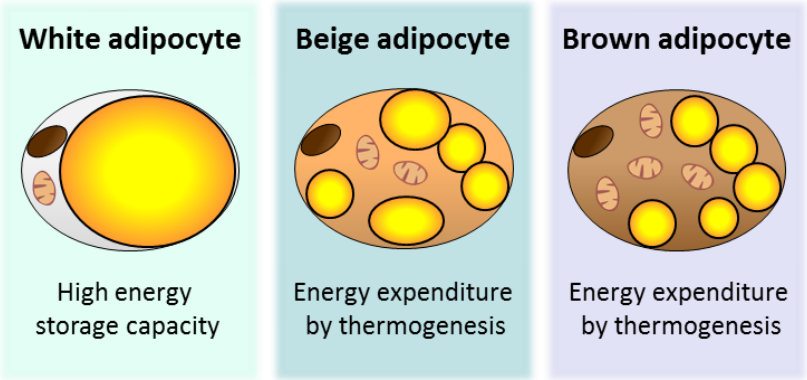

Figure 1: Different types of adipocytes: White, beige and brown. Schematic illustration showing the three different types of adipocytes. White adipocytes are unilocular and have a high capacity to store TG in their lipid droplet, specific TG storage organelles (depicted in yellow). Upon appropriate stimulation, a brown-fat-like gene expression program can be induced in WAT, resulting in the so-called beige adipocytes. Beige and brown adipocytes have numerous lipid droplets, a high mitochondria content and anticipate energy by heat generation.

Locations

WAT is distributed in subcutaneous (e.g. inguinal fat) as well as visceral regions in the body. The visceral AT, surrounding the inner organs, can be divided in omental, mesenteric, retroperitoneal, perirenal, gonadal (e.g. epididymal) and pericardial fat. Brown adipocytes are localized in BAT depots within the interscapular, axillary and perirenal region (Bjorndal et al., 2011; Cypess et al., 2009; Ikeda et al., 2018; van Marken Lichtenbelt et al., 2009; Virtanen et al., 2009). Perirenal BAT is located at the site of the renal hilum, whereas perirenal WAT is located at the opposite site at the renal capsule and posterior to the capsule (de Jong et al., 2015). Beyond the different types of AT, also the localization of WAT in the body has different metabolic outcomes. For instance, it is well established that primarily subcutaneous fat depots are prone to browning upon appropriate stimulation (Sidossis and Kajimura, 2015) resulting in a lower risk for the development of metabolic disorders. Enhanced storage of fat in visceral AT depots is implicated in obesity-associated metabolic diseases, e.g. Type 2 diabetes mellitus (T2DM) (Lee et al., 2013b). Depot-specific functions might be due to differential developmental processes (Gesta et al., 2006; Yamamoto et al., 2010) or distinct paracrine and endocrine signals (Girard and Lafontan, 2008). Moreover, visceral fat releases

fatty acids (FA) and hormones, which due to the fat depot's specific location, directly proceed to the liver through the portal vein, thus having a more pronounced effect on hepatic metabolism due to its location in the body (Huang-Doran et al., 2010).

1.1.2 Adipocyte development

1.1.2.1 Development of white adipocytes

Adipogenesis, the development of mature adipocytes, is progressing in two sequential phases. In the first phase, which is known as determination or commitment, pluripotent stem cells undergo commitment to the adipocyte lineage when appropriately stimulated (Covas et al., 2008). The second phase, known as terminal differentiation, involves a multistep genetic program that is mediating the conversion from preadipocytes to mature adipocytes (Tang and Lane, 2012).

Cell culture models: powerful tools to study the transcriptional cascades orchestrating adipocyte cell differentiation

The molecular machinery controlling terminal differentiation is more comprehensively studied due to commercially available preadipocyte cell lines that paved the way to understand a large part of this cellular process. Among these cellular models, the 3T3-L1 preadipocyte cell line is the best established one, serving as the "gold standard" to study the transcriptional cascade controlling terminal differentiation in the last decades. The 3T3-L1 preadipocyte cell line, which was derived from 17-19-day-old Swiss 3T3 mouse embryos, is able to give rise to spherical adipocytes filled with lipid droplets upon stimulation with adipogenic inducers (Green and Kehinde, 1974). Thus, it is serving as a convenient model to study the development of adipocytes, as we have done in our study.

Differentiation of two-day confluent 3T3-L1 cells can be induced by applying an adipogenic cocktail, containing 1-Methyl-3-isobutylxanthine (IBMX), dexamethasone, and insulin (MDI) in the presence of fetal calf serum (Green and Kehinde, 1975; Rubin et al., 1978; Russell and Ho, 1976). Commonly, adipogenesis in primary preadipocyte cultures or mouse embryonic fibroblasts (MEFs) is additionally stimulated by peroxisome proliferator-activated receptor γ (PPARγ) ligands, such as thiazolidinediones (TZD) like troglitazone or rosiglitazone (Kim et al., 2007b; Rhee et al., 2008). Upon induction of adipocyte differentiation, growth-arrested preadipocytes reenter the cell cycle und undergo several rounds of cell division, a process known as mitotic clonal expansion (MCE), before acquiring the adipocyte phenotype (Bernlohr et al., 1985; Tang et al., 2003). Whether MCE is required for adipogenesis is

strongly debated, as various preadipocyte cellular models are capable of differentiating without post-confluence mitosis (Cho and Jefcoate, 2004; Entenmann and Hauner, 1996). Nevertheless, approximately 16-20 hours after induction of 3T3-L1 differentiation, alterations in gene expression of cell-cycle proteins involved in S-phase entry can be observed and synchronously DNA replication is initiated (Tang et al., 2003). In 3T3-L1 cells, MCE is accompanied by sequential activation of a battery of adipogenic transcription factors that finally promote adipocyte development (Tang et al., 2003).

Adipogenesis is generally depicted as a transcriptional cascade orchestrating adipocyte cell differentiation (Farmer, 2006) (Figure 2). Numerous transcription factors, coactivators and negative regulators act together to induce adipocyte specific gene expression and consequently adipocyte development. In the following, the focus was centered on the factors which are relevant to the thesis content. The addition of the adipogenic inducers, insulin, dexamethasone and IBMX is activating the Insulin-like growth factor 1 receptor (IGF1R) signaling pathways, the glucocorticoid receptor (GR)- and the cAMP-dependent pathway, respectively (Elks and Manganiello, 1985; Rubin et al., 1978; Smith et al., 1988).

Insulin, acting through the IGF1R, is essential for the initiation of adipogenesis (Smith et al., 1988). The two closely related hormones insulin and IGF1 are able to bind and activate the respective other receptor, although with reduced affinity than to their own receptors (Boucher et al., 2010). Once activated by insulin, IGF1R or insulin receptor (IR) elicit the activation of a cascade of intracellular events ultimately leading to the activation of the serine/threonine kinase Akt, also known as Protein kinase B (Xu and Liao, 2004). Akt is an important signaling mediator in the IGF1 receptor signaling cascade and is necessary for inducing adipocyte differentiation as it is crucial for controlling glucose uptake and metabolism in 3T3-L1 cells (Kohn et al., 1996; Magun et al., 1996; Xu and Liao, 2004). Insulin- or IGF1-induced phosphorylation of Akt in the threonine 308 (Thr308) and serine 473 (Ser473) residues is a required step in promoting Akt activity (Alessi et al., 1996).

Subsequently, cAMP response element-binding protein (CREB) is activated by the protein kinase Akt through phosphorylation at Ser133 (Du and Montminy, 1998). CREB phosphorylation at Ser133 accelerates the capacity to activate CREB-dependent transcription, a process mandatory for adipocyte differentiation (Klemm et al., 1998; Reusch et al., 2000). CREB can be also activated by phosphorylation at Ser133 through an insulin-dependent ERK1/2 activation or by its most important activator cAMP-dependent protein kinase A (PKA) (Ginty et al., 1994; Gonzalez and Montminy, 1989; Klemm et al., 1998). IBMX inhibits phosphodiesterases, thereby increasing intracellular cAMP levels and promoting CREB phosphorylation.

Immediately after induction of differentiation, a member of the CCAAT/enhancer-binding protein (C/EBP) family, the C/EBPβ transcription factor is induced. Several lines of evidence have implicated CREB in the regulation of C/EBPβ transcription in adipocytes (Bradley et al., 2003; Niehof et al., 1997; Zhang et al., 2004b). The C/EBP protein family belongs to the family of basic leucine zipper (bZIP) transcription factors (Landschulz et al., 1988). These proteins possess a C-terminal leucine zipper domain for dimerization and a basic domain for DNA binding (Landschulz et al., 1988). Several representatives of this protein family have been identified, among them C/EBPβ, C/EBPδ and C/EBPα. These transcription factors can homodimerize or heterodimerize with each other, subsequently bind to the same C/EBP consensus sequences and can thereby activate transcription (Landschulz et al., 1989; Williams et al., 1991). The C/EBPβ mRNA directs the production of three isoforms: full-length 38-kDa C/EBPβ (LAP*), 34-kDa (LAP) and 17-kDa LIP through alternative translation from different AUG codons (Descombes and Schibler, 1991). While LAP* and LAP contain the N-terminal trans-activating and the C-terminal bZIP domain, the truncated form, LIP, consists of only the C-terminal part of C/EBPβ, retaining its DNA binding capacity and the ability to form dimers with other protein isoforms of all C/EBP family members but it lacks the ability to activate transcription (Descombes and Schibler, 1991). Thus, C/EBPβ LIP blocks adipocyte differentiation (Yeh et al., 1995). C/EBPβ is regulated by glucocorticoid signaling through GR by hindering the interaction of C/EBPβ with the transcriptional co-repressor histone deacetylase 1 (HDAC1) and by promoting the acetylation of C/EBPβ. Beyond acetylation, C/EBPβ activity is known to be modulated by other posttranslational modifications (PTMs), such as phosphorylation, as further described in chapter 1.3.1.

Another key player in the transcriptional network that triggers adipocyte differentiation, C/EBPδ, is rapidly induced by glucocorticoids, like dexamethasone, acting through the GR (MacDougald et al., 1994; Yeh et al., 1995).

Yeh et al. showed that ectopic expression of C/EBPβ and also, but to a somewhat lesser extent, of C/EBPδ in 3T3-L1 preadipocytes promotes C/EBPα expression and is able to induce adipocyte differentiation in the absence of adipogenic stimuli (Yeh et al., 1995). C/EBPβ and C/EBPδ play important roles in activating the late adipogenic program by promoting the expression of the master adipocyte regulators C/EBPα and PPARγ (Hamm et al., 2001; Wu et al., 1996; Yeh et al., 1995) that control terminal differentiation (Cristancho and Lazar, 2011). This notion was supported by the identification of C/EBP regulatory elements at the *pparγ* and *c/ebpα* loci (Christy et al., 1991; Clarke et al., 1997). Ectopic expression of PPARγ and C/EBPα promotes adipocyte differentiation in the absence of hormonal inducers (Freytag and Geddes, 1992; Freytag et al., 1994; Lin and Lane, 1994; Tontonoz et al., 1994b). Conversely, blocking C/EBPα or PPARγ expression inhibits

adipocyte differentiation (Lin and Lane, 1992; Rosen et al., 1999). Altogether, these findings indicate that PPARγ and C/EBPα are required for the adipocyte differentiation program. In mice, two different PPARγ isoforms (PPARγ1 and PPARγ2) are produced through alternative splicing (Zhu et al., 1995), of which PPARγ2 is primarily adipocyte-specific (Tontonoz and Spiegelman, 2008). Adipogenesis can be governed by both isoforms (Mueller et al., 2002; Zhang et al., 2004a). PPARγ acquires the ability to bind to peroxisome proliferator response elements (PPRE) after heterodimerization with the retinoid X receptor (RXR) (Kliewer et al., 1992; Tontonoz and Spiegelman, 2008). Moreover, C/EBPα and PPARγ, together, coordinate the expression of the majority of genes determining the adipocyte phenotype (Lefterova et al., 2008).

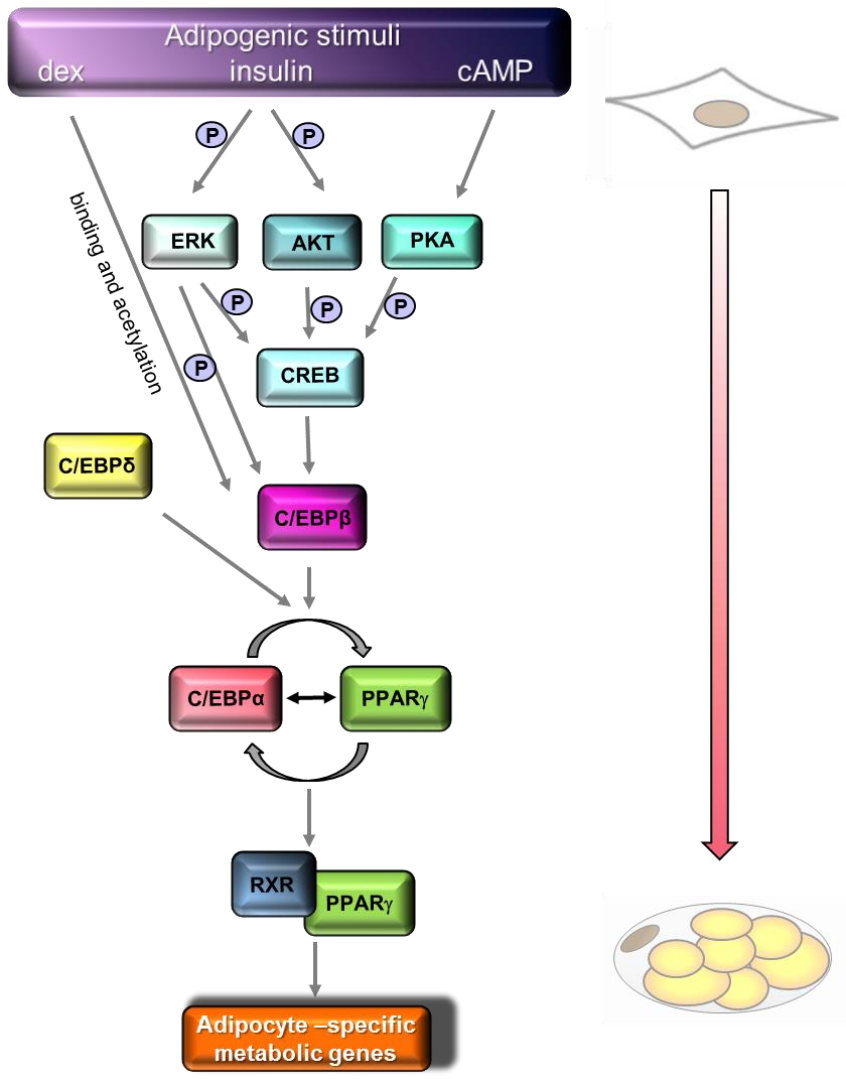

Figure 2: Induction of adipogenesis by a cascade of transcription factors. Simplified scheme of adipogenic transcription factors. Adipogenesis can be induced in fibroblast-like preadipocytes by applying an adipogenic cocktail, containing insulin, IBMX and dexamethasone in the presence of serum. Consequently, a transcription factor cascade is triggered leading to the expression of C/EBPβ and the master regulators of adipogenesis C/EBPα and PPARγ. Finally, their activation is resulting in the expression of adipocyte-specific metabolic genes that are responsible for the lipid-laden mature adipocyte phenotype.

White adipocyte precursors in vivo

In the last decades, the study of distinct *in vitro* systems, such as 3T3-L1 cells, has largely contributed to dissecting the molecular events driving white adipocyte development. However, unravelling the mechanisms contributing to fat development *in vivo* had proven difficult until recent years. Technological advances now allow the identification and isolation of adipocyte precursors *in vivo* which provides a valuable tool for the investigation of adipocyte development in health and diseases, like obesity (Berry et al., 2014; Cristancho and Lazar, 2011). The developmental origin of WAT is still unclear, however it is suggested that it largely depends on the individual AT depots. Subcutaneous fat descends from different mesenchymal lineages. In contrast, visceral adipocytes are proposed to derive from the lateral plate mesoderm (Chau et al., 2014). Moreover, it seems that even a certain AT depot constitutes of adipocytes that origin from distinct lineages (Sanchez-Gurmaches and Guertin, 2014). Especially the characterization of cell surface marker profiles using flow cytometry and fluorescence-activated cell sorting (FACS)-based approaches has largely contributed to the identification of precursors with a high capacity to differentiate into adipocytes (Berry et al., 2014). These surface markers include, for instance, $CD24^+$; platelet-derived growth factor receptor β ($PDGFR\beta^+$); stem cells antigen 1 ($Sca\text{-}1^+$); $CD34^+$ and many more (Berry et al., 2014; Hepler et al., 2017). It is very likely that these precursor populations overlap or that they have specialized roles in the respective AT depot (Hepler et al., 2017).

The mature white adipocyte

The adipocyte cell identity can be established and maintained since C/EBPα and PPARγ are able to auto-regulate their own expression as well as that of the respective other (Rosen et al., 2002; Wu et al., 1999). It is well-known that PPARγ is required to maintain the mature adipocyte phenotype (Tamori et al., 2002). ChIP-Seq analysis in differentiating 3T3-L1 cells revealed binding of the PPARγ:RXR heterodimer to about 75 % of the up-regulated genes (Nielsen et al., 2008). Moreover, C/EBPα binding sites highly overlap with the PPARγ binding sequences suggesting that together they bind to about 60 % of all genes that are up-regulated during adipogenesis and among them particularly to genes that control major adipocyte-specific functions such as TG synthesis and storage (Lefterova et al., 2008). In addition to its role in the regulation of early adipogenesis, also C/EBPβ is involved in controlling adipocyte-specific gene expression in mature adipocytes, supported by the finding that C/EBPβ binds to C/EBP sites in developed adipocytes (Lefterova et al., 2008; MacDougald et al., 1995). Knockdown studies demonstrated that PPARγ, C/EBPα and

C/EBβ are all required for activating adipocyte-specific gene expression in mature 3T3-L1 cells (Lefterova et al., 2008) (Figure 3).

As a member of the nuclear receptor superfamily, PPARγ is activated through ligand binding and in the following induces the expression of downstream target genes. Natural PPARγ ligands encompass 15-deoxy-$\Delta^{12,14}$ prostaglandin J2 (Forman et al., 1995; Kliewer et al., 1995), the oxidized lipid components 9- and 13-hydroxyoctadeca-9*Z*,11*E*-dienoic acids (9- and 13-HODE) of oxidized low density lipoprotein (Nagy et al., 1998), oxidized alkyl phospholipids (McIntyre et al., 2003), fatty acids and eicosanoids (Forman et al., 1997; Kliewer et al., 1997).

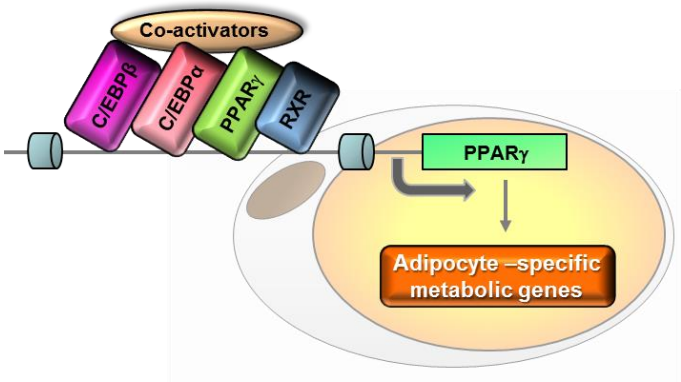

Figure 3: Transcriptional control of adipocyte-specific gene expression in mature adipocytes. In mature adipocytes, PPARγ can auto-regulate its own expression in conjunction with the transcription factors C/EBPα, and C/EBPβ, co-activators and RXR. Finally, this leads to the maintenance of adipocyte-specific gene expression and cell fate (adapted from Cristancho and Lazar, 2011).

1.1.2.2 Development of brown adipocytes

Brown adipocytes emerge from progenitor cells residing in the dermomyotome, which can also differentiate into skeletal muscle cells. These precursors express engrailed 1 (EN1), myogenic factor 5 (MYF5) and paired-box protein 7 (PAX7) (Atit et al., 2006; Lepper and Fan, 2010; Seale et al., 2008).

In recent years, nearly 50 regulators of brown and beige adipocyte development have been identified. In this section the function of the key regulators of brown adipocyte differentiation will be discussed.

The brown adipocyte fate is determined by the expression of several genes, including bone morphogenetic protein 7 (BMP7), early B cell factor 2 (EB2F), Ewing sarcoma (EWS) and Y-box binding protein 1 (YBX1). EWS interacts with its binding partner YBX1 to induce BMP7 expression (Park et al., 2013). BMP7 is crucial for inducing BAT development (Tseng et al., 2008). The brown and beige selective marker EBF2 plays an important role in the brown preadipocyte fate commitment (Seale, 2015).

The core transcriptional cascade comprising PPARγ and the C/EBP proteins orchestrates adipocyte differentiation in all types of fat cells. The specific mechanisms controlling white, beige and brown development and identity operate in addition to the general adipogenic program (Seale, 2015). Notably, external stimuli and cell type-selective regulators modulate the activity and expression of these transcription factors in different types of fat cells. PPARγ regulates many brown adipocyte-specific functions, for instance it is required for inducing UCP1 expression (Sears et al., 1996). C/EBPβ expression is elevated in BAT compared to WAT and its expression is induced by cold exposure (Kajimura et al., 2009; Karamitri et al., 2009). PPARα expression is considerably increased in brown compared to white adipocytes. The protein participates in controlling mitochondrial β-oxidation (see chapter 1.1.3.3) in several cell types, including brown fat cells. Moreover, it induces the expression of key brown adipocyte-specific genes, such as UCP1, PR domain containing 16 (PRDM16) and PPARγ coactivator 1 (PGC1α) (Barbera et al., 2001; Hondares et al., 2011). The transcriptional co-regulator PRDM16 interacts with C/EBPβ and PPARγ in order to induce the expression of BAT-specific genes and thereby promotes brown adipocyte differentiation (Kajimura et al., 2009; Seale et al., 2008). Acting together with Mediator complex subunit 1 (MED1), PRDM16 promotes the activity of PPARγ and the thyroid receptor (TR) to induce UCP1 expression (Iida et al., 2015). Moreover, PRDM16 interacts with ZFP516 in order to induce brown adipogenesis and thermogenesis (Dempersmier et al., 2015). However, PRDM16 was shown to be not necessary for activation of brown fat-specific gene expression in embryos or young animals and, thus, other factors are believed to compensate for PRDM16 (Seale, 2015). Nevertheless, PRDM16 is required for the suppression of many white adipocyte-specific genes, e.g. resistin (Harms et al., 2014). In addition to its function in determining brown preadipocyte fate commitment, EBF2 promotes brown adipocyte differentiation by recruiting PPARγ to brown adipocyte-specific DNA binding sites (Rajakumari et al., 2013). The process of brown adipogenesis and some of the key factors participating in it is shown in Figure 4.

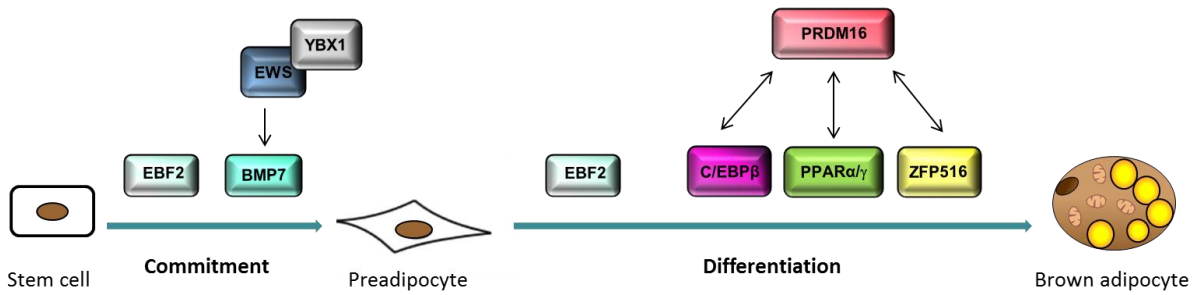

Figure 4: Brown adipogenesis. Schematic illustration showing some of the key factors regulating brown preadipocyte commitment and brown adipocyte differentiation (adapted from Seale, 2015).

1.1.2.3 Development of beige adipocytes

Brown and beige adipocytes descend from different lineages. Beige adipocytes can origin from progenitor cells expressing PDGFRα or Sca-1 or from smooth muscle-like precursors expressing myosin heavy chain 11 (MYH11). Beige adipocytes develop upon various internal or external stimuli, such as chronic cold exposure, PPARγ agonists or β-adrenergic stimulation (Kajimura et al., 2015). Many of the above stated regulators for brown adipocyte differentiation play a similar role in beige adipocyte adipogenesis. EBF2 as well as BMP7 also regulate the cell fate commitment of beige preadipocytes (Inagaki et al., 2017; Stine et al., 2016). Similar to brown adipocytes, RDM16 promotes beige adipocyte differentiation by inducing the expression of beige adipocyte-specific genes and repressing WAT-selective genes (Seale et al., 2011). Furthermore, PPARγ, C/EBPβ and ZFP516 participate in inducing beige adipocyte differentiation (Inagaki et al., 2017). Moreover, Krüppel-like factor 11 (KLF11) mediates the induction of beige adipocyte-specific gene expression triggered by the PPARγ agonist rosiglitazone through interaction with PPARγ (Loft et al., 2015). The process of beige adipocyte differentiation and some of the key factors participating in it is illustrated in Figure 5.

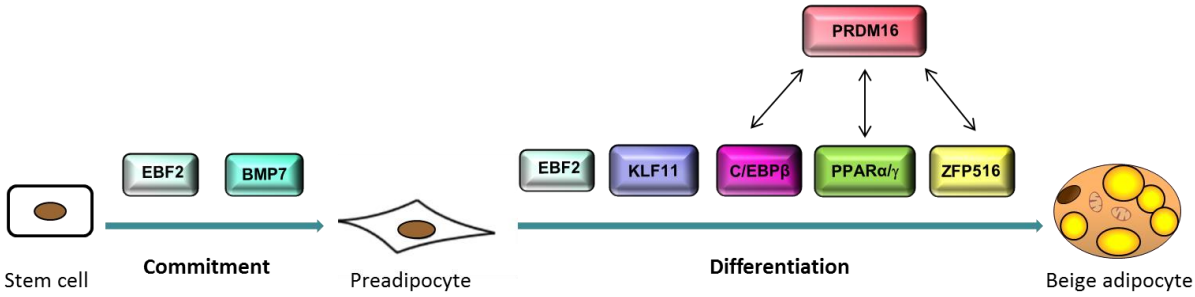

Figure 5: Beige adipogenesis. Schematic illustration showing some of the factors regulating beige preadipocyte commitment and beige adipocyte differentiation (adapted from Seale, 2015).

1.1.3 Functional characteristics

1.1.3.1 Adipose tissue as a fuel reservoir

One of the roles of WAT is to store TG under conditions of caloric excess and to make this energy available during times of energy deprivation. WAT represents the major TG storage site in the body (Rosen and Spiegelman, 2006). In periods of over nutrition or reduced energy expenditure, AT is capable of expanding via two different mechanisms: either by the enlargement of fat cells (hypertrophy) or by an increase in adipocyte cell number (hyperplasia) (Rutkowski et al., 2015). While adipocyte hyperplasia is associated with a healthier metabolic phenotype, hypertrophy was shown to be linked to numerous metabolic

disturbances (Bjorntorp et al., 1971). Prior to hyperplasia, hypertrophy occurs in AT in order to meet the need for additional fat storage capacity. Only when a certain adipocyte size is reached, factors are released in order to trigger preadipocyte proliferation and differentiation (Krotkiewski et al., 1983).

AT is highly dynamic in terms of energy storage and release. Nutrients are stored in form of TG under conditions of energy surplus and this energy is made available during times of energy deprivation. TG, which are built-up from one glycerol-3-phosphate (G3P) and three FA molecules, are chemically inert molecules and thus serve as a “safe” form to store excess energy (Frayn et al., 2006). The mechanisms involved in their formation (lipogenesis) and break-down (lipolysis) will be described in the following.

Lipogenesis

Lipogenesis is defined as the process by which TG are formed and it is primarily stimulated by insulin. This process includes the synthesis of FA and glycerol, their activation and finally their esterification to produce TG (Rutkowski et al., 2015).

There are two major sources for FA to form TG: FA either originate from hydrolyzed dietary TG or can be synthesized *de novo*, a process primarily occurring in the liver but also to a lesser extent in other tissues (Saponaro et al., 2015). Uptake of dietary FA into the adipocyte is controlled by a broad array of FA binding and transport proteins, such as fatty acid translocase (CD36) (Coburn et al., 2000), fatty acid-binding protein 4 (FABP4) (Hunt et al., 1986; Spiegelman et al., 1983) and like fatty acid transport protein 1 (FATP1) (Hirsch et al., 1998; Schaffer and Lodish, 1994). A surplus of glucose can be converted to lipids by *de novo* lipogenesis (Saponaro et al., 2015). Glucose uptake is mediated by numerous glucose transporters, like glucose transporter type 4 (GLUT4). GLUT4 is specifically expressed in insulin-sensitive tissues, such as skeletal muscle or AT. Upon insulin signaling, this protein translocates to the cell membrane for facilitating glucose entry (Furtado et al., 2002). Breakdown of glucose by glycolysis and the citric acid cycle (processes which will not be discussed further as it would be beyond the scope of this thesis) generates Acetyl-CoA. FA can be synthesized *de novo* from Acetyl-CoA by a mechanism encompassing, first, the action of Acetyl-CoA carboxylase 1 (ACC1) to produce Malonyl-CoA and, second, the activity of fatty acid synthase (FAS) to generate FA from Malonyl-CoA (Wakil and Abu-Elheiga, 2009).

These FA are subsequently activated by the conversion to acyl-CoA products by Acyl-coenzyme A synthetase (ACS) (Watkins, 1997). Glycerol becomes activated when it is converted to G3P. G3P can be either produced during glycolysis, but a significant proportion

is generated by glyceroneogenesis, a process predominantly occurring in the liver or AT (Saponaro et al., 2015). During glyceroneogenesis, G3P can be generated from non-carbohydrate substrates. The key regulator and rate-limiting enzyme of this process, phosphoenolpyruvate carboxykinase (PEPCK), mediates the decarboxylation of oxaloacetate to form phosphoenolpyruvate. Hence, it is established to have a crucial role in TG synthesis (Olswang et al., 2002).

Finally, FA acyl-CoA is esterified with G3P to form TG.

Lipolysis

For energy mobilization during times of energy demand, TG are hydrolyzed to FA through a process termed lipolysis (Rutkowski et al., 2015). This mechanism can be triggered by various stimuli, including β-adrenergic signaling or cAMP-dependent activation of PKA (Fain and Garcija-Sainz, 1983; Honnor et al., 1985a, b). Importantly, lipolysis is suppressed by insulin in the fed state (Ahmed et al., 2010; Choi et al., 2010).
The lipid droplet-associated protein perilipin 1 is essential for controlling the hormonal regulation of lipolysis of TG and can be multiply phosphorylated by PKA (Greenberg et al., 1991). In the basal state, lipolysis is repressed and perilipin 1 is bound to comparative gene identification-58 (CGI-58), also known as Abhd5, thereby capturing it to the surface of the lipid droplet (Subramanian et al., 2004; Yamaguchi et al., 2004). PKA-mediated phosphorylation of perilipin 1 stimulates the rapid release of CGI-58 into the cytosol (Granneman et al., 2007; Granneman et al., 2009; Subramanian et al., 2004; Yamaguchi et al., 2007). Upon release from perilipin 1, CGI-58 binds to ATGL (Granneman et al., 2009), the first and rate-limiting enzyme of lipolysis (Haemmerle et al., 2006), thereby stimulating its TG hydrolase activity and acting as its co-activator (Lass et al., 2006). ATGL is highly expressed in adipose tissue and was demonstrated to be bound to the lipid droplet surface. Activated ATGL catalyzes the initial step in lipolysis and hydrolyzes the first fatty acid from the TG. It has a high substrate specificity for TG, while it poorly hydrolyses diacylglycerols (DG) and monoacylglycerols (MG) (Jenkins et al., 2004; Villena et al., 2004; Zimmermann et al., 2004). The main DG hydrolase hormone sensitive lipase (HSL) has a broad substrate specificity, being able to catalyze the breakdown of TG, DG, MG, cholesteryl esters, retinyl esters and short-chain carbonic acid esters (Zechner et al., 2017). PKA phosphorylates HSL and thereby triggers its translocation to the lipid droplet surface and interaction with perilipin 1 (Egan et al., 1992; Granneman et al., 2007; Miyoshi et al., 2006). Subsequently, HSL catalyzes the hydrolysis of DG to MG, thereby producing a further fatty acid (Rodriguez et al., 2010). Finally, MG is hydrolyzed by monoacylglycerol lipase (MGL) and releases glycerol

and the third fatty acid, which can be secreted by the adipocytes into the circulation (Vaughan et al., 1964).

The mechanisms involved in lipolysis and lipogenesis are depicted in Figure 6.

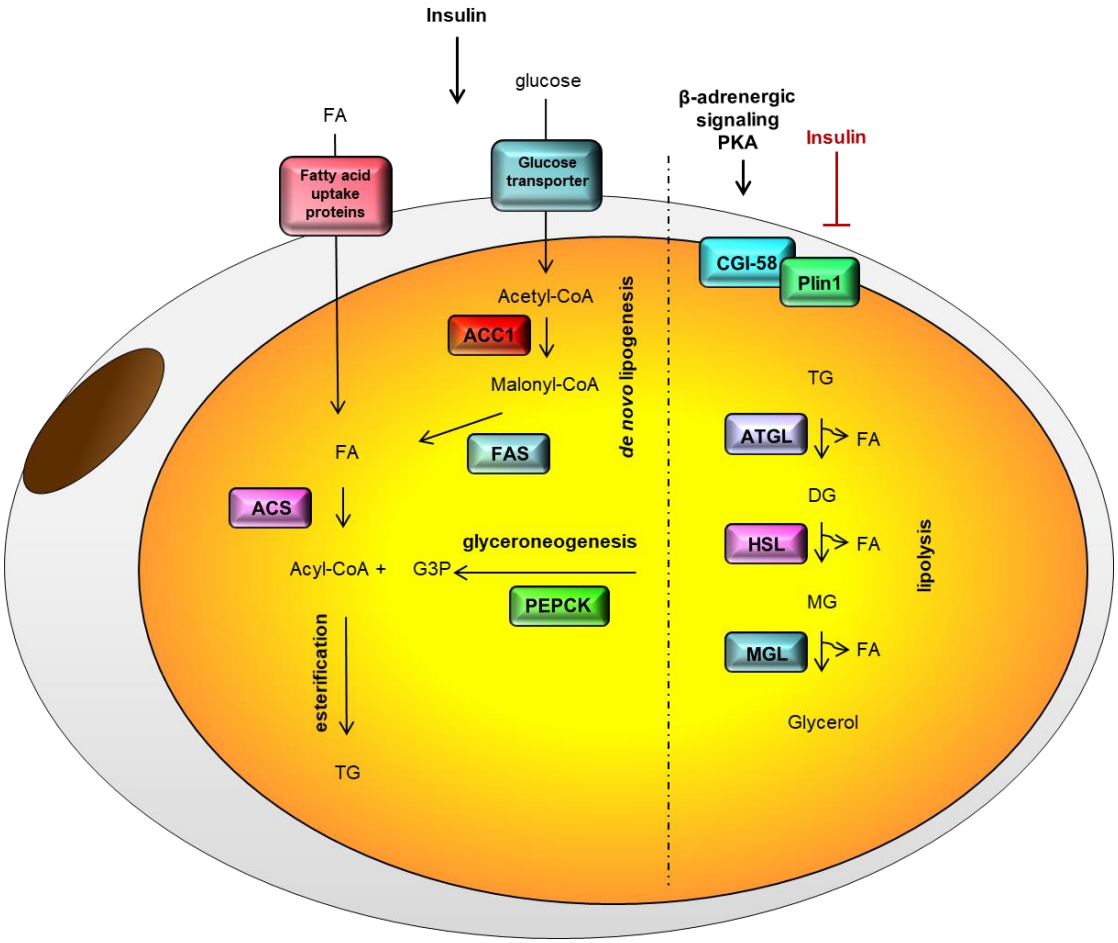

Figure 6: Lipolysis and fatty acid re-esterification have to be carefully balanced in an adipocyte. Scheme showing the processes of lipolysis and lipogenesis in an adipocyte. Lipolysis, the sequential breakdown of TG to glycerol and FA via a set of proteins (including CGI-58, perilipin 1 (Plin1), ATGL, HSL and MGL), can be, for instance, triggered by β-adrenergic stimulation or PKA signaling. In contrast, insulin inhibits lipolysis. Lipogenesis, a process involving the synthesis of FA and glycerol, their activation and finally their esterification to produce TG, is promoted by insulin signaling. FA are synthesized *de novo* from Acetyl-CoA. Subsequently, they are activated by ACS. G3P is generated by glyceroneogenesis, a process in which PEPCK is the rate-limiting step that mediates the decarboxylation of oxaloacetate to form phosphoenolpyruvate. Subsequently, Acyl-CoA and G3P are esterified to form TG (adapted from Rutkowski et al., 2015).

1.1.3.2 Adipose tissue as an endocrine organ

While in former times AT function was believed to be exclusively restricted to the storage of energy surplus, nowadays AT is recognized as an endocrine organ (Ahima and Flier, 2000; Galic et al., 2010; Kershaw and Flier, 2004). As such, it affects distinct target organs, such as the liver, skeletal muscle or brain, in order to regulate glucose and lipid metabolism, thus controlling energy homeostasis, blood pressure and inflammation. The AT regulates energy homeostasis by modulating feeding behavior and energy expenditure (Fasshauer and

Bluher, 2015). AT is able to influence these processes by nutritional or neuronal pathways and through the release of numerous hormones, chemoattractants or cytokines, so called, adipokines (Kershaw and Flier, 2004; Rosen and Spiegelman, 2006; Song et al., 2009). Particularly, the discoveries of leptin and adiponectin in the 1990s for the first time suggested that AT was a regulator of systemic energy homeostasis (Stern et al., 2016). Up to now, more than 600 potential hormones secreted by the AT have been identified (Lehr et al., 2012). The factors secreted by the AT exert specific functions to fine-tune distinct biological processes, like, glucose metabolism (e.g. leptin, adiponectin, FGF21 or resistin), insulin sensitivity (e.g. leptin, adiponectin or RBP4), insulin secretion (e.g. apelin or nesfatin-1), lipid metabolism (e.g. apelin), inflammation (e.g. tumor necrosis factor alpha (TNFα), monocyte chemoattractant protein 1 (MCP1), resistin or interleukins), vascular growth and function (e.g. vascular endothelial growth factor (VEGF)), blood pressure (e.g. apelin or angiotensinogen) or appetite regulation (e.g. leptin) (Fasshauer and Bluher, 2015) (Figure 7). Moreover, BAT releases factors (the so-called brown adipokines or batokines) to modulate systemic metabolism and mediate its beneficial metabolic effects (Kajimura, 2017). Despite the diversity of adipokines controlling a vast variety of biological functions, below it will be only focused on the adipokines that are relevant to this thesis.

Adiponectin functions as an insulin sensitizer (Berg et al., 2001) and positively contributes to healthy AT expansion, thereby protecting from ectopic lipid deposition (Xu et al., 2003; Yamauchi et al., 2001). Adiponectin was demonstrated to enhance skeletal muscle FA oxidation and glucose uptake, thereby improving insulin sensitivity (Ceddia et al., 2005; Fruebis et al., 2001; Yamauchi et al., 2002). Leptin's best-established function is to act on the hypothalamus in order to regulate food consumption and energy expenditure, consequently affecting body weight (Halaas et al., 1995). Leptin plasma levels are highly correlated with fat mass and adipocyte size (Florant et al., 2004; Shimizu et al., 1997; Skurk et al., 2007). Leptin resistance often emerges with increasing adiposity and is resulting in devastating consequences, such as the failure to suppress food intake and enhance energy expenditure, thus promoting even further body weight gain (Dalamaga et al., 2013). Moreover, leptin exerts positive effects on glucose homeostasis independently of affecting food intake and energy expenditure (Berglund et al., 2012). In states of cellular stress adipocytes release cytokines, e.g. TNFα, or chemoattractants, MCP1, thereby triggering AT inflammation (Bluher, 2016). Expression of TNFα in the AT is increased in obese rodents and humans and it can be positively correlated with insulin resistance. It alters the gene expression of metabolic organs, such as AT or liver, and impairs insulin signaling (Kershaw and Flier, 2004). MCP1 mediates the infiltration of immune cells into the AT. MCP1 levels are also increased in obese rodents and humans (Kwon and Pessin, 2013).

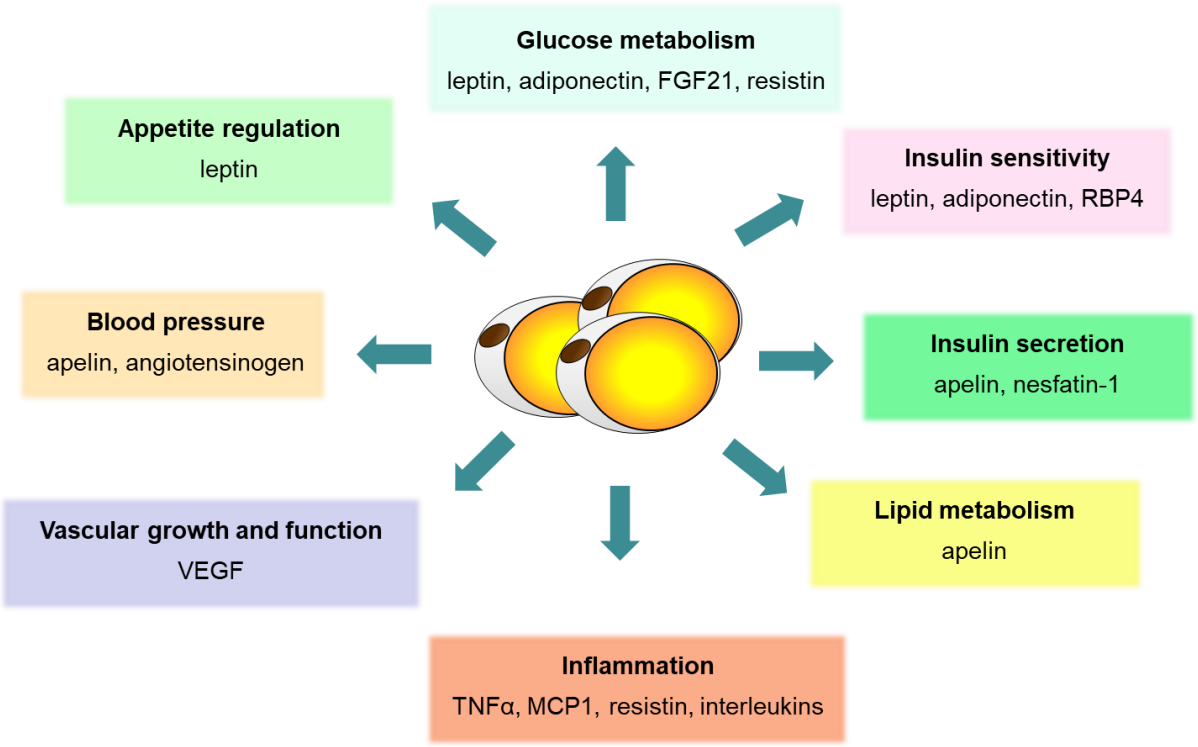

Figure 7: Adipose tissue is an endocrine organ that maintains whole-body energy homeostasis. Illustration summarizing the relevance of AT as an endocrine organ in controlling various biological processes by releasing a broad variety of adipokines in the circulation.

1.1.3.3 Adipose tissue thermogenesis

As stated above brown and beige adipocytes can expend energy in form of heat (Cannon and Nedergaard, 2004; Harms and Seale, 2013). By this mechanism thermogenic cells can promote weight loss and improve systemic energy metabolism and glucose/lipid homeostasis (Harms and Seale, 2013). BAT was described to become activated when animals have a high energy intake in order to protect from weight gain (Rothwell and Stock, 1979). Accordingly, mice with less BAT display an increase in body weight (Lowell et al., 1993). Moreover, browning of WAT has been shown to have anti-obesity and anti-diabetic effects in rodent models (Wu et al., 2013).

Oxidation of FA in the AT is required for cold-induced thermogenesis by generating the energy needed to fuel thermogenesis and for the transcriptional regulation of BAT thermogenesis (Lee et al., 2015). Although skeletal muscle is the primary site of fuel oxidation, most tissues have a oxidative capacity to some extend, including AT. Glucose is metabolized via glycolysis to generate energy. For the oxidation of lipids, first, TG are transported in the blood via lipoproteins and are subsequently hydrolized by lipoprotein lipase (LPL) (Eckel, 1989). Subsequently, FA uptake is facilitated by various membrane proteins, like FATPs, FABPs or CD36. Activation of FA is mediated by the attachment of

coenzyme A (CoA) to form acyl-CoAs (Glatz et al., 2010). FA are degraded to produce energy in the mitochondria by β-oxidation (Bartlett and Eaton, 2004). Due to the impermeability of the mitochondrial membrane to acyl-CoAs, these molecules are converted to acylcarnitines by the enzyme carnitine palmitoyltransferase 1 (CPT1) that is located at the outer mitochondrial membrane, an essential mechanism governing the FA up-take into mitochondria for following oxidation (Rufer et al., 2009). While the isoform CPT1a is expressed in various tissues, including liver and AT, the CPT1b isorform is predominantly expressed in skeletal muscle, heart and testis (Houten and Wanders, 2010). Carnitine acylcarnitine translocase (CACT) facilitates the entry of acylcarnitines into the mitochondria (Longo et al., 2006). Subsequently, acylcarnitines have to be transformed into their initial precursors, acyl-CoAs, a process catalyzed by CPT2 which resides in the inner mitochondrial membrane (Rufer et al., 2009). Finally, acyl-CoAs are degraded during β-oxidation, a cyclic process which involves the action of a four-step enzymatic cascade. Each cycle shortens the acyl-CoA molecules by two carbon atoms and generates acetyl-CoA and the electron carriers nicotinamide adenine dinucleotide (NADH) and flavin adenine dinucleotide ($FADH_2$). The acyl-CoA molecules afterwards undergo further cycles of β-oxidation, acetyl-CoA is used in the citric acid cycle and NADH and $FADH_2$ provide electrons to the respiratory electron transport chain (Houten and Wanders, 2010). The electron transport chain comprises five different complexes that use electrons released from glycolysis or β-oxidation to produce energy in form of adenosine triphosphate (ATP). Electrons are transported between the complexes via membrane-embedded ubiquinone and soluble cytochrome c (CytC). First, the proton-pumping enzyme complex I (NADH–ubiquinone oxidoreductase) accepts electrons from NADH and catalyzes the reduction of ubiquinone to ubiquinol. Additionally, electrons enter the electron transport chain via Complex II (succinate–quinone oxidoreductase). Ubiquinol subsequently delivers the electrons to complex III (cytochrome bc_1), which facilitates the reduction of the ultimate electron acceptor CytC. Subsequently, CytC is oxidized by complex IV (cytochrome c oxidase), thereby producing protons. The resulting proton gradient across the mitochondrial membrane drives ATP synthase, that generates ATP.

The thermogenic activity of brown and beige adipocytes primarily depends on the increased expression of UCP1, a protein localized on the inner mitochondrial membrane, which permits a leak of protons generated by the electron transport chain across the mitochondrial membrane. Consequently, substrate oxidation becomes uncoupled from ATP synthesis and the energy produced during oxidation is dissipated as heat (Cannon and Nedergaard, 2004) (Figure 8). Additionally, recent studies described mechanisms of UCP1-independent thermogenesis. For instance, SERCA2b-mediated calcium cycling has been reported to control beige AT thermogenesis (Ikeda et al., 2018). Moreover, beige fat was shown to

govern energy expenditure and thermogenesis through a creatine-driven substrate cycle (Kazak et al., 2015).

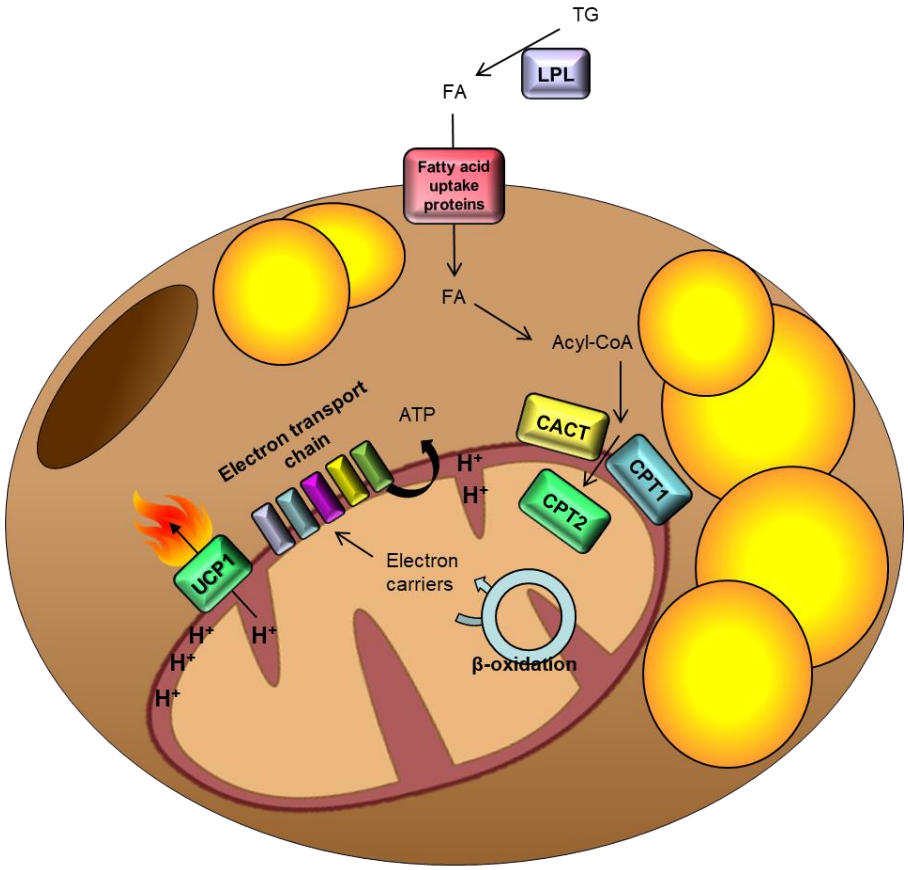

Figure 8: Brown and beige adipocytes dissipate energy by heat generation. Simplified illustration showing the oxidation of FA and the subsequent heat generation (thermogenesis) by brown and beige adipocytes. Primarily, circulating TG are hydrolyzed by LPL. The resulting FA enter the cell via membrane proteins. FA are converted to acyl-CoA, subsequently CPT1 catalyzes the transformation to acylcarnitines. CACT mediates the uptake of acylcarnitines into the mitochondria. CPT2 converts them to acyl-CoA molecules, which afterwards undergo β-oxidation, a process that generates electron carriers. These release their electrons in the electron transport chain, generating a proton (H^+) gradient in the mitochondrial membrane. UCP1 uncouples substrate oxidation from ATP synthesis by allowing a H^+ leak across the mitochondrial membrane.

Thermogenesis can be triggered by multiple external stimuli, for instance by cold exposure. At the molecular level, cold exposure triggers catecholamine release from sympathetic nerves, thereby activating β-adrenergic signaling (Collins, 2011). This is consequently resulting in increased cAMP levels and a PKA-mediated activation of CREB and ATF2 transcription factors, finally inducing the expression of UCP1 and PGC1α (Cao et al., 2004). UCP1 and PGC1α expression can be additionally directly regulated by PPARγ and C/EBPβ and thereby control thermogenesis (Kajimura et al., 2009; Karamanlidis et al., 2007; Seale et al., 2008). The transcriptional co-activator PGC1α, which is highly expressed upon cold exposure, is pivotal for activating a thermogenic gene program in brown and beige adipocytes (Puigserver et al., 1998; Tiraby et al., 2003). PRDM16 interacts with PGC1α and promotes its transcriptional activity (Seale et al., 2007). Moreover, ligand-bound TR forms a

complex with PGC1α, PRDM16 and MED1 to induce UCP1 expression (Chen et al., 2009; Iida et al., 2015). ZFP516, which is activated upon cold stimulation, interacts with PRDM16 in order to activate the expression of UCP1 and PGC1α, thereby promoting thermogenesis (Dempersmier et al., 2015). Altogether, these transcription factors, among others, are responsible for inducing thermogenesis in differentiated brown and beige adipocytes (Figure 9).

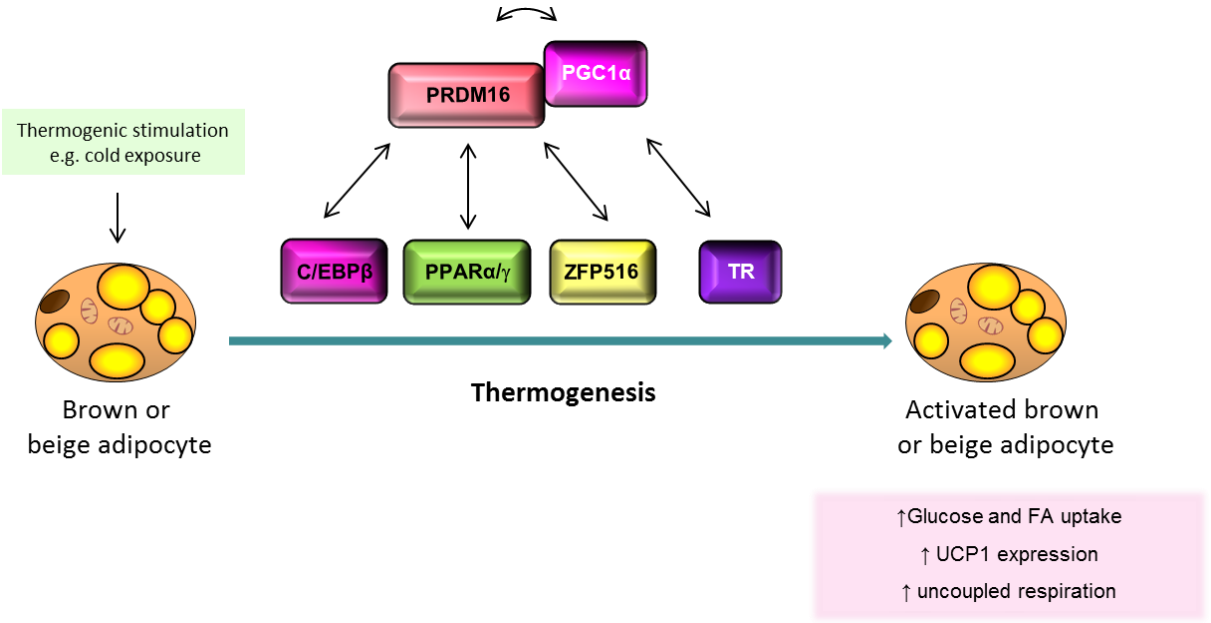

Figure 9: Molecular mechanism triggering thermogenesis in brown and beige adipocytes. Schematic illustration highlighting the most critical factors involved in activating thermogenesis in brown and beige adipocytes. Ultimately, nutrient uptake, UCP1 expression and uncoupled respiration is promoted, thereby energy is dissipated in form of heat (adapted from Seale, 2015).

1.1.4 Organ crosstalk in energy/metabolic balance and the role of adipose tissue

Metabolism comprises biochemical processes in living organisms that either produce or consume energy. It can be divided in three classes: the degradation of molecules to generate energy (catabolism), the synthesis of molecules (anabolism) and waste disposal (in form of reactive oxygen species, carbon dioxide, ammonia). These processes are essential survival processes. In this context, the flux rates of energy and substances and the maintenance of whole-body energy homeostasis are pivotal features in a living organism. The term whole-body energy homeostasis refers to the balance between the energy that is consumed and the energy needed by an organism. Basal metabolic rate, regulation of body temperature, non-shivering thermogenesis, physical activity, growth and reproduction are processes which contribute to a body's energy expenditure, whereas energy intake is reflected by the amount of energy resorbed from food in form of glucose, FA or amino acids (Figure 10). In order to

prevent energy imbalances, excess energy can be stored in numerous tissues in form of carbohydrates (e.g. glycogen) or lipids (e.g. TG) which can be mobilized and utilized in times of energy demand. Thus, energy homeostasis can be fine-tuned by various processes, including regulation of food intake, energy expenditure and energy storage. Any defects in this systems could result in energy imbalance and consequently disease (Rozman et al., 2014). Chronic excessive energy intake beyond the energy demands of an organism results in obesity, reflected by an exorbitant accumulation of AT (Hardy et al., 2012).

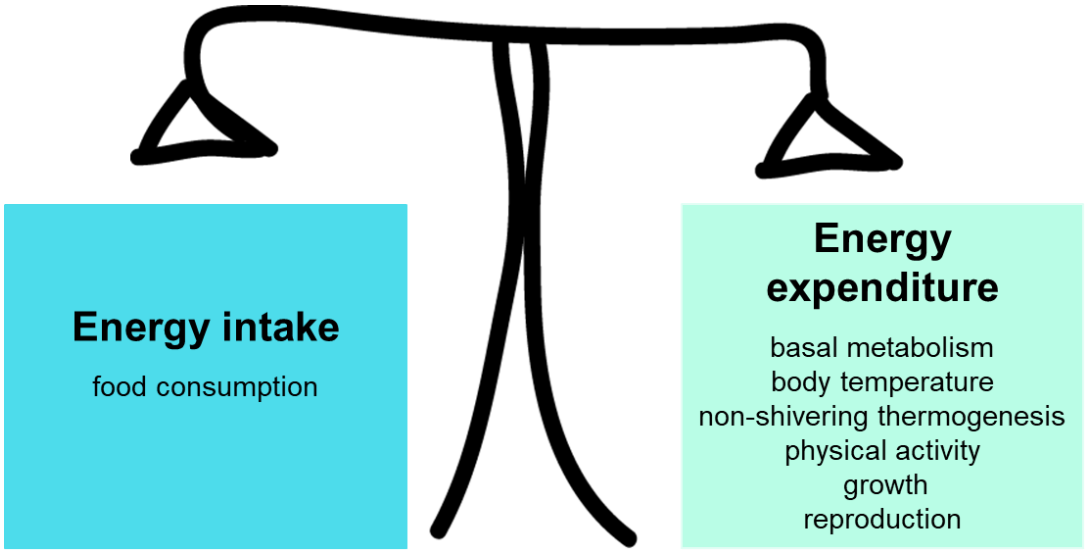

Figure 10: The balance between energy intake and expenditure in whole-body energy homeostasis. The energy homeostasis of an organism can be maintained by the careful control of the balance between the amount of energy consumed (by feeding) and expended (through basal metabolism, body temperature control, non-shivering thermogenesis, physical activity and reproduction) in order to preserve life functions.

The body's principal energy source is glucose. It not only generates energy when it is oxidized but also serves as an element for biosynthesis of molecules (Houten and Wanders, 2010). Only under certain conditions, for instance during fasting, a switch from glucose to FA oxidation takes place in order to preserve the glucose supply to tissues that are incapable of fat oxidation, such as the brain (Bartlett and Eaton, 2004; Frayn et al., 2006; Houten and Wanders, 2010). Thus, blood glucose levels are maintained rather steady, despite changes in food consumption or energy expenditure, an important prerequisite for preservation of life functions. Beside glucose, the body can use FA in order to generate energy or use them in biosynthetic reactions (Houten and Wanders, 2010). Glucose and lipid metabolism are controlled by the concerted action of different tissues, the so-termed tissue or organ crosstalk. These metabolically active organs and tissues, including the brain, gastrointestinal tract, liver, skeletal muscle and AT, are able to sense the nutrient status and can in turn convey signals to other organs in order to adapt to alterations in glucose and lipid levels

(Herman and Kahn, 2006; Rosen and Spiegelman, 2006; Tirone and Brunicardi, 2001) (Figure 11).

The brain is involved in this crosstalk by direct or indirect nutrient sensing and signaling to peripheral organs (Ruud et al., 2017). Below the current stage of knowledge regarding the inter-organ crosstalk between the AT, liver, pancreas and muscle contributing to metabolic balance will be discussed.

Ingested food passes the gastrointestinal tract, an important player in the regulation of glucose and lipid metabolism. It transmits signals by secreting hormones (e.g. Ghrelin or GLP-1), through gut microbiota-derived molecules or via nerve fibers in order to control various processes, such as the digestive function, regulation of satiety, glucose homeostasis and energy balance (Monteiro and Batterham, 2017). Water-insoluble lipids, such as TG or cholesterol, are transported through the circulation by lipoproteins. These particles contain cholesterol esters, TG, free cholesterol, phospholipids and apolipoproteins, which mediate the formation and function of lipoproteins. Lipoproteins can be classified into chylomicrons, chylomicron remnants, VLDL, IDL, LDL, HDL and Lp (a). Dietary lipids are transported in chylomicrons from the intestine to muscle and AT where they are metabolized by LPL and chylomicron remnants are generated. These are subsequently taken up by the liver. The endogenous lipoprotein pathway starts with the transport of TG by VLDL from the liver to muscle and AT, where LPL releases FA and IDL. Subsequently IDL is further metabolized to generate LDL, which is mainly taken up in the liver but also other tissues. Reverse cholesterol transport starts with the formation of premature HDL by the liver and intestine, which can include cholesterol and phospholipids released from cells, thereby giving rise to mature HDL. Cholesterol is then transported to the liver by HDL (Feingold and Grunfeld, 2000).

Upon increasing glucose levels, for example after a meal, the pancreas secretes insulin, which promotes glucose uptake into the AT, liver and muscle for oxidation or for storage as glycogen or as TG. Moreover, insulin inhibits hepatic glucose output by blocking glycogenolysis (breakdown of glycogen to glucose) and gluconeogenesis (synthesis of glucose). AT stores FA in form of TG during periods of caloric excess (Frayn et al., 2006; Houten and Wanders, 2010). Excess TG storage in tissues other than AT is often referred to as ectopic lipid deposition, which is associated with lipotoxicity and insulin resistance (Rutkowski et al., 2015; Vegiopoulos et al., 2017). Lipid accumulation in the muscle impairs insulin-stimulated glucose uptake (Dresner et al., 1999; Roden et al., 1996), whereas ectopic lipid deposition in the liver results in altered insulin signaling impairing glycogen synthesis (Samuel and Shulman, 2016). Furthermore, insulin fails to suppress hepatic glucose output,

while consistently stimulating FA synthesis (Brown and Goldstein, 2008). Thus, functioning as a lipid buffer, the AT indirectly controls glucose homeostasis (Rosen and Spiegelman, 2006). The liver can store FA in form of TG or glucose in form of glycogen in conditions of energy surplus. However, exceeding lipid acummulation in the liver can ultimately result in nonalcoholic fatty liver disease (NAFLD), which ranges from hepatic steatosis, inflammation, fibrosis to cirrhosis (Browning and Horton, 2004; Neuschwander-Tetri and Caldwell, 2003). Moreover, the liver is the major site for glyceroneogenesis and *de novo* lipogenesis, a process stimulated by insulin, thereby regulating glucose and lipid metabolism (Saponaro et al., 2015). In times of energy need, low insulin levels as well as the secretion of other hormones, for instance glucagon secreted by the pancreas, inhibits glucose oxidation and induces hepatic glucose output through glycogenolysis or gluconeogenesis (Herman and Kahn, 2006; Rosen and Spiegelman, 2006).

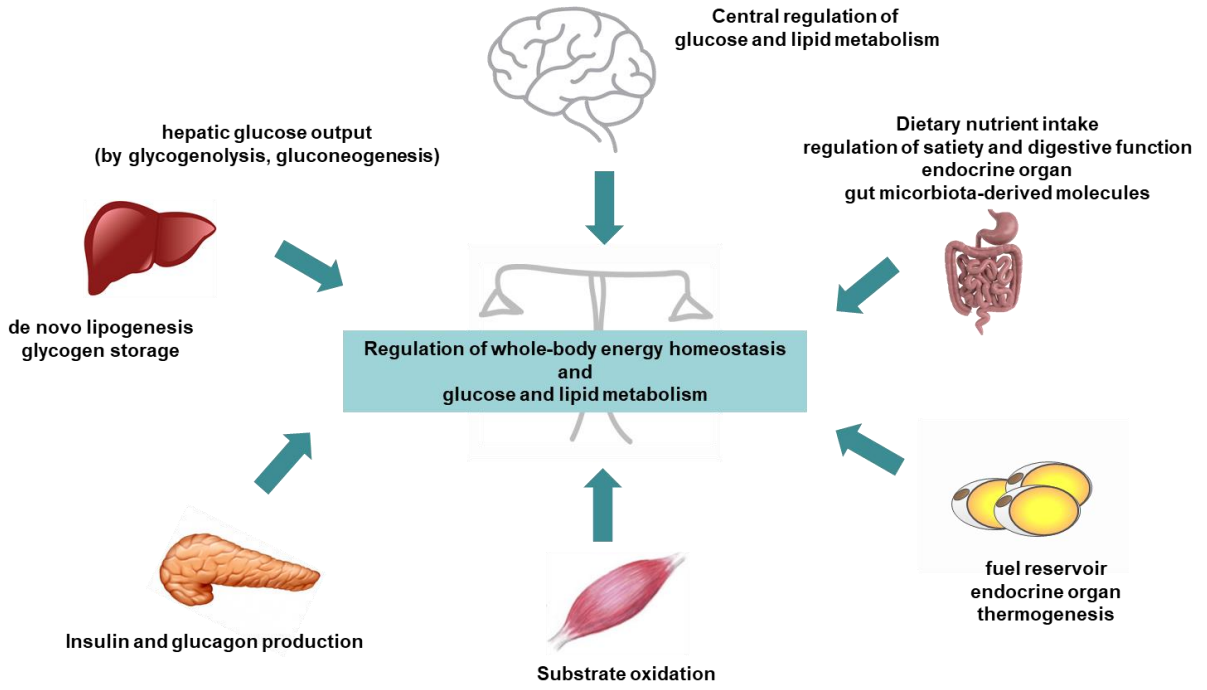

Figure 11: Tissue crosstalk involved in glucose and fatty acid metabolism. Simplified scheme showing the key functions of metabolic organs in glucose and lipid metabolism. The brain controls glucose and lipid metabolism by signaling to metabolic target organs. The gut not only takes up dietary nutrients but also regulates satiety and digestive function and secretes hormones and gut microbiota-derived molecules in order to regulate glucose/lipid metabolism and energy balance. The AT is functioning as a lipid buffer, thereby controlling glucose homeostasis. Moreover, by adipokine secretion AT affects distinct target organs, such as the liver, skeletal muscle or brain, in order to regulate glucose and lipid metabolism and energy homeostasis. Further, it is able to dissipate energy in form of heat. Muscle is the major site for fuel oxidation in the body. The key function if the pancreas is the secretion of insulin and glucagon. The liver is able to affect glucose homeostasis by storing excessive glucose as glycogen or by performing de novo lipogenesis. Moreover, it can generate glucose and release it in the circulation either by glycogenolysis or gluconeogenesis.

Disturbances in glucose homeostasis, insulin resistance and T2DM

Glucose intolerance is manifested as state of dysregulated glucose homeostasis in which the glucose concentration in the blood is elevated after a certain amount of time following a defined load of glucose compared to a healthy organism. Insulin resistance represents one major underlying factor of glucose intolerance (Nathan et al., 2007). Systemic insulin resistance is reflected by a decline in glucose disposal rate, meaning the rate of glucose clearance from the blood, in response to a certain insulin concentration (Reaven, 1988). Although insulin resistance can be triggered by various factors, obesity is the most prevalent origin of it (Johnson and Olefsky, 2013). Systemic insulin resistance in most cases is secondary to impaired insulin signaling in metabolically active tissues, such as liver, skeletal muscle or AT (Hardy et al., 2012). In this context, the failure to promote insulin-mediated GLUT4 translocation is one contributor to insulin resistance in muscle and AT (Leto and Saltiel, 2012). Paradoxically, during an insulin resistant state in the liver, insulin fails to suppress hepatic glucose output, while consistently stimulating FA synthesis (Brown and Goldstein, 2008). In skeletal muscle insulin resistance has been linked to a reduction in insulin-mediated glucose uptake and glycogen synthesis. Insulin resistance in the AT, caused by AT dysfunction, has been associated with altered glucose uptake and failure in suppressing lipolysis (Hardy et al., 2012). Metabolic abnormalities, like glucose intolerance and insulin resistance are precursors for the development of T2DM (Nathan et al., 2007; Reaven, 1988). T2DM is a chronic disease characterized by high blood glucose levels secondary to insulin deficiency which results from insulin resistance and dysfunction in the pancreatic β-cells to produce insulin (Ashcroft and Rorsman, 2012; Chatterjee et al., 2017). Under normal conditions, β-cells initially compensate insulin resistance by secreting more insulin. However, pathological conditions, such as inflammatory, metabolic or ER stress, in combination with genetic susceptibility might result in β-cell dysfunction or even death in T2DM. Ultimately, due to β-cell dysfunction the pancreas fails to compensate for the glucose overload in the blood (Halban et al., 2014). T2DM can be affected by lifestyle or environmental factors, including age, pregnancy, energy-dense diets, lack in physical exercise and obesity but also by genetic factors which are potentiated by an unhealthy lifestyle (Ashcroft and Rorsman, 2012; Grarup et al., 2014; Kolb and Martin, 2017). In 2017, about 425 million people were estimated to suffer from diabetes (Bennett, 2018). Around 90 % of them are assumed to be T2DM patients. Additionally, the number of undiagnosed cases is thought to reach almost 200 million and the disease prevalence is steadily rising globally (Chatterjee et al., 2017). These statistics emphasize that T2DM represents a major global health problem, particularly as it is associated with many pathologies, including heart disease, stroke and microvascular complications, such as blindness, kidney damage and peripheral neuropathy (Ashcroft and Rorsman, 2012). Thus, T2DM increases morbidity and

mortality, primarily due to cardiovascular disease (Inzucchi et al., 2012). Therefore, T2DM places a severe economic burden on societies (Seuring et al., 2015). Nowadays, good metabolic control in T2DM, meaning lowering blood glucose levels on the long term, can only be achiebed by a combination of changes in lifestyle, such as an appropriate diet, more physical exercise and body weight loss, and a pharmacological treatment (Marin-Penalver et al., 2016). However, in addition to developing a successful treatment regimen also discovering possibilities for curing or even preventing the disease is a major research task.

1.1.5 Lipodystrophy and obesity

1.1.5.1 Lipodystrophy

Lipodystrophy is a condition that is characterized by a partial or complete absence of AT, which can be acquired or emerge from a genetic defect (Asterholm et al., 2007; Fiorenza et al., 2011). The most common form of lipodystrophy is caused by antiretroviral therapy of human immunodeficiency virus (HIV) (Koutkia and Grinspoon, 2004). In contrast to lean individuals, in which the AT constitutes of healthy ‘empty’ adipocytes, in lipodystrophic patients the residual AT is highly abnormal and dysfunctional with varying adipocyte size (Huang-Doran et al., 2010).

AT inflammation

AT tissue inflammation has been found in patients with HIV-associated lipodystrophy and in lipodystrophic mice. However, it is still under debate whether AT inflammation is a cause of insulin resistance in lipodystrophy or if additional factors might contribute to the development of metabolic dysregulation (Herrero et al., 2010; Johnson et al., 2004; Lagathu et al., 2007).

Ectopic lipid deposition due to decreased TG storage capacity

Frequently, the decreased capacity to store TG in the AT in lipodystrophy results in high levels of circulating lipids that accumulate in ectopic organs, such as the liver, muscle or pancreas (Asterholm et al., 2007; Huang-Doran et al., 2010; Vegiopoulos et al., 2017).

Dysregulated adipokine secretion

Due to the absence or dysfunction of AT, circulating adipokine levels, such as of leptin and adiponectin, are reduced (Haque et al., 2002), which is consequently worsening the metabolic status. This is particularly devastating in the case of leptin as the deficiency of this hormone promotes hyperphagia and thus even further contributes to the increase in ectopic storage of lipids (Savage, 2009).

Lipodystrophy-associated metabolic disturbances

Reinforcing that AT is an endocrine organ regulating whole-body metabolic homeostasis; lipodystrophy is commonly associated with local and systemic inflammation, insulin resistance, hyperglycemia, dyslipidemia, hypertension or even T2DM (Asterholm et al., 2007; Vegiopoulos et al., 2017). One major cause for the metabolic dysregulations in lipodystrophy is the ectopic lipid accumulation triggered by the absence AT and the consequent spillover of lipids in the circulation (Asterholm et al., 2007; Huang-Doran et al., 2010; Vegiopoulos et al., 2017). As lipodystrophy displays almost the same metabolic outcomes as obesity, lipodystrophic mouse models represent a valuable tool to study not only the mechanisms underlying impaired accumulation of AT but also the excess of it and the contribution of these two opposing pathologies to metabolic dysfunction (Asterholm et al., 2007; Savage, 2009).

1.1.5.2 Obesity

As stated above, obesity results from a chronic imbalance between energy intake and expenditure. Genetic as well as environmental factors contribute to the development of this complex disease. It is well established that the excessive consumption of energy-rich food and reduced physical exercise in developed societies nowadays are major drivers of the rising obesity numbers (Speakman, 2004). Currently, obesity reaches epidemic proportions with nearly 712 million obese adults worldwide (Collaborators et al., 2017). The excess in bodyweight due to an overabundance of AT is implicated in many human health problems like T2DM, NAFLD, dyslipidemia, certain forms of cancer and cardiovascular diseases (Kopelman, 2000). Increasing rates of obesity and its associated metabolic disorders and the lack of efficient treatment options are major public health and economic burdens of our time (O'Neill and O'Driscoll, 2015). Lifestyle changes, such as dieting or exercise often do not result in sustainable weight loss (Dansinger et al., 2005; Leblanc et al., 2011) and anti-obesity medications, so far, cause serious side effects (Di Dalmazi et al., 2013). Bariatric surgery, the most efficient way to reduce obesity and its comorbidities, is mainly applied in morbidly obese patients due to the risk of surgical complications and the constant need for reoperation (Chang et al., 2014). Hence, understanding the mechanisms involved in obesity and the discovery of new anti-obesity drugs is a crucial research task worldwide.

Ectopic lipid deposition

One biological function of AT is to store lipids in periods of caloric surplus. In obesity, when the maximal storage capacity is reached or the capability for lipid storage is impaired, the spillover of lipids accumulates in other organs, such as liver or muscle (Hardy et al., 2012).

Obesity-associated AT inflammation and alterations in adipokine secretion

Obesity triggers the recruitment of various immune cells to the AT, including neutrophils, mast cells, lymphocytes and macrophages (Johnson and Olefsky, 2013). With proceeding obesity, the amount of AT macrophages increases and in particular rather in visceral than in subcutaneous fat depots (Cancello et al., 2005; Cinti et al., 2005; Harman-Boehm et al., 2007; Weisberg et al., 2003). Several factors contribute to the induction of AT inflammation and recruitment of immune cells. The environment of energy surplus and the failure to respond to it by adipocyte hyperplasia results in adipocyte hypertrophy (Arner et al., 2010). The expansion of adipocytes causes cellular stress, changing the adipokine secretion profile and promoting the release of pro-inflammatory cytokines, such as TNFα, or chemoattractants, like MCP1, thereby recruiting immune cells which in turn secrete even more cytokines and contribute to AT and systemic inflammation (Bluher, 2016). Furthermore, limited AT expandability and vascularization promotes hypoxia and consequently AT inflammation (Rutkowski et al., 2015). Ultimately, adipocyte hypertrophy is resulting in apoptosis, triggering the release of cellular components, further attracting immune cells to the AT (Bluher, 2016; Grant and Dixit, 2015). It is well established that macrophages cluster around apoptotic adipocytes in crown-like structures (Cinti et al., 2005). Moreover, obesity was reported to be partly responsible for the phenotype switch of the alternately activated M2 macrophages to the pro-inflammatory M1 macrophages (Fujisaka et al., 2009; Lumeng et al., 2007). A surge of total number of macrophages and a rise in the ratio of M1 to M2 macrophages constitutes a major sign of AT inflammation that is related to obesity and its associated metabolic disturbances (Reilly and Saltiel, 2017). In contrast to these findings referring to chronic AT inflammation, a more recent study indicated that acute inflammatory responses are required for AT remodeling and expansion, thus maintaining whole-body metabolic homeostasis and preventing chronic systemic inflammation (Wernstedt Asterholm et al., 2014). Additionally, AT inflammation might be essential for adaptive responses to energy surplus since it regulates angiogenesis in order to restrain hypoxia and induces insulin resistance to prevent exceeding energy accumulation in cells (Arner et al., 2011; Chung et al., 2006; Saltiel, 2012).

Obesity-associated insulin resistance

Various factors have been reported to contribute to the development of obesity-associated insulin resistance. Among them, altered lipid metabolism, including high levels of circulating lipids or deposition in ectopic organs, is known to cause systemic insulin resistance (Samuel and Shulman, 2012). AT inflammation in obesity might be responsible for chronic systemic inflammation that at least partially contributes to the development of obesity-related metabolic disorders (Bluher, 2016; Hotamisligil, 2006; Stolarczyk, 2017). In fact, obese patients that display an insulin resistance commonly show signs of AT inflammation, while

obese individuals with persisting insulin sensitivity do not demonstrate AT inflammation (Hardy et al., 2011; Kloting et al., 2010). Accordingly, improvements in insulin sensitivity and glucose tolerance by body weight reduction was found to be accompanied with decreased circulating inflammatory markers (Gumbau et al., 2014; Haffner et al., 2005; Oberbach et al., 2006).

AT is important for maintaining whole-body energy homeostasis, consequently AT dysregulation has devastating effects, such as metabolic impairments. AT dysfunction is reflected by an enhanced recruitment of immune cells to the AT, ectopic lipid accumulation, hypoxia, impaired autophagy and apoptosis and insulin resistance in adipocytes (Bluher, 2009, 2013). Paradoxically, the absence (lipodystrophy) as well as the overabundance (obesity) of AT are associated with AT inflammation, altered adipokine secretion, high circulating FA and TG levels, resulting in ectopic lipid deposition, leading together to systemic inflammation and finally insulin resistance (Asterholm et al., 2007; Savage, 2009; Vegiopoulos et al., 2017) (Figure 12).

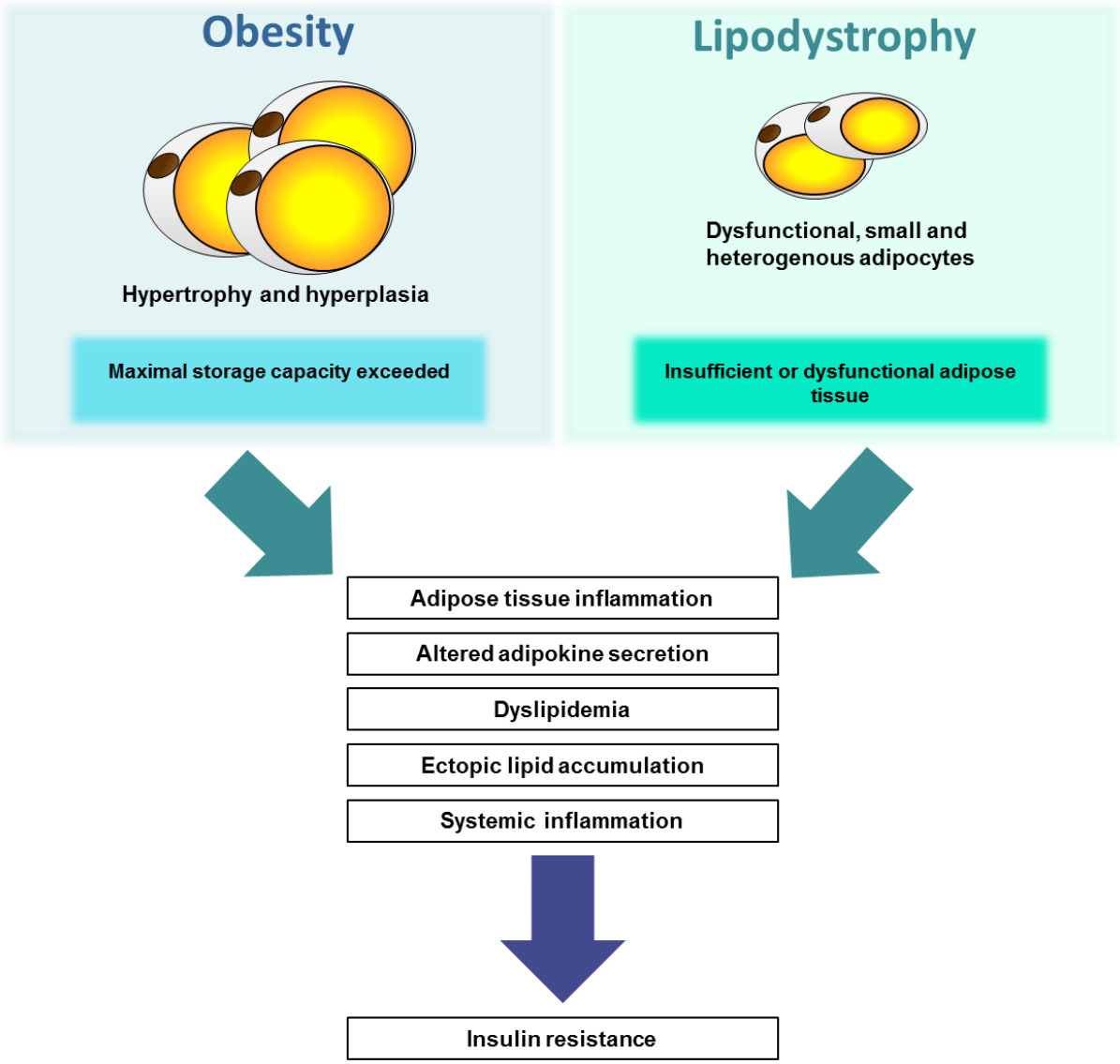

Figure 12 Obesity vs Lipodystrophy: Two opposing phenotypes with similar devastating metabolic outcomes. Schematic illustration showing the metabolic dysfunctions of these two pathologies associated with AT dysfunction. While in obesity, adipocyte hypertrophy and hyperplasia can only cope to a certain extend with the excess of lipids, either insufficient or dysfunctional AT in lipodystrophy cannot serve as a buffer for toxic lipids. Thus, both disorders results in AT inflammation and changes in the adipokine profile. The lipid overspill leads to dyslipidemia and subsequently ectopic lipid deposition and finally systemic inflammation. Consequently, both pathologies cause a systemic insulin resistance (adapted from Vegiopoulos et al., 2017).

1.2 Neddylation

The PTM neddylation is the conjugation of Neural precursor cell-expressed, developmentally downregulated 8 (Nedd8) to its target proteins (Enchev et al., 2015). The 76 amino acid polypeptide Nedd8 with a molecular weight of 8 kDa was originally identified in a cDNA library screen and was described to be developmentally-downregulated in the mouse brain (Kumar et al., 1992; Kumar et al., 1993). Nedd8 is one of the best-characterized ubiquitin-like proteins (UBLs) sharing a 60% identity and 80% homology with ubiquitin. Nedd8 is involved

in the development of various diseases, including cancer (Kumar et al., 1993; Watson et al., 2011).

1.2.1 Ubiquitin and UBL conjugation pathways

Ubiquitination, also known as ubiquitylation, is a PTM, whereby the small protein ubiquitin is covalently conjugated to target proteins via a tightly controlled three-step enzymatic cascade. Ubiquitination mediates various processes in eukaryotic cells by targeting proteins for proteasomal degradation or altering the function of target proteins (Hershko and Ciechanover, 1998). A variety of protein families was discovered that share mechanistic characteristics with the ubiquitination pathway. These proteins are referred to as UBLs, which encompass 17 distinct proteins, among them Nedd8, SUMO, ATG8, ATG12, URM1, UFM1, FAT10 and ISG15, to name the most prominent examples (Cappadocia and Lima, 2018).

Ubiquitin and many UBLs are expressed as inactive precursors that require proteolytic processing at the C-terminus, to expose a glycine (Gly) residue that serves as site for substrate conjugation. This process is catalyzed by specific proteases termed deubiquitinating enzymes (DUBs) in case of ubiquitin and UBLs-specific proteases (ULPs) in case of UBLs (Amerik and Hochstrasser, 2004). Subsequently, ubiquitin or UBLs must be activated by a specific ATP- dependent enzyme that is called E1 or E1-like enzyme (Haas et al., 1982). Afterwards, ubiquitin or UBLs are passed from the E1 to the E2 or E2-like enzyme, also termed Ub-conjugating or Ubl-conjugating enzyme. Finally, the C-terminal Gly residue of ubiquitin or UBLs is covalently linked to the ε-amino group of a lysine (K or Lys) in a substrate protein, a process catalyzed by a set of E3 protein ligases (Cappadocia and Lima, 2018). E2 enzymes display a structural overlap between E1 and E3 binding sites, resulting in mutually exclusive E1-E2 and E2-E3 interactions, thus ensuring the unidirectional progression of the sequential enzymatic cascade (Eletr et al., 2005; Huang et al., 2005).

Target proteins can be modified with a single molecule or with chains of ubiquitin or UBLs, dictating distinct functional outcomes. For instance, ubiquitin can itself be modified at one of its seven Lys, resulting in different types of polyubiquitin chains (Adhikari and Chen, 2009). K48-linked polyubiquitin chains, for example, are well-established to be involved in targeting proteins for degradation by the 26S proteasome (Chau et al., 1989; Thrower et al., 2000). In contrast, mono-, oligo-, or polyubiquitination via other ubiquitin Lys residues, like K63, mediates various cellular functions, like DNA repair, gene transcription, signal transduction, endocytosis or vesicular trafficking (Chan and Hill, 2001; Haglund et al., 2003; Hurley et al., 2006; Kirkin and Dikic, 2007; Mukhopadhyay and Riezman, 2007). Additionally, also

monoubiquitination has been recently associated with targeting proteins for proteasomal degradation (Braten et al., 2016). Moreover, it has been shown that ubiquitin can also be covalently attached to N-terminal α-amino groups either as a single molecule or in order to form linear polyubiquitin chains (Scaglione et al., 2013; Tatham et al., 2013; Tokunaga et al., 2009).

Four main classes of ubiquitin E3 ligases exist, that mediate the covalent conjugation of the modifier to target proteins: the really interesting new gene (RING) finger domain-containing type, the homologous to E6-AP carboxyl terminus (HECT) type, the U-box type and the plant homeodomain (PHD)-finger type (Nakayama and Nakayama, 2006). The largest family of RING E3s is the family of cullin RING ligases (CRLs), which are composed of a domain with a RING motif, a cullin scaffold protein and one or more cullin-specific subunits that are responsible for substrate recognition and adaptor functions. CRL activity is regulated by the covalent conjugation of cullin scaffold proteins with the UBL Nedd8 (Petroski and Deshaies, 2005), which will be discussed in more detail below. The ubiquitination cascade is depicted in Figure 13.

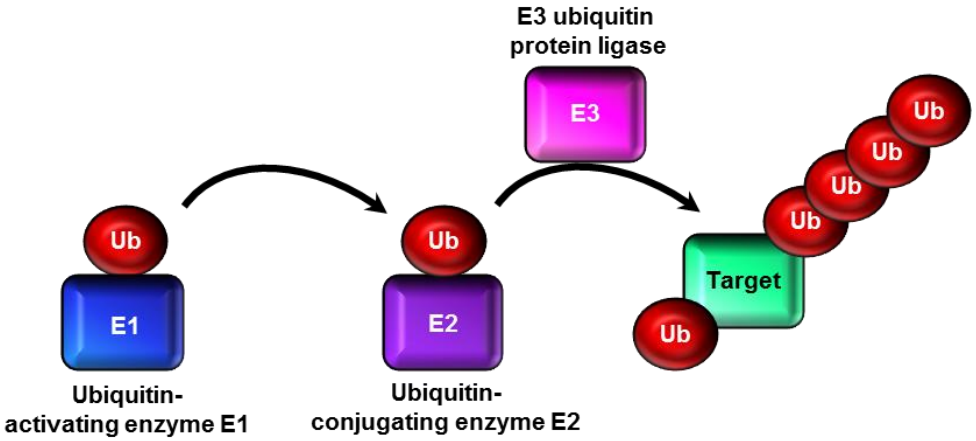

Figure 13: The ubiquitination pathway. Ubiquitination is a posttranslational protein modification whereby the small protein ubiquitin is covalently attached to target proteins via a three-step enzymatic cascade involving the ubiquitin-activating enzyme E1, the ubiquitin-conjugating enzyme E2 and the E3 ubiquitin protein ligase. Target proteins can be mono-ubiquitinated or poly-ubiquitinated, leading to different biological outcomes. Targeting proteins for proteasomal degradation represents the best-established ubiquitin function, but also, for instance, the localization, function or interaction with partner proteins can be changed upon ubiquitination.

1.2.2 The neddylation pathway

Similar to ubiquitin, the covalent conjugation of Nedd8 to substrates is mediated by a cascade, comprising the three successively acting enzymes E1, E2 and E3 (Gong and Yeh, 1999; Kamitani et al., 1997; Liakopoulos et al., 1998; Osaka et al., 1998; Yeh et al., 2000). Analogous to ubiquitin, Nedd8 is synthesized as an 81-amino acid precursor protein that is subsequently cleaved to expose its C-terminal Gly76 residue, its site for substrate

recognition. This process is catalyzed by deneddylating enzymes, such as NEDP1 (also known as SENP8 or DEN1) or UCH-L3 (Kamitani et al., 1997; Mendoza et al., 2003; Wada et al., 1998). After exposing the C-terminal attachment site, Nedd8 is adenylated in an ATP-dependent reaction by the heterodimeric E1 Nedd8-activating enzyme (NAE), comprising the subunits Nae1, also called Appbp1, and ubiquitin-activating enzyme 3 (Uba3). Nedd8 is then transferred to an Uba3 cysteine side chain via thiolester linkage (Gong and Yeh, 1999), followed by the transfer of the activated Nedd8 to the E2 Nedd8-conjugating enzymes Ubc12, also known as Ube2m, or Ube2f, forming another thiolester linkage (Gong and Yeh, 1999). Notably, Ube2f has been demonstrated to mediate solely the conjugation of Nedd8 to cullin 5 (Huang et al., 2009). A set of E3 ligases finally mediates the transfer of Nedd8 to the ε-amino group of Lys residues of target proteins (Enchev et al., 2015) (Figure 14). Until now, only approximately 10 different Nedd8 E3 ligases have been identified, of which the majority consists of the RING domain structure and also can serve as ubiquitin E3 ligase (Zhao et al., 2014; Zhou et al., 2018). Among them the RING-box proteins Rbx1 and Rbx2, also known as ROC1/2, are the most prominent ones that are responsible for the neddylation and ubiquitination of cullin substrates (Huang et al., 2009; Kamura et al., 1999; Morimoto et al., 2003). DCN1 also catalyzes the neddylation of cullin proteins in yeast and *C. elegans* (Kurz et al., 2005). Mouse double minute 2 homolog (Mdm2) neddylates and ubiquitinates p53 and itself (Bottger et al., 1997; Haupt et al., 1997; Kubbutat et al., 1997; Xirodimas et al., 2004).

Until now, not much knowledge has been generated on the possible types and functions of Nedd8 chains. It was reported that Lys11, Lys22, Lys27, Lys33, Lys48, Lys54 and Lys60 can be conjugated in order to form Nedd8 chains (Jeram et al., 2010; Jones et al., 2008; Xirodimas et al., 2008). Moreover, evidence suggests that Nedd8 can form mixed chains with ubiquitin and other UBLs (Jones et al., 2008; Swatek and Komander, 2016; Xirodimas et al., 2008) and can function as terminator of the mixed modifier chain (Singh et al., 2012).
Like ubiquitin, Nedd8 can be de-conjugated from target proteins by de-neddylating enzymes, among them the constitutive photomorphogenesis 9 (COP9) signalosome (CSN) is the most-extensively studied one, which is removing Nedd8 from cullins. CSN consists of 8 subunits, of which CSN5 was characterized to be the catalytic one (Cope et al., 2002; Lyapina et al., 2001; Schwechheimer et al., 2001). In addition to its role in the proteolytic processing of the Nedd8 precursor, Nedp1 has also been described to be involved in de-neddylating primarily non-cullin targets and hyper-neddylated cullins (Chan et al., 2008; Mergner et al., 2015; Wu et al., 2003).

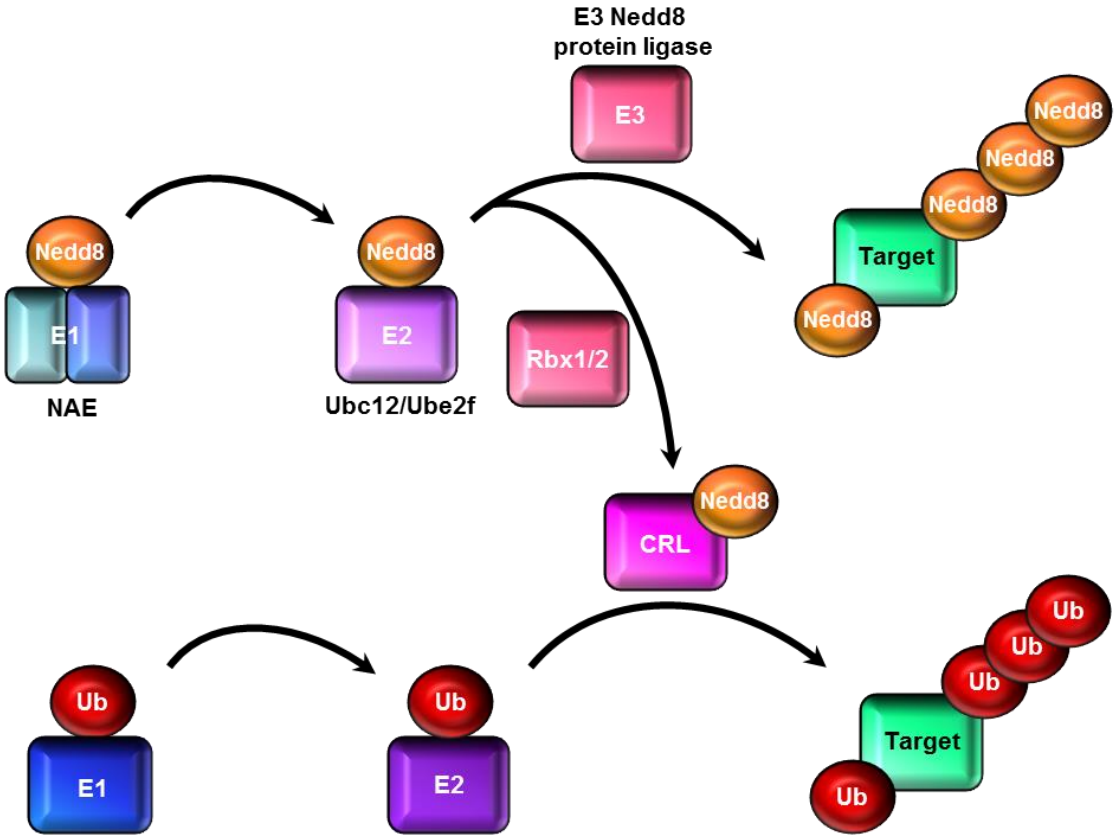

Figure 14: Interaction of the Nedd8 conjugation pathway with the ubiquitination pathway. Like ubiquitin, Nedd8 is covalently attached to substrate proteins via an enzymatic cascade, comprising the heterodimeric Nedd8-activating enzyme 1 NAE, the Nedd8 conjugating enzymes Ubc12 or Ube2f and the E3 Nedd8 protein ligase. Neddylation controls ubiquitination by modifying cullin proteins, scaffold proteins of the CRL of the ubiquitination pathway, and thereby fine-tuning their function. Rbx1/2 represent the most prominent E3 ligases mediating cullin neddylation. In summary, neddylation regulates ubiquitination and is thus involved in cell cycle control. In recent years, many Nedd8 targets have been identified unraveling new roles of neddylation beyond its crosstalk with the ubiquitination pathway.

1.2.3 Neddylation: substrates, biological functions and involvement in pathologies

Neddylation of target proteins conveys the regulation of various cellular functions, such as transcriptional regulation, signal transduction and cell cycle control and thus plays important roles under physiological conditions and in disease (Enchev et al., 2015). Neddylation of various substrates has been discovered to be involved in the development of cancer (Soucy et al., 2010). The best characterized targets of neddylation are the cullins, a family of structurally related proteins, comprising cullin1, 2, 3, 4A, 4B, 5 and 7, PARC and Apc2, which are functioning as molecular scaffolds of CRLs (Pan et al., 2004; Petroski and Deshaies, 2005; Watson et al., 2011) (summarized in Table 1). The conjugation of Nedd8 to cullin scaffold proteins is essential for the enzymatic function of CRLs, which target cellular proteins for proteasomal degradation. Thus, one function of the neddylation cascade is the regulation of the ubiquitination rate and the subsequent degradation of the proteins whose

ubiquitination is dependent on the CRL activity (Boh et al., 2011; Merlet et al., 2009; Saha and Deshaies, 2008). By controlling the stability of various cellular proteins, CRLs are involved in the regulation of cell signaling, cell cycle progression, DNA damage repair and other signaling pathways (Brown and Jackson, 2015; Sarikas et al., 2011). Thus dysregulated cullin neddylation has been implicated in cancer (Soucy et al., 2010). Moreover, up-regulation of Nedd8 pathway enzymes, like NAE and Ubc12, has been associated with several cancer types, such as lung cancer, liver cancer, colorectal cancer, intrahepatic cholangiocarcinoma, nasopharyngeal carcinoma and esophageal squamous cell carcinoma (Barbier-Torres et al., 2015; Chen et al., 2016; Gao et al., 2014; Hua et al., 2015; Li et al., 2014; Xie et al., 2017; Xie et al., 2014). Despite its most prominent role in cell cycle control and cancer, additional cellular functions and pathologies regulated by Nedd8 conjugation, are just beginning to be explored. Our group lately identified the role of neddylation in mature synapses and in synaptogenesis during neuronal development. In more detail, neddylation of the scaffolding protein PSD-95 is essential for the maturation, stability and function of dendritic spines (Vogl et al., 2015). There is increasing evidence that neddylation might be deregulated in obesity and metabolism (Dubiel et al., 2017; Park et al., 2016), as discussed below. In a recent study, dysregulated neddylation was reported to have an impact on liver fibrosis. Increased Nedd8 expression was found in humans as well as in two mouse models of liver fibrosis. Importantly, neddylation inhibition strongly reduced hepatocyte death, inflammation and hepatic fibrosis (Zubiete-Franco et al., 2017). In recent years many targets of neddylation have been identified. These Nedd8 substrates are summarized in Table 1.

Table 1: Nedd8 targets as well as their functions and implications in pathologies

Substrates	Function	Pathology	References
APP intracellular domain (AICD)	AICD neddylation inhibits its transcriptional activity	Not described	(Lee et al., 2008)
Breast cancer-associated protein 3 (BCA3)	BCA3 neddylation suppresses NFκB-dependent transcription	Not described	(Gao et al., 2006)
BRCA1-associated protein 2 (BRAP2)	Neddylation of BRAP2 inhibits NFκB nuclear translocation	Not described	(Takashima et al., 2013)
Cullins: Cullin1, 2, 3, 4A, 4B, 5 and 7, PARC and Apc2	Best-characterized Nedd8 targets. Cullins are molecular scaffolds of CRLs. Neddylation of cullins regulates CRL activity and thus controls ubiquitination and consequently proteasomal degradation	Dysregulated cullin neddylation is implicated in cancer	(Boh et al., 2011; Brown and Jackson, 2015; Merlet et al., 2009; Pan et al., 2004; Petroski and Deshaies, 2005; Saha and Deshaies, 2008; Sarikas et al., 2011; Soucy et al., 2010; Watson et al., 2011)

E2F transcription factors	Neddylation controls the transcriptional activity of E2Fs, transcription factors that regulate cell cycle progression	Nedd8 conjugation to E2Fs promotes their pro-apoptotic activity and thus could have implications in cancer	(Aoki et al., 2013; Loftus et al., 2012)
Epidermal growth factor receptor (EGFR)	Neddylation of EGFR results in increased ubiquitination followed by endocytic internalization	Not described	(Marmor and Yarden, 2004; Oved et al., 2006)
ICE	Effector caspase. Nedd8 conjugation to ICE abrogates its activity to cleave its substrate PARP1 in *D. melanogaster* and thus has an anti-apoptotic activity	Not described	(Broemer et al., 2010)
HIF1α/HIF2α	Nedd8 regulates HIF1α protein stability	Not described	(Ryu et al., 2011)
Histone H4	Poly-neddylation on histone H4 and consecutive ubiquitination amplifies the signal for the DNA damage response cascade	Not described	(Ma et al., 2013)
Hu antigen R (HuR)	HuR is overexpressed in certain cancer types. Nedd8 conjugation stabilizes HuR	By regulating HuR stability neddylation is involved in liver and colon cancer	(Abdelmohsen and Gorospe, 2010; Embade et al., 2012)
L11	The ribosomal protein L11 is neddylated by Mdm2, thereby protecting L11 from degradation and stabilizing p53 during nucleolar stress	Not described	(Sundqvist et al., 2009)
Mdm2	The E3 ligase Mdm2 displays an auto-ubiquitination and auto-neddylation activity. Mdm2 neddylation stabilizes the protein. Mdm2 is able to catalyze the conjugation of Nedd8 to the tumor suppressor proteins p53 and p73, thereby inhibiting their transcriptional activity	Cancer	(Watson et al., 2006; Watson et al., 2010; Xirodimas et al., 2004)
NEMO	Subunit of the IκB kinase that activates NFκB signaling. Neddylation of NEMO inhibits NFκB signaling	Not described	(Noguchi et al., 2011)

p53	See Mdm2		
p73	See Mdm2		
Parkin and PINK1	Nedd8 conjugation to parkin and PINK1 leads to increased E3 ligase activity of parkin and stabilization of PINK1	Parkin was shown to be neddylated on multiple Lys residues in patients suffering from Parkinson's disease (PD)	(Choo et al., 2012)
PPARγ	PPARγ neddylation stabilizes the protein by preventing its ubiquitination. Thereby, neddylation has a role in adipogenesis and obesity	Obesity	(Park et al., 2016)
PSD-95	Nedd8 conjugation to PSD-95 controls its localization to dendritic spines. Thus, neddylation is required for the maturation, stability and function of spines	Not described	(Vogl et al., 2015)
SMAD-specific E3 ubiquitin-protein ligase 1 (SMURF1)	The HECT-domain ubiquitin E3 ligase SMURF1 displays an auto-neddylation activity. Neddylation of SMURF1 increases its ubiquitin E3-ligase activity	Cancer	(Xie et al., 2014)
Tyr kinase transforming growth factor-β type II receptor (TGFβRII)	Nedd8 conjugation to TGFβRII stabilizes and prolongs its signaling by promoting its endocytosis	TGFβRII neddylation might be implicated in leukemia	(Zuo et al., 2013)
von Hippel-Lindau disease tumor suppressor (VHL)	Neddylated VHL promotes fibronectin matrix assembly	Neddylation of VHL is required for the assembly of the fibronectin matrix and to prevent tumorigenesis	(Stickle et al., 2004)

1.2.4 The NAE Inhibitor MLN4924

The ubiquitin-proteasome system (UPS) is responsible for the controlled degradation of intracellular proteins which play important roles in various cellular functions. As discussed above, dysregulation of the UPS can result in the development of cancer and other diseases. CRLs are important control points of the UPS and the up-regulation of CRL activity is implicated in various types of cancer. The Nedd8 conjugation cascade, which leads to the neddylation of CRLs, is therefore supposed to have a critical regulatory role in the UPS (Soucy et al., 2009). The potent and selective NAE inhibitor MLN4924 (Pevonedistat),

developed by Millenium Pharmaceuticals, is able to block the activity of NAE. The MLN4924 molecule resembles the structure of adenosine 5'-monophosphate (AMP), which is an intermediate formed by NAE (Soucy et al., 2009). The inhibitor is able to inhibit NAE by forming a covalent NEDD8-MLN4924 adduct in the NAE active site, which cannot be utilized for further enzymatic reactions and thus inhibits the neddylation pathway (Brownell et al., 2010). Consequently, MLN4924 inhibits the turnover of many CRL substrates resulting in CRL substrate accumulation and DNA damage (Soucy et al., 2010). Thereby, MLN4924 induces cell death pathways in various cancer cell models (Brownell et al., 2010; Jia et al., 2011; Luo et al., 2012; Pan et al., 2012; Soucy et al., 2009). The drug is currently in clinical trials for the treatment of distinct cancer types (Sarantopoulos et al., 2016; Shah et al., 2016; Swords et al., 2018; Swords et al., 2017).

1.3 Posttranslational modifications in adipocyte biology

Although in the last years the role of certain PTMs, mainly phosphorylation and acetylation, of key players in fat development has been analyzed, not much knowledge has been generated regarding the function of other PTMs in the context of adipogenesis and adipocyte cell fate. Unravelling the role of PTMs in the molecular mechanisms driving adipogenesis and fat storage offers a new therapeutic potential to treat obesity and its associated comorbidities. In this framework PTMs play a pivotal role as they orchestrate differentiation programs and cellular functions by controlling stability, function, localization, partner interactions, etc. PTMs, such as phosphorylation, acetylation, glycosylation, methylation, ubiquitination or sumoylation control, amongst others, transcription factor function and enable the access of RNA polymerases to promoter sites (Filtz et al., 2014). MS-based quantitative proteomics nowadays allows the characterization of the proteome and its modifiers in a high-throughput manner. Several studies using this approach demonstrated that in 3T3-L1 cells the phosphoproteome changes upon stimulation with adipogenic inducers (Humphrey et al., 2013; Rabiee et al., 2017; Wu et al., 2009). These studies revealed that in general phosphorylation is involved in transmitting cellular signals. Within the first 4 hours of adipogenesis mainly already expressed proteins get phosphorylated, e.g. cell membrane receptors. These signals are then subsequently propagated and amplified via molecular networks involving protein interaction and modification. Finally, this is resulting in the phosphorylation of proteins positively or negatively regulating gene expression, RNA splicing and RNA processing (Rabiee et al., 2017; Wu et al., 2009). Furthermore, acetylation of the ε-amino group of lysine residues in proteins has emerged as a key posttranslational modification regulating adipocyte differentiation as adipogenesis induction triggers an overall and sequential change in protein acetylation (Xu et al., 2013).

1.3.1 Posttranslational modifications of key adipocyte transcription factors: PPARγ, C/EBPα and C/EBPβ

PTMs control various cellular processes and developmental programs, including adipogenesis. In recent years, more research has taken into account the relevance of the posttranslational control of adipocyte development and fat formation, therefore also the role of ubiquitin and UBLs, such as SUMO or Nedd8, is beginning to be explored. The transcription factors C/EBPβ, C/EBPα and PPARγ act together in order to activate adipocyte-specific gene expression (Lefterova et al., 2008). The function of these factors is tightly regulated by PTMs, as summarized in Table 2.

Table 2: PTMs of key adipogenic transcription factors

Transcription factor	PTM	Function of PTM	Model	References
PPARγ	Phosphorylation on Ser112	Decreases PPARγ transcriptional activity	JEG-3 cells	(Adams et al., 1997)
			NIH 3T3 cells	(Camp and Tafuri, 1997)
			Rat-IR cells	(Hu et al., 1996)
		Prevention of PPARγ phosphorylation protects mice from diet induced insulin resistance	Whole-body PPARγ2 Ser112 mutant mice	(Rangwala et al., 2003)
	Ubiquitination	Proteasomal degradation	NIH 3T3 cells	(Floyd and Stephens, 2002)
			NIH 3T3 cells	(Hauser et al., 2000)
			NIH 3T3 cells	(Kilroy et al., 2009)
			3T3-L1 cells	(Kilroy et al., 2012)
			H1299 cells, 3T3-L1 cells	(Kim et al., 2014)
	SUMOylation	Decreases PPARγ transcriptional activity	COS-7 cells	(Chung et al., 2011)
			NIH 3T3 cells	(Ohshima et al., 2004)
			HeLa cells	(Yamashita et al., 2004)
		KO of SUMOylation in MEFs decreases PPARγ transcriptional targets and prevents high fat diet (HFD)-induced body weight gain	Whole-body SUMO1 KO mice	(Mikkonen et al., 2013)

	Neddylation	Stabilizes the protein by preventing its ubiquitination. Role of neddylation in adipogenesis and obesity	HEK293 cells 3T3-L1 cells, human AT-derived stem cells, mice injected with MLN4924	(Park et al., 2016)
C/EBPα	Phosphorylation on Ser21	Regulates GLUT4 expression in adipocytes, required for maintaining whole-body glucose homeostasis	NIH 3T3 cells, C/EBPα$^{-/-}$ MEFs, Whole-body C/EBPα Ser21 mutant mice	(Cha et al., 2008)
	Ubiquitination	Not described		
	SUMOylation	Role in lung differentiation	Lungs from Sprague-Dawley rats	(Chen et al., 2017)
		Hepatocyte differentiation	Rat hepatocytes	(Sato et al., 2006)
		Hematopoietic stem/progenitor cell development	Zebrafish	(Yuan et al., 2015)
C/EBPβ	Phosphorylation on Thr188	After around 4 h after adipogenic stimulation phosphorylation of Thr188 "primes" C/EBPβ for the following phosphorylation on Ser184 and Thr179	3T3-L1 cells	(Kim et al., 2007a; Li et al., 2007; Tang et al., 2005; Zhang et al., 2012)
		Enhances C/EBPβ protein stability		
	Phosphorylation on Ser184 and Thr179	Induces a conformational change that facilitates dimerization through its leucine zipper domain which enables the accessibility of the adjacent basic regions to the C/EBP regulatory element		
	Acetylation at multiple sites		293T cells, 3T3-F442A cells	(Cesena et al., 2007)
			3T3-L1 cells, NIH 3T3 cells	(Wiper-Bergeron et al., 2007)
	Acetylation on K39	Promotes C/EBPβ transcriptional	CHO-GHR cells	(Cesena et al., 2007)

		activity on C/EBPα and PPARγ promoters	293T cells, CHO-GHR cells	(Cesena et al., 2008)
	Ubiquitination	In macrophages ubiquitination activates C/EBPβ and promotes M2 macrophage polarization	Macrophages from C57Bl6 mice	(Ye et al., 2012)
		In myoblasts ubiquitin modification targets C/EBPβ for proteasomal degradation and promotes myogenesis	C2C12 cells	(Fu et al., 2015)
	SUMOylation on Lys133	Increases ubiquitination and decreases protein stability and transcriptional activity and inhibits adipogenesis	3T3-L1 cells, COS-7 cells	(Chung et al., 2010)
			3T3-L1 cells	(Liu et al., 2013)
	Poly(ADP-ribosyl)ation (PARylation)	Inhibits DNA binding and transcriptional activity	3T3-L1 cells	(Luo et al., 2017)

1.3.2 Neddylation in adipocyte development, function and obesity

There is emerging evidence that neddylation might play a role in adipocytes. Several studies indicated that CSN- and CAND1-dependent modification of CRL is crucial for adipogenesis (Dubiel et al., 2013; Dubiel et al., 2015; Huang et al., 2012). Although these studies showed a role for CRL activity in adipogenesis, they did not address the role of neddylation-mediated modification of CRL function. A more recent study demonstrated that neddylation of membrane-bound Cul3 is essential for adipocyte differentiation of LiSa-2 cells (Dubiel et al., 2017). So far, almost all potential roles of neddylation in adipocyte biology were described to be dependent on cullin or CRL function. However, during the course of this study, Park et al. described for the first time a non-cullin dependent function of neddylation in adipocytes. The authors reported that neddylation of PPARγ is required for adipogenesis. Moreover, neddylation inhibition protected mice from body weight gain and glucose intolerance during obesity induction (Park et al., 2016). Despite the growing evidence for the involvement of neddylation in adipocyte function, the molecular mechanisms mediating Nedd8 effects on adipocytes and the role of neddylation in obese mice are still largely unexplored and Nedd8 targets that govern these processes remain to be identified.

2 Rationale and thesis objectives

Neddylation is a posttranslational protein modification controlled by a multistep enzymatic cascade. It is considered to have an important role in cell cycle progression and cancer, regulation of cell signaling and developmental programming processes. However, the role of Nedd8 conjugation in nonreplicating postmitotic cells remains almost unexplored. Particularly, its biological relevance in adipocyte physiology is largely unknown. Thus, this study aimed to delineate the role of neddylation in adipocyte biology and obesity. Within this framework, the objectives of this study were:

1. to investigate the expression of neddylation pathway proteins during 3T3-L1 adipocyte differentiation

2. to identify the role of neddylation in adipocyte differentiation and fat storage by inhibiting the Nedd8 conjugation pathway by different means in adipocyte cellular models

3. to characterize the molecular pathways involved in the effects of neddylation inhibition on adipogenesis and fat storage

4. to explore the *in vivo* role of neddylation in obesity and metabolism

    - by studying the expression of Nedd8 proteins in AT from lean and HFD-induced obese mice

    - by characterizing a conditional adipocyte-specific knock-out (KO) mouse model (*Nae1Adipo*CreER^{T2} mice), in which Nae1, the subunit of the E1 enzyme of the pathway, is ablated in the AT concomitantly during the induction of obesity and in already obese mice

    - by investigating the effects of peripheral global neddylation inhibition by subcutaneous MLN4924 injections in already obese mice

3 Materials and Methods

3.1 Consumables, plasmids, antibodies, primers and solutions

Following commercially available cell lines were used in this project:

Table 3: Commercially available cell lines

Cell line	Supplier
3T3-L1 cells	ATCC
HEK293 cells	ATCC

The following reagents were used in this study:

Table 4: Kits and reagents

Kits and reagents	Supplier
Acrylamide/Bis–acrylamide 30% solution	Sigma-Aldrich
Adiponectin ELISA Kit mouse	Crystal Chem Inc.
Agar-Agar	Merck
Agarose	Carl Roth
Amaxa® Cell Line Nucleofector® Kit L (VCA-1005)	Lonza
Amaxa® Cell Line Nucleofector® Kit V (VCA-1003)	Lonza
Ampicillin	Sigma-Aldrich
Ammonium chloride	Merck
Ammonium persulfate	Sigma-Aldrich
β-Mercaptoethanol	Sigma-Aldrich
Beetle-Juice Luciferase assay Firefly	PJK
Benzoic acid	Sigma-Aldrich
Biorad Protein Assay	Biorad
Biotin	Sigma-Aldrich
Bovine Serum	Gibco
Bovine Serum Albumin (BSA)	Carl Roth
cAMP [^{125}I] Radioimmunoassay Kit	PerkinElmer
Chloroform	Merck
Collagenase Type IV	Life Technologies
Cycloheximide	Sigma-Aldrich

DAPI	Vector Laboratories
Dexamethasone	Sigma-Aldrich
Dimethyl sulfoxide (DMSO)	Sigma-Aldrich
dNTPs	Invitrogen
Dulbecco's modified Eagle medium (DMEM)	Gibco
DMEM/F12 + GLUTAMAX	Gibco
Dynabeads Protein G	Invitrogen
EDTA	Merck
Enzychrom Glucose Assay Kit	BioAssay Systems
Enzychrom Triglyceride Assay Kit	BioAssay Systems
Ethanol (different concentrations)	Merck
Ethidium Bromide	Carl Roth
Fetal calf serum (FCS)	Gibco
Formaldehyde	Sigma-Aldrich
Forskolin	Sigma-Aldrich
Glucose	Carl Roth
Glycerol	Sigma-Aldrich
Glycin	Carl Roth
High-fat diet D12451	Research Diets
HiSpeed Maxi Kit	Qiagen
Hydrogen Chloride (HCl)	Merck
2-hydroxypropyl-beta-cyclodextrin (HPBCD)	ONBIO
Immobilon	Millipore
Insulin	Sigma-Aldrich
Insulin ELISA Kit Ultra sensitive mouse	Crystal Chem Inc.
3-Isobutyl-1-methylxanthine (IBMX)	Sigma-Aldrich
Isopropanol	Merck
Isoproterenol	Sigma-Aldrich
Leptin ELISA Kit mouse	Crystal Chem Inc.
L-Glutamine	Biochrom
Lipofectamine2000	Invitrogen
Lipolysis Assay Kit for 3T3-L1 cells	Zenbio
Mayer's Hematoxylin Solution	Sigma-Aldrich
Methanol	Sigma-Aldrich
MLN4924 (Pevonedistat)	Activebiochem

MG132	Calbiochem
$MgCl_2$	Invitrogen
NEFA-HR(2) Kit	Wako
N-ethylmaleimide (NEM)	Sigma-Aldrich
NP-40	Sigma-Aldrich
Oil red O	Sigma-Aldrich
One Shot™ TOP10 Chemically Competent *E. coli*	Invitrogen
OptiMEM	Invitrogen
1,10-orthophenathroline (OPT)	Sigma-Aldrich
PageRuler™ Prestained Protein Ladder	Fermentas GmbH
Paraformaldehyde	Carl Roth
Paraplast	Carl Roth
Pierce™ Streptavidin Magnetic beads	ThermoFisher Scientific
Penicillin + Streptavidine mix	Biochrom AG
Phosphatase inhibitor cocktail	Roche
Poly-D-lysine	Sigma-Aldrich
PonceauS solution	Sigma-Aldrich
Potassium hydroxide (KOH)	Merck
Potassium hydrogen carbonate ($KHCO_3$)	Merck
Protease inhibitor cocktail	Sigma-Aldrich
Proteinase K	Sigma-Aldrich
Pfu DNA Polymerase	ThermoFisher Scientific
PVDF membrane	Millipore
QIAprep Spin Miniprep Kit	Qiagen
QIAquick PCR Purification Kit	Qiagen
QIAquick Gel Extraction Kit	Qiagen
QuantiFast SYBR Green RT-PCR Kit	Qiagen
QuantiTect Reverse Transcription Kit	Qiagen
Restriction enzymes	New England Biolabs
RNase A	Sigma-Aldrich
RNase free water	Qiagen
Roti-Load	Carl Roth
Roti-Histokitt	Carl Roth
SERVA gradient (4-20 %) gels	SERVA
Skimmed Milk Powder	Carl Roth

Sodium Chloride (NaCl)	Carl Roth
Sodium deoxycholate	Merck
Sodium dodecyl sulphate (SDS)	Merck
Sodium hydroxide (NaOH)	Sigma-Aldrich
Sodium pyruvate (100×)	Gibco
Sunflower seed oil	Sigma-Aldrich
Tamoxifen	Sigma-Aldrich
Tamoxifen food pellets LAS CRdiet CreActive TAM400	LASvendi
Taq DNA Polymerase	Invitrogen
TEMED	Carl Roth
Trichloroacetic acid	Carl Roth
Tris-HCl	Carl Roth
Triton X-100	Carl Roth
TRIzol	Invitrogen
Trypan Blue	Gibco
Trypsin/EDTA	Gibco
Tween 20	Sigma-Aldrich
VECTASTAIN Elite ABC HRP Kit (Peroxidase, Standard)	Vector Laboratories
Xylol	Carl Roth
Yeast extract	Carl Roth

Following plasmids were used in this project:

Table 5: Plasmids

Plasmid	**Source**
pcDNA3.1(-) mouse C/EBPβ LAP	Peter Johnson (unpublished) Addgene Plasmid #12557
pcDNA3.1(-) 1xFLAG-tagged mouse C/EBPβ LAP	cloned
pcDNA3.1(-) 6xHis-BIO-tagged mouse C/EBPβ	cloned
pcDNA3.1(-) 6xHis-BIO-tagged mouse C/EBPβmut LAP	Genesynthesis (BioCat)
pcDNA3.1(+) 3xFLAG-tagged mouse Nedd8	Vogl et al., 2015
pcDNA3.1(+) 6xHis-BIO-tagged mouse Nedd8	Vogl et al., 2015
pcDNA3.1(+) mouse Ubc12-C111S	Yosef Yarden

pcDNA3.1 myc-His A FLAG-tagged mouse PPARγ	Spiegelman, 2000 Addgene Plasmid #8895
pGL3 PPARγ 1.0kb promoter-Luc	Teddy T.C.Yang, 2002
pGL C/EBPα-luc	Zao Yue
mMTV–Luc	Paez-Pereda
pmaxGFP® Vector	Lonza (Vector as part of Cat#VCA-1005)

Following antibodies were used in this study:

Table 6: Antibodies

Antibody	**Supplier**
Rabbit polyclonal anti-β-actin	Cell Signaling, Cat#4967
Mouse monoclonal anti-β-actin (clone C4)	Millipore, Cat#MAB1501
Rabbit monoclonal anti-Akt	Cell Signaling, Cat#4691
Rabbit polyclonal anti-Phospho-Akt (Ser473)	Cell Signaling, Cat#9271
Rabbit polyclonal anti-C/EBPα	Cell Signaling, Cat#2295
Rabbit polyclonal anti-C/EBPβ (LAP)	Cell Signaling, Cat#3087
Rabbit polyclonal anti-C/EBP (C-19)	Santa Cruz, Cat#sc-150
Mouse monoclonal anti-Creb (86B10)	Cell Signaling, Cat#9104
Rabbit polyclonal anti-Phospho-Creb (Ser133)	Cell Signaling, Cat#9191S
Rabbit polyclonal anti-Erk1/2	Cell Signaling, Cat#9102
Rabbit polyclonal anti-Phospho-Erk1/2 (Thr202/Tyr204)	Cell Signaling, Cat#9101
Rabbit polyclonal anti-Nae1	Novus Biologicals, Cat#NBP1-92163
Rabbit monoclonal anti-Nedd8 (Y297)	Genetex, Cat#GTX61205
Rabbit monoclonal anti-Nedd8 (Y297)	Abcam, Cat#ab81264
Normal rabbit IgG	Santa Cruz, Cat#sc-2027
Mouse monoclonal anti-FLAG® M2	Sigma-Aldrich, Cat#F3165
Streptavidin-HRP	Cell Signaling, Cat#3999
Mouse monoclonal anti-PPARγ (E-8)	Santa Cruz, Cat#sc-7273
Rabbit polyclonal anti-Ubc12	Lifespan BioSciences, Cat#LS-B432
Rabbit polyclonal anti-UCP1	Abcam, Cat#ab10983
Chicken polyclonal anti-GFP	Abcam, Cat#ab13970
Mouse monoclonal anti-TFIIB (2F6A3H4)	Cell Signaling, Cat#4169
Goat anti-chicken IgG antibody	Molecular Probes, Cat#A11039
Goat anti-rabbit IgG, HRP-linked antibody	Cell Signaling, Cat#7074

Horse anti-mouse IgG, HRP-linked antibody	Cell Signaling, Cat#7076
Biotinylated goat anti-rabbit secondary antibody	Vector Laboratories, Cat#BA-1000

Following primers were used for qRT-PCR:

Table 7: Primers used for qRT-PCR

Name	**sequence 5' - 3'**
mACC1_f	GCG TCG GGT AGA TCC AGT T
mACC1_r	CTC AGT GGG GCT TAG CTC TG
mACO_f	GCA CCA TTG CCA TTC GAT ACA
mACO_r	CCA CTG CTG TGA GAA TAG CCG T
mActin_f	CGG TTC CGA TGC CCT GAG GCTCTT
mActin_r	CGT CAC ACT TCA TGA TGG AAT TGA
mAdiponectin_f	GGA GAG AAA GGA GAT GCA GGT
mAdiponectin_r	CTT TCC TGC CAG GGG TTC
mCD36_f	TTC ACG GGC GTC CAG AA
mCD36_r	GAT CTT GCT GAG TCC GTT CCA
mC/EBPα_f	AAA CAA CGC AAC GTG GAG A
mC/EBPα_r	GCG GTC ATT GTC ACT GGT C
mC/EBPβ_f	TGA TGC AAT CCG GAT CAA
mC/EBPβ_r	CAC GTG TGT TGC GTC AGT C
mCidea_f	AAA CCA TGA CCG AAG TAG CC
mCidea_r	AGG CCA GTT GTG ATG ACT AAG AC
mCox7a1_f	CGA AGA GGG GAG GTG ACT C
mCox7a1_r	AGC CTG GGA GAC CCG TAG
mCox8b_f	CCA GCC AAA ACT CCC ACT T
mCox8b_r	GAA CCA TGA AGC CAA CGA C
mCPT1a_f	TCC ATG CAT ACC AAA GTG GA
mCPT1a_r	TGG TAG GAG AGA GCA GCA CCT T
mCPT1b_f	CTG TTA GGC CTC AAC ACC GAA C
mCPT1b_r	CTG TCA TGG CTA GGC TGT ACA T
mCytc_f	GCA AGC ATA AGA CTG GAC CAA A
mCytc_r	TTG TTG GCA TCT GTG TAA GAG AAT C
mElovl3_f	TTC TCA CGC GGG TTA AAA ATG G

mElovl3_r	GAG CAA CAG CTA GAC GAC CAC
mF4/80_f	CTT TGG CTA TGG GCT TCC AGT C
mF4/80_r	GCA AGG AGG ACA GAG TTT ATC GTG
mFABP4_f	AAG AGA AAA CGA GAT GGT GAC AA
mFABP4_r	CTT GTG GAA GTC ACG CCT TT
mFAS_f	GCT GCT GTT GGA AGT CAG C
mFAS_r	AGT GTT CGT TCC TCG GAG TG
mFATP1_f	CGC TTT CTG CGT ATC GTC TG
mFATP1_r	GAT GCA CGG GAT CGT GTC T
mGlut4_f	GAC GGA CAC TCC ATC TGT TG
mGlut4_r	GCC ACG ATG GAG ACA TAG C
mHSL_f	GCG CTG GAG GAG TGT TTT T
mHSL_r	CGC TCT CCA GTT GAA CCA AG
mIRS2_f	GTG GGT TTC CAG AAC GGC CT
mIRS2_r	ATG GGG CTG GTA GCG CTT CA
mLCAD_f	ATG GCA AAA TAC TGG GCA TC
mLCAD_r	TCT TGC GAT CAG CTC TTT CA
mLPL_f	CTG GTG GGA AAT GAT GTG G
mLPL_r	TGG ACG TTG TCT AGG GGG TA
mMCAD_f	AAC ACT TAC TAT GCC TCG ATT GCA
mMCAD_r	CCA TAG CCT CCG AAA ATC TGA A
mMCP1_f	AGG TCC CTG TCA TGC TTC TG
mMCP1_r	GCT GCT GGT GAT CCT CTT GT
mPEPCK_f	CTT CTC TGC CAA GGT CAT CC
mPEPCK_r	TTT TGG GGA TGG GCA C
mPGC1α_f	CCC AGG CAG TAG ATC CTC TTC AA
mPGC1α_r	CCT TTC GTG CTC ATA GGC TTC ATA
mPGC1β_f	CTT GAC TAC TGT CTG TGA GGC
mPGC1β_r	CTC CAG GAG ACT GAA TCC AGA G
mPPARα_f	TCA GGG TAC CAC TAC GGA GT
mPPARα_r	CTT GGC ATT CTT CCA AAG CG
mPPARγ_f	GAA AGA CAA CGG ACA AAT CAC C
mPPARγ_r	GGG GGT GAT ATG TTT GAA CTT G
mPRDM16_f	CAG CAC GGT GAA GCC ATT C

mPRDM16_r	GCG TGC ATC CGC TTG TG
mSREBP1c_f	GGT TTT GAA CGA CAT CGA AGA
mSREBP1c_r	CGG GAA GTC ACT GTC TTG GT
mTNFα_f	CCA GAC CCT CAC ACT CAG ATC
mTNFα_r	CAC TTG GTG GTT TGC TAC GAC
mTFIIB_f	TGG AGA TTT GTC CAC CAT GA
mTFIIB_r	GAA TTG CCA AAC TCA TCA AAA CT
mUcp1_f	GGC CTC TAC GAC TCA GTC CA
mUcp1_r	TAA GCC GGC TGA GAT CTT GT

Following primers were used for ChIP assays:

Table 8: Real-time PCR primers for ChIP assays

Name	**sequence 5' - 3'**
C/EBPβ binding site at PPARγ promoter _f	TTC AGA TGT GTG ATT AGG AG
C/EBPβ binding site at PPARγ promoter _r	AGA CTT GGT ACA TTA CAA GG

Following primers were used for genotyping of the *Nae1Adipo*CreER^{T2} mouse line:

Table 9: Primers for genotyping

Name	**sequence 5' - 3'**
Nae1 lox f	AGG AAA ATC AGG ATT TAG TTC ATA TTT CC
Nae1 lox r	CAT GAA ATC CAC TGT TCC ATT TAA TGG C
AdipoCreER^{T2} f	TGG TGC ATC TGA AGA CAC TAC A
AdipoCreER^{T2} r	TGC TGT TGG ATG GTC TTC ACA G

Following primers were used for cloning:

Table 10: Primers for cloning

Name	**sequence 5' - 3'**
HisBIO f	TAT CTC GAG ACC ATG CAT CAT CAC CAC CAT CAT G
HisBIO r	ATG GAA TTC TAA CGC CGA TCT TGA TTA GAC CTT GAC
FLAG f	TCG AGA TGG ACT ACA AGG ACG ACG ATG ACA AGA G
FLAG r	AAT TCT CTT GTC ATC GTC GTC CTT GTA GTC CAT C

All primers were obtained from Sigma-Aldrich.

Following buffers and solutions were used:

Table 11: Buffers and solutions

Buffer/solution	**composition**
Cell lysis buffer for C/EBPβ homodimerization assay	50 mM Tris-HCl pH 7.4 150 mM NaCl 1 mM EDTA 1 % Triton X-100
Cell lysis buffer for cellular fractionation	10 mM HEPES-NaOH, pH 7.9 1.5 mM MgCl2 10 mM KCl 1 mM DTT 0.5 % NP-40 0.1 mM EDTA 0.1 mM EGTA
Cell lysis buffer for ChIP	10 mM HEPES-KOH, pH 7.9 1.5 mM MgCl2 10 mM KCl 0.5 % Igepal
Dexamethasone	10 mM in 100 % Ethanol
Dilution buffer for ChIP	0.01 % SDS 1.1 % Triton-X100 1.2 mM EDTA 16.7 mM Tris-HCl, pH 8.1 167 mM NaCl
Elution buffer for ChIP	1 % SDS 50 mM Tris-HCl, pH 8.0 1 mM EDTA 50 mM $NaHCO_3$
Guanidinium-HCl lysis buffer	6 M guanidinium-HCl 10 mM Tris-HCl 0.1 M Na2HPO4/NaH2PO4 (pH 8.0) 10 mM β-mercaptoethanol
High salt wash buffer for ChIP	0.01 % SDS 1 % Triton-X100 2 mM EDTA

	20 mM Tris-HCl, pH 8.1 500 mM NaCl
IBMX	0.0115 g/ml in 0.5 M KOH
Insulin for cellular cultures	1 mg/ml in 0.02 M HCL
4x Laemmli Buffer	50 % (v/v) Glycerol 125 mM Tris, pH6.8 4 % SDS 0.08 % (w/v) Bromphenol blue 5 % β-Mercaptoethanol
LB agar plates	10 g/l Peptone 5 g/l Yeast extract 10 g/l NaCl 15 g/l Agar Adjust to pH7.0 Add selective antibiotic
LB medium	10 g/l Peptone 5 g/l Yeast extract 10 g/l NaCl Adjust to pH7.0
LiCl wash buffer for ChIP	0.25 M LiCl 1 % Igepal 1 % SOD 1 mM EDTA 10 mM Tris-HCl, pH 8.1
Lower Tris buffer for gel electrophoresis	182 g/l Tris Adjusted to pH8.8 4 g/l SDS
Low salt wash buffer for ChIP	0.01 % SDS 1 % Triton-X100 2 mM EDTA 20 mM Tris-HCl, pH 8.1 150 mM NaCl
Nuclear lysis buffer for cellular fractionation	20 mM HEPES-NaOH, pH 7.9 25 % glycerol 1.5 mM MgCl2 420 mM NaCl 0.1 mM EDTA

	0.1 mM EGTA
Nuclear lysis buffer for ChIP	1 SDS 10 mM EDTA 50 mM Tris-HCl pH 8.1
1x PBS	137 mM NaCl 2,7 mM KCl 20 mM Na_2HPO_4 2 mM KH_2PO_4 adjust tp pH7.4
RIPA lysis buffer	50 mM Tris 150 mM NaCl 1 % NP-40 0.5 % Sodium deoxycholate 0.1 % SDS
SDS-PAGE Running buffer	25 mM Tris pH 8,8 192 mM Glycin 0,1 % SDS
50x TAE buffer	2 M Tris 1 M acetic acid 100 mM EDTA, pH 8.0
1x TBS	50 mM Tris 150 mM NaCl Adjusted to pH7.6
TE buffer for ChIP	10 mM Tris-HCl pH8.0 1 mM EDTA
Transfer Buffer for Western Blotting	25 mM Tris 192 mM Glycin 15 % Methanol
Upper Tris buffer for gel electrophoresis	60,5 g/l Tris Adjusted to pH 6.8 4 g/l SDS
Urea washing buffer, pH8.0	8 M urea 0.1 M Na_2HPO_4/NaH_2PO_4 (pH 8.0) 0.01 M Tris-HCl 10 mM β-mercaptoethanol 0.1 % Triton X-100
Urea washing buffer, pH6.3	8 M urea

	0.1 M Na_2HPO_4/NaH_2PO_4 (pH 6.3) 0.01 M Tris-HCl 10 mM β-mercaptoethanol 0.1 % Triton X-100

3.2 Animals

3.2.1 Animals and animal housing

Animal experiments were carried out at the Max Planck Institute of Psychiatry, Munich and at the Max Planck Institute of Heart and Lung Research, Bad Nauheim. All experiments were performed under standard laboratory conditions (22±1 °C, 55 %±5 % humidity) with food (standard rodent chow diet, Altromin 1324, or HFD, Research Diets D12451) and water *ad libitum* under a 12 h light/dark schedule. All procedures conducted in this study conform to the international standards for use of laboratory animals, and were performed in accordance with the Guide for the Care and Use of Laboratory Animals of the Government of Bavaria (Gz.ROB-55.2Vet-2532.Vet_02-13-46) and the Government of Darmstadt (V 54-19c20/15-B20/1116). All efforts were made to minimize both the suffering and number of animals used in the present study.

3.2.2 Mouse strains and transgenic mouse lines

- Male C57BL/6N mice for subcutaneous MLN4924 injections to study the effects of peripheral inhibition of the neddylation pathway on obesity and metabolism.

- Male C57BL/6 mice for primary cell culture of inguinal WAT.

- *Nae1Adipo*CreER^{T2} mouse line to study the effects of fat specific ablation of the neddylation pathway on obesity and metabolism. The *Adipo*CreER^{T2} mouse line was created by A. Sassmann (Sassmann et al., 2010). Nae1 knockout mice were developed by A.M. Vogl (Vogl et al., 2015). By breeding the two lines together, A.M. Vogl created the *Nae1Adipo*CreER^{T2} mouse line.

3.2.3 Genotyping

Genomic DNA was extracted from mouse tail biopsies by alkaline lysis. For this purpose, 100 µl of 50 mM NaOH were added to small pieces of mouse tails and then they were boiled for 30 min at 95 °C. After cooling down the tissue lysates to 4 °C, 30 µl of 1 M Tris-HCl pH7.2 were added for neutralization. Tissue lysates, which were subsequently used as PCR templates, were kept at 4 °C for short-term storage and at -20 °C for long-term storage. For genotyping by PCR, 1 µl of the tissue lysates, containing genomic DNA, 2.5 µl 10x PCR buffer, 0.75 µl 50 mM $MgCl_2$, 2.5 µl 2 mM dNTPs, 1.25 µl 10 µM primers (Table 9), 0.125 µl Taq DNA Polymerase (5 U/µl stock solution) were mixed. PCRs were conducted using the

following program: 95 °C for 5 min, 35 cycles of 95 °C for 45 sec, 58 °C for 30 sec, 72 °C for 30 sec, followed by 72 °C for 7 min. After amplifying the desired genomic DNA sequence, PCR samples were mixed with 5x loading buffer and were loaded on a 1 % (w/v) ethidium bromide agarose gel (1x TAE). Separated bands were analyzed using a UV-transilluminator and the Intas GDS software.

3.3 Procedures with plasmid DNA

3.3.1 Preparation of plasmid DNA

For Mini Preps, a single colony was inoculated in 2 ml LB medium with a selective antibiotic O.N. on a shaker at 37°C. For Maxi Preps, a single colony was inoculated in 200 ml LB medium with a selective antibiotic O.N. at 37°C with vigorous shaking. Plasmid DNA was isolated from bacteria using DNA isolation Kits (QIAprep Spin Miniprep Kit or HiSpeed Plasmid Maxi Kit) according to the manufacturer's instructions.

3.3.2 Cloning

The vector pcDNA3.1(-) mouse C/EBPβ LAP was a gift from Peter Johnson (Addgene, plasmid # 12557). FLAG- and 6xHis-BIO tags were fused to the N-Terminus of mouse C/EBPβ LAP by cloning 1xFLAG- and 6xHis-BIO tags in pcDNA3.1(-) mouse C/EBPβ LAP.

PCR for amplification of desired DNA sequence

Prior to cloning into vectors, desired DNA sequences were amplified by PCR. For this purpose, 1 µg plasmid DNA, 5 µl Pfu Buffer + $MgSO_4$, 5 µl dNTPs (2 mM), 1 µl of each primer (10 µM) (Table 10) and 0.5 µl Pfu DNA Polymerase (1.25 U/µl) were mixed. The PCR program was carried out according to the manufacturer's protocol. After amplifying the desired DNA sequence, small aliquots of the PCR samples were supplemented with 5x loading buffer and were loaded on a 1 % (w/v) ethidium bromide agarose gel (1x TAE) in order to analyze the sizes of the PCR products. DNA bands were visualized using a UV-transilluminator and the Intas GDS software. Next, the PCR products were purified using the QIAquick PCR Purification Kit.

Restriction digest of plasmid DNA and PCR products

For restriction digest of plasmid DNA or PCR products, 10U of restriction enzyme were used per µg of DNA in a 50 µl reaction supplemented with the appropriate NEB buffer. Digestion reactions were performed for 5 h at 37 °C and were afterwards heat inactivated for 15 min at 70 °C.

Extraction of DNA fragments from ethidium bromide agarose gels

Following restriction digests, DNA fragments were separated by agarose gel electrophoresis. Samples were mixed with 5x loading buffer and were loaded on a 1 % (w/v) ethidium bromide agarose gel (1x TAE). Separated DNA fragments were visualized using a UV-transilluminator and the Intas GDS software and the appropriate bands were cut using a scalpel. QIAquick Gel Extraction Kit was used according to manufacturer´s protocol to purify DNA fragments.

Ligation reaction and transformation into bacteria

For ligation, vectors and inserts (1:3 molar ratio), 1 µl of T4 ligase buffer (10x), 1 U T4 DNA ligase were mixed and H_2O was added up to 10 µl reaction volume. The reaction was incubated for 1 h at RT, followed by an O.N. incubation at 4 °C. On the next day, the reaction was heat inactivated for 15 min at 70 °C. Subsequently, TOP10 chemically competent bacteria were transformed with 2 µl of the ligation reaction. Colonies were inoculated and DNA was isolated as described in 3.3.1. Successful ligation was confirmed by restriction enzyme analysis and sequencing.

3.3.3 Creation of mutant plasmids by genesynthesis

The pcDNA3.1(-) 6xHis-BIO-tagged mouse C/EBPβmut LAP was generated from the wild-type pcDNA3.1(-) mouse C/EBPβ LAP by exchanging all Lys to Arg (AGG) by gene synthesis (BioCat GmbH).

3.4 Cell Culture

3.4.1 Primary cell culture from adipose tissue

For primary adipocyte cell culture, the stromal vascular fraction (SVF) from inguinal fat was prepared from 6- to 8-week-old C57BL/6 mice. For this purpose, the inguinal adipose depot was dissected and all fat pads were collected in 10 ml PBS. Subsequently, the fat pads were

cut with scalpels in a dish filled with digestion buffer (Dulbecco's modified Eagle's medium (DMEM)/F12 + GLUTAMAX, 10^5 U/l Penicillin/Streptomycin, 0.15 % Collagenase Type IV and 2 % BSA). Then, tissue was digested in 20 ml digestion buffer for 50 min at 37 °C in a shaking water bath. Tissue homogenate was filtered through a 100 µm cell strainer that was subsequently washed with 10 ml DMEM/F12 + GLUTAMAX and 10^5 U/l Penicillin/Streptomycin. Tissue homogenate and washing solution were combined and centrifuged at 400 x g for 10 min at RT. The supernatant was removed and the pellet was resuspended in 4 ml erythrocyte lysis buffer (154 mM NH_4Cl, 10 mM $KHCO_3$, 0.1 mM EDTA) and incubated for 20 min at RT. After centrifugation at 400 x g for 10 min at RT, the supernatant was discarded and the pellet was resuspended in 10 ml culture medium (DMEM/F12 + GLUTAMAX, 10 % fetal calf serum (FCS) and 10^5 U/l Penicillin/Streptomycin) and filtered through a 30 µm cell strainer. Primary SV cells were seeded, on the following day cells were washed with phosphate buffered saline (PBS) and new culture medium was added to the cells. Cells were maintained at 37 ºC and 5 % CO_2. Adipocyte differentiation was induced in preadipocyte cultures by treating one-day confluent cells for 48 hours with medium containing 10 % FCS, 0.5 mM IBMX, 1 µM dexamethasone, 5 µg/ml insulin and 1 µM rosiglitazone. Two days after induction, cells were switched to differentiation medium containing 10 % FCS and 5 µg/ml insulin. Depending on the demands of each experiment primary preadipocyte cells were treated with different concentrations of DMSO or MLN4924 during the first two days of differentiation or every second day from day 8 of differentiation on as indicated in the results section.

3.4.2 Mouse embryonic fibroblast preparation and culture

MEFs were prepared from mouse embryos (E13.5). For this purpose, embryos were decapitated and internal organs were removed from the abdominal cavity. The carcass was cut and subsequently digested in 1 ml 0.25 % trypsin/1 mM EDTA for 30 min at 37 °C, gently shaking. After removing the trypsin solution, tissue pieces were first washed with 10 ml and then resuspended in 1.5 ml DMEM containing 10 % FCS. Next, cells were dissociated by trituration with a Pasteur pipette. After adding 5.5 ml DMEM supplemented with 10 % FCS, cells were filtered through a 30 µm cell strainer. MEFs were maintained in DMEM containing 10 % FCS, 2 mM L-Glutamine and 1 mM Sodium Pyruvate at 37 °C and 5 % CO_2. In order to induce adipocyte differentiation of MEF cells, two days post-confluent cells were treated with 10 % FCS, 0.115 µg/ml IBMX, 1 µg/ml insulin, 1 µM dexamethasone and 10 µM troglitazone. Subsequently, cells were treated every second day with 1 µg/ml insulin. MEF cells were treated with DMSO or MLN4924 during the first two days of differentiation as indicated in the results section.

3.4.3 3T3-L1 cell culture, differentiation protocol and transfection

The 3T3-L1 preadipocyte cell line was derived from Swiss 3T3 mouse fibroblasts (Green and Kehinde, 1974). 3T3-L1 cells were cultured in DMEM supplemented with 10 % Bovine Serum (BS), 10^5 U/l Penicillin/Streptomycin, 2 mM L-Glutamine and 1 mM Sodium Pyruvate at 37 ºC and 5 % CO_2. When cells reached 80 % confluency, they were washed with PBS, trypsinized, counted and subsequently propagated in cell culture flasks or seeded according to the demands of each experiment.

For differentiation of 3T3-L1 cells into adipocytes, two days post-confluent cells were treated with 10 % FCS, 0.115 µg/ml IBMX, 0.001 mg/ml insulin and 1 µM dexamethasone. Next, cells were treated every second day with 1 µg/ml insulin. 3T3-L1 cells were treated with different concentrations of DMSO or MLN4924 during the first two days of differentiation or every second day from day 8 of differentiation as indicated in the results section. Depending on the demands of each experiment, 1 µM rosiglitazone or 20 µg/ml cycloheximide (CHX) were added to the cells.

3T3-L1 preadipocytes and adipocytes were transfected using the Amaxa Cell Line Nucleofector Kit V and L, respectively. Subsequently, cells were maintained for a 48 h incubation period.

3.4.4 HEK293 cell culture and transfection

HEK293 (human embryonic kidney) cells were cultured in DMEM, 10 % FCS, 10^5 U/l Penicillin/Streptomycin, 2 mM L-Glutamine and 1 mM Sodium Pyruvate at 37 ºC and 5 % CO_2. When cells reached confluency, they were washed with PBS, trypsinized, counted and subsequently propagated or seeded on Poly-D-Lysine (PDL)-coated cell culture plates according to the demands of each experiment.

HEK293 cells were seeded in culture medium in PDL-coated cell culture dishes 48 h prior to transfection. Cells were transiently transfected using Lipofectamine 2000 in DMEM, containing 1 % FCS, 2 mM L-Glutamine and 1 mM Sodium Pyruvate. After 18 h the transfection medium was replaced by DMEM, containing 1 % FCS, 2 mM L-Glutamine and 1 mM Sodium Pyruvate. For experiments with BIO-tagged constructs, 4 µM biotin was added to the medium. Cells were incubated for another 48 h. According to the demands of each experiment, during this incubation time some cellular cultures were treated for 24 h with DMSO or 1 µM MLN4924 and the last 6 h with 10 µM MG-132.

3.4.5 Oil red O staining

Adipocytes were stained with Oil Red O (ORO), a red fat soluble dye, which is used for staining TG and lipids, to determine the quantity of lipid droplet containing cells and the lipid content per well. In addition to ORO, cells were counterstained with haematoxylin. For the staining procedure 0.05 g ORO powder were diluted in 25 ml 60 % isopropanol, boiled briefly, cooled down to RT and filtered through a 0.22 µm filter. Cells were washed with 500 µl PBS and subsequently fixed using 500 µl 4 % formaldehyde per well. After an incubation time of 30 min at RT cells were washed with 500 µl dH_2O. Subsequently, cells were stained with 500 µl ORO solution per well for 1 h at RT. Next, two washing steps with dH_2O were followed by the staining with 300 µl Mayer's Hematoxylin Solution per well for 5 min at RT. Cells were washed with running tab water for 5 min at RT. Tab water was removed and dH_2O was added before taking pictures of the stained cells in different magnifications. For quantification, ORO was extracted from the cells by adding 1 ml 60 % isopropanol per well. Each sample was measured at 510 nm in a SmartSpec Plus Photometer.

3.5 RNA isolation and real-time PCR

In order to extract total RNA, 1 ml Trizol was added to cells or tissue, samples were homogenized and subsequently centrifuged for 15 min at 13,200 rpm at 4 °C. Supernatants were transferred to a new tube and incubated for 5 min at RT. Subsequently, 200 µl chloroform were added and tubes were shaken vigorously by hand for 15 sec. After an incubation time of 3 min at RT, samples were centrifuged for 15 min at 13,200 rpm at 4 °C. The aqueous phase, containing RNA, was transferred into new Eppendorf tubes. Next, 500 µl isopropanol were added to the samples. Tubes were inverted two times and samples were incubated for 10 min at RT. Samples were again centrifuged for 15 min at 13,200 rpm at 4 °C and supernatants were discarded afterwards. Pellets were washed with 1 ml 75 % ethanol. Samples were vortexed and subsequently centrifuged for 5 min at 13,200 rpm at 4 °C. Supernatants were discarded, samples were spun down briefly and afterwards the rest of the liquid was removed with a pipette. The pellet was dried for 10 min at 60 °C and subsequently dissolved in RNase free water. RNA was dissolved for 10 min at 50-60 °C.

RNA was diluted in RNase free water to a final concentration of 1 µg RNA in 10 µl. cDNA was generated with the QuantiTect Reverse Transcription Kit. Real-time PCR (qRT-PCR) was performed using the QuantiFast SYBR Green RT-PCR Kit and the Roche Light Cycler. For this purpose, 2 µl of cDNA, were pipetted in a 96-well plate. 5 µl QuantiFast SYBR Green

RT-PCR Master Mix, 1 µl of the left and right primer (10 µM) respectively (Table 7), and 1 µl RNase free water were mixed and added to each sample. RT – mix served as a negative control. It contained three different samples treated as the other samples but the enzyme reverse transcriptase was replaced by RNase free water. Following cycle parameters were used: One cycle for preincubation at 95 °C for 5 min, 40 cycles for amplification (10 sec at 95 °C for denaturation and 30 sec at 60 °C for primer annealing and elongation per cycle), one cycle of 10 sec at 50 °C for determining the melting curve and for 30 sec cooling down to 42 °C. RNA amounts were quantified using three different internal standards (Standard 1/1, Standard 1/10, Standard 1/100). Results were normalized to the RNA expression of the housekeeping genes TFIIB or β-Actin. Samples and standards were measured in triplicates. Absolute quantification of the PCR products as wells as melting point analysis was carried out using the Light Cycler Software Version 4.05.

3.6 Immunoblotting

First, lysates from tissue or cells were prepared using RIPA lysis buffer (Table 11), supplemented with protease inhibitor cocktail and phosphatase inhibitor cocktail. When neddylated proteins were analysed 20 mM N-Ethylmaleimide (NEM), an inhibitor of cysteine peptidases, and 2 mM 1,10-Phenanthroline monohydrate (OPT), an inhibitor of metalloproteases, were added to the RIPA lysis buffer in order to prevent de-neddylation of the analysed proteins. Samples were sonicated with the SONIFIER® Cell disruptor B15 using output control 6, 40 % duty cycle and 7 impulses. Lysates were centrifuged at 12000 rpm for 5 min at 4 °C and supernatants were in the following analyzed by immunoblotting. Protein concentrations were measured by Bradford Assay. Protein extracts were mixed with dH_2O and Roti-Load or 4x Laemmli buffer (Table 11). Samples were heated for 5 min at 95 °C and centrifuged for 5 min at 13,200 rpm at 4 °C. PageRuler™ Prestained Protein Ladder and samples were separated by SDS-PAGE on SERVA gradient (4-20 %) gels or 8-15 % self-made polyacrylamide gels. Proteins were transferred to 0.45 µm PVDF membranes using a wet transfer system. To control transfer efficiency, the membranes were stained with PonceauS solution. In the following step, the PVDF membranes were blocked in 5 % milk powder dissolved in 1x Tris-buffered saline (TBS) solution containing 0.1 % Tween 20 (TBST) for 1 h at RT. After the O.N. incubation at 4 °C of the primary antibodies, diluted in either 5 % BSA or 5 % milk solution, the membranes were washed three times in TBST for 5 min. Subsequently, the membranes were incubated with a horseradish peroxidase-IgG conjugated secondary antibody diluted in either 5 % BSA or 5 % milk solution for 1 h at RT. All antibodies used in this study are listed in Table 6. Membranes were washed three times in TBST before visualizing the proteins of interest by using the chemiluminescent substrate

Immobilon. Immunoreactive bands were measured with the ChemiDoc™ MP imaging system. Data were analyzed using Image Lab 4.0 Software (Biorad).

3.7 Pull-down assays

For pull-down assays, cells were plated in 10 cm dishes and treated according to the demands of each experiment. Following the protocol for denaturing conditions, cells were lysed in 1 ml Guanidinium-HCl buffer (Table 11) containing protease inhibitor cocktail and were subsequently sonicated. Cell lysates were incubated with 50 µl magnetic Streptavidin beads overnight at 4 °C. Beads were successively washed once with 750 µl Guanidinium-HCl buffer containing 0.1 % Triton X-100, once with 750 µl urea buffer, pH 8.0 (Table 11) and three times with 750 µl urea buffer, pH 6.3 (Table 11). Proteins were eluted by boiling in 150 µl 4x Laemmli buffer, separated by SDS-PAGE and analyzed by immunoblotting.

3.8 C/EBPβ homodimerization assay

For C/EBPβ homodimerization assays, cells were plated in 10 cm dishes and treated according to the demands of the experiment. Cell lysates were prepared in mild lysis buffer (Table 11) containing protease inhibitors and phosphostop. Cells were centrifuged for 20 min at 13,000 rpm at 4 °C and supernatants were incubated with magnetic Streptavidin beads O.N. at 4 °C. Beads were washed three times with 750 µl TBS and proteins were eluted by boiling in 150 µl 4x Laemmli buffer. C/EBPβ homodimerization was analyzed by immunoblotting.

3.9 Cellular fractionation of 3T3-L1 cells

For cellular fractionation experiments, 3T3-L1 cells were plated in 10 cm dishes and treated with DMSO or 1 µM MLN4924. Cells were washed two times with 10 ml PBS and trypsinized at the indicated time points. Cells were centrifuged for 10 min at 100xg at 4 °C. The cell pellet was washed once with 1 ml ice cold PBS and subsequently centrifuged for 10 min at 100xg at 4 °C. Cell pellets were frozen at -80 °C. Next, cells were lysed using 250 µl cellular lysis buffer (Table 11) containing protease inhibitors and phosphates inhibitors by occasionally mixing for 15 min. In order to sediment nuclei, samples were centrifuged for 10 min at 6,000 rpm at 4 °C. Supernatants were analyzed as cytosolic fraction by immunoblotting. Pelleted nuclei were washed twice with 500 µl ice cold PBS and afterwards lysed for 30 min at 4 °C using 50 µl nuclear extraction buffer (Table 11) containing protease

inhibitor and phosphatase inhibitor. Samples were again centrifuged for 10 min at 6,000 rpm at 4 °C. Supernatants were analyzed as nuclear fraction by immunoblotting.

3.10 Immunocytochemistry

3T3-L1 cells were plated on chloroform/100 % EtOH-treated coverslips, differentiated and co-transfected with pcDNA3.1(+) mouse Ubc12-C111S and a vector expressing GFP, following the std. protocols. On day 7 of differentiation, after staining with ORO, cells were permeabilized with 0.1 % Triton X-100 in PBS, blocked in 5 % BSA in PBS/0.1 % Triton X-100, and incubated at 4 °C with α-GFP primary antibody. After 24 h, cells were incubated with a green-fluorescent α-chicken secondary antibody for 2 h. Coverslips were mounted in mounting medium containing DAPI and slides were sealed with Roti® Histokitt. Images were acquired on a Zeiss AXIO fluorescence microscope and were processed with AxioVision software (Zeiss). Random areas were picked in a blinded fashion, and a minimum of 100 nuclei per coverslip were counted.

3.11 Lipolysis assay

3T3-L1 cells were plated in 96-well plates, treated with DMSO, 3 µM MLN4924 or 1 µM Isoproterenol for the indicated time period. FA concentration in the medium was measured using the Lipolyis Assay Kit for 3T3-L1 cells (Zenbio) following the manufacturer's instructions.

3.12 Flow cytometry

For flow cytometry analysis, 3T3-L1 cells were plated in 6-well plates and induced to differentiate. 3T3-L1 adipocytes were treated with DMSO or 3 µM MLN on day 8 of differentiation for 24 h or with 10 µM isoproterenol (ISO) for the last 1 h, respectively. Subsequently, cells were rinsed in medium and transferred into a 15 ml falcon tube. Cells were centrifuged for 3 min at 1200 rpm. Next, the medium was removed and cells were washed with 5 ml PBS twice. After washing, the cell pellet was dissolved in 1 ml PBS. Cells were kept on ice for 10 min. For the fixation of the cells, 3 ml ice-cold absolute ethanol was added drop wise while slowly vortexing. Next, samples were centrifuged for 4 min at 2000 rpm at 4 °C. Approximately 3 ml supernatant were removed and cells were resuspended in the rest of the liquid and transferred into Eppendorf tubes. Cells were centrifuged for 3 min at 4000 rpm at 4 °C and supernatant was removed afterwards. Cells

were washed twice with 1 ml ice-cold PBS with a centrifugation step of 3 min at 4000 rpm at 4 °C in between. Next, supernatant was removed completely and cells were resuspended in 500 µl PI mix containing 1 ml PBS, 50 µl PI and 1 µl RNase A. After incubating 30 min at 37 °C, side scatter (SS) and forward scatter (FS) were determined by flow cytometry using the Beckman Coulter EPICSTMXLTM flow cytometry apparatus and data was analyzed using EXPO32 Software.

3.13 Reporter gene assays

3T3-L1 cells were transfected using the Amaxa Cell Line Nucleofector V or L Kit and were subsequently seeded in 24-well plates. Two days after transfection, 3T3-L1 cells were washed once with 500 µl PBS, subsequently lysed with 100 µl Passive Lysis Buffer and frozen at -80 °C. Next, cell lysates were de-frozen and centrifuged for 1 min at 13,000 rpm at 4 °C. Reporter activity for luciferase was measured in a TriStar photometer by adding 50 µl Luciferin to 20 µl cell lysate. Luciferase activity was normalized to GFP fluorescence emission measured in a TriStar photometer.

3.14 cAMP assay

3T3-L1 cells were cultured in Std. Medium supplemented with 10 % BS. Two days after, cells were serum deprived in Std. Medium supplemented with 1 % BSA without antibiotics for 4 h. IBMX (0.115 µg/ml), insulin (1 µg/ml) and 10 % FCS were added together with DMSO or 1 µM MLN4924 or 5 µM forskolin to the cultures. Cells were treated for the indicated time periods. For measuring intracellular cAMP levels, cells were incubated with 6 % trichloracetic acid (TCA) overnight at 4 °C. Supernatants were collected in 10 ml glass tubes, TCA was extracted twice using 3 ml diethyl ether saturated with water. Subsequently, samples were lyophilized O.N. Finally, cAMP content was measured by J. Stalla using the cAMP [^{125}I] Radioimmunoassay Kit.

3.15 Chromatin Immunoprecipitations

3.15.1 ChIP in 3T3-L1 cells

For Chromatin Immunoprecipitation (ChIP) experiments, 3T3-L1 cells were plated in 10 cm dishes and were treated for 24 h with DMSO or 1 µM MLN4924. In order to crosslink proteins to DNA, 270 µl 37 % Formaldehyde were added to the plates containing 10 ml medium. After incubating for 10 min at RT, the crosslinking reaction was stopped by adding 1 ml 1.25 M

Glycine per plate for 5 min at RT. Then, medium was removed and dishes were placed on ice. Cells were washed twice with ice cold PBS and subsequently scraped gently with 1 ml PBS containing protease inhibitor cocktail. Cells were pelleted by centrifuging for 10 min at 100xg at 4 °C. Supernatants were discarded and cells were lysed for 15 min on ice in 300 µl cell lysis buffer (Table 11) containing protease inhibitor cocktail. Samples were centrifuged for 10 min at 6000 rpm at 4 °C. Pelleted nuclei were lysed by adding 200 µl nuclei lysis buffer (Table 11) containing protease inhibitor cocktail. DNA was sheared by sonicating 14 x (15 sec continuous sonication, 1 min to cool in between). After sonication, samples were centrifuged for 20 min at 13,200 rpm at 4 °C. Supernatants were aliquoted for IPs (OD_{260nm} = 10) and diluted up to a volume of 500 µl with dilution buffer (Table 11) containing protease inhibitor cocktail. Protein G beads were washed three times with dilution buffer and samples were pre-cleared for 30 min with 10 µl pre-washed Protein G beads. Next, 1 % Input was taken and frozen at -80 °C. Afterwards, the respective antibodies (Table 6) were added to the supernatants and incubated rotating O.N. at 4 °C. On the next day, Protein G beads were washed three times in dilution buffer and subsequently blocked with 0.1 µg per µl beads BSA. Beads were washed three times with dilution buffer and 50 µl pre-washed / blocked Protein G beads were added to the samples and incubated rotating for 30 min at 4 °C. Beads were washed once for 5 min with 500 µl low salt buffer (Table 11), once for 5 min with 500 µl high salt buffer (Table 11), once for 5 min with 500 µl LiCl buffer (Table 11) and once for 5 min with 500 µl TE buffer (Table 11). Then, 200 µl elution buffer (Table 11) were added to the inputs and set aside at RT. Meanwhile, supernatants were removed from beads and 100 µl elution buffer was added and incubated for 15 min at RT. The elution step was repeated once more and the two eluates were combined. To reverse crosslinking, 8 µl 5 M NaCl were added to the inputs and IPs and incubated for O.N. at 65°C. Next, the samples were incubated with 1 µl RNase A for 30 min at 37 °C. Later, 4 µl 0.5 M EDTA, 8 µl 1 M Tris-HCl and 1 µl Proteinase K were added to the samples and incubated for 1 h at 45 °C. DNA fragments were purified using QIAquick PCR Purification Kit and afterwards stored at -20°C until further analysis by qRT-PCR. Samples were measured in triplicates. Results were normalized to Inputs.

3.15.2 ChIP in mouse adipose tissue

Epididymal fat was homogenized in 1 ml cell lysis buffer (Table 11) containing protease inhibitor cocktail and incubated for 15 min on ice, meanwhile vortexing every 5 min. Samples were centrifuged for 10 min at 6000 rpm at 4 °C. Supernatants were discarded and nuclei were washed three times with ice-cold PBS containing protease inhibitor cocktail. In between each washing step, nuclei were centrifuged for 10 min at 6000 rpm at 4 °C. Subsequently,

nuclei were cross-linked for 10 min in 500 µl 1 % formaldehyde solution. Formaldehyde was quenched with 50 µl 1.25 M glycine for 5 min. After centrifuging for 10 min at 6000 rpm at 4 °C supernatants were discarded and nuclei were washed three times with ice-cold PBS containing protease inhibitor cocktail. In between each washing step, nuclei were centrifuged for 10 min at 6000 rpm at 4 °C. Nuclei were lysed in 500 µl nuclei lysis buffer (Table 11) containing protease inhibitor cocktail and samples were incubated for 20 min at RT. DNA was sonicated on ice/EtOH 5x (10 sec continuous sonication, 1 min to cool in between). Sonicated samples were centrifuged for 20 min at 13,200 rpm at 4 °C. Supernatants were aliquoted for IPs (OD_{260nm} = 5) and diluted up to a volume of 500 µl with dilution buffer (Table 11) containing protease inhibitor cocktail. For further steps the protocol described in chapter 3.15.1 was followed.

3.16 *In vivo* experiments

3.16.1 Induction of Nae1 Knock-out in the fat tissue in lean and obese mice

Experimental mice were single-housed 1 week before and during the experiments and kept under standard laboratory conditions. Male mice of 2 months of age were used in all experiments. Age-matched *Nae1*^{floxed} mice were used as controls. The control and KO (*Nae1*^{floxed} and *Nae1Adipo*CreER^{T2}) mice were divided in 2 sets: KO of the Nae1 gene in the fat tissue of lean *Nae1Adipo*CreER^{T2} mice was induced by injecting intraperitoneally 2 mg tamoxifen (10 % ethanol in sunflower seed oil) per day for 3 days and subsequent feeding with tamoxifen food pellets (LAS CRdiet CreActive TAM400, LASvendi) for 7 days. After tamoxifen dependent Cre-lox recombination mice were fed either standard rodent chow diet or HFD for 14 weeks. A second set of animals was fed for 9 weeks with a HFD. Subsequently, the KO of the Nae1 gene in the AT of obese *Nae1Adipo*CreER^{T2} mice was induced by injecting intraperitoneally 2 mg tamoxifen (10 % ethanol in sunflower seed oil) per day for 5 days. Then mice were fed either standard rodent chow diet or HFD for 8 weeks.

3.16.2 Treatment with the neddylation inhibitor MLN4924

Eight weeks old C57BL/6N mice were fed a HFD for 8 weeks. Diet-induced obese mice were subsequently injected daily, subcutaneously with 90 mg/kg MLN4924, diluted in 20 % (w/v) 2-hydroxypropyl-β-cyclodextrin, or vehicle for 2 months. During vehicle/MLN4924 treatment, mice were fed with either standard rodent chow diet or HFD for 7 weeks.

3.16.3 Indirect calorimetry

Energy expenditure (EE), oxygen consumption (VO_2), respiratory exchange ratio (RER), food and water consumption and locomotor activity were analyzed by an indirect calorimetry system (Phenomaster, TSE Systems) over a period of 48 h. Before data collection, all mice were acclimatized to the system for 48 h.

3.16.4 Glucose tolerance test

Animals were subjected to 6 h of fasting 1 h after the onset of the light phase. Subsequently, mice were injected intraperitoneally with 2 g glucose per kg body weight (20 % w/v D-glucose in 0.9 % w/v saline). Tail blood glucose levels (mg/dl) were measured with a handheld glucometer (Contour next, Bayer) before (0 min) and at 15, 30, 60 and 120 min after injection.

3.16.5 Measurement of plasma parameters

After sacrificing the animals, trunk blood was collected in EDTA-coated microvette tubes, immediately chilled on ice, centrifuged at 5,000 rpm for 10 min at 4 °C, and plasma was stored at –80 °C For measurement of plasma parameters following Kits were used: EnzyChrom™ Glucose Assay Kit, EnzyChromTM Triglyceride Assay Kit, Mouse Leptin ELISA Kit, NEFA Kit, Adiponectin ELISA Kit, Insulin ELISA Kit.

3.16.6 Tissue harvest and preparation

Tissues were isolated and either snap frozen in liquid nitrogen for protein and RNA analysis or fixed in 4 % paraformaldehyde. Prior to embedding the tissues in Paraplast for histology, tissues were washed once with PBS and subsequently incubated in 70 % ethanol O.N. at 4 °C. On the next day tissues were further de-hydrated by incubation for 2 h in 96 % ethanol, for 2 h in 99.8 % ethanol and in xylol till the tissues were transparent. Finally, tissues were embedded in Parablast.

3.16.7 Histology

Sections at 8 µm were prepared of Paraplast-embedded tissues using a microtome (Leica). For hematoxylin & eosin staining, WAT and liver sections were deparaffinised in xylol and

rehydrated by incubating the sections twice for 5 min in xylol, twice for 2 min in 100 % ethanol, twice for 2 min in 96 % ethanol, twice for 2 min in 70 % ethanol, and removing the ethanol by washing twice with dH_2O. Afterwards, sections were stained for 5 min in hematoxylin. Next sections were rinsed with dH_2O and subsequently washed with running tab water for 10 min. Sections were then stained for 3 min in eosin, rinsed with dH_2O and dehydrated again by incubating the sections once for 1 min in 70 % ethanol, twice for 1 min in 96 % ethanol, twice for 1 min in 100 % ethanol and twice for 5 min in xylol. Then sections were embedded using the Roti-Histokitt. Pictures of the tissue were taken with a Zeiss AXIO microscope and were processed with AxioVision software (Zeiss). Adipocyte area was determined by quantifying the adipocyte area from 3 animals per study group using the Adiposoft image analysis Software.

For perilipin immunohistochemistry, sections were re-hydrated in a graded alcohol series (45 min in xylol, 5 min in xylol, two times for 10 min in 100 % ethanol, two times for 10 min 95 % ethanol and two times for 5 min in 70 % ethanol). Subsequently sections were rinsed for 10 min in dH_2O. Antigen retrieval was performed by washing the sections in 0.01 M sodium citrate (pH 6.0), boiling them for 5 min in the microwave at 100 %, letting them cool down for 5 min at RT, boiling them for 3 min in the microwave at 70 % and finally cooling them down to RT for 20 min. Sections were rinsed twice in PBS and endogenous peroxidase was quenched by incubation in 0.1 % H_2O_2 (in PBS) for 5 min. After blocking for 1 h in 1.5 % goat serum, two successive washing steps in PBS, α-perilipin antibody diluted in 2 % goat serum was incubated ON at 4 °C. On the next day sections were washed twice in PBS for 2 min and the secondary antibody diluted in PBS was incubated for 30 min at RT. After two consecutive washing steps with PBS, ABC reagent was incubated for 30 min at RT. Sections were subsequently washed with PBS and 0.05 M Tris-HCl (pH 7.4) for 5 min, respectively. DAB staining (2 ml DAB in 100 ml 100 mM Tris-HCl, pH 7.6 and 0.01 % H_2O_2) was performed for 45 sec to 1 min and then the reaction was stopped with dH_2O. Next sections were washed twice with PBS for 5 min and nuclei were stained with hematoxylin. For this purpose sections were incubated in hematoxylin for 5 min, rinsed in dH_2O and incubated in running tab water for 10 min. Sections were de-hydrated again by incubating the sections twice for 1 min in 70 % ethanol, twice for 1 min in 96 % ethanol, twice for 1 min in 100 % ethanol and twice for 5 min in xylol. Then sections were embedded using the Roti-Histokitt.

3.16.8 Bomb calorimetry

Bomb calorimetry was performed by Ralf Elvert. Feces samples were dried at 60 °C, homogenized and squeezed to a pill for determination of energy content in an oxygen bomb

calorimeter (model 6300, Parr Instruments, Frankfurt/Main, Germany). For the analysis of solid feces samples, the bomb calorimeter was calibrated using benzoic acid for calorimetrical determination with a guaranteed caloric value of 26.47 kJ/g.

3.17 Statistical analysis

For cell culture, each condition was tested at least in triplicates. Each data set was obtained from at least three independent experiments. Data distribution was assumed to be normal, but this was not formally tested. Mice were assigned to the various experimental groups on the basis of genotype. Age-matched littermates were used as controls in all experiments. No randomization was used. All statistical analyses were performed using GraphPad Prism 7 software. Multiple comparison analyses were performed by using one- or two-way analysis of variances followed by Tukey's or Bonferroni's *post hoc* tests. Student's test was used for comparisons of two groups. Two-sample Z-test for proportions was performed for scoring of cells with or without lipid droplets after Ubc12 C111S overexpression and for FACS analysis. Differences were considered statistically significant at $*p < 0.05$. All results are presented as mean ± SEM.

4 Results

Neddylation is a PTM that exerts the regulation of various cellular functions, including cell cycle control as the best-established one (Enchev et al., 2015). Nevertheless, the role of neddylation in adipocyte development and function remained largely unknown. In this regard, especially the detection and characterization of Nedd8 targets and their roles in adipocytes awaited further investigation.

4.1 Neddylation increases during 3T3-L1 differentiation

With this in mind, we first attempted to investigate the role of neddylation in adipocyte development by analyzing the expression of proteins involved in the neddylation pathway by immunoblotting during the time course of 3T3-L1 adipocyte differentiation. The 3T3-L1 preadipocyte cell line can be differentiated into adipocytes in the presence of MDI (Green and Kehinde, 1974), and is thus frequently used as a model to study adipocyte differentiation. Using this tool we observed that the expression of the regulatory subunit of the E1 enzyme NAE, Nae1, changed during 3T3-L1 adipocyte maturation. Additionally, neddylation of the E2 enzyme Ubc12, the conjugating enzyme of the pathway, increased during adipogenesis (Figure 15), pointing towards an upregulation of neddylation pathway members during 3T3-L1 differentiation. Supporting this finding, we observed an increase in the pattern of neddylated proteins during 3T3-L1 adipogenesis (Figure 15). Interestingly, the smear of neddylated proteins, revealed by immunoblotting with an α-Nedd8 antibody, suggests that there are many additional neddylated substrates in 3T3-L1 cells beyond the Cullins (at ~ 95 kDa), the canonical neddylation targets. This observation is of particular importance, as the role of non-Cullin neddylation is still controversial (Enchev et al., 2015).

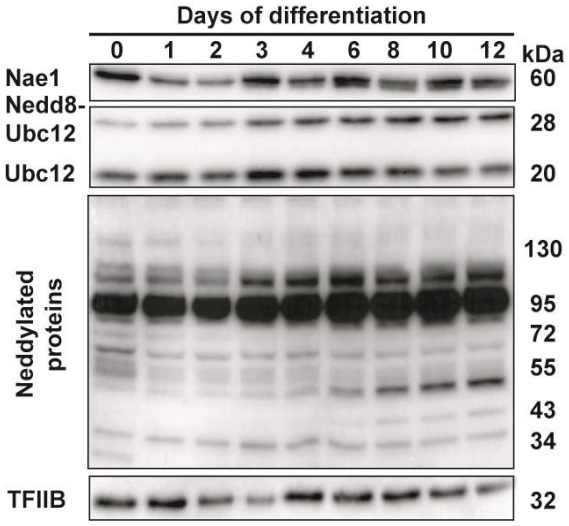

Figure 15: Neddylation increases during 3T3-L1 adipocyte differentiation. 3T3-L1 cells were differentiated for two days in culture medium with MDI followed by insulin. Protein lysates were extracted at the indicated time points. Immunoblots of Nae1, Ubc12 and Nedd8 during 3T3-L1 adipocyte differentiation are shown. Equal protein loading was confirmed by normalization to TFIIB expression.

4.2 Neddylation is crucial for adipocyte differentiation

Given the positive relationship between increasing neddylation and progression of adipocyte differentiation, we hypothesized that Nedd8 conjugation to substrate proteins might regulate adipogenesis. Thus, we attempted to validate this hypothesis using different approaches of neddylation inhibition. Neddylation was abolished during adipogenesis by either treating the cells with the specific Nae1 inhibitor MLN4924 or overexpressing a dominant negative Ubc12 (Ubc12 C111S) enzyme.

4.2.1 The Nae1 inhibitor MLN4924 impairs adipocyte differentiation in a dose-dependent manner

The potent and selective inhibitor MLN4924 is able to block the activity of Nae1, thus resulting in the disruption of Nedd8 conjugation to substrate proteins (Soucy et al., 2009). In order to explore the role of neddylation during adipocyte differentiation, MLN4924 was used as a pharmacological tool to inhibit the neddylation pathway. Simultaneous with the initiation of the differentiation process, 3T3-L1 preadipocytes were treated for two days with different concentrations of the neddylation inhibitor. Since MLN4924 was dissolved in DMSO, this solvent was used as a control for all subsequent experiments. After 14 days of 3T3-L1 adipocyte differentiation, cells were fixed, stained with the fat-soluble dye Oil Red O (ORO) and hematoxylin and pictures were taken by light microscopy. The more lipid droplets the cells contained the more they were stained with the red dye. TG content was photometrically

determined as a functional read-out. As evidenced by ORO staining, we observed dose-dependent inhibitory effects of MLN4924 on lipid droplet accumulation in 3T3-L1 cells (Figure 16A-B). As shown in Figure 16, adipocyte differentiation was completely blocked at concentrations of 500 nM and 1000 nM MLN4924. Cell viability after MLN4924 treatment was confirmed by counterstaining the cells with hematoxylin, ruling out putative cytotoxic effects of the drug.

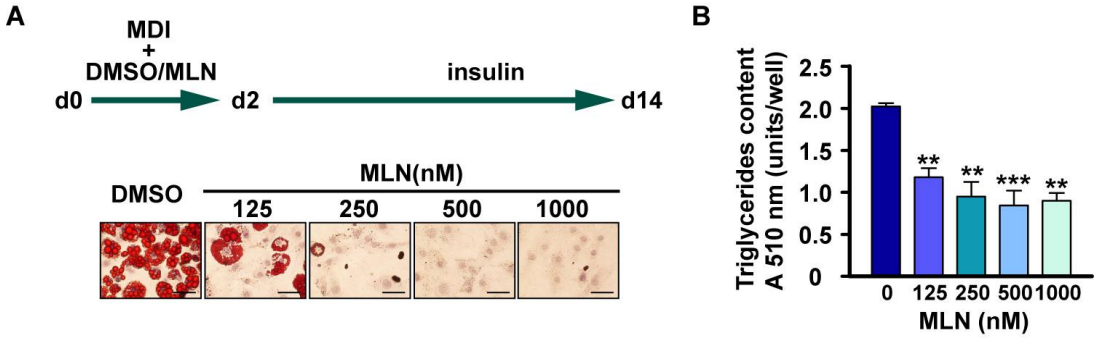

Figure 16: The neddylation inhibitor MLN4924 blocks adipocyte differentiation in a dose-dependent manner. (A-B) 3T3-L1 cells were differentiated for two days in culture medium with MDI followed by insulin. During the first two days of differentiation cells were treated with DMSO or different concentrations of MLN4924 (MLN). Cells were stained with ORO and hematoxylin on day 14. **(A)** Schematic diagram showing culture conditions. Representative images showing ORO (red) and hematoxylin staining of 3T3-L1 cells on day 14. **(B)** TG content was determined by quantifying ORO staining. Data are presented as mean ± SEM (n=3). Significance was determined by one-way ANOVA with Bonferroni's multiple comparison test. $**p < 0.01$ and $***p < 0.001$ DMSO vs. MLN treatment. Scale bars in (A) represent 50 µm.

Additionally, MLN4924 drug kinetics was performed by treating the cells with 1 µM MLN4924 and daily fixation and staining with ORO and hematoxylin from day 0 to day 14 of differentiation. These experiments revealed that neddylation blockade at this concentration completely abrogated 3T3-L1 adipocyte development (Figure 17A-B).

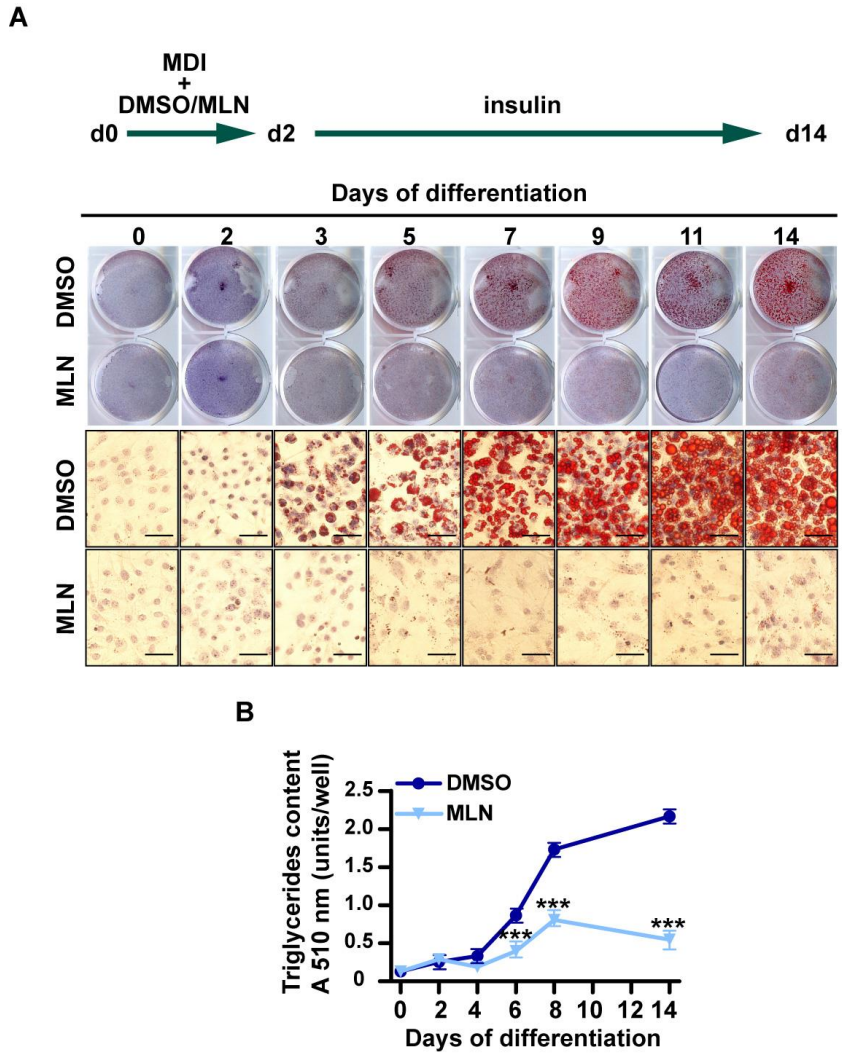

Figure 17: MLN4924 inhibits adipocyte differentiation. (A-B) 3T3-L1 cells were differentiated for two days in culture medium with MDI followed by insulin. During the first two days of differentiation cells were treated with DMSO or 1 µM MLN. Cells were stained with ORO and hematoxylin on different time points of differentiation. **(A)** Schematic diagram showing culture conditions. Representative images (of the whole cell culture well and by light microscopy) showing ORO (red) and hematoxylin staining of 3T3-L1 cells on different time points of differentiation. **(B)** TG content was determined by quantifying ORO staining. Data are presented as mean ± SEM (n=3). Significance was determined by two-way ANOVA with Bonferroni's multiple comparison test. $**p < 0.01$ and $***p < 0.001$ DMSO vs. MLN treatment. Scale bars in (A) represent 50 µm.

In a complementary set of experiments, we aimed to validate these results in other cellular models. Using PCC of inguinal WAT and MEFs we could confirm that neddylation inhibition by MLN4924 treatment at a concentration of 1 µM attenuates adipocyte differentiation in these cell cultures (Figure 18A-D). These experiments strongly support the relevance of neddylation in regulating adipocyte differentiation.

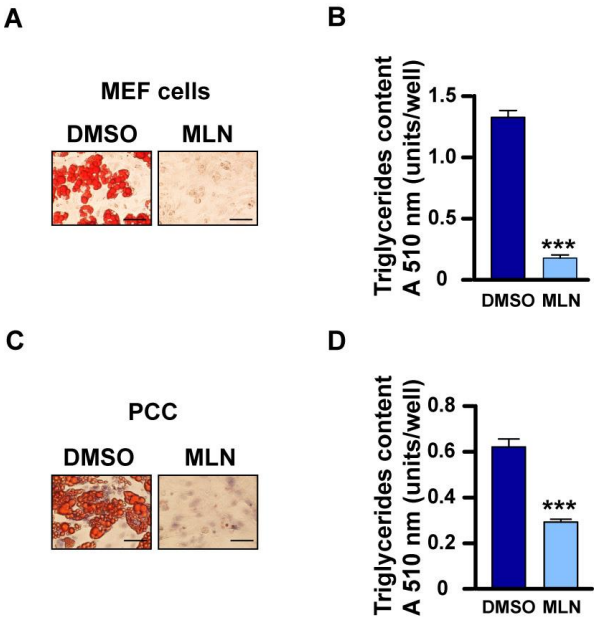

Figure 18: MLN4924 blocks adipocyte differentiation of MEFs and primary preadipocytes. (A-B) MEFs were induced to differentiate by treating the cells for two days with MDI and troglitazone followed by insulin. During the first two days of differentiation cells were treated with DMSO or 1 µM MLN and stained with ORO and hematoxylin on day 14. **(A)** Representative images showing ORO and hematoxylin staining of differentiated MEFs on day 14. **(B)** TG content was determined by quantifying ORO staining. **(C-D)** PCC of inguinal fat were induced to differentiate by treating the cells for two days with MDI and rosiglitazone followed by insulin. During the first two days of differentiation cells were treated with DMSO or 1 µM MLN and stained with ORO and hematoxylin on day 14. **(C)** Representative images showing ORO and hematoxylin staining of differentiated PCC on day 14. **(D)** TG content was determined by quantifying ORO staining. Data are presented as mean ± SEM (n=3). Significance was determined by unpaired two-side t test. $*p < 0.05$ and $***p < 0.001$ DMSO vs. MLN treatment. Scale bars in (A,C) represent 50 µm.

4.2.2 MLN4924-induced blockade of adipogenesis is reversible

Importantly, MLN4924 induced effects on adipocyte differentiation could be reverted when the drug was removed and cells were re-treated with adipogenic inducers (Figure 19A-B). As demonstrated by ORO staining, MLN4924-treated cells, that were re-stimulated to differentiate, reached the same TG content as control cells (Figure 19A-B). The fact that 3T3-L1 cells are able to recover after wash-out of the drug and repeated stimulation of differentiation ruled out potential cytotoxic effects. Moreover, the cells still conserve their biological function as preadipocytes, which can be transformed into mature adipocytes upon MDI treatment.

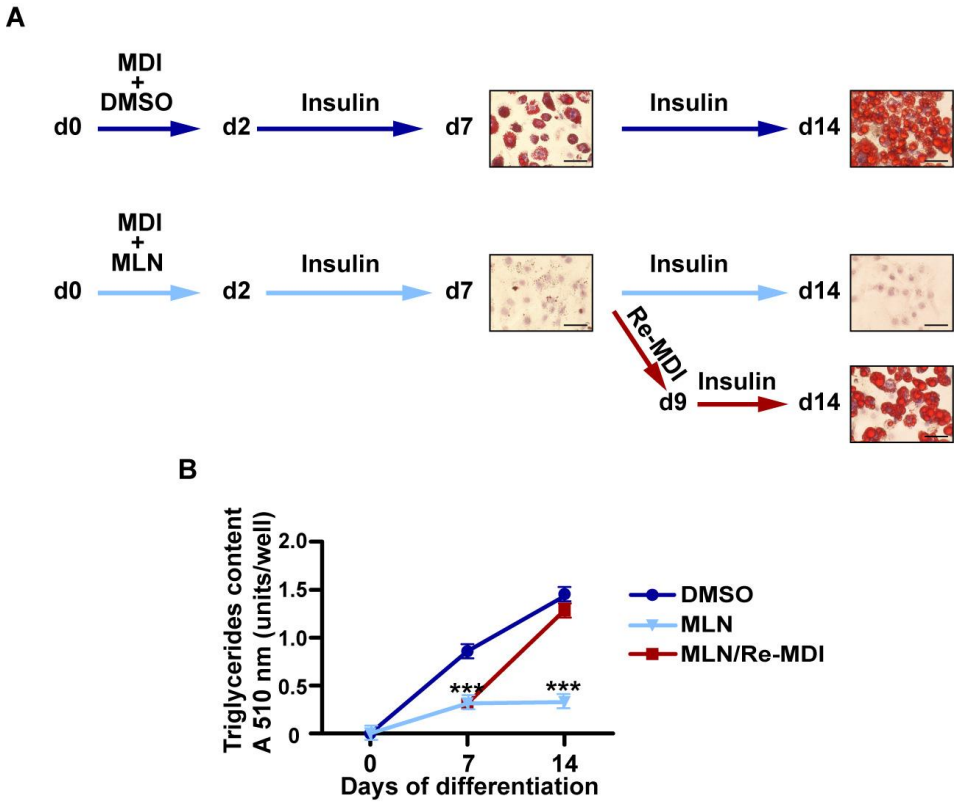

Figure 19: Reversion of MLN4924-induced effects on adipocyte differentiation. (A-B) 3T3-L1 cells were differentiated for two days in culture medium with MDI followed by insulin. During the first two days of differentiation cells were treated with DMSO or 1 µM MLN4924 (MLN). On day 7 part of the MLN4924-treated cell cultures was again incubated with MDI followed by insulin (Re-MDI). **(A)** Schematic diagram showing culture conditions. Representative images showing ORO and hematoxylin staining on day 7 and 14 after differentiation. **(B)** TG content was determined by quantifying ORO staining. Data are presented as mean ± SEM (n=3). Significance was determined by two-way ANOVA with Bonferroni's multiple comparison test. $**p < 0.01$ and $***p < 0.001$ DMSO vs. MLN treatment. Scale bars in (A) represent 50 µm.

4.2.3 Overexpression of the dominant negative Ubc12 protein, Ubc12 C111S, blocks adipocyte differentiation

To corroborate the role of neddylation in adipogenesis by other means than using the pharmacological neddylation inhibitor MLN4924, differentiating 3T3-L1 adipocytes were transfected with a dominant negative Ubc12 protein. The point mutant Ubc12 C111S, in which the cysteine residue 111 was substituted by the amino acid serine, captures Nedd8 and prevents the following conjugation to substrate proteins (Wada et al., 2000). The effects of overexpressing the dominant negative Ubc12 enzyme on 3T3-L1 adipogenesis were evaluated by immunocytochemistry. Cells were co-transfected with Ubc12 C111S and a GFP-expression plasmid, subsequently cells were fixed, stained with ORO and GFP was detected by an α-GFP antibody. Thus, successfully transfected cells could be visualized by green fluorescence. Cells co-transfected with the dominant negative Ubc12 C111S did not differentiate into adipocytes (85 % of control cells differentiated into mature adipocytes, whereas only 21 % of Ubc12 C111S-transfected cells contained lipid droplets) (Figure 20A-

B). Thus, downregulation of the neddylation pathway with this genetic tool further reinforced the importance of neddylation in the regulation of adipogenesis.

A

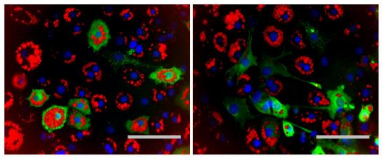

B

	without LD	with LD
Control	15 %	85 %
Ubc12 C111S	79 %	21 %

Figure 20: Overexpression of the dominant-negative Ubc12 protein blocks adipocyte differentiation. (A-B) 3T3-L1 cells were differentiated for two days in culture medium with MDI followed by insulin. Cells were co-transfected with a GFP expressing plasmid and either control or Ub12 C111S expressing vectors. Immunocytochemistry against GFP as well as ORO and DAPI staining was performed on day 14 after differentiation. **(A)** Representative images of fluorescence microscopy showing green fluorescent cells stained with ORO and DAPI (blue). **(B)** Quantification of green fluorescent cells that were regarded as successfully transfected cells (considered as 100 %) with or without lipid droplets (LD) by manual counting (n=100). Two-sample Z-test for proportions was performed for scoring of cells with or without lipid droplets after Ubc12C111S overexpression. $p<0.001$ (cells without LD Control vs. Ubc12C111S; cells with LD Control vs. Ubc12C111S). Scale bars in (A) represent 100 µm.

4.3 Neddylation is required for the maintenance of the adipocyte cellular morphology

Using both, genetic and pharmacological tools, we inhibited the neddylation pathway in order to evaluate the role of neddylation in adipocyte differentiation. We found that neddylation is required for adipocyte development. Consequently, we sought to define the role of neddylation in mature adipocytes.

4.3.1 MLN4924 treatment leads to lipid droplet loss in mature adipocytes

To examine the effects of neddylation blockade on mature adipocytes, 3T3-L1 cells were incubated every second day with different concentrations of MLN4924 and DMSO from day 8 of differentiation on. Since the expression of adipogenic proteins does not change significantly from 8 days after stimulation of adipogenesis on, these cells can be considered as fully developed adipocytes (Tamori et al., 2002). Lipid droplet content was evaluated by ORO staining. As shown in Figure 21A-B, blocking the neddylation pathway by MLN4924 treatment resulted in a dose- dependent lipid droplet loss in 3T3-L1 mature adipocytes respect to control cells. Higher MLN4924 concentrations were required to induce lipid droplet loss in mature adipocytes as 3 µM of the compound exerted the strongest effects. Thus, this concentration was used in all the following experiments regarding mature adipocytes.

Treatment of 3T3-L1 adipocytes with 3 µM MLN4924 revealed that the drug exhibits time-dependent effects on lipid droplet loss in mature adipocytes (Figure 21C-D).

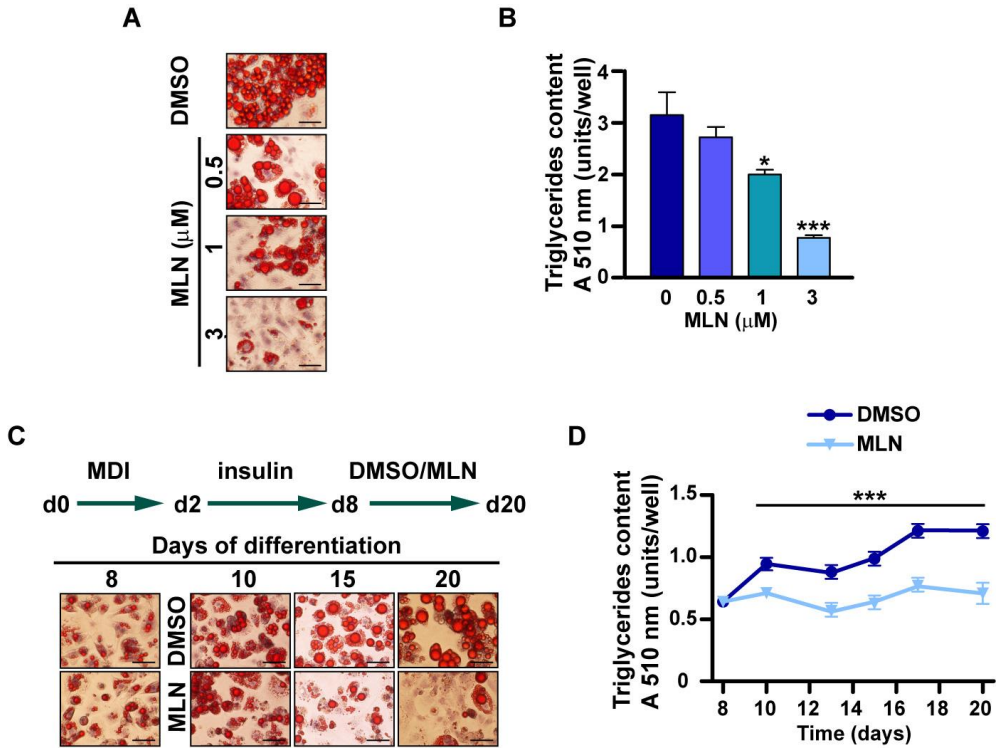

Figure 21: MLN4924 treatment reduces triglyceride content in a dose- and time-dependent manner. (A-B) 3T3-L1 cells were differentiated for two days in culture medium with MDI followed by insulin. Then, 3T3-L1 adipocytes were treated with DMSO or different concentrations of MLN from day 8 of differentiation on. Cells were stained with ORO and hematoxylin on day 17 of differentiation. **(A)** Representative images showing ORO and hematoxylin staining on day 17 of differentiation. **(B)** TG content was determined by quantifying ORO staining. **(C-D)** 3T3-L1 cells were differentiated for two days in culture medium with MDI followed by insulin. 3T3-L1 adipocytes were treated with DMSO or 3 µM MLN every second day from day 8 of differentiation on and stained with ORO and hematoxylin on different time points. **(C)** Schematic diagram showing culture conditions. Representative images showing ORO and hematoxylin staining at different time points after MLN treatment. **(D)** TG content was determined by quantifying ORO staining. Data are presented as mean ± SEM (n=3). Significance was determined by two-way ANOVA with Bonferroni's multiple comparison test. ∗p < 0.05 and ∗∗∗p < 0.001 DMSO vs. MLN treatment. Scale bars in (A,C) represent 50 µm.

In accordance with our findings obtained in 3T3-L1 cells, a substantial decrease in lipid droplet content was observed when neddylation was blocked by the pharmacological neddylation inhibitor in differentiated PCC from inguinal fat (Figure 22A-B).

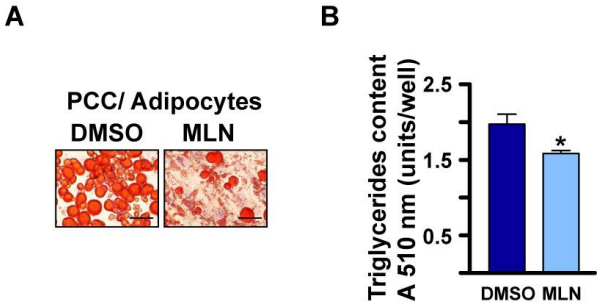

Figure 22: MLN4924 decreases triglyceride content in primary adipocytes. (A-B) PCC of inguinal fat were induced to differentiate by treating the cells for two days with MDI and rosiglitazone followed by insulin.

Subsequently, PCC were treated with DMSO or 3 µM MLN every second day from day 8 of differentiation on. ORO and hematoxylin staining was performed on day 14. **(A)** Representative images showing ORO and hematoxylin staining on day 14 of differentiation. **(B)** TG content was determined by quantifying ORO staining. Data are presented as mean ± SEM (n=3). Significance was determined by unpaired two-side t test. ∗p < 0.05 DMSO vs. MLN treatment.

Moreover, flow cytometry analysis of 3T3-L1 adipocytes revealed that DMSO-treated cells contained a population of large, high-scatter cells not observed in MLN4924-treated cells. Cells treated with the inhibitor rather displayed a similar profile as cells treated with the lipolytic drug isoproterenol, indicating a decreased intracellular lipid accumulation in both cultures (Figure 23). Taken together, this suggests that neddylation might control lipid storage in adipocytes. However, it is of note that compared to the effects on adipogenesis, in general the result of inhibiting neddylation in developed adipocytes was milder.

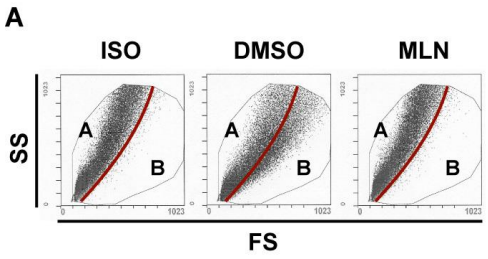

Figure 23: MLN4924 decreased intracellular lipid accumulation. (A-B) 3T3-L1 cells were differentiated for two days in culture medium with MDI followed by insulin. 3T3-L1 adipocytes were treated with DMSO or 3 µM MLN on day 8 of differentiation for 24 h or with 10 µM isoproterenol (ISO) for the last 1 h, respectively. Side scatter (SS) and forward scatter (FS) were determined by flow cytometry on day. **(A)** Representative flow cytometry plots showing gating scheme for 3T3-L1 cells based on size. Gates A and B represent the distribution of the dots in the plot after treatment with ISO. Gates were then applied to the DMSO and MLN plots. (B) Percentages of cells in region A and B are shown. Statistical significance was determined by Two-sample Z-test for proportions. DMSO vs ISO p< 0,001; DMSO vs MLN p<0.001, MLN vs ISO p=0.8810 n.s.

4.3.2 MLN4924-induced lipid droplet loss in adipocytes is reversible

We found that neddylation blockade using the pharmacological inhibitor MLN4924 induces lipid droplet loss in mature adipocytes. Notably, washing out the drug and applying the pro-lipogenic hormone insulin reverted the lipid droplet loss in 3T3-L1 adipocytes, indicating that treated cells preserved their adipocyte function and maintained the ability to store TG (Figure 24A-B). Accordingly, TG content of cells pre-treated with MLN4924 followed by insulin incubation was considerable elevated compared to cultures without insulin (Figure 24A-B). These results point to the fact that the lipid droplet loss in adipocytes triggered by neddylation blockade is reversible.

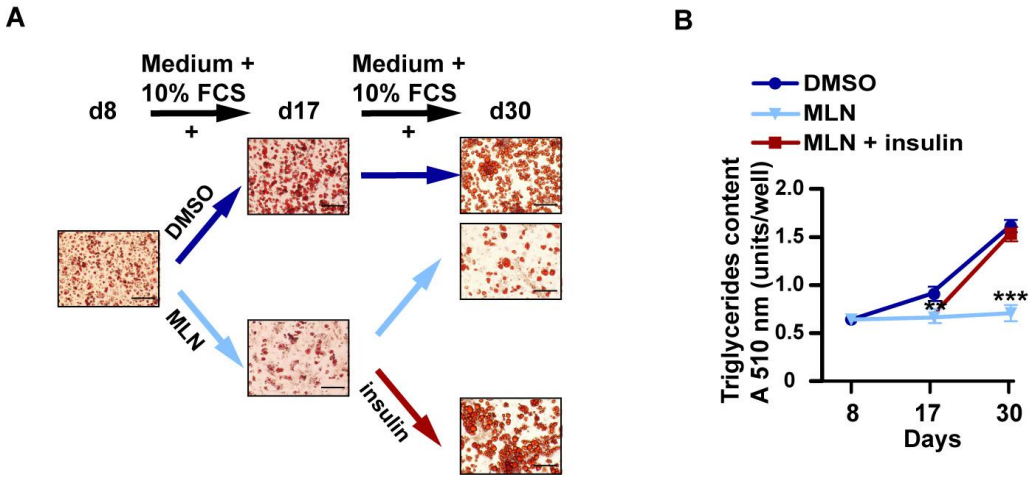

Figure 24: MLN4924-induced effects on lipid droplet loss can be reverted by adding the pro-lipogenic hormone insulin. (A-B) 3T3-L1 cells were differentiated for two days in culture medium with MDI followed by insulin. Then, 3T3-L1 adipocytes were treated with DMSO or 3 µM MLN every second day from day 8-17. Subsequently, cells were cultured with or without insulin until day 30. ORO and hematoxylin staining was performed at the indicated time points. **(A)** Schematic diagram showing culture conditions. Representative images showing ORO and hematoxylin staining at day 8, day 17 and day 30 of differentiation. **(B)** TG content was determined by quantifying ORO staining. Data are presented as mean ± SEM (n=3). Significance was determined by two-way ANOVA with Bonferroni's multiple comparison test. $**p < 0.01$ and $***p < 0.001$ DMSO vs. MLN treatment. Scale bars in (A) represent 50 µm.

4.4 Neddylation controls adipogenesis by modulating key adipogenic transcription factors

We identified neddylation as a critical regulatory pathway of adipocyte development and fat storage. Which signaling pathways involved in adipogenesis and lipid storage are controlled by neddylation? Which potential Nedd8 targets might contribute to this regulation?

4.4.1 MLN4924 treatment reduces C/EBPα and PPARγ expression during adipogenesis

We first sought to define the underlying molecular mechanisms causing the MLN4924-mediated inhibitory effects on adipogenesis. Adipocyte differentiation is a process, involving a cascade of transcription factors in addition to cell-cycle proteins which control gene expression and lead to adipocyte development. Also, various coactivators and negative regulators are necessary for this process (Farmer, 2006). The transcription factors C/EBPα and PPARγ are the master transcriptional regulators of adipogenesis and adipocyte function as they control the induction of many adipocyte-specific metabolic genes (Lefterova et al., 2008). Hence, western blotting and qRT-PCR analysis was performed in order to characterize the impact of MLN4924 treatment on the expression of these key transcription factors during 3T3-L1 adipocyte differentiation. For this purpose, 3T3-L1 differentiation was

induced by MDI in the presence of DMSO or 1 µM MLN4924 and protein or mRNA lysates were extracted at the indicated time points. Importantly, blockade of the neddylation pathway using the pharmacological inhibitor abrogated the mRNA and protein expression of the key transcription factors of the adipogenic gene program, C/EBPα and PPARγ (Figure 25A-B).

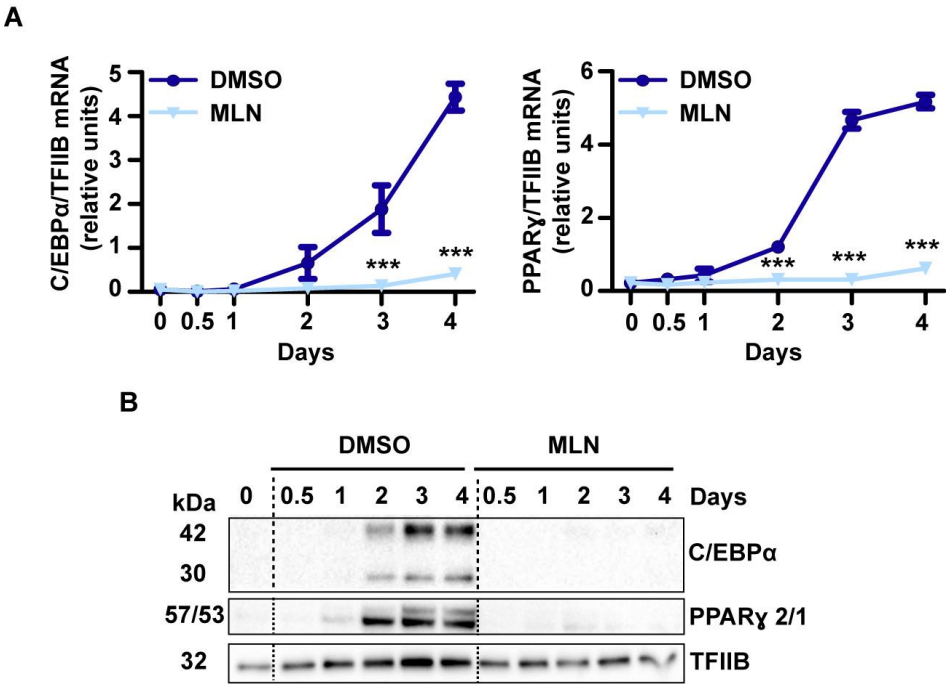

Figure 25: MLN4924 treatment inhibits C/EBPα and PPARγ expression. (A-B) 3T3-L1 cells were differentiated for two days in culture medium with MDI followed by insulin. During the first two days of differentiation cells were treated with DMSO or 1 µM MLN. **(A)** Relative mRNA levels of PPARγ and C/EBPα during 3T3-L1 adipocyte differentiation normalized to TFIIB. **(B)** Immunoblots of PPARγ and C/EBPα during 3T3-L1 adipocyte differentiation. Equal protein loading was confirmed by TFIIB expression. Data are presented as mean ± SEM (n=3). Significance was determined by two-way ANOVA with Bonferroni's multiple comparison test. ***p < 0.001 DMSO vs. MLN4924 treatment.

4.4.2 Neddylation exerts its effects upstream of PPARγ

Park et al. recently demonstrated that PPARγ neddylation is fundamental for its protein stability and is thus crucial for adipogenesis (Park et al., 2016). To examine the putative PPARγ neddylation we took advantage of the HEK293 cell line which is a valuable tool for protein binding studies. These cells are easy to culture, to transfect and do not express several adipocyte-specific proteins. As such, they provide a perfect low ‘noise’ cellular model for studying the biology of these proteins. To assess the impact of neddylation inhibition on PPARγ protein expression and stability, we analyzed protein extracts from HEK293 cells ectopically expressing FLAG-PPARγ2 by western blotting. Blocking the neddylation pathway by using the genetic tool Ubc12 C111S did not alter PPARγ protein expression (Figure 26A). Cycloheximide (CHX) is a protein synthesis inhibitor that allows monitoring the stability of

proteins. Making use of CHX chase assays, we found that MLN4924 treatment did not impair PPARγ protein stability (Figure 26B-C).

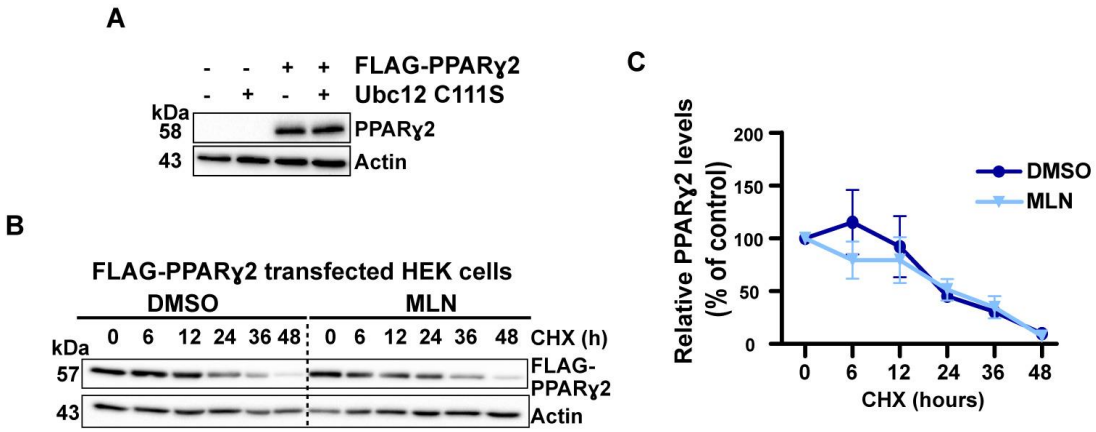

Figure 26: Neddylation inhibition does not affect PPARγ protein stability. (A) HEK293 cells were transiently transfected with FLAG-PPARγ and Ubc12 C111S constructs for 48 h. Immunoblotting against PPARγ was performed. Equal protein loading was confirmed by Actin expression. **(B-C)** For CHX chase assays, HEK293 cells were transiently transfected with FLAG-PPARγ and treated 24h later with DMSO or 1 µM MLN. CHX (20 µg/ml) was added to the cultures 12 h after treatment. Protein lysates were analyzed at different time points by immunoblotting. **(B)** Immunoblot using anti-FLAG antibody. Equal protein loading was confirmed by normalization to Actin expression. **(C)** Bands were densitometrically analyzed, normalized to the Actin bands and quantitative data are indicated as percentages of control values obtained from cells before CHX addition (time point 0). Data are presented as mean ± SEM (n=3). No statistical difference was determined by two-way ANOVA with Bonferroni's multiple comparison test.

Additionally, putative covalent binding of Nedd8 to PPARγ was judged by pull-down assays under denaturing conditions in which biotinylated Nedd8 (BIO-Nedd8) was purified using magnetic streptavidin beads and FLAG-PPARγ2 was visualized by western blotting with an α-PPARγ antibody. Given that we failed to detect PPARγ neddylation (Figure 27) and PPARγ protein stability was unaffected by neddylation inhibition (Figure 26), it remains controversial whether PPARγ is a target of neddylation that could mediate the effects of neddylation blockade on adipocyte differentiation and fat storage.

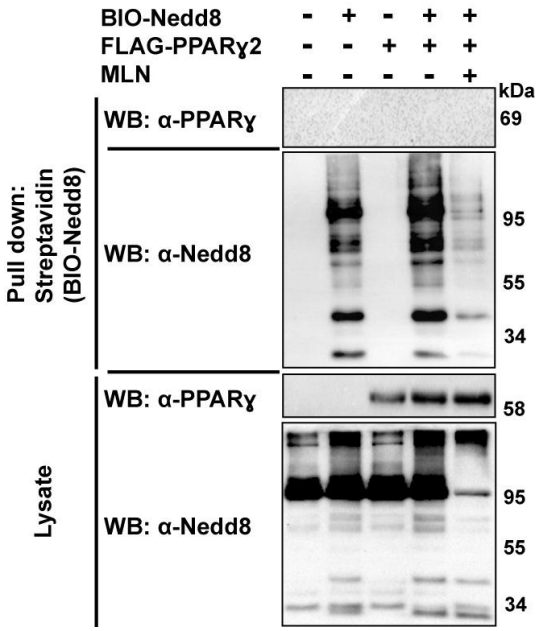

Figure 27: PPARγ is not neddylated. Extracts from HEK293 cells transfected with 6xHisBio-tagged Nedd8 (BIO-Nedd8) and FLAG-tagged PPARγ (FLAG-PPARγ) constructs for 72 h and treated with DMSO or 1 µM MLN and 10 µM MG-132 for the last 6 h were purified under denaturing conditions with streptavidin beads (Pull down: Streptavidin). Cell lysates and pull downs were analyzed by immunoblotting with antibodies as indicated.

We performed reversion experiments by co-treating MLN4924-treated 3T3-L1 adipocytes with rosiglitazone. The PPARγ agonist was able to restore the MLN4924-mediated effects on adipogenesis and lipid droplet loss (Figure 28). In adipocytes, PPARγ and C/EBPα expression is controlled by a cross-regulatory loop, which is important in the maintenance of adipocyte cell identity (Wu et al., 1999). Thus, in the presence of rosiglitazone, PPARγ might be able to boost its own expression. If PPARγ was a direct target of neddylation and its protein stability was negatively influenced by neddylation inhibition as claimed by Park et al. (Park et al., 2016), we would assume that rosiglitazone could not revert MLN4924-induced effects on adipogenesis and mature adipocytes. These data therefore suggest that neddylation may target proteins upstream of PPARγ during adipogenesis and in the lipid-filled adipocyte. As a consequence, PPARγ and C/EBPα expression might be compromised.

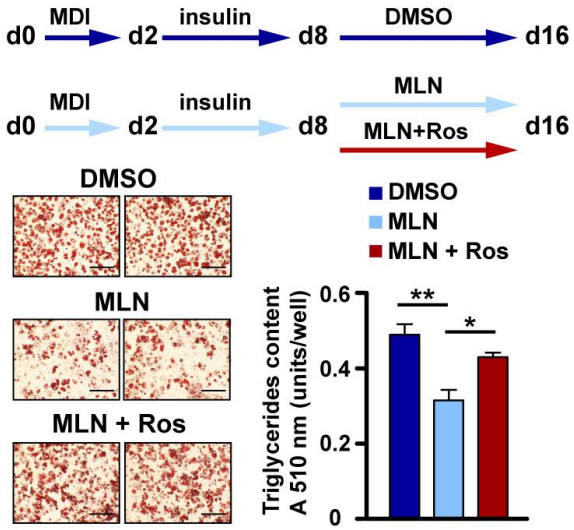

Figure 28: Rosiglitazone reverts MLN4924-induced effects on lipid storage. Schematic diagram showing culture conditions. 3T3-L1 cells were differentiated for two days in culture medium with MDI followed by insulin. 3T3-L1 adipocytes were treated with DMSO or 3 µM MLN alone or 3 µM MLN and 1 µM rosiglitazone (Ros) every second day from day 8-16. Representative images showing ORO and hematoxylin staining of 3T3-L1 cells on day 16 of differentiation. TG content was determined by quantifying ORO staining. Data are presented as mean ± SEM (n=3). Significance was determined by one-way ANOVA with Tukey's multiple comparison test. $*p < 0.05$ and $**p < 0.01$. Scale bars represent 200 µm.

4.4.3 Neddylation inhibition decreases C/EBPβ DNA binding and transcriptional activity during adipogenesis

C/EBPβ is an important element in the control of C/EBPα and PPARγ expression and therefore it is a crucial mediator of adipocyte development (Cao et al., 1991; Christy et al., 1991; Clarke et al., 1997; Wu et al., 1996; Wu et al., 1995). Due to the profound downregulation of PPARγ and C/EBPα, we aimed to delineate the effects of neddylation blockade on the expression of their upstream regulator C/EBPβ. Hence, 3T3-L1 cells were induced to differentiate, were treated with DMSO or 1 µM MLN4924 and protein and mRNA lysates were obtained at the indicated time points. Immunoblotting and qRT-PCR analysis demonstrated that neddylation inhibition did neither impact C/EBPβ protein nor mRNA levels (Figure 29A-B). However, as assessed by reporter gene assays using PPARγ- and C/EBPα-promoter-Luc reporter constructs, we found that the transcriptional activity of C/EBPβ was compromised when neddylation was blocked by Ubc12 C111S overexpression (Figure 29C-D). Thus, neddylation inhibition attenuates C/EBPβ transcriptional activity.

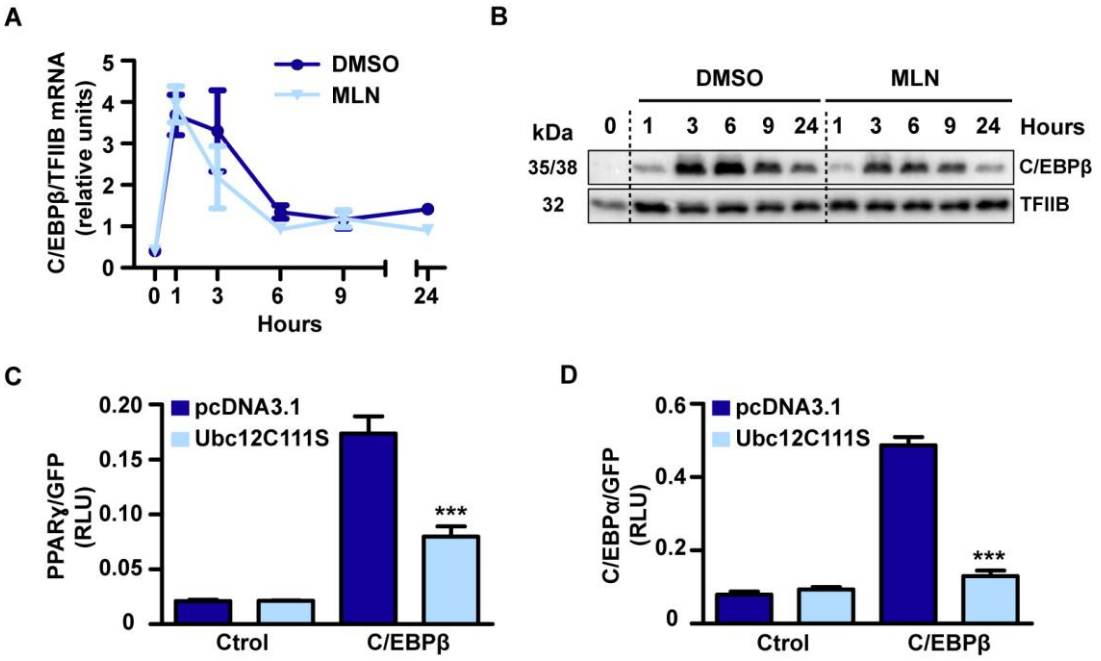

Figure 29: Neddylation inhibition attenuates C/EBPβ transcriptional activity. (A-B) 3T3-L1 cells were differentiated for two days in culture medium with MDI followed by insulin. During the first two days of differentiation cells were treated with DMSO or 1 µM MLN. **(A)** Relative mRNA levels of C/EBPβ during 3T3-L1 adipocyte differentiation normalized to TFIIB. **(B)** Immunoblot of C/EBPβ during treatment of differentiated 3T3-L1 cells. Equal protein loading was confirmed by TFIIB expression. **(C-D)** 3T3-L1 cells were transiently co-transfected on day 2 of differentiation with PPARγ promoter-luciferase (prom-LUC) or C/EBPα prom-Luc reporter construct and GFP-, C/EBPβ-, control- or Ubc12C111S- expression plasmids and incubated for 48 h. Relative luciferase units (RLU) were calculated by normalizing luciferase activity to GFP activity in the same sample. Data are presented as mean ± SEM (n=3). Significance was determined by two-way ANOVA with Bonferroni's multiple comparison test. ***p < 0.001 control vs. Ubc12 C111S.

Neddylation could modulate protein activity via different mechanisms, like altering protein stability, protein-protein and protein-DNA interactions, as well as cellular localization (Enchev et al., 2015). We examined the impact of neddylation blockade on C/EBPβ protein stability in 3T3-L1 cells by performing a CHX chase assay. For this purpose, we treated 3T3-L1 cells with DMSO or 1 µM MLN4924 simultaneously with the induction of differentiation by MDI. After 12 h, cells were additionally treated with 20 µg/ml CHX and proteins were extracted at the indicated time points. As revealed by this assay, C/EBPβ protein stability remained unaffected by neddylation inhibition (Figure 30A). The decrease in C/EBPβ transcriptional activity could be secondary to changes in cellular localization. Following a subcellular fractionation protocol in 3T3-L1 cells, we observed that neddylation inhibition does not change the cellular localization of C/EBPβ, which was exclusively found in the nucleus (Figure 30B). Because of its bZIP domain C/EBPβ can homodimerize, which facilitates the binding to certain DNA regulatory regions, consequently activating transcription (Landschulz et al., 1989; Williams et al., 1991). We tested if impaired C/EBPβ homodimerization induced by neddylation blockade might account for the reduced C/EBPβ transcriptional activity. By pull down analysis in HEK293 cells expressing FLAG-tagged- as well as 6xHisBio-

tagged- C/EBPβ (FLAG-C/EBPβ and BIO-C/EBPβ), we could show that neddylation blockade does not impair C/EBPβ homodimerization (Figure 30C). Considering that neddylation inhibition did neither affect C/EBPβ protein stability, homodimerization nor cellular localization, we hypothesized that neddylation might directly influence the C/EBPβ DNA binding to regulatory gene elements. Thus, chromatin immunoprecipitation coupled with quantitative real-time PCR (ChIP-qRT-PCR) was employed in order to study C/EBPβ binding to the PPARγ promoter in the presence of the neddylation inhibitor. Therefore, we analyzed C/EBPβ binding to the PPARγ promoter in lysates of undifferentiated and one-day-differentiated 3T3-L1 cells that were treated with DMSO or 1 µM MLN4924 and purified C/EBPβ using an α-C/EBPβ antibody or IgG as control. This experiment revealed that, indeed, MLN4924 treatment dramatically attenuates the binding of C/EBPβ to the PPARγ promoter (Figure 30D), proposing neddylation modulates C/EBPβ DNA binding and by this mechanism controls its transcriptional activity which is critical for PPARγ and C/EBPα expression. Taken together, these data strongly suggest that modulation of C/EBPβ DNA binding and consequently transcriptional activity by neddylation inhibition may account for the attenuation of adipogenesis. Even though we cannot exclude the participation of other proteins in mediating the effects of neddylation inhibition on adipocyte differentiation, C/EBPβ may be at least one of the neddylation targets involved in the regulation of adipogenesis.

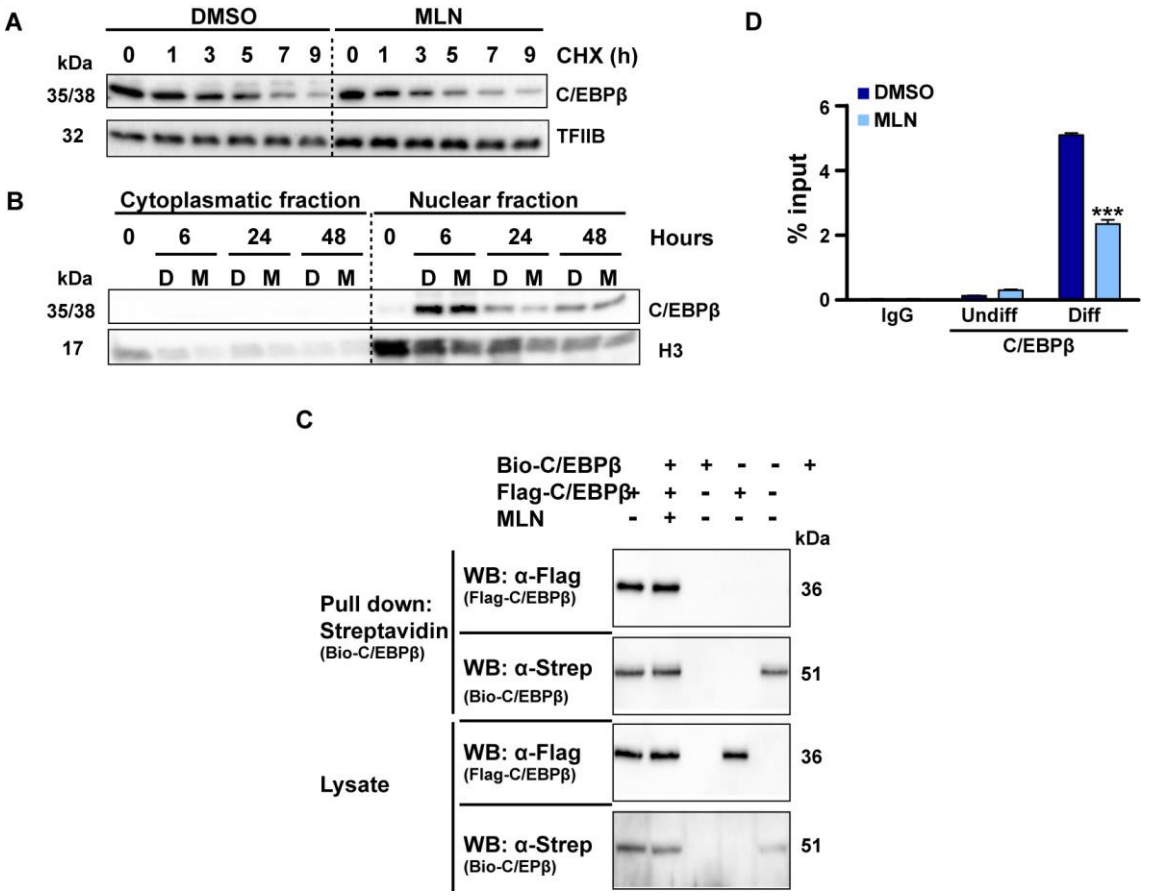

Figure 30: MLN4924 treatment reduces C/EBPβ DNA binding activity but does not affect C/EBPβ protein stability, localization and homodimerization. (A) For CHX chase assays, 3T3-L1 cells were induced to differentiate with MDI and treated with DMSO or 1 µM MLN. CHX (20 µg/ml) was added to the cultures 12 h after treatment. Lysates were analyzed at different time points by immunoblotting against C/EBPβ. Equal protein loading was confirmed by normalization to TFIIB expression. **(B)** 3T3-L1 cells were induced to differentiate and treated with DMSO (D) or 1 µM MLN4924 (M). A cellular fractionation protocol was employed at the indicated time points. Cytoplasmic and nuclear fractions were analyzed by immunoblotting against C/EBPβ. Histone H3 confirms separation of the cytosolic and nuclear fractions. **(C)** Extracts from HEK293 cells transfected for 72 h with 6xHisBio-tagged C/EBPβ (BIO-C/EBPβ) and FLAG-tagged C/EBPβ (FLAG-C/EBPβ) and treated with DMSO or 1 µM MLN and 10 µM MG-132 for the last 6 h were purified under non-denaturing conditions with streptavidin beads (Pull down: Streptavidin). Cell lysates and pull downs were analyzed by immunoblotting with antibodies as indicated. **(D)** Results from ChIP-qRT-PCR assays for C/EBPβ binding to the PPARγ gene promoter performed in 3T3-L1 cells 24 h after differentiation or in undifferentiated cells in the presence of DMSO or 1 µM MLN. Amounts of immunoprecipitated DNA were normalized to inputs. IgG was used as a negative control. Data are presented as mean ± SEM (n=3). Significance was determined by two-way ANOVA with Bonferroni's multiple comparison test. ***p < 0.001 DMSO vs. MLN treatment.

4.4.4 Neddylation inhibition does not affect adipogenic factors regulating C/EBPβ expression and activity

The induction of differentiation and the following activation of early adipogenic factors is promoting the expression or modulating the activity of the key transcription factor C/EBPβ (Farmer, 2006). Thus, we screened for potential neddylation targets among factors driving early adipogenesis and orchestrating the metabolic program of adipocytes upstream of C/EBPβ. Therefore, adipocyte differentiation was induced in 3T3-L1 cells by MDI, cells were

treated with DMSO or 1 µM MLN4924 and protein lysates were extracted at the indicated time points. Immunoblotting revealed that the activation by phosphorylation of different important factors induced during early adipocyte development, such as Erk1/2, Akt and CREB, was not altered under MLN4924 treatment respect to control cells (Figure 31). Moreover, comparable unphosphorylated protein expression was found between treated and control cultures.

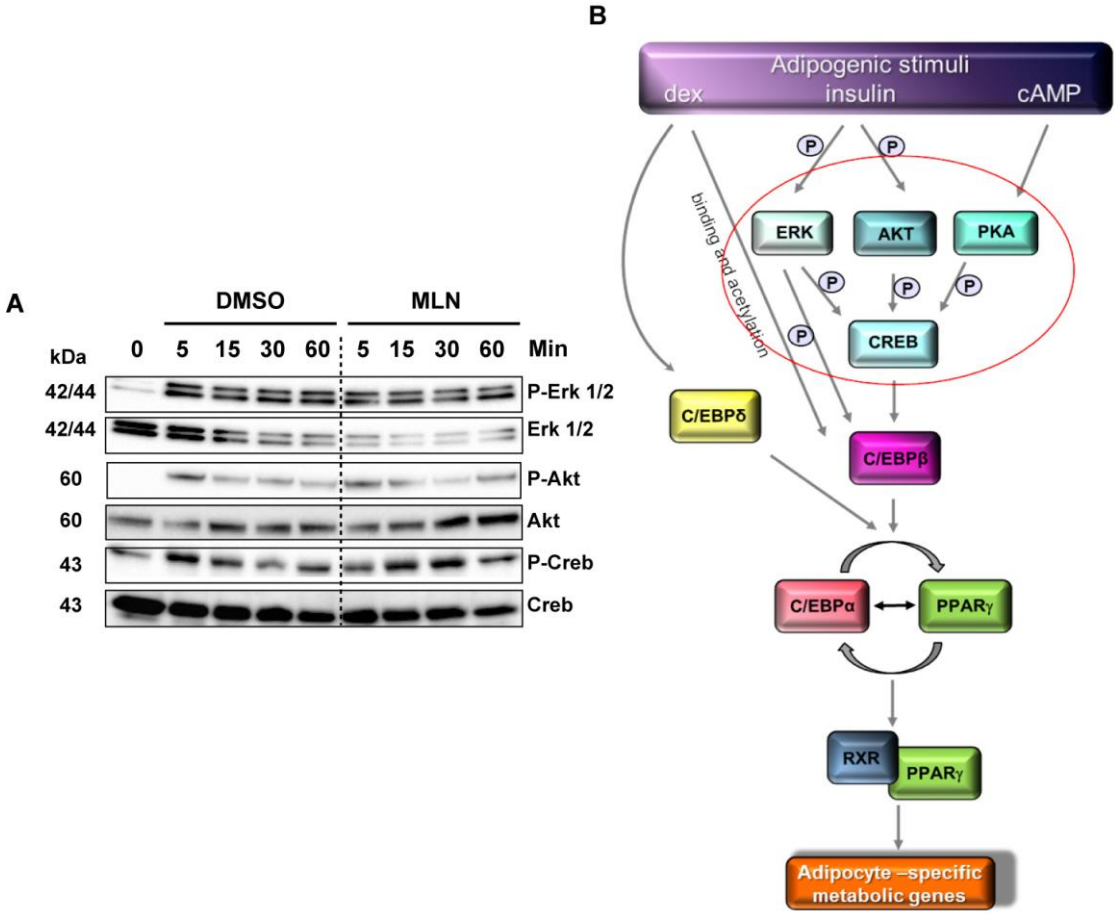

Figure 31: MLN4924 treatment does not control activation of early adipogenic factors. (A) 3T3-L1 cells were differentiated for two days in culture medium with MDI followed by insulin. During the first two days of differentiation cells were treated with DMSO or 1 µM MLN. Protein lysates were extracted at the indicated time points during treatment of differentiating 3T3-L1 cells. Immunoblots of the indicated proteins are shown. **(B)** Simplified scheme to illustrate the role of the early adipogenic transcription factors investigated (highlighted with red circle) in the process of adipogenesis.

Elevation of intracellular cAMP levels has been associated with crucial events in the early program of adipocyte differentiation (Petersen et al., 2008). Radioimmunoassays were employed to assess the impact of neddylation inhibition on intracellular cAMP concentrations. For this purpose, 3T3-L1 cells were differentiated, treated with DMSO, 1 µM MLN4924 or 5 µM forskolin and intracellular cAMP was extracted. As depicted in Figure 32, basal intracellular cAMP levels remained unaffected by MLN4924 treatment. Forskolin induced the rise in intracellular cAMP production by activating the adenylyl cyclase. The

resulting increase in intracellular cAMP concentration was not affected by the pharmacological inhibitor, indicating that neddylation may not regulate the induction of cAMP release (Figure 32).

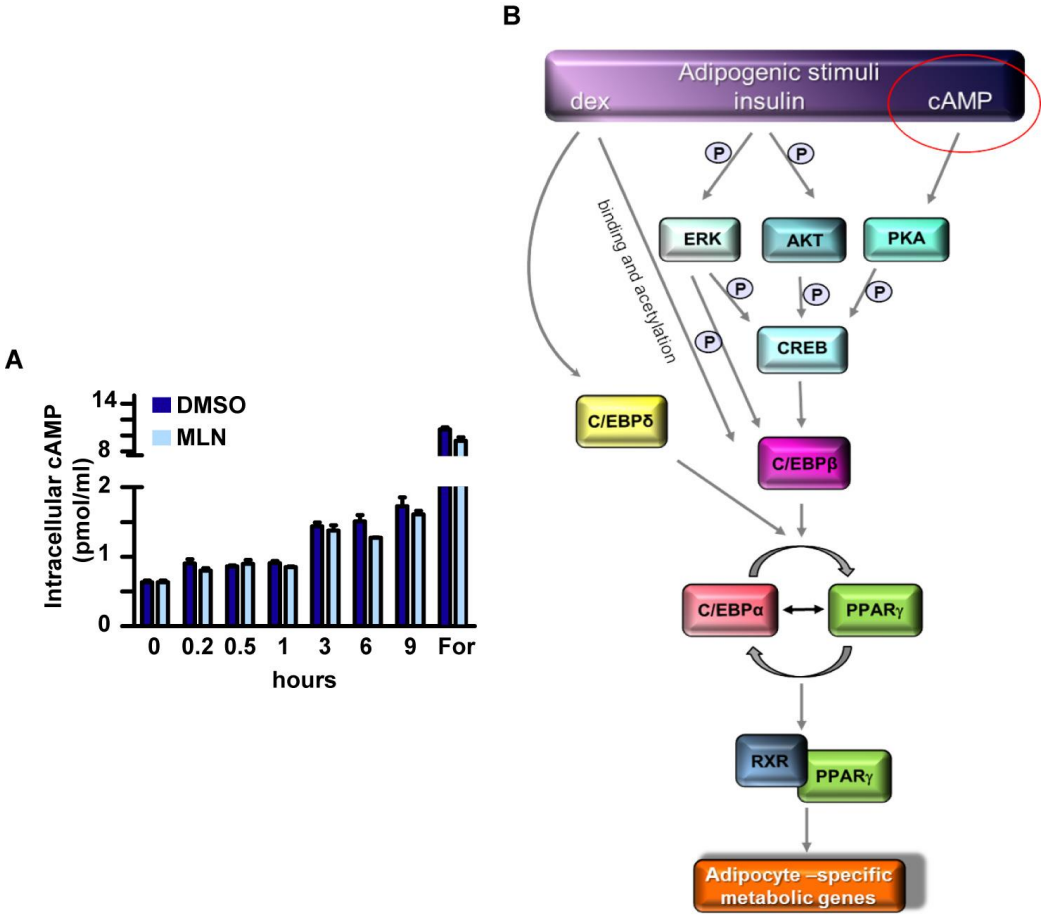

Figure 32: MLN4924 treatment does not affect intracellular cAMP levels. (A) 3T3-L1 cells were serum deprived for 4 h. 0.115 µg/ml IBMX, 1 µg/ml insulin and 10 % FCS were added together with DMSO or 1 µM MLN or 5 µM forskolin (For) to the cultures. cAMP levels were measured after the indicated time periods. Data are presented as mean ± SEM (n=3). No statistical difference was determined by one-way ANOVA with Bonferroni's multiple comparison test. **(B)** Simplified scheme to illustrate the role of cAMP (highlighted with red circle) in the process of adipogenesis.

Due to the importance of GR activation in adipocyte differentiation (Rubin et al., 1978), we assessed the ability of neddylation blockade to modulate the dexamethasone-induced transcription of the MTV promoter, which serves as a readout for GR activity. For this purpose, we made use of reporter gene assays in 3T3-L1 cells in which neddylation was blocked by MLN4924 treatment. These assays indicated that neddylation inhibition had no effect on GR signaling. Particularly, GR activation was not affected by treatment with the inhibitor neither under supplementation of normal MDI nor dexamethasone alone (Figure 33). Reduced GR activation in the absence of dexamethasone confirmed the specificity of the system (Figure 33). Altogether, neddylation inhibition did not affect the factors contributing to adipogenesis investigated that act upstream of C/EBPβ.

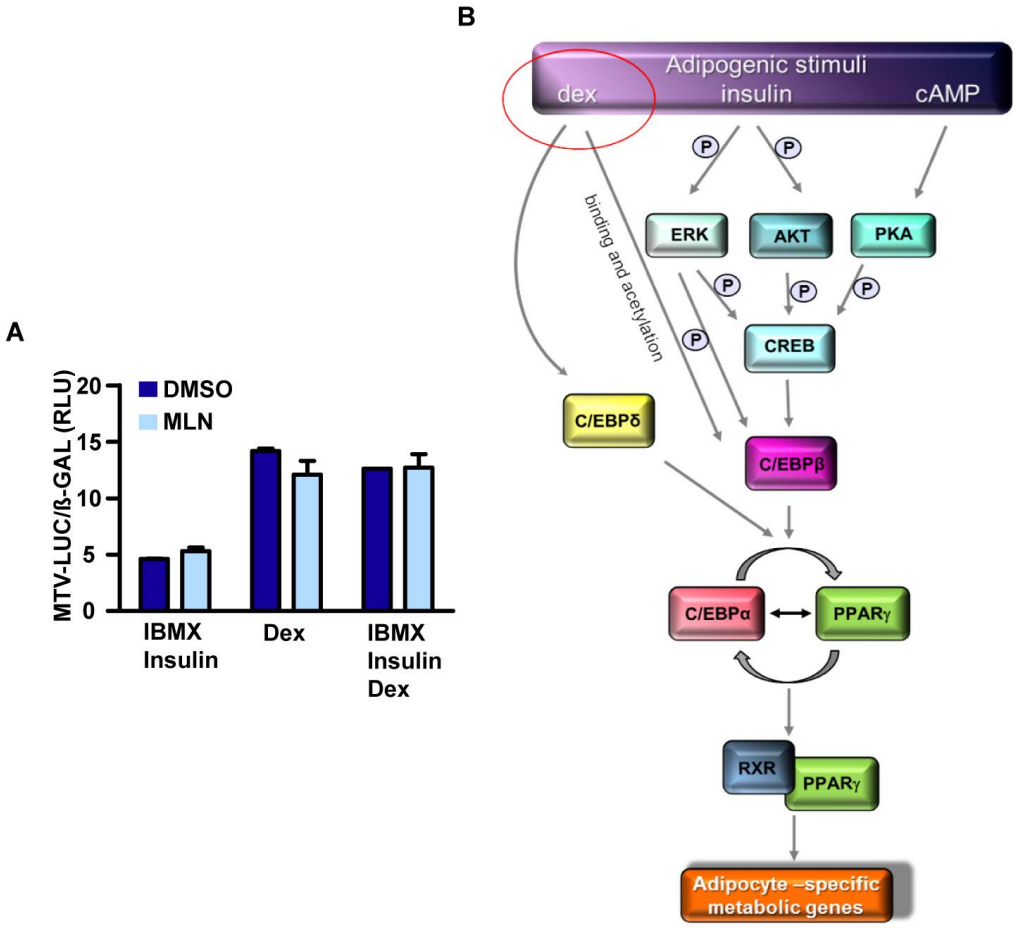

Figure 33: MLN4924 treatment does not impact GR signaling. (A) 3T3-L1 cells were transfected with MTV promoter-luciferase (MTV-LUC) and β-galactosidase (β-GAL) constructs. Cells were cultured in Std. medium containing IBMX and insulin, dexamethasone (Dex) alone or IBMX, insulin and Dex (MDI) and treated with DMSO or 1 µM MLN. RLU were calculated by normalizing luciferase activity to β-GAL activity in the same sample. Data are presented as mean ± SEM (n=3). No statistical difference was determined by one-way ANOVA with Bonferroni's multiple comparison test. **(B)** Simplified scheme to illustrate the role of dexamethasone-mediated GR signaling (highlighted with red circle) in the process of adipogenesis.

4.4.5 C/EBPβ is a target of neddylation

The finding that C/EBPβ transcriptional activity and DNA binding was markedly reduced and that the factors controlling C/EBPβ expression and activity remained unaffected by neddylation inhibition points towards C/EBPβ as a potential Nedd8 target. To examine the putative C/EBPβ neddylation we again took advantage of the HEK293 cell line. Therefore, we first validated the suppression of C/EBPβ transcriptional activity on the PPARγ promoter by genetic neddylation inhibition in these cells (Figure 34).

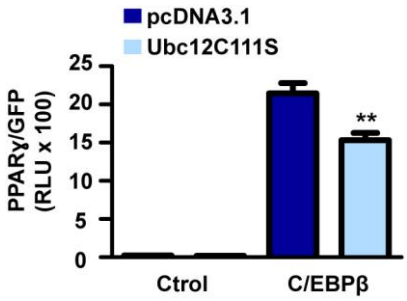

Figure 34: Neddylation inhibition decreases C/EBPβ transcriptional activity in HEK293 cells. HEK293 cells were transiently co-transfected with PPARγ promoter-luciferase (prom-LUC) reporter construct and GFP-, C/EBPβ-, control- or Ubc12C111S- expression plasmids and incubated for 48 h. RLU were calculated by normalizing luciferase activity to GFP activity in the same sample. Data are presented as mean ± SEM (n=3). Significance was determined by two-way ANOVA with Bonferroni's multiple comparison test. $**p < 0.01$ control vs. Ubc12 C111S.

Next, we studied the putative covalent binding of Nedd8 to C/EBPβ by pull-down assays. Biotin-tagged Nedd8 (6xHisBio-tagged Nedd8 (BIO-Nedd8)) and FLAG-tagged C/EBPβ (FLAG-C/EBPβ) or vice versa 6xHisBio-tagged C/EBPβ (BIO-C/EBPβ) and 3xFLAG-tagged Nedd8 (FLAG-Nedd8) were ectopically expressed in HEK293 cells and biotin-tagged proteins were pulled down by direct binding to magnetic streptavidin beads and analyzed by WB. These assays revealed two distinct bands of neddylated C/EBPβ, indicating a di-neddylation of the protein (Figure 35A-B). The observed bands were drastically reduced by the treatment with the specific neddylation inhibitor MLN4924 (Figure 35A-B), strongly suggesting that C/EBPβ is neddylated. Substrate proteins are targeted by Nedd8 on specific lysine residues (Xirodimas, 2008). As a control experiment, we created a HisBio-tagged C/EBPβ lysine null version (BIO-C/EBPβ mut), in which all lysines were mutated to arginines, thus preventing a putative neddylation of the protein. Indeed, the C/EBPβ mutant construct was not undergoing neddylation, as shown by pull down assays (Figure 35C). In summary, these experiments emphasized that C/EBPβ is a true bona fide target of Nedd8.

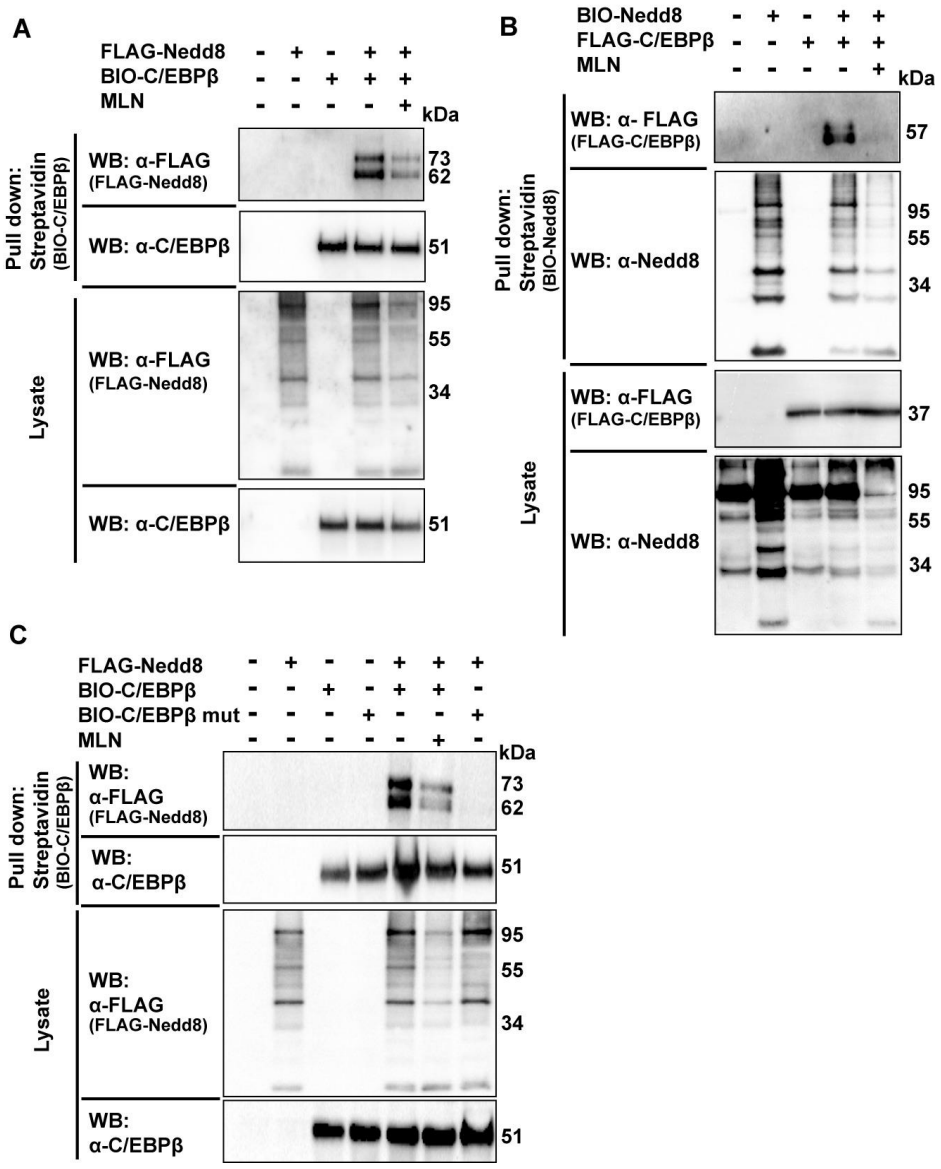

Figure 35: C/EBPβ is neddylated in HEK293 cells. (A-C) Extracts from HEK293 cells transfected for 72 h with **(A)** FLAG-tagged Nedd8 (FLAG-Nedd8) and 6xHisBio-tagged C/EBPβ (BIO-C/EBPβ), **(B)** BIO-Nedd8 and FLAG-C/EBPβ or **(C)** BIO-C/EBPβ or BIO-C/EBPβ mut and FLAG-Nedd8 constructs and treated with DMSO or 1 µM MLN and 10 µM MG-132 for the last 6 h were purified under denaturing conditions with streptavidin beads (Pull down: Streptavidin). Cell lysates and pull downs were analyzed by immunoblotting with antibodies as indicated.

4.5 Neddylation regulates lipid metabolism and insulin sensitivity in differentiated adipocytes

As shown above, we discovered that neddylation is crucial for maintaining the TG storage capacity. Accordingly, we explored the underlying molecular mechanisms responsible for the reduction in lipid droplet content triggered by neddylation inhibition.

4.5.1 Neddylation inhibition impairs the expression of adipocyte-specific metabolic genes

A balance between lipogenesis to synthesize TG and lipolysis is crucial for the function of a healthy adipocyte (Rutkowski et al., 2015). Both, an enhancement of lipolysis or a reduction of FA uptake and lipogenesis could potentially lead to a decrease in TG content of adipocytes. Thus, we aimed to specify the effects of neddylation blockade on these two cellular processes. In this regard, lipolysis assays were conducted. For this purpose, 3T3-L1 adipocytes (day 8 of differentiation) were treated with DMSO, 3 µM MLN4924 or 1 µM isoproterenol. FA release by 3T3-L1 adipocytes was evaluated by determining the FA content in the medium after treatment. Surprisingly, MLN4924-treated cells displayed a decrease in FA release in the medium after 1 and 3 hours, pointing to a deterioration of lipolysis in these cells (Figure 36). Nevertheless, under stimulated conditions using isoproterenol, MLN4924-treated cells still conserved the ability to perform lipolysis to the same extent as control cells, indicating that the induced lipolytic activity on adipocytes under neddylation blockade is not impaired (Figure 36). After 24 and 48 hours treatment, we observed that control cells re-uptake the FAs from the medium in order to use them for TG synthesis (Figure 36). Strikingly, in MLN4924-cultured cells FA levels were found to be increased in the medium after 24 and 48 hours of treatment in respect to controls, indicating that impaired fatty acid uptake and re-utilization might be responsible for the lipid droplet loss in adipocytes upon neddylation inhibition (Figure 36).

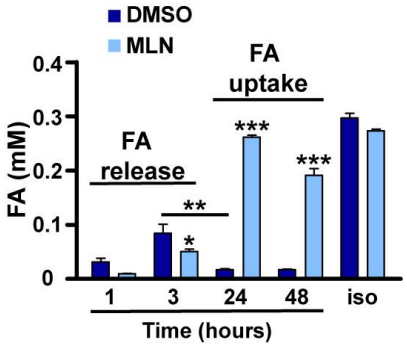

Figure 36: MLN4924 treatment decreases lipolysis and fatty acid uptake. Time course of FA release from differentiated 3T3-L1 cells was obtained. 3T3-L1 cells were differentiated for two days in culture medium with MDI followed by insulin. On day 14 of differentiation, medium was exchanged for assay medium and cells were treated with DMSO or 3 µM MLN for the indicated time points. FA concentration was assessed in the medium using a lipolysis assay kit. Results from FA release after 1h incubation with 10 µM isoproterenol (iso) are also shown. Data are presented as mean ± SEM (n=3). Statistical significance is shown as $*p \leq 0.05$, $**p \leq 0.01$, $***p \leq 0.001$. Significance was determined by two-way ANOVA with Bonferroni's multiple comparison test or by one-way ANOVA with Bonferroni's multiple comparison test (DMSO 3 h vs 24 h).

Apart from its role in adipogenesis, PPARγ plays a key role in the regulation of TG synthesis in mature adipocytes, controlling processes like FA uptake and lipogenesis (Ahmadian et al., 2013; Kersten, 2001). Thus, we examined if changes in PPARγ expression could account for

the lower lipid content in MLN4924-treated cells. Indeed, when 3T3-L1 adipocytes were treated with 3 µM of the inhibitor from day 8 of differentiation on, mRNA and protein levels of PPARγ were massively downregulated in respect to control cells (Figure 37A-B). Moreover, C/EBPα mRNA and protein expression was severely impaired (Figure 37A-B).

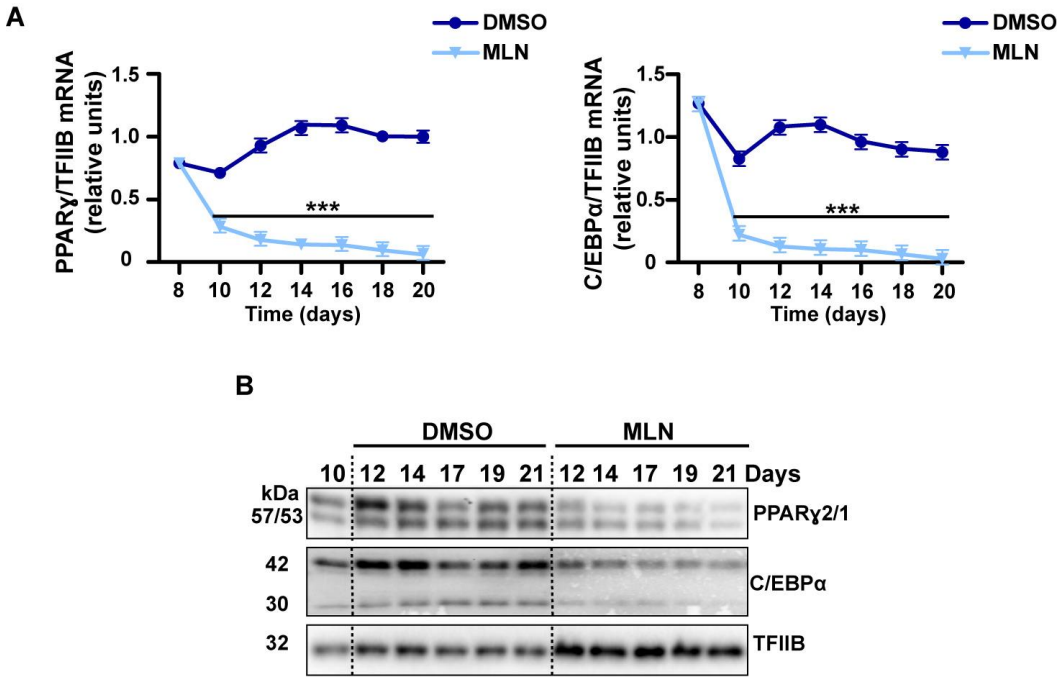

Figure 37: MLN4924 treatment reduces the expression of PPARγ and C/EBPα. (A-B) 3T3-L1 cells were differentiated for two days in culture medium with MDI followed by insulin. Differentiated 3T3-L1 cells were treated every second day with DMSO or 3 µM MLN from day 8 of differentiation on. **(A)** Relative mRNA levels of PPARγ and C/EBPα in 3T3-L1 cells during treatment normalized to TFIIB expression. **(B)** Immunoblots of PPARγ and C/EBPα during treatment of differentiated 3T3-L1 cells. Equal protein loading was confirmed by TFIIB expression. Data are presented as mean ± SEM (n=3). Significance was determined by two-way ANOVA with Bonferroni's multiple comparison test. ***p < 0.001 DMSO vs. MLN treatment.

C/EBPα and PPARγ are key regulators of TG synthesis and glucose homeostasis in mature adipocytes. PPARγ activates many adipocyte genes involved in FA uptake, like LPL, CD36, FATP1 and FABP4 (Chawla and Lazar, 1994; Martin et al., 2000; Nagy et al., 1998; Schoonjans et al., 1996; Tontonoz et al., 1994a) and TG hydrolysis, such as HSL (Deng et al., 2006). The PPARγ downstream targets involved in lipid metabolism, like LPL, FATP1, FABP4, CD36 and HSL, were profoundly reduced in MLN4924-treated compared to DMSO-treated cells (Figure 38A). Consequently, lipid metabolism in adipocytes was compromised when neddylation was inhibited.

Furthermore PPARγ is able to induce genes involved in glyceroneogenesis, like PEPCK (Tontonoz et al., 1995), insulin signaling and glucose uptake, including IRS2 and GLUT4 (Smith et al., 2001; Wu et al., 1998) and adipokines, such as adiponectin (Gustafson et al., 2003). MLN4924 treatment downregulated the mRNA expression of genes involved in glucose metabolism, like PEPCK, GLUT4, IRS2 and adiponectin (Figure 38B).

TG are synthesized by FA, which partially origin from *de novo* lipogenesis (Saponaro et al., 2015). Neddylation inhibition markedly decreased transcription of genes involved in lipogenesis, like SREBP1c, FAS and ACC1 (Figure 38C), even though they are not under the control of PPARγ. This indicates that neddylation inhibition completely impaired adipocyte function.

PPARγ was reported to suppress inflammation and PPARγ activation attenuates MCP1 expression (Panzer et al., 2002; Sharma and Staels, 2007). Therefore, we tested the effects of MLN4924-mediated PPARγ downregulation on MCP1 mRNA levels. In fact, neddylation inhibition massively enhanced the expression of MCP1 in 3T3-L1 cells (Figure 38D).

In conclusion, these observations likely indicate that neddylation is essential to promote lipid accumulation and adipokine secretion by modulating PPARγ and C/EBPα expression. Downregulation of these master genes resulted in the dramatic decrease of their adipocyte-specific downstream target genes, impaired adipocyte function and might additionally trigger pro-inflammatory pathways.

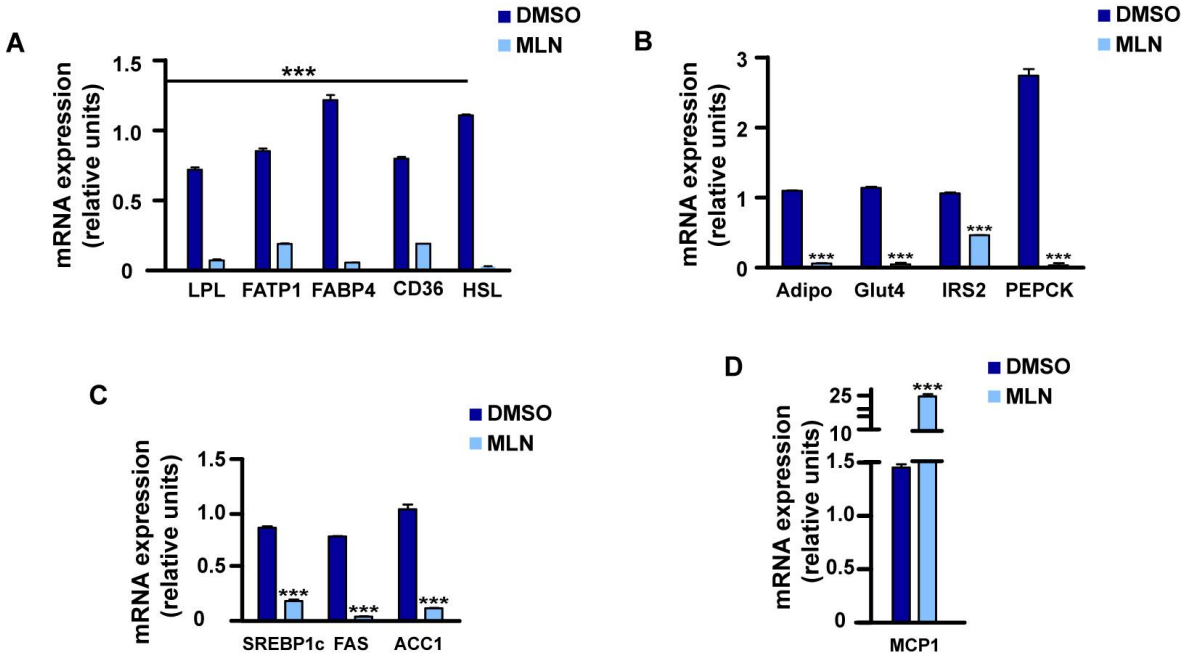

Figure 38: MLN4924 treatment decreases the expression of adipocyte-specific genes. (A-D) 3T3-L1 cells were differentiated for two days in culture medium with MDI followed by insulin. Differentiated 3T3-L1 cells were treated every second day with DMSO or 3 µM MLN from day 8 of differentiation on. Relative mRNA levels of the indicated genes involved in FA uptake, glucose transport and insulin signaling, glyceroneogenesis, lipogenesis and inflammation in 3T3-L1 cells on day 20 of differentiation. mRNA levels were normalized to TFIIB expression. Data are presented as mean ± SEM (n=3). Significance was determined by unpaired two-side t test. ***p < 0.001 DMSO vs. MLN treatment.

4.5.2 Neddylation blockade decreases C/EBPα and PPARγ expression by inhibiting C/EBPβ transcriptional activity in mature adipocytes

As shown above, decreased PPARγ and C/EBPα levels were observed, when 3T3-L1 mature adipocytes were treated with the neddylation inhibitor MLN4924. Since we have identified C/EBPβ as a putative target of neddylation in preadipocytes and because C/EBPβ is an important regulator of PPARγ expression also in the mature adipocyte (Lefterova et al., 2008), we aimed to further unravel the effects of neddylation inhibition on C/EBPβ in differentiated 3T3-L1 cells. In this context, we treated 3T3-L1 cells from day 8 of differentiation on with DMSO or 3 µM MLN4924 and we studied the effects of neddylation inhibition on C/EBPβ expression. As observed in 3T3-L1 preadipocytes, we found that C/EBPβ mRNA as well as protein levels remained unaffected by MLN4924 treatment (Figure 39A-B). Further, we observed a decreased C/EBPβ transcriptional activity on CEBPα and PPARγ promoters in mature adipocytes in luciferase reporter assays (Figure 39C-D). Altogether these results provide strong evidence that neddylation might be required for adipocyte cellular identity and function and point towards C/EBPβ as a potential neddylation target also in differentiated adipocytes.

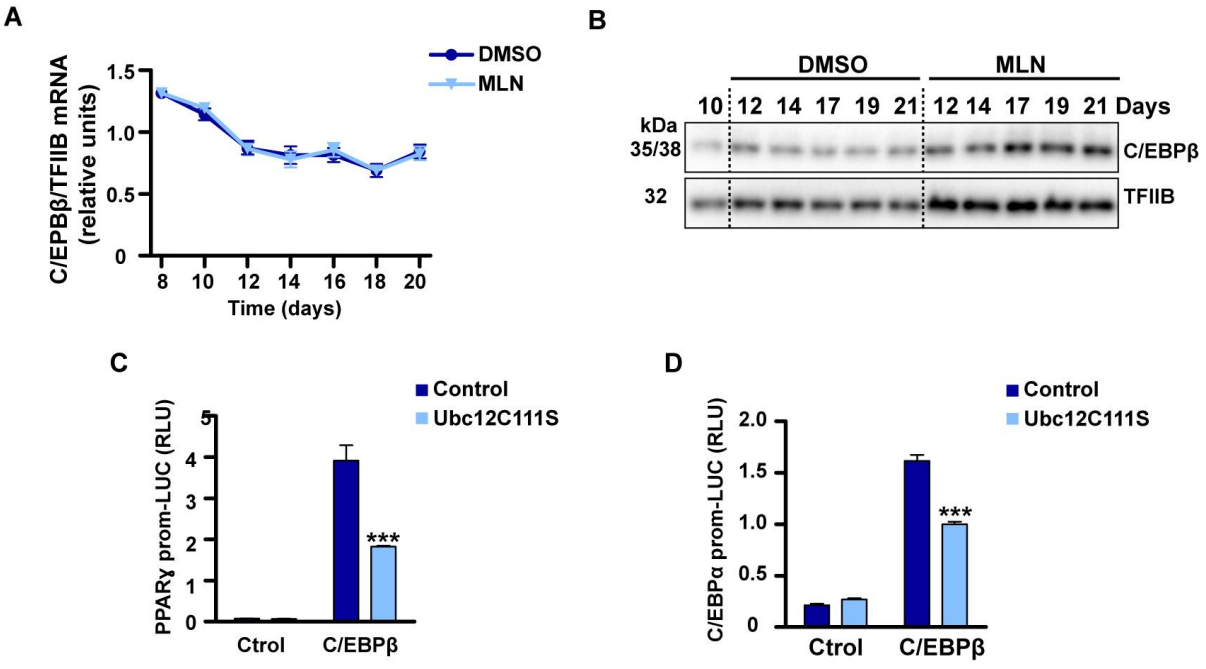

Figure 39: Neddylation inhibition reduces C/EBPβ transcriptional activity in adipocytes. (A-B) 3T3-L1 cells were differentiated for two days in culture medium with MDI followed by insulin. Differentiated 3T3-L1 cells were treated every second day with DMSO or 3 µM MLN4924 (MLN) from day 8 of differentiation on. **(A)** Relative mRNA levels of C/EBPβ in 3T3-L1 cells during treatment normalized to TFIIB expression. **(B)** Immunoblot of C/EBPβ during treatment of differentiated 3T3-L1 cells. Equal protein loading was confirmed by TFIIB expression. **(C-D)** Differentiated 3T3-L1 cells were transiently co-transfected on day 8 of differentiation with PPARγ promoter-luciferase (prom-LUC) or C/EBPα prom-Luc reporter construct and GFP-, C/EBPβ-, control- or Ubc12C111S-expression plasmids and incubated for 48 h. RLU were calculated by normalizing luciferase activity to GFP activity in the same sample. Data are presented as mean ± SEM (n=3). Significance was determined by two-way ANOVA with Bonferroni's multiple comparison test. ***p < 0.001 control vs. Ubc12 C111S.

4.6 Neddylation increases in obese mice

Our *in vitro* data point to an important regulatory role of the neddylation pathway in adipocyte development and function. These results encouraged us to characterize the physiological relevance of AT neddylation *in vivo*. It is well-established that feeding an obesogenic HFD (45 kcal%) for 8 weeks induces obesity and insulin resistance (de Wilde et al., 2009). Therefore, we followed this approach for inducing obesity in mice. First, we explored the relevance of neddylation in obesity by examining the pattern of neddylated proteins in AT of mice receiving either chow diet or HFD for 8 weeks. We found an increase in neddylated proteins in subcutaneous (sc) WAT of HFD-fed mice in comparison to chow-fed animals, whereas we did not detect a difference in the visceral (vis) WAT between HFD- and chow-fed mice (Figure 40). This observation suggests that Nedd8 conjugation might be involved in obesity in mice.

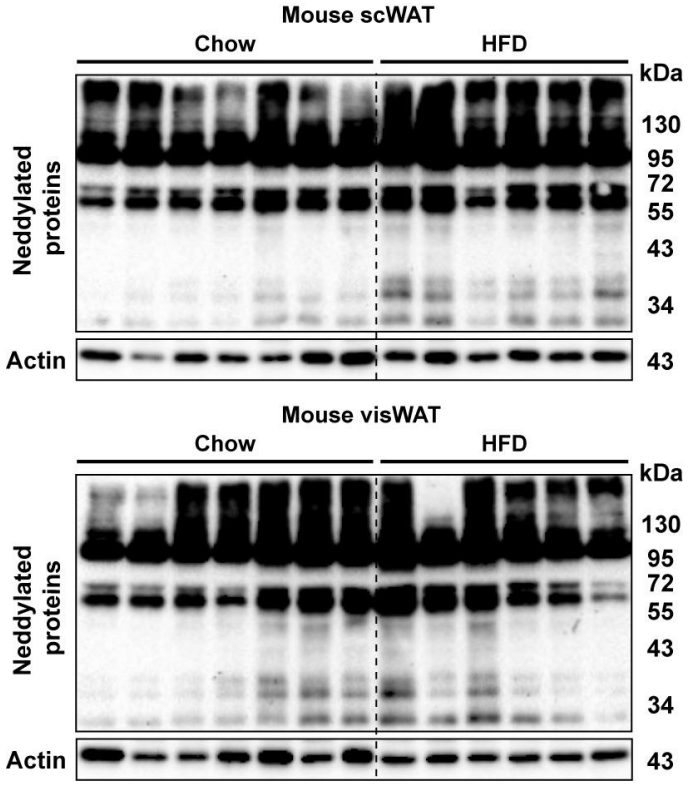

Figure 40: Increased adipose tissue neddylation in obese mice. Immunoblots of Nedd8 in sc and vis WAT of mice fed chow or HFD for 8 weeks. Equal protein loading was confirmed by normalization to Actin expression (n= 6-7 mice per group).

4.7 *Nae1* knock-out mice: a model to study the relevance of adipose tissue neddylation *in vivo*

To further investigate the physiological role of AT neddylation *in vivo*, we established a mouse model in which Nae1 was specifically deleted in the AT in an inducible manner by crossing mice with floxed *Nae1* alleles (Vogl et al., 2015) with mice carrying a tamoxifen-inducible CreER^{T2} transgene under control of the adiponectin promoter (*Adipo*CreER^{T2}) (Sassmann et al., 2010) (Figure 41). Thereby, we generated a tool which allows the deletion of neddylation specifically in adipocytes. To circumvent potential adverse effects of tamoxifen (Hesselbarth et al., 2015), also control mice carrying floxed *Nae1* alleles but not the *Adipo*CreER^{T2} transgene were treated with the drug.

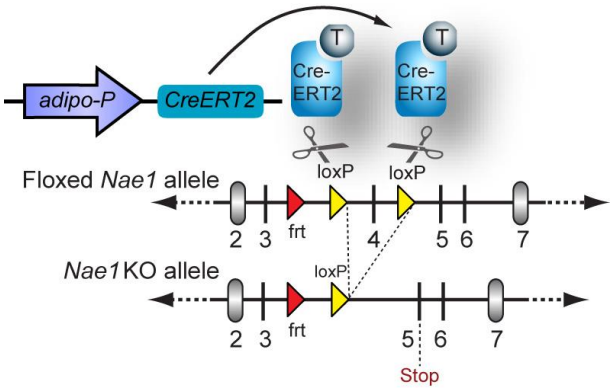

Figure 41: Tamoxifen-inducible adipose tissue-specific KO of *Nae1*. Schematic illustration of the system used for tamoxifen (T)-inducible *Adipo-Cre*ER^{T2} transgene activity resulting in *Nae1* knock out (KO).

4.8 Adipose tissue-specific ablation of the neddylation pathway reduces obesity but impairs metabolic homeostasis

First, we sought to investigate the effects of AT-specific neddylation ablation in HFD-induced obese mice. For this purpose, *Nae1Adipo*CreER^{T2} (KO) and control (Ctrl) littermates were fed a HFD for 9 weeks prior to tamoxifen administration. *Nae1* KO was induced by intraperitoneal tamoxifen injections. Then mice were divided in two sets: a first set of animals received chow diet and a second set continued with HFD feeding (Figure 42A). Successful deletion of *Nae1* in WAT was verified by qRT-PCR analysis comparing the Nae1 mRNA expression levels between the different genotypes and diets (Figure 42B). Additionally, *Nae1* KO was further validated by immunoblotting comparing the pattern of neddylated proteins in the different ATs between KO and control mice (Figure 42C). Liver tissue was used as a negative control (Figure 42B-C).

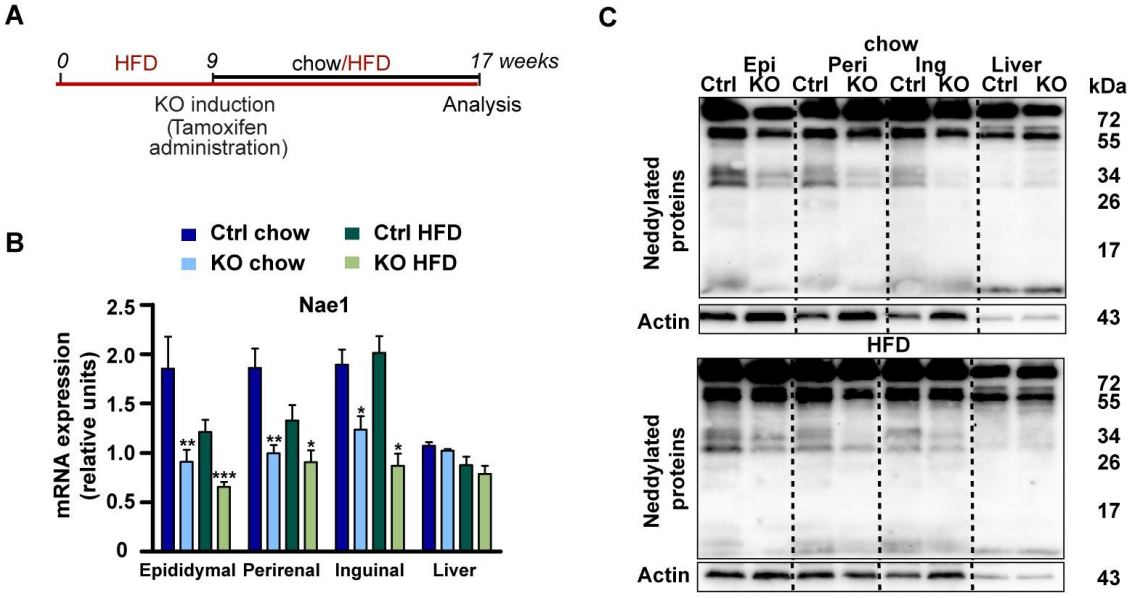

Figure 42: Tamoxifen-inducible adipose tissue-specific KO of *Nae1* in obese mice. (A) Diagram showing the *in vivo* experimental design. *Nae1Adipo*CreER^{T2} (KO) and Control *Nae1*^{floxed} (Ctrl) mouse lines were fed a HFD for 9 weeks prior to tamoxifen injection. Afterwards, mice were fed a chow or a HFD. **(B)** Relative mRNA levels of Nae1 in WAT and liver normalized to Actin (n= 7-11 mice per group). **(C)** Immunoblots of Nae1 in WAT and liver of chow- and HFD-fed mice. Equal protein loading was confirmed by normalization to Actin expression. Data are presented as mean ± SEM. Statistical significance is shown as $*p \leq 0.05$, $**p \leq 0.01$, $***p \leq 0.001$. Significance was determined by unpaired two-side t test.

4.8.1 Conditional fat-specific inactivation of the neddylation pathway reduces HFD-induced obesity but promotes adipose tissue dysfunction

Obese *Nae1Adipo*CreER^{T2} mice fed a HFD exhibited a major loss of body weight approximately from 25 days on after the induction of *Adipo*Cre mediated recombination, whereas a less profound but significant decrease in body weight was observed in chow-fed animals (Figure 43A-B). *Nae1* deletion in WAT of obese mice resulted in a marked diminution of epididymal, perirenal and inguinal fat pads in comparison to control animals, regardless of the diet (Figure 43C). While the AT of control mice was rich in unilocular white adipocytes with sparse extracellular matrix, the AT of *Nae1* KO mice was highly abnormal and showed a dramatic rise in stromal-vascular cells, as visualized by H&E staining of the AT sections (Figure 43D). Adipocytes of these mice were variable in size which may account for the reduction in fat weight.

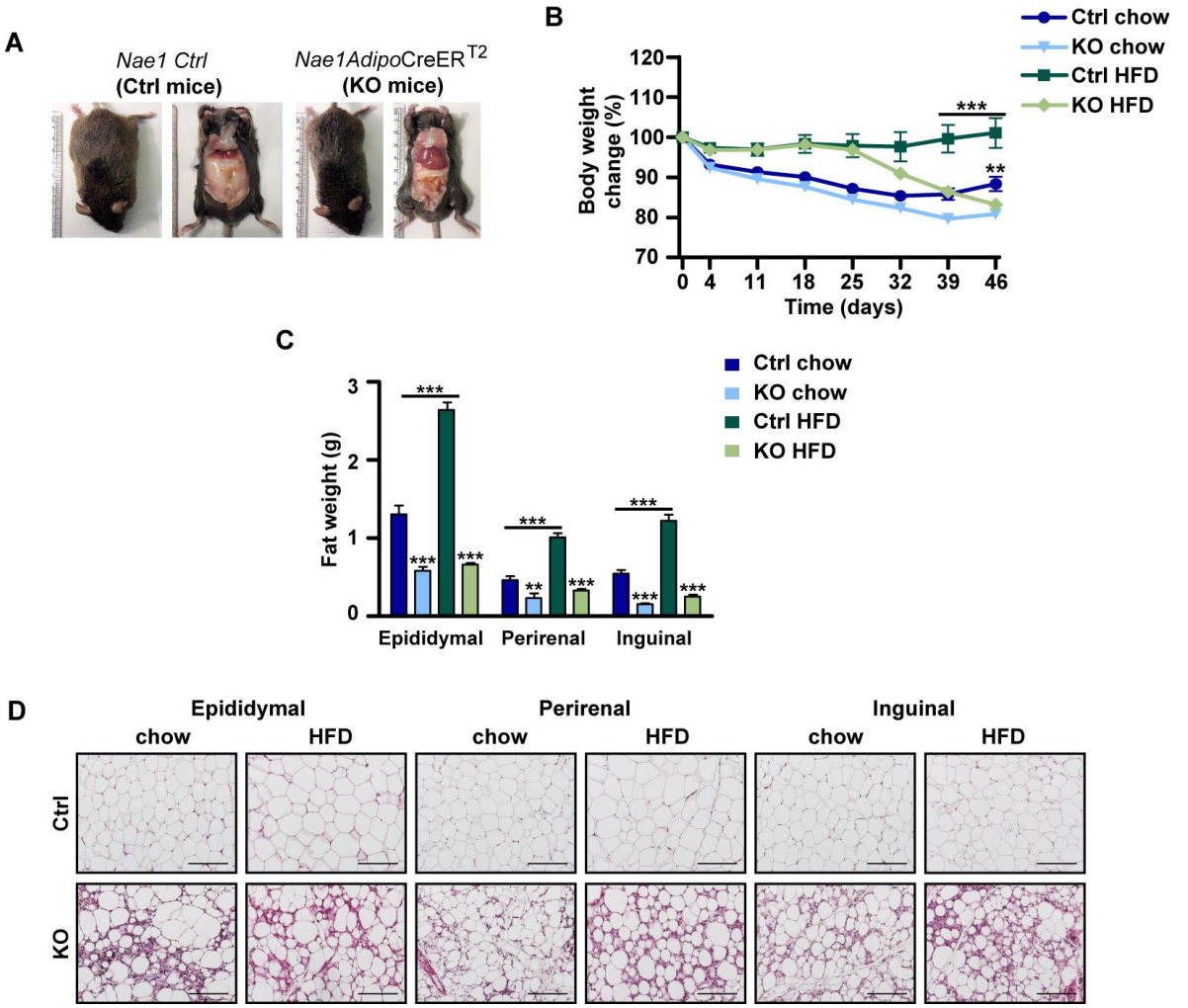

Figure 43: Adipose-specific neddylation ablation in obese mice reduces adiposity but results in abnormal adipose tissue. (A) Pictures of HFD-fed Ctrl and *Nae1Adipo*CreER^{T2} littermates in week 17. **(B)** Body weight change relative to the initial weight was assessed over 46 days after tamoxifen administration (n= 8-11 mice per group). **(C)** WAT weights in Ctrl and *Nae1Adipo*CreER^{T2} KO mice (n= 8-11 mice per group). **(D)** Images showing HE staining of WAT sections. Data are presented as mean ± SEM. Statistical significance is shown as ∗∗p ≤ 0.01, ∗∗∗p ≤ 0.001. Significance was determined by two-way ANOVA with Bonferroni's multiple comparison test. Scale bars in (D) represent 175 µm.

Consistent with the results obtained in 3T3-L1 cells, C/EBPβ binding to the PPARγ promoter was reduced in WAT of chow-fed *Nae1Adipo*CreER^{T2} mice and it showed a tendency to decrease in HFD-fed mice (Figure 44A). Consequently, PPARγ mRNA expression was downregulated in KO animals respect to Ctrls independently of the diet (Figure 44B). This finding further emphasizes C/EBPβ as a neddylation target *in vivo*. As already previously stated, PPARγ is a key regulator of adipocyte function and survival. Thus, we aimed to evaluate adipocyte survival in WAT of *Nae1Adipo*CreER^{T2} mice. Adipocyte death was detected by immunohistochemistry for the essential lipid droplet-associated protein perilipin (Cinti et al., 2005; Wernstedt Asterholm et al., 2014), which is a direct target of PPARγ (Dalen et al., 2004). No perilipin immunoreactivity was observed on lipid droplets of dead adipocytes surrounded by macrophages, which were only found in WAT of

*Nae1Adipo*CreER^{T2} mice (Figure 44C). In contrast, perilipin was detected in adjacent, viable adipocytes, more frequently present in WAT of control littermates (Figure 44C). As follows, adipocyte cell death may account substantially for the decrease in body weight and the depletion of AT mass in *Nae1Adipo*CreER^{T2} mice.

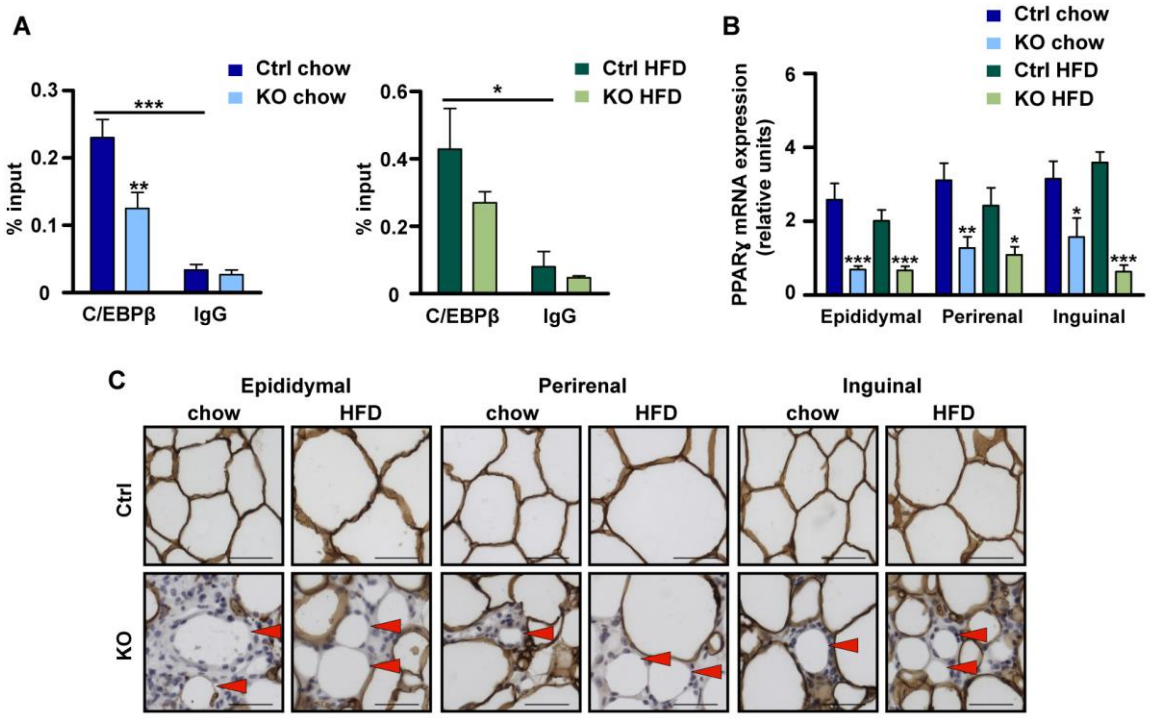

Figure 44: Fat-specific neddylation ablation in obese mice results in decreased C/EBPβ DNA binding, reduced PPARγ expression and adipocyte death. (A) ChIP-qRT-PCR assays for C/EBPβ binding to the PPARγ gene promoter performed in WAT. Amounts of immunoprecipitated DNA were normalized to inputs. IgG was used as a negative control. **(B)** Relative mRNA levels of PPARγ in WAT normalized to Actin (n= 7-11 mice per group). **(C)** Images showing perilipin expression assessed by anti-perilipin immunostaining (brown) and hematoxylin staining (blue) in WAT sections. Red arrows indicate dying adipocytes with perilipin-negative lipid droplets. Data are presented as mean ± SEM. Statistical significance is shown as ∗p ≤ 0.05, ∗∗p ≤ 0.01, ∗∗∗p ≤ 0.001. Significance was determined by unpaired two-side t test. Scale bars in (D) represent 85 μm.

Considering *Nae1Adipo*CreER^{T2} mice displayed reduced AT PPARγ levels and showed signs of adipocyte death, we consequently examined the expression of adipocyte-specific metabolic genes that determine the adipocyte phenotype, including adiponectin, genes involved in FA uptake, lipogenesis, glucose uptake and insulin signaling, glyceroneogenesis and lipolysis, many of which are regulated by PPARγ. Notably, ablating the neddylation pathway specifically in the AT, we could mostly confirm our findings in 3T3-L1 cells.

HFD feeding in Ctrl mice had largely no effect on the mRNA expression of genes involved in FA uptake, such as LPL, FATP1 and FABP4, and the lipolytic enzyme HSL respect to chow-fed Ctrl mice (Figure 45). WAT of *Nae1Adipo*CreER^{T2} mice exhibited a downregulated mRNA expression of the majority of the genes investigated, in comparison to control littermates,

independently of the diet (Figure 45). In fact, chow-fed and HFD-fed *Nae1Adipo*CreER^{T2} mice displayed similar mRNA levels of these genes in all WAT depots tested (Figure 45).

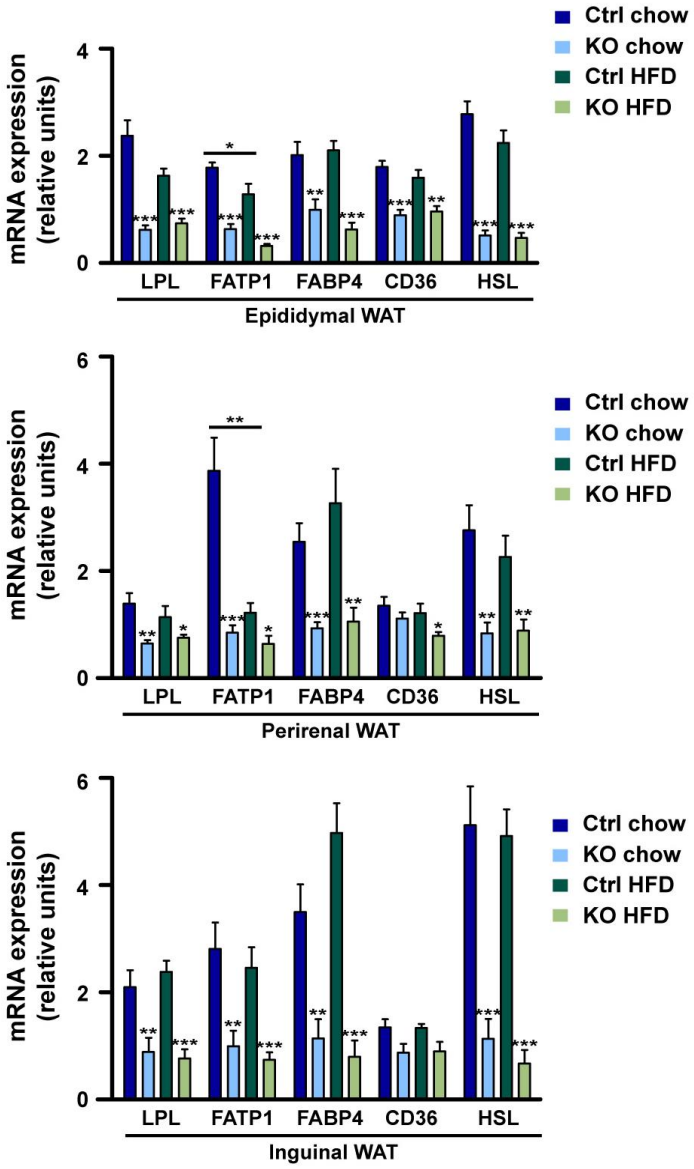

Figure 45: Adipose tissue-specific neddylation ablation in obese mice reduces mRNA expression of PPARγ downstream genes involved in FA uptake and lipolysis. Relative mRNA levels of the indicated genes in WAT normalized to Actin (n= 7-11 mice per group). Data are presented as mean ± SEM. Statistical significance is shown as ∗p ≤ 0.05, ∗∗p ≤ 0.01, ∗∗∗p ≤ 0.001. Significance was determined by unpaired two-side t test.

Furthermore, expression of genes involved in insulin signaling and glucose transport, such as GLUT4 and IRS2, glyceroneogenesis, like PEPCK and the adipokine adiponectin remained largely unchanged in AT of HFD-fed compared to chow-fed Ctrl mice (Figure 46). Notably, fat-specific neddylation ablation almost consistently reduced the mRNA expression of these genes, independently of the diet (Figure 46). Thus, similar mRNA expression levels were observed between chow-fed and HFD-fed *Nae1Adipo*CreER^{T2} mice in all AT depots tested (Figure 46).

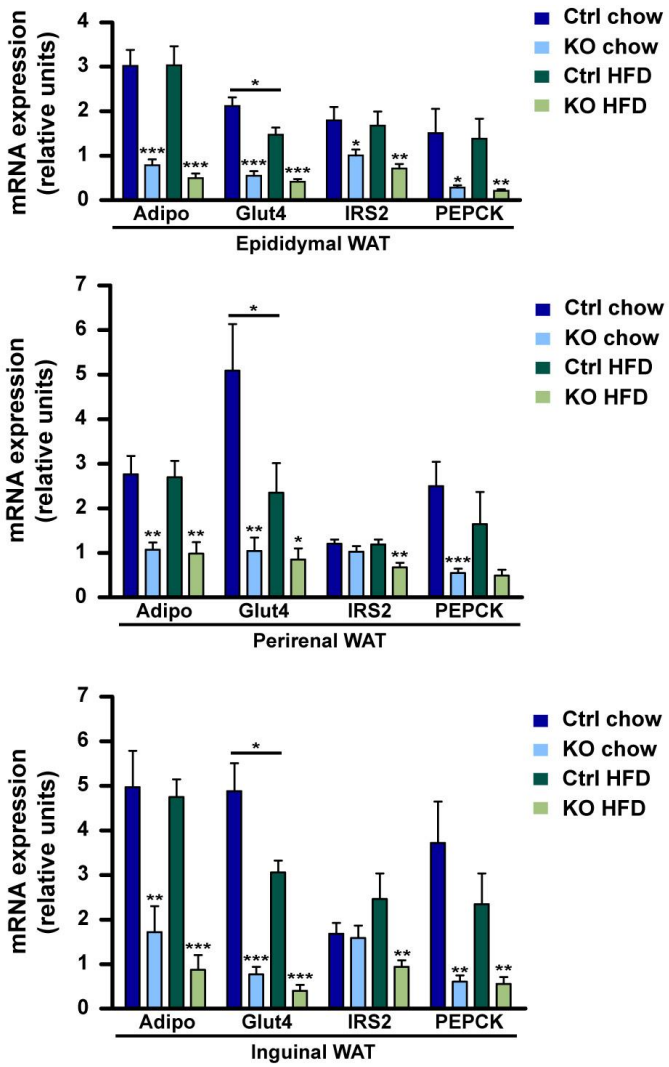

Figure 46: Adipose tissue-specific neddylation ablation in obese mice reduces mRNA expression of PPARγ downstream genes involved in glucose homeostasis, insulin signaling and glyceroneogenesis. Relative mRNA levels of the indicated genes in WAT normalized to Actin (n= 6-11 mice per group). Data are presented as mean ± SEM. Statistical significance is shown as $*p \leq 0.05$, $**p \leq 0.01$, $***p \leq 0.001$. Significance was determined by unpaired two-side t test.

Strikingly, genes involved in lipogenesis, like SREBP1c, FAS and ACC1 were partially severely downregulated by HFD feeding in Ctrl mice (Figure 47). Fat-specific neddylation ablation triggered a dramatic reduction of mRNA levels of the majority of genes involved in lipogenesis in AT of chow-fed and HFD-fed *Nae1Adipo*CreER^{T2} mice (Figure 47). The WAT mRNA levels of these genes of chow-fed as well as HFD-fed *Nae1Adipo*CreER^{T2} mice were reduced to a similar extend (Figure 47).

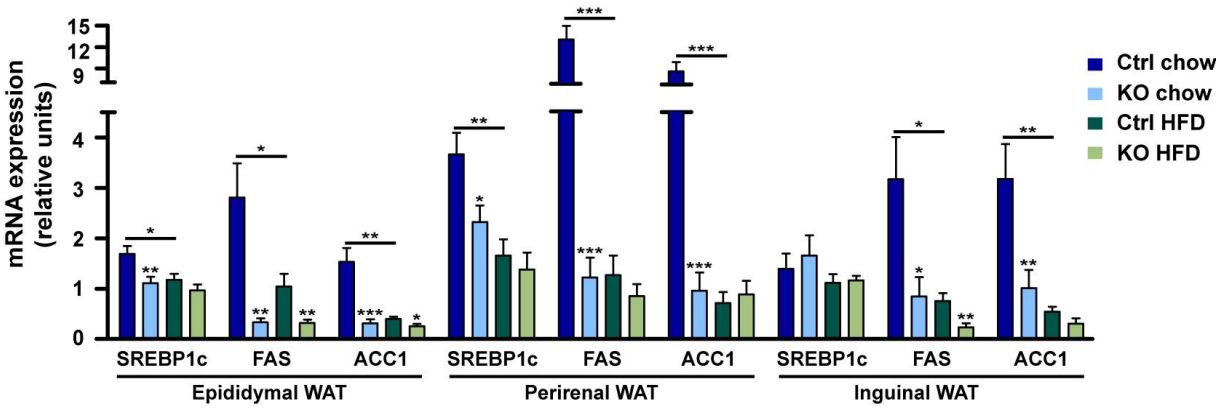

Figure 47: Adipose tissue-specific neddylation ablation in obese mice reduces mRNA expression of genes involved in lipogenesis. Relative mRNA levels of the indicated genes in WAT normalized to Actin (n= 7-11 mice per group). Data are presented as mean ± SEM. Statistical significance is shown as ∗p ≤ 0.05, ∗∗p ≤ 0.01, ∗∗∗p ≤ 0.001. Significance was determined by unpaired two-side t test.

Altogether, these data support the notion that adipose specific neddylation inhibition reverts HFD-induced obesity by promoting a dramatic diminution of fat tissue triggered by AT dysfunction and cell death. This indicates that neddylation is crucial for AT expansion as well as adipocyte survival *in vivo*.

Moreover, qRT-PCR analysis showed that HFD feeding per se increased MCP1 mRNA levels in perirenal and epididymal fat, however not in inguinal fat. In chow-fed mice, *Nae1* KO increased MCP1 expression respect to Ctrl mice (Figure 48). HFD-fed *Nae1Adipo*CreER^{T2} mice displayed similar MCP1 levels in perirenal and epididymal fat depots as chow-fed *Nae1Adipo*CreER^{T2} mice, but lower levels than observed on HFD-fed Ctrl mice (Figure 48). Only in the case of inguinal fat, HFD feeding potentiated the effects of fat-specific neddylation ablation on MCP1 mRNA expression (Figure 48). HFD alone did mostly not change the macrophage F4/80 mRNA levels in WAT (Figure 48). However, F4/80 mRNA expression was elevated in *Nae1Adipo*CreER^{T2} mice, which was even potentiated by HFD feeding (Figure 48). The inflammatory marker TNFα remained almost unaltered by HFD feeding and AT-specific neddylation ablation, as mRNA levels were only found to be increased in inguinal WAT of KO mice fed a HFD (Figure 48). In summary, these data together with the histological findings indicate a rise in inflammation and an enhanced recruitment of macrophages in the AT of *Nae1* KO mice.

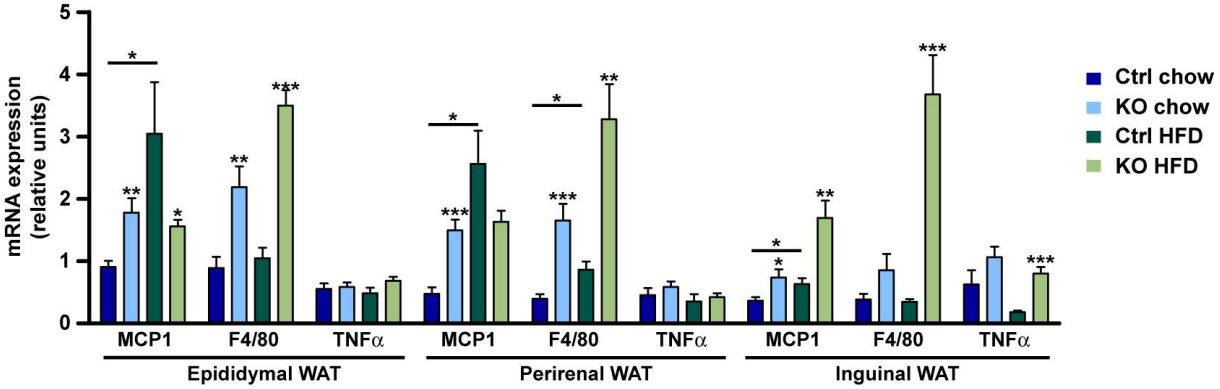

Figure 48: Adipose-tissue specific neddylation ablation in obese mice leads to adipose tissue inflammation. Relative mRNA levels of the indicated genes in WAT normalized to Actin (n= 6-11 mice per group). Data are presented as mean ± SEM. Statistical significance is shown as $*p \leq 0.05$, $**p \leq 0.01$, $***p \leq 0.001$. Significance was determined by unpaired two-side t test.

4.8.2 Conditional fat specific inactivation of the neddylation pathway in obese mice causes severe metabolic disturbances

Neddylation seems to control adipocyte survival and function on the posttranslational level *in vivo*. KO of *Nae1* caused a severe lipodystrophic phenotype. Metabolic abnormalities, including hypertriglyceridemia, high levels of circulating FA, hepatic steatosis and disturbances in glucose metabolism, are frequently observed in mouse models with partial or complete loss of fat tissue (Asterholm et al., 2007). Thus, we next studied the metabolic consequences of the *Nae1* ablation in AT of mice fed control and obesogenic diets. *Nae1Adipo*CreER^{T2} mice displayed severe hyperglycemia and hyperinsulinemia in comparison to Ctrl animals independently of the diet (Figure 49A-B). Moreover, *Nae1Adipo*CreER^{T2} mice displayed a markedly impaired glucose tolerance during a glucose tolerance test (GTT) (Figure 49C). Plasma levels of adiponectin, an insulin-sensitizing hormone, were demonstrated to be decreased in lipodystrophic mouse models due to the reduction in fat mass (Ye and Scherer, 2013). Consistent with the alterations in adiponectin mRNA expression in AT and the decrease in fat mass, plasma levels of adiponectin were reduced in *Nae1Adipo*CreER^{T2} animals (Figure 49D). Taken together, the lipodystrophic phenotype in *Nae1Adipo*CreER^{T2} was accompanied by a profound metabolic dysfunction. These data indicate a potential involvement of AT neddylation in the protection against peripheral insulin resistance, although this hypothesis was not further tested.

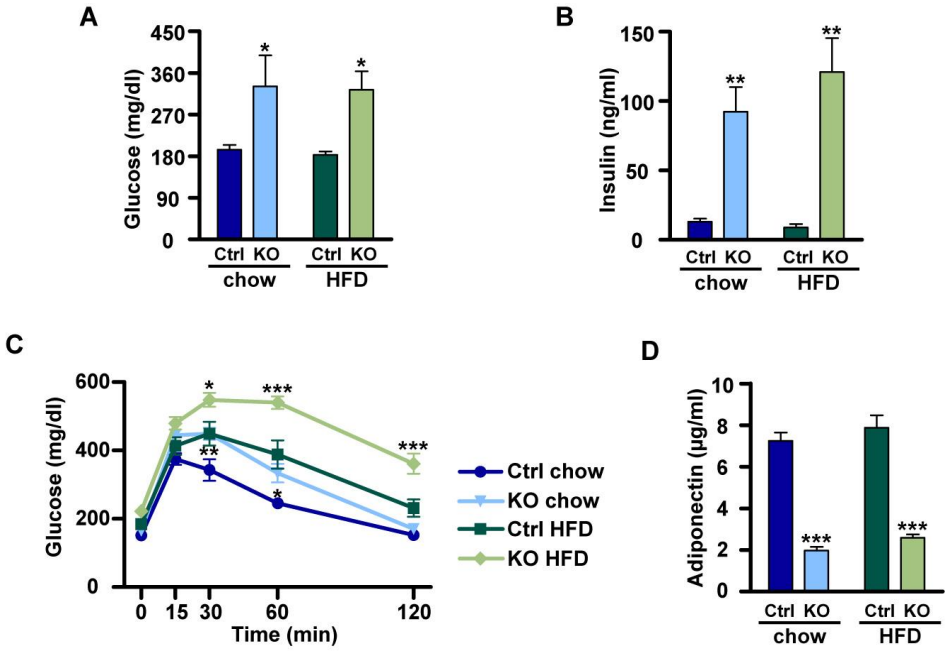

Figure 49: Fat-specific neddylation ablation in obese mice impairs glucose homeostasis. (A) Plasma glucose levels (n= 4-6 mice per group). **(B)** Plasma insulin levels (n= 4-6 mice per group). **(C)** Intraperitoneal glucose tolerance test (GTT) (n= 8-12 mice per group). **(D)** Plasma adiponectin levels (n=4-6 mice per group). Data are presented as mean ± SEM. Statistical significance is shown as $*p \leq 0.05$, $**p \leq 0.01$, $***p \leq 0.001$. Significance was determined by two-way ANOVA with Bonferroni's multiple comparison test.

To our surprise, plasma TG levels in *Nae1Adipo*CreER^{T2} animals remained unchanged regardless of the diet (Figure 50A). The loss of AT mass was associated with an increase in plasma FA levels in chow-fed KO animals, whereas no changes were observed in HFD-fed *Nae1Adipo*CreER^{T2} mice (Figure 50B). The unexpected lack in increased plasma FA in HFD-fed animals could have resulted from compensatory effects of ectopic lipid disposition in the liver. Indeed, HFD-fed *Nae1Adipo*CreER^{T2} mice developed hepatosteatosis, correlated with higher liver weights and histological evidence of lipid accumulation (Figure 50C-E). Moreover, the unchanged circulating FA levels in HFD-fed *Nae1Adipo*CreER^{T2} mice may be explained by a pronounced increase in FA oxidation as reflected by a lower respiratory exchange ratio (RER) during the dark phase respect to HFD-fed Ctrl mice (Figure 50F). The RER can be assessed by indirect calorimetry and reflects which substrate is oxidized. When primarily glucose is oxidized, the RER is close to 1, whereas it is close to 0.7 when fat is the major fuel used (Speakman, 2013). Thus, the RER is a measure to assess metabolic flexibility, meaning the ability of an organism to adapt substrate oxidation to fuel availability (Galgani et al., 2008). The glucose intolerance of the KO mice might contribute to promote FA utilization over glucose oxidation as cellular glucose uptake may be impaired. In contrast to HFD-fed *Nae1Adipo*CreER^{T2} mice, no signs of liver steatosis and no changes in RER were detected in chow-fed KO mice (Figure 50F).

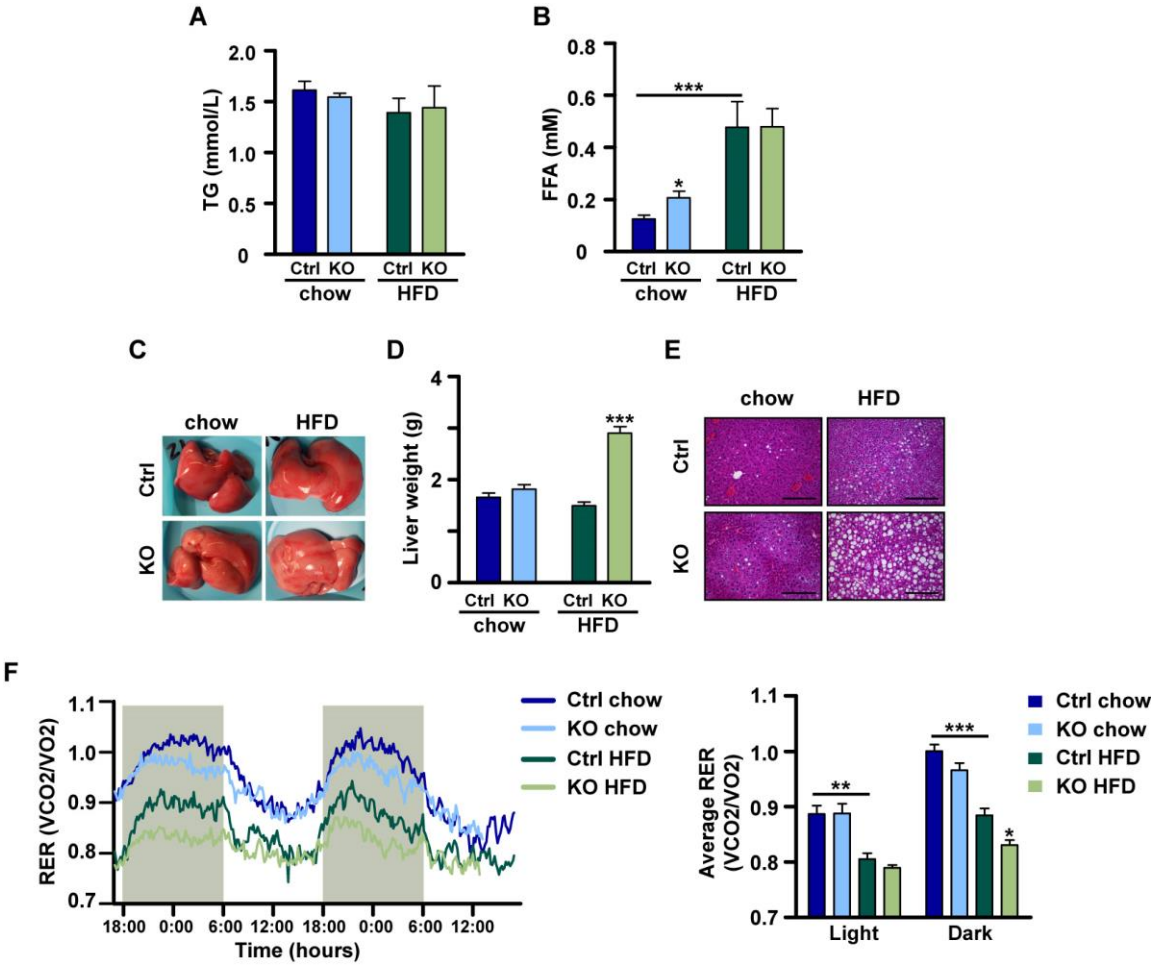

Figure 50: Fat-specific neddylation ablation in obese mice results in hepatic steatosis and metabolic inflexibility. (A) Plasma TG levels (n= 4-6 per group). **(B)** Plasma FA levels (n= 4-6 per group). **(C-D)** Representative pictures of liver and liver weight of Ctrl and *Nae1Adipo*CreER^{T2} KO mice (n= 8-11 mice per group). **(E)** Representative images showing HE staining of liver sections. **(F)** RER and average RER measured during the light and dark cycle (shaded region) in Ctrl and *Nae1Adipo*CreER^{T2} KO mice (n= 6-10 mice per group). Data are presented as mean ± SEM. Statistical significance is shown as ∗p ≤ 0.05, ∗∗p ≤ 0.01, ∗∗∗p ≤ 0.001. Significance was determined by two-way ANOVA with Bonferroni's multiple comparison test in (B,D,F) and by one-way ANOVA with Bonferroni's multiple comparison test in (B,F Ctrl chow vs Ctrl HFD). Scale bars in (E) represent 200 µm.

No changes were observed in locomotor activity, energy expenditure or oxygen consumption in *Nae1Adipo*CreER^{T2} mice, which thus cannot account for the effects on body weight loss (Figure 51A-C). Importantly, HFD-fed *Nae1Adipo*CreER^{T2} mice demonstrated a decreased food intake, which might partially explain the decrease in AT mass in HFD-fed KO animals (Figure 51D). In contrast, no changes in food intake were observed in chow-fed KO mice (Figure 51D). The reduced leptin plasma levels in *Nae1* KO mice that display diminished and dysfunctional AT (Figure 51E) are in accordance with the accepted fact that leptin plasma levels positively correlate with fat mass (Florant et al., 2004; Shimizu et al., 1997; Skurk et al., 2007). As leptin regulates food intake (Halaas et al., 1995), the decreased food consumption observed in HFD-fed KO mice contradicts the reduced leptin plasma levels that would in fact promote hyperphagia. In summary, diminished AT weight, together with

impaired adipocyte function and increased inflammation in *Nae1Adipo*CreER^{T2} mice, gives rise to metabolic disturbances, which reflect many side-effects of human lipodystrophy including glucose intolerance, hyperglycemia, and hyperinsulinemia, decreased plasma adiponectin levels and hepatic steatosis. Thus, AT neddylation might be an important regulator of metabolic homeostasis in mice.

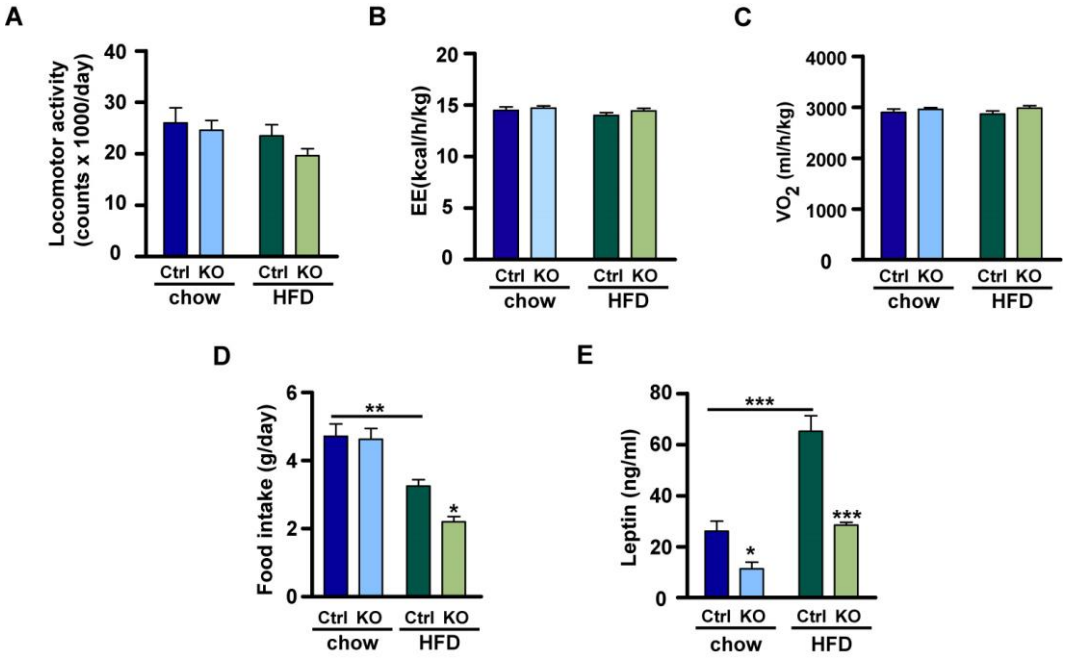

Figure 51: Fat-specific neddylation ablation in obese mice reduces food intake despite decreased leptin levels but does not affect locomotor activity or energy expenditure. (A) Locomotor activity of mice (n= 6-10 mice per group). **(B-C)** Energy expenditure (EE) and oxygen consumption (VO_2) in mice (n= 6-10 mice per group). **(D)** Food intake of mice (n= 6-10 mice per group). **(E)** Plasma leptin levels (n= 4-6 per group). Data are presented as mean ± SEM. Statistical significance is shown as $*p \leq 0.05$, $**p \leq 0.01$, $***p \leq 0.001$. Significance was determined by two-way ANOVA with Bonferroni's multiple comparison test in (D-E) and by one-way ANOVA with Bonferroni's multiple comparison test in (D-E, Ctrl chow vs Ctrl HFD).

4.9 Adipose tissue-specific ablation of the neddylation pathway prevents HFD-induced obesity but leads to metabolic dysfunction

In a second *in vivo* experiment we aimed to deepen our knowledge of the physiological role of AT neddylation by inducing the fat-specific *Nae1* KO simultaneously with the initiation of HFD feeding. In this second model we measured the most relevant parameters in order to complement our data obtained in the first model of *Nae1* KO in HFD-induced obese mice. Due to the fact that neddylation increases with adiposity (at least in scWAT) and *Nae1* deletion in HFD-induced obese mice results in a dramatic phenotype, this second model allowed us to explore whether the lipodystrophic phenotype in *Nae1* KO mice depends on the neddylation status of obese mice. Moreover, this complementary experiment enabled us

to investigate whether *Nae1* ablation showed a phenotype under stress situation like HFD or not compared to mice fed a chow diet before the obese phenotype was established. For this purpose, *Nae1* KO was induced by tamoxifen administration and afterwards mice received either a standard rodent chow diet or a HFD during the time course of the experiment (Figure 52A). *Nae1* deletion specifically in AT of *Nae1Adipo*CreER^{T2} mice after tamoxifen administration was confirmed by western blotting and brain tissue was used as a negative control (Figure 52B).

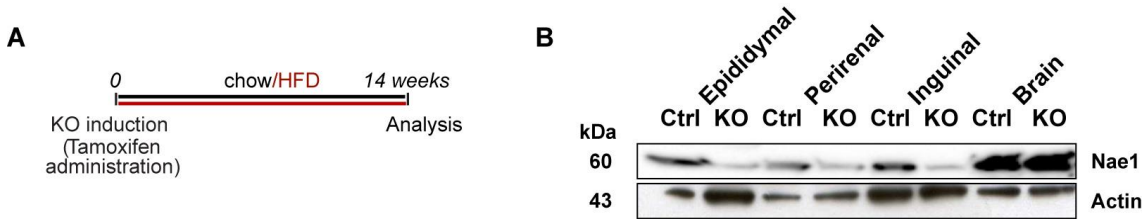

Figure 52: Tamoxifen-inducible adipose tissue-specific KO of *Nae1*. (A) Diagram showing the *in vivo* experimental design. *Nae1* KO and Ctrl mouse lines were treated with tamoxifen and subsequently fed a chow diet or HFD for 14 weeks. **(B)** Immunoblots of Nae1 in WAT and brain of HFD-fed mice. Equal protein loading was confirmed by normalization to Actin expression.

4.9.1 Conditional fat specific ablation of the neddylation pathway protects against HFD-induced obesity by decreasing adipose tissue mass and food intake

Fat specific KO of *Nae1* prevented HFD-induced body weight gain, while mice under chow diet displayed a similar body weight respect to Ctrl animals (Figure 53A-B). Moreover, KO of *Nae1* resulted in decreased epididymal and inguinal fat depot mass respect to Ctrl mice, indistinctly of the diet. Perirenal fat mass of *Nae1Adipo*CreER^{T2} mice tended to be reduced reaching significance only in mice under HFD (Figure 53C). The protection against body weight gain in KO mice under HFD could be attributed to the lower fat mass. Nevertheless, despite the reduction of fat mass in chow-fed KO mice, these mice did not display a decreased body weight compared to chow-fed Ctrl mice. Taken together, *Nae1Adipo*CreER^{T2} mice displayed a lipodystrophic phenotype, confirming the findings in HFD-induced obese *Nae1* KO mice.

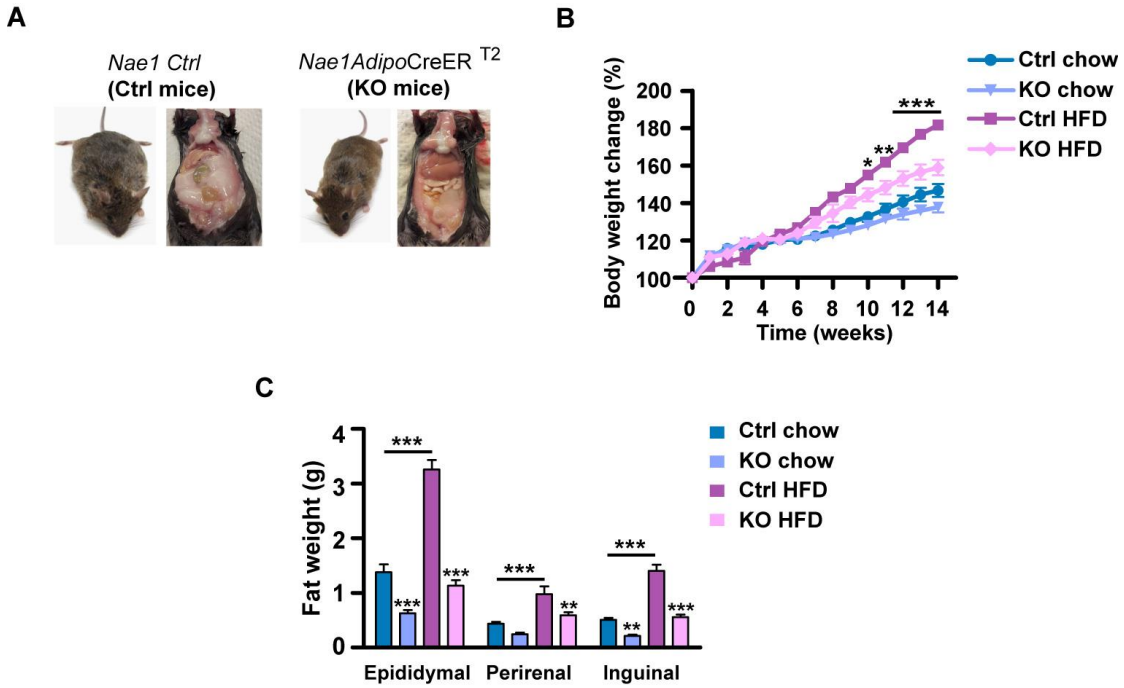

Figure 53: Adipose tissue-specific ablation of the neddylation pathway prevents HFD-induced obesity. (A) Representative pictures of HFD-fed Ctrl and *Nae1Adipo*CreER^{T2} littermates in week 14. **(B)** Body weight change relative to the initial weight was assessed over 14 weeks after tamoxifen administration (n= 9-10 mice per group). **(C)** WAT weights in Ctrl and *Nae1Adipo*CreER^{T2} KO mice (n= 9-10 mice per group). Data are presented as mean ± SEM. Statistical significance is shown as $*p \leq 0.05$, $**p \leq 0.01$, $***p \leq 0.001$. Significance was determined by two-way ANOVA with Bonferroni's multiple comparison test in (B,C) and by one-way ANOVA with Bonferroni's multiple comparison test (C, Ctrl chow vs Ctrl HFD).

Locomotor activity, food intake and energy expenditure were assessed in mice that underwent *Nae1* KO simultaneously with HFD-mediated induction of obesity. *Nae1Adipo*CreER^{T2} mice showed no changes in locomotor activity (Figure 54A) and energy expenditure (Figure 54C) and thus these parameters cannot explain the protection against HFD-induced increase in AT mass. However, both, HFD- and chow-fed *Nae1Adipo*CreER^{T2} mice, demonstrated a decreased food intake, which might partially account for the low AT mass (Figure 54B). Although it was not formerly tested in this complementary experiment, we hypothesize that the KO of *Nae1* simultaneously with obesity induction might also result in adipocyte death and consequently AT dysfunction, which probably contributes to the protection against HFD-induced increase in fat mass and body weight.

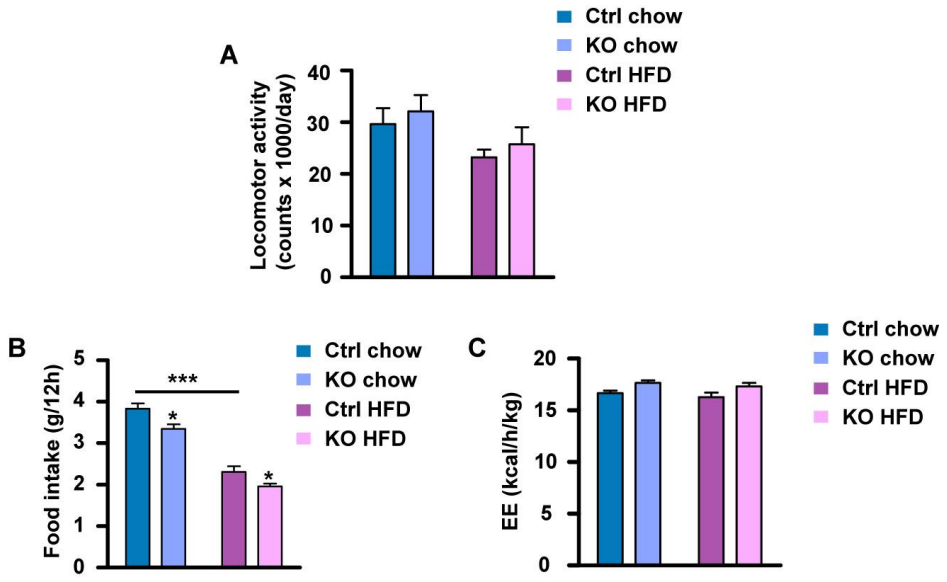

Figure 54: Adipose-tissue specific neddylation ablation reduces food intake but does not alter locomotor activity and energy expenditure. (A) Locomotor activity of mice (n= 8 mice per group). **(B)** Food intake of mice (n= 8 mice per group). **(C)** Energy expenditure (EE) in mice (n= 8 mice per group). Data are presented as mean ± SEM. Statistical significance is shown as $*p \leq 0.05$, $***p \leq 0.001$. Significance was determined by two-way ANOVA with Bonferroni's multiple comparison test in (B) and by one-way ANOVA with Bonferroni's multiple comparison test in (B, Ctrl chow vs Ctrl HFD).

4.9.2 Conditional adipocyte specific ablation of the neddylation pathway leads to hepatic steatosis and metabolic dysfunction

Fat specific ablation of the neddylation pathway resulted in the protection against HFD-induced rise in AT mass and body weight. Following the observations in HFD-induced obese *Nae1Adipo*CreER^{T2} mice, we next aimed to characterize the metabolic consequences of the *Nae1* ablation in the model of simultaneous obesity-induction. While *Nae1* KO in the AT of chow-fed animals did not result in hepatic steatosis, liver steatosis was triggered by HFD feeding in *Nae1* KO mice, corroborated by higher liver weights (Figure 55A-B). Non-fasting plasma TG levels were not altered in *Nae1Adipo*CreER^{T2} animals indistinctly of the diet (Figure 55C). Surprisingly, plasma FA levels in HFD-fed *Nae1Adipo*CreER^{T2} animals were significantly reduced, whereas this effect was less pronounced in chow-fed animals (Figure 55D). Taken together these findings indicate that deletion of *Nae1* in the fat tissue promotes fat re-direction to the liver for storage. Moreover, the significant decrease in circulating FA levels in HFD-fed KO mice may be also explained by a pronounced increase in FA oxidation as reflected by a lower RER during the dark phase, independently of the diet (Figure 55E).

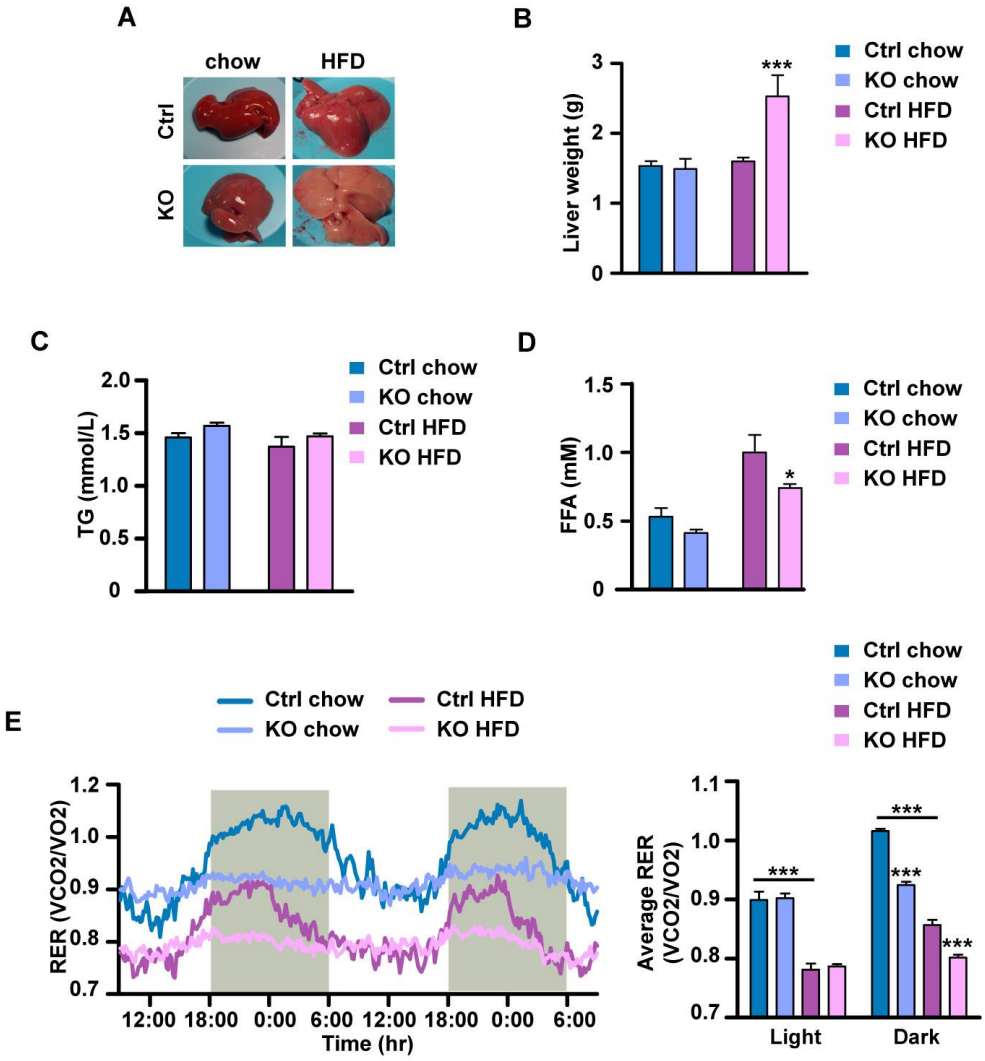

Figure 55: Adipose tissue-specific ablation of the neddylation pathway causes hepatic steatosis and impairs metabolic flexibility. (A) Representative liver pictures of Ctrl and *Nae1Adipo*CreER^{T2} KO mice. **(B)** Liver weight of Ctrl and *Nae1Adipo*CreER^{T2} KO mice (n= 9-10 mice per group). **(C)** Plasma TG levels (n= 9-10). **(D)** Plasma FA levels (n= 9-10 per group). **(E)** RER and average RER measured during the light and dark cycle (shaded region) in Ctrl and *Nae1Adipo*CreER^{T2} KO mice (n= 8 mice per group). Data are presented as mean ± SEM. Statistical significance is shown as $*p \leq 0.05$, $***p \leq 0.001$. Significance was determined by two-way ANOVA with Bonferroni's multiple comparison test in (B,D,E) and by one-way ANOVA with Bonferroni's multiple comparison test in (E Ctrl chow vs Ctrl HFD).

Due to the metabolic dysfunction observed in the first *Nae1* KO model, we sought to examine the consequences of *Nae1* deletion simultaneously with HFD-feeding on glucose homeostasis. Plasma adiponectin levels were decreased when neddylation was ablated in WAT probably due to the loss of AT (Figure 56A). While unexpectedly plasma glucose levels were not changed, plasma insulin levels in HFD-fed KO animals were found to be severely elevated (Figure 56B-C). Thus, a compensatory insulin production may rescue KO mice from hyperglycemia. Accordingly, *Nae1Adipo*CreER^{T2} animals under HFD demonstrated to be glucose intolerant during a GTT (Figure 56D). KO mice fed a standard chow diet showed a

similar glucose tolerance in respect to control littermates (Figure 56D). The glucose intolerance of the KO mice might contribute to promote FA utilization over glucose oxidation during the dark phase. Collectively, AT-specific neddylation ablation protects against HFD-induced obesity but leads to a lipodystrophic phenotype accompanied by a metabolic dysfunction in mice, confirming and complementing our data on the AT-specific *Nae1* deletion in HFD-induced obese mice.

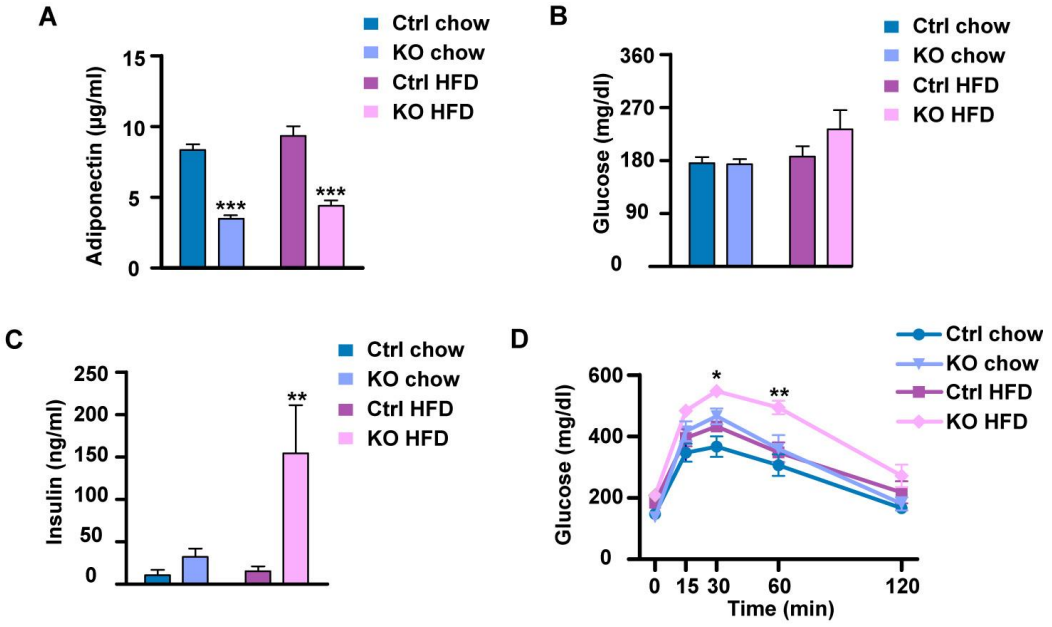

Figure 56: Fat-specific neddylation ablation leads to metabolic disturbances. (A) Plasma adiponectin levels (n= 9-10mice per group). **(B)** Plasma glucose levels (n= 9-10 mice per group). **(C)** Plasma insulin levels (n= 9-10 mice per group). **(D)** Intraperitoneal GTT (n= 9-10 mice per group). Data are presented as mean ± SEM. Statistical significance is shown as $*p \leq 0.05$, $**p \leq 0.01$, $***p \leq 0.001$. Significance was determined by two-way ANOVA with Bonferroni's multiple comparison test (A,C,D).

4.10 Peripheral neddylation inhibition reduces obesity and associated metabolic disorders

Fat-specific neddylation deletion in HFD-fed mice resulted in a lipodystrophic phenotype associated with liver steatosis and metabolic dysfunction. However, the ubiquitous expression of Nedd8 suggests that neddylation may have other non-adipocyte functions controlling obesity and metabolism. In fact, a recent study showed that the peripheral administration of the pharmacological inhibitor, MLN4924 protected mice against HFD-induced obesity (Park et al., 2016). Nevertheless, the therapeutic relevance of MLN4924 in the treatment of obesity and associated metabolic disorders still remains to be defined. Thus, we studied the impact of a global peripheral deletion of the neddylation pathway, by injecting MLN4924 in mice previously fed an obesogenic diet. After MLN429 or vehicle injection, mice were fed were fed either a chow or a HFD (Figure 57A). Neddylation inhibition by MLN4924

administration in different tissues, such as WAT, BAT and liver was monitored by assessing the pattern of neddylated proteins (Figure 57B-C).

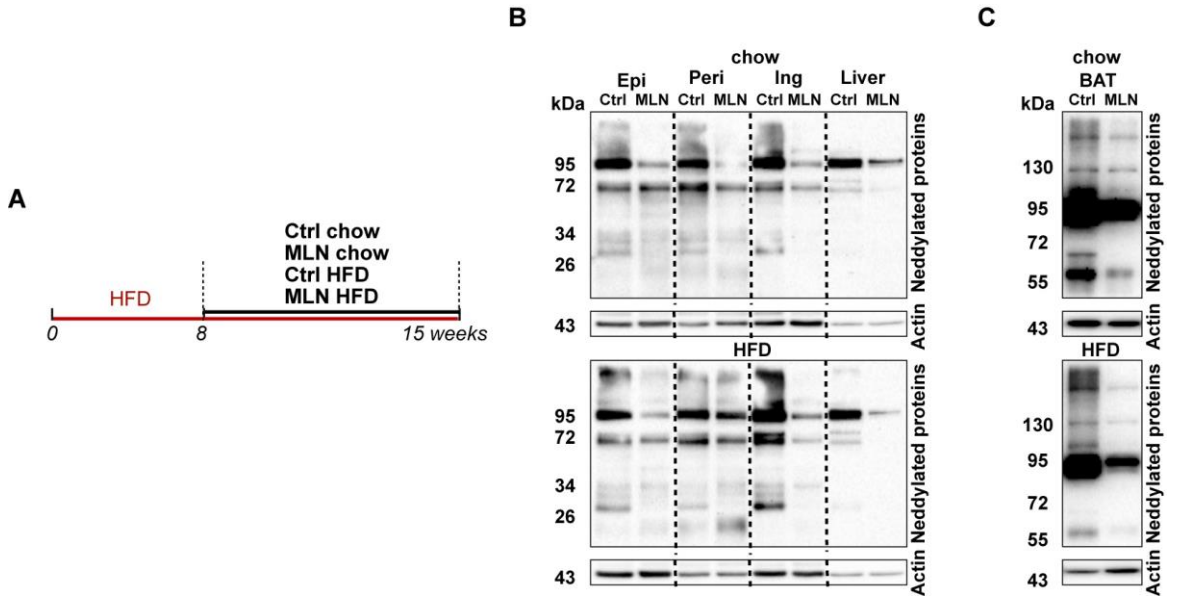

Figure 57: Peripheral neddylation inhibition by subcutaneous injections of MLN4924. (A) Diagram showing the *in vivo* experimental design. Mice were fed a HFD for 8 weeks. Afterwards, mice were fed a chow or a HFD and daily subcutaneously injected with vehicle (Ctrl) or MLN4924 (MLN). **(B-C)** Immunoblots for Nedd8 in WAT, BAT and liver of Ctrl and MLN-treated mice fed a normal chow diet (upper panel) or a HFD (lower panel). Equal protein loading was confirmed by normalization to Actin expression.

4.10.1 MLN4924 administration reduces HFD-induced obesity by decreasing adipose tissue mass and adipocyte size

In line with our observations in the *Nae1Adipo*CreER^{T2} KO model, also peripheral inhibition of the neddylation pathway resulted in body weight loss in obese mice. Notably, MLN4924 treatment reduced body weight in mice fed a HFD, while chow-fed animals displayed similar body weights (Figure 58A-B). The decrease in body weight was triggered by a reduction of fat mass in HFD-fed mice (Figure 58C). Global neddylation inhibition did not decrease AT mass in chow-fed animals, going in line with the unchanged body weight (Figure 58C). Moreover, as evidenced by H&E staining of AT sections, smaller polygonal healthy functional adipocytes without signs of inflammation were observed in MLN4924 treated animals compared to control mice (Figure 58E). Adipocyte area reduction was assessed in H&E-stained AT sections using the Adiposoft software. This approach revealed a decrease in average adipocyte area in WAT of MLN4924 treated mice respect to controls, though not always significant (Figure 58D).

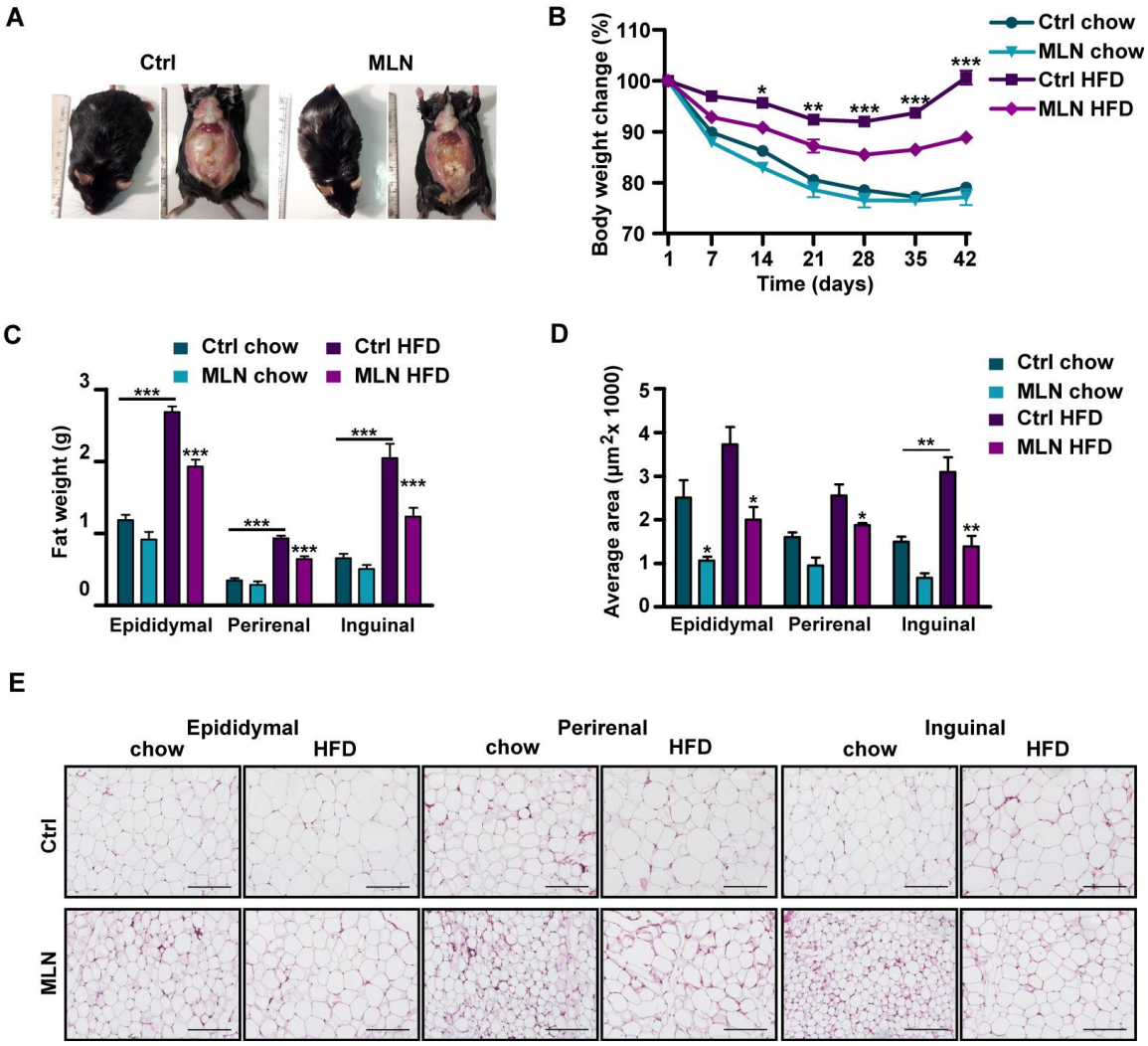

Figure 58: MLN4924 administration in HFD-induced obese mice reduces adiposity and adipocyte size. (A) Pictures of HFD-fed Ctrl and MLN-treated mice in week 15. **(B)** Body weight change relative to the initial weight was assessed over 42 days during vehicle or MLN administration (n= 9-10 mice per group). **(C)** WAT weights in Ctrl and MLN-treated mice (n= 9-10 mice per group). **(D)** Average adipocyte area (n=3 mice per group). **(E)** Images showing HE staining of WAT sections. Data are presented as mean ± SEM. Statistical significance is shown as $*p \leq 0.05$,$**p \leq 0.01$, $***p \leq 0.001$. Significance was determined by two-way ANOVA with Bonferroni's multiple comparison test in (B-D), and by one-way ANOVA with Bonferroni's multiple comparison test in (C-D, ctrl chow vs ctrl HFD). Scale bars represent 175 µm (E).

Moreover, perilipin immunoreactivity was observed on lipid droplets of adipocytes in MLN4924- as well as vehicle-treated animals without signs of macrophage infiltration (Figure 59A), suggesting neddylation inhibition by MLN4924 treatment does not impact adipocyte survival. Going in line, qRT-PCR showed that MCP1 expression in WAT of HFD-fed MLN4924-treated mice and specifically in epididymal fat in chow-fed MLN4924-treated animals decreased respect to Ctrl mice (Figure 59B). Importantly, HFD per se increased the expression of MCP1, although histological analysis did not reveal signs of macrophage infiltration. This suggests that AT inflammation triggered by HFD was still in a preliminary stadium, in which the AT is secreting higher MCP1 levels but immune cells were not yet recruited to the AT. This preliminary stadium of inflammation could potentially progress with

continuous HFD feeding. MLN4924 administration is able to rescue the beginning inflammation induced by HFD.

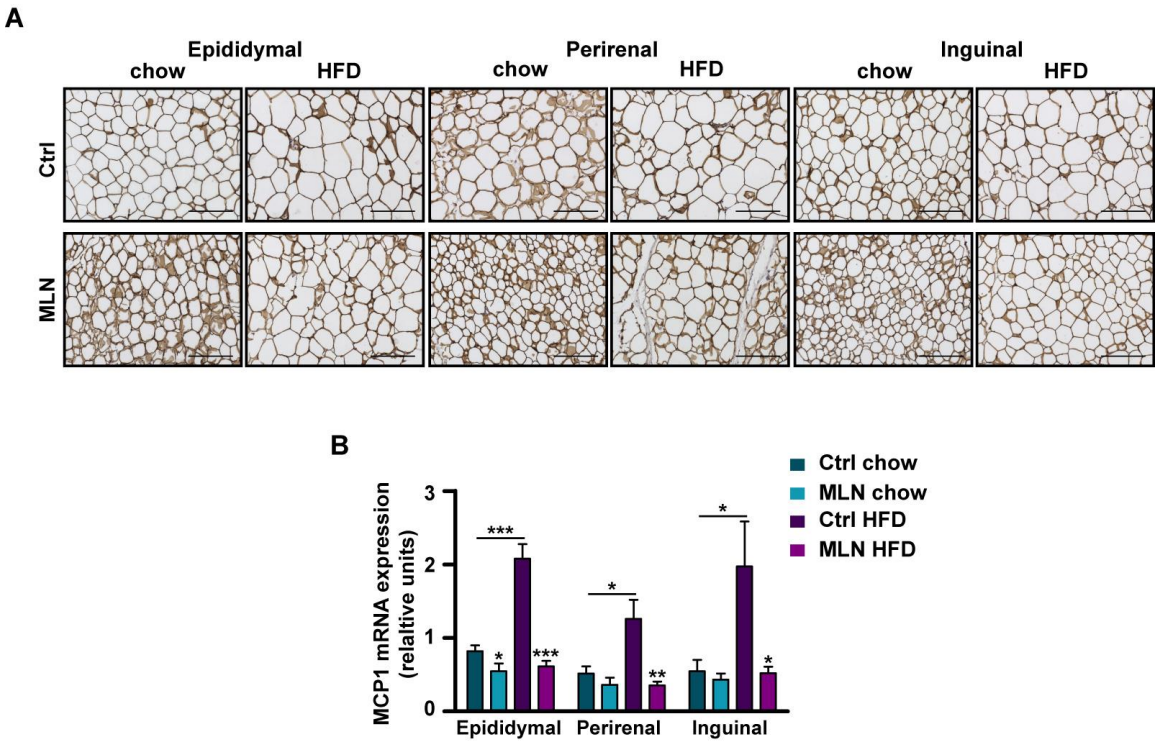

Figure 59: MLN4924 treatment in HFD-induced obese mice does not result in adipocyte death and decreases MCP1 expression in adipose tissue. (A) Representative images showing perilipin expression assessed by anti-perilipin immunostaining (brown) and hematoxylin staining (blue) in WAT sections. **(B)** Relative mRNA levels of MCP1 in different WATs normalized to Actin (n= 8-10 mice per group). Data are presented as mean ± SEM. Statistical significance is shown as $*p \leq 0.05$,$**p \leq 0.01$, $***p \leq 0.001$. Significance was determined by unpaired two-side t test. Scale bars in (A) represent 175 µm.

In order to explore the potential roles of C/EBPβ and PPARγ in the morphological changes of adipocytes upon MLN4924 treatment, we first examined the degree of C/EBPβ binding to the PPARγ promoter in WAT of MLN4924-treated and Ctrl animals. In contrast to our data obtained in 3T3-L1 cells and our findings in the KO model, WAT of MLN4924 treated mice displayed a similar C/EBPβ DNA binding to the PPARγ promoter, as revealed by ChIP assays (Figure 60A). This surprising result may indicate that compensatory mechanisms, that prevent the direct inhibitory effects on C/EBPβ in the AT, are triggered by global MLN4924 treatment *in vivo.* Accordingly, peripheral MLN4924 administration elevated PPARγ mRNA expression in WAT. PPARγ levels in the MLN4924-treated mice were either similar or higher than in Ctrl animals (Figure 60B). Furthermore, in epididymal and perirenal WAT the MLN4924 treatment restored the reduction of PPARγ expression caused by HFD (Figure 60B).

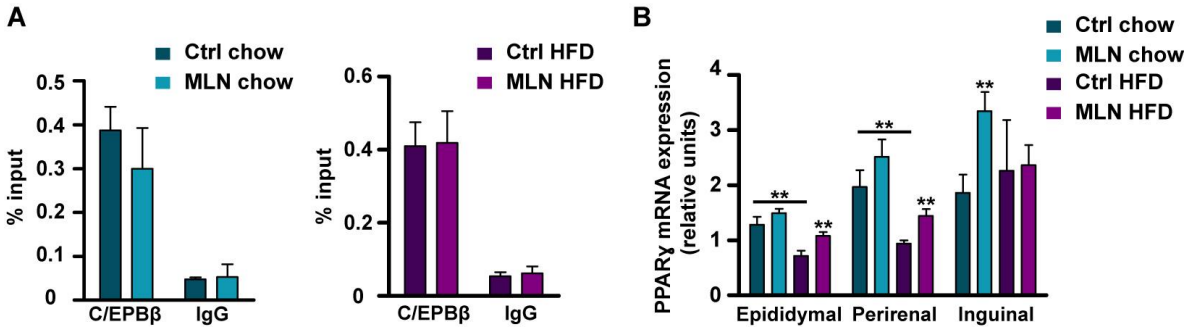

Figure 60: MLN4924 treatment in HFD-induced obese mice increases PPARγ expression in WAT. (A) ChIP-qRT-PCR assay for C/EBPβ binding to the PPARγ gene promoter in WAT. Amounts of immunoprecipitated DNA were normalized to inputs. IgG was used as a negative control. **(B)** Relative mRNA levels of PPARγ in different WATs normalized to Actin (n= 7-8 mice per group). Data are presented as mean ± SEM. Statistical significance is shown as $**p \leq 0.01$. Significance was determined by unpaired two-side t test in (B).

Consequently, we aimed to investigate the mRNA expression of metabolic genes that control the maintenance of adipocyte cellular identity. Performing qRT-PCR, we found that peripheral neddylation inhibition largely reverted the HFD-induced alterations on adipocyte-specific gene expression (Figure 61-63). Genes involved in FA uptake and lipolysis were found to be mostly elevated, independently of the diet, when neddylation was blocked in the periphery (Figure 61). Additionally, global neddylation inhibition mostly resulted in an increased expression of genes regulating glucose utilization and glyceroneogenesis (Figure 62). Furthermore, neddylation blockade in the periphery partially increased lipogenic gene expression in WAT of HFD-fed MLN4924-treated mice (Figure 63). In fact, mRNA expression of genes regulating lipogenesis was decreased by HFD per se and peripheral neddylation blockade partially restored it (Figure 63). Altogether, MLN4924 treatment largely reverted HFD-induced alterations in adipocyte gene expression, although not always significant, thereby improving adipocyte function. Thus, adipocyte-specific or peripheral neddylation ablation, both, results in lean phenotypes but with distinct outcomes on AT “health” and function.

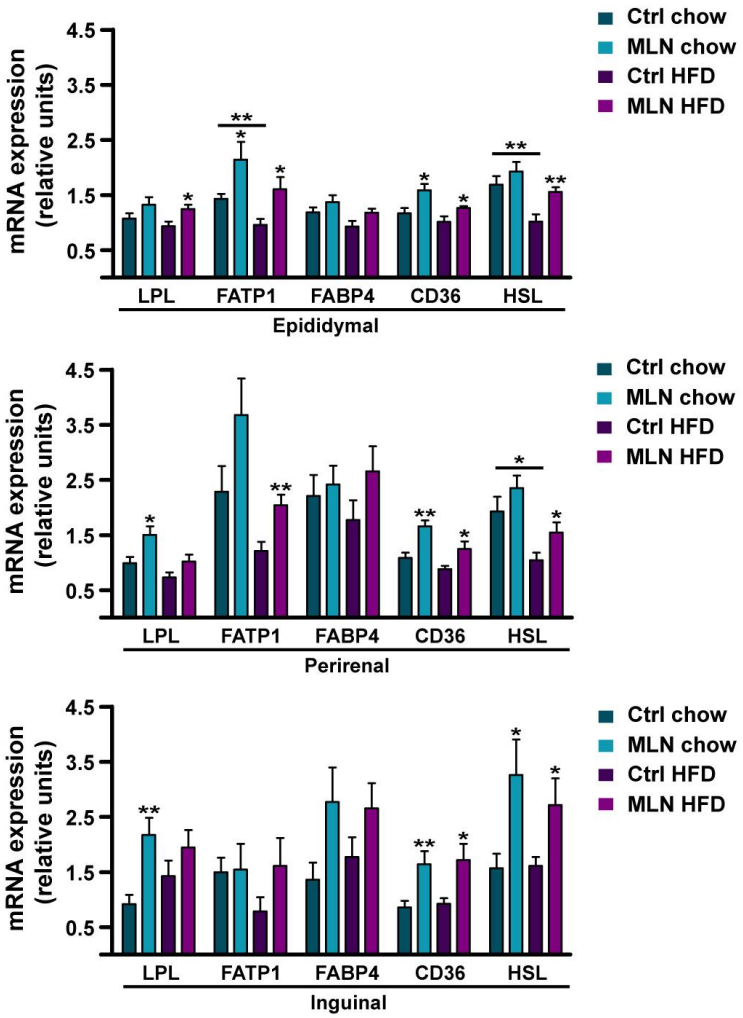

Figure 61: MLN4924 administration in HFD-induced obese mice increases mRNA expression of PPARγ downstream genes involved in FA uptake and lipolysis. Relative mRNA levels of the indicated genes in WAT normalized to Actin (n= 8-10 mice per group). Data are presented as mean ± SEM. Statistical significance is shown as $*p \leq 0.05$, $**p \leq 0.01$, $***p \leq 0.001$. Significance was determined by unpaired two-side t test.

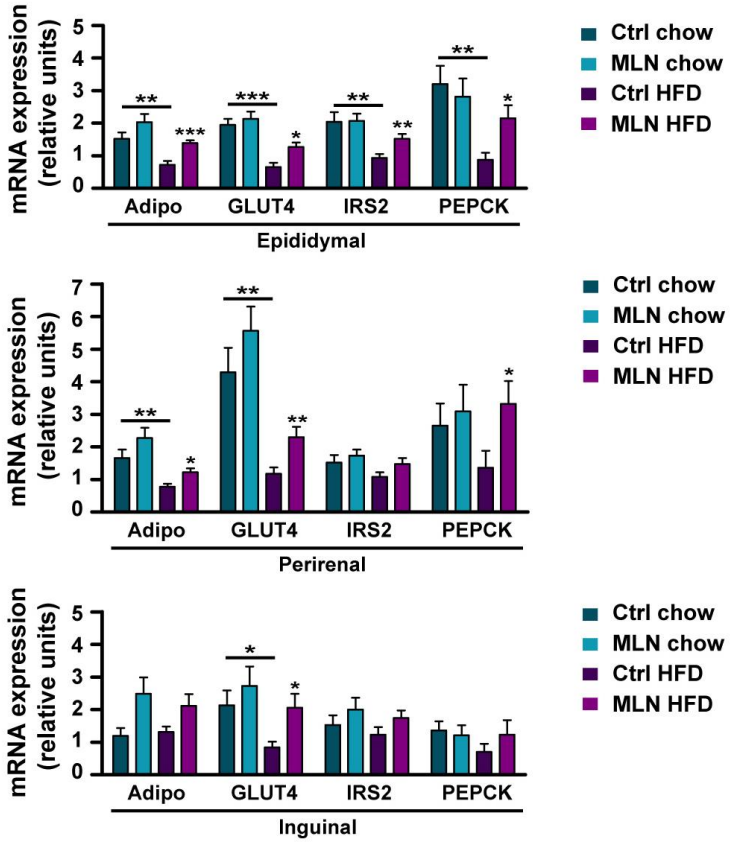

Figure 62: MLN4924 administration in HFD-induced obese mice increases mRNA expression of PPARγ downstream genes involved in glucose homeostasis, insulin signaling and glyceroneogenesis. Relative mRNA levels of the indicated genes in WAT normalized to Actin (n= 7-9 mice per group). Data are presented as mean ± SEM. Statistical significance is shown as ∗p ≤ 0.05, ∗∗p ≤ 0.01, ∗∗∗p ≤ 0.001. Significance was determined by unpaired two-side t test.

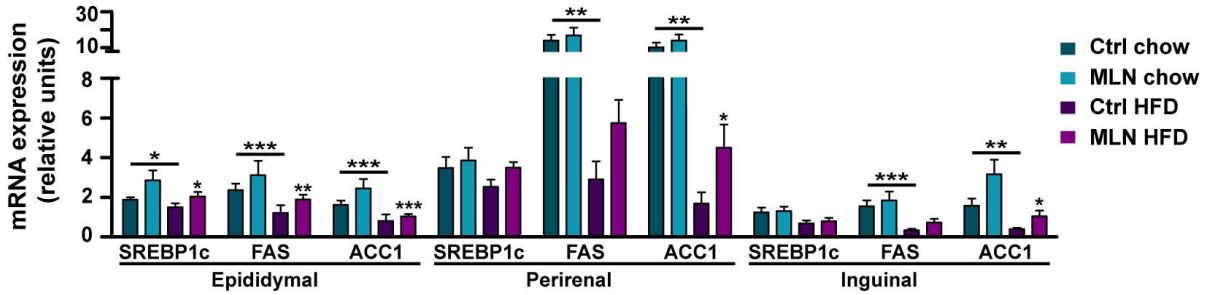

Figure 63: MLN4924 administration in HFD-induced obese mice increases mRNA expression of genes involved in lipogenesis. Relative mRNA levels of the indicated genes in WAT normalized to Actin (n= 7-9 mice per group). Data are presented as mean ± SEM. Statistical significance is shown as ∗p ≤ 0.05, ∗∗p ≤ 0.01, ∗∗∗p ≤ 0.001. Significance was determined by unpaired two-side t test.

4.10.2 MLN4924 injection restores HFD-induced impairment of thermogenesis in obese mice

Due to the ability of MLN4924 to revert HFD-induced body weight gain and improve AT morphology and function, we investigated a possible role of MLN4924 treatment in BAT remodeling or in the induction of browning. First, we examined the expression of thermogenic

genes in interscapular BAT by qRT-PCR. MLN4924 treatment did not significantly change the expression of the majority of thermogenic genes tested, such as UCP1, cell death-inducing DNA fragmentation factor alpha-like effector A (Cidea), PGC-1-α/β and PRDM16, between control and MLN4924-treated mice (Figure 64A). Accordingly, UCP1 protein expression remained unchanged upon MLN4924 treatment (Figure 64B). Only fatty acyl chain elongase, Elovl3, was found to be increased in BAT of MLN4924-treated mice in respect to Ctrls independent of the diet (Figure 64A). Elovl3 was described to have an important role in lipid recruitment and β-oxidation in BAT (Westerberg et al., 2006). A higher Elovl3 expression (Figure 64A) might be required to restore intracellular very long chain FA pools when the FA turnover rate is high. Consequently, we further investigated the impact of MLN4924 treatment on β-oxidation in this AT depot. Indeed, MLN4924 treatment in mice fed a HFD, partially promoted the expression of genes involved in β-oxidation, although these effects were not always statistically significant. Acyl-coenzyme A oxidase (ACO) expression increased in BAT of HFD-fed MLN4924-treated mice respect to Ctrl (Figure 64C). Long-chain acyl-CoA dehydrogenase (LCAD) expression tended to increase upon MLN4924 treatment in HFD-fed mice, although this increase was not statistically significant (Figure 64C). Accordingly, also the expression of genes promoting mitochondrial activity was partially elevated. Cox8b was significantly elevated in BAT of HFD-fed mice treated with the drug (Figure 64A).

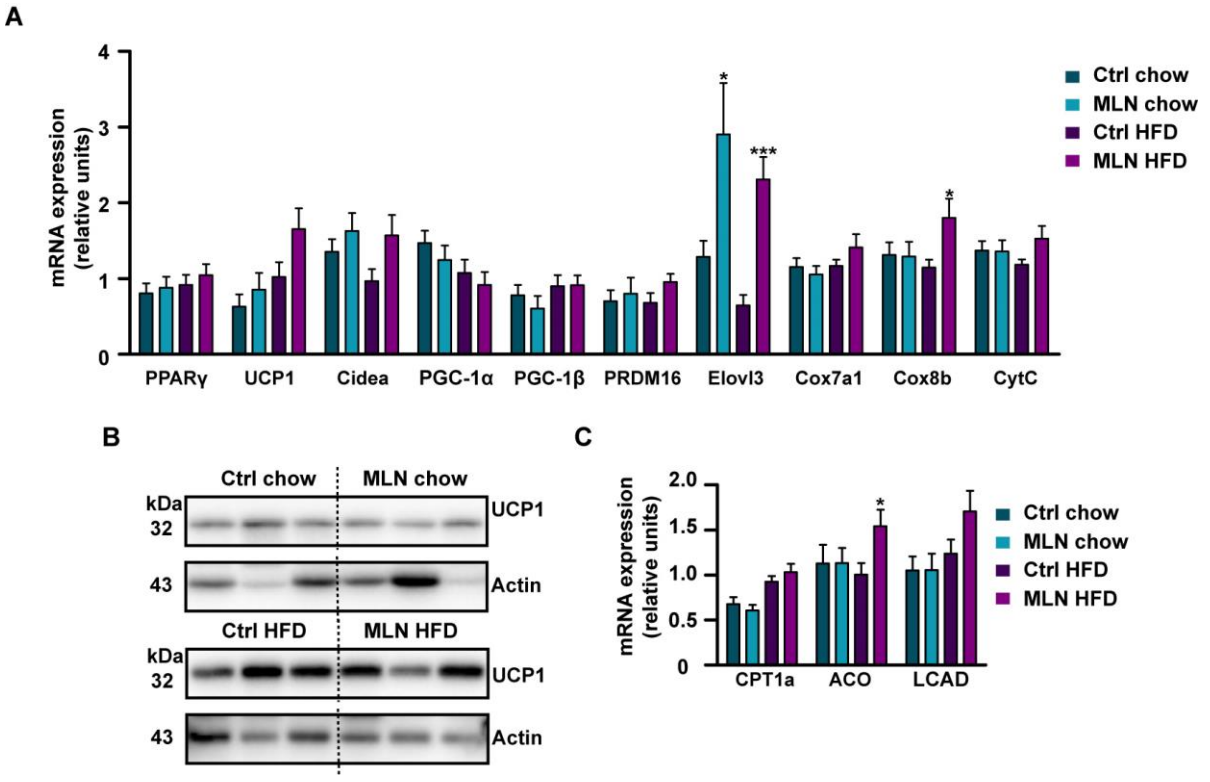

Figure 64: MLN4924 administration did largely not result in a promotion of β-oxidation and thermogenesis in interscapular BAT. (A) Relative mRNA levels of the indicated genes in BAT normalized to Actin (n= 7-10 mice per group). **(B)** Immunoblot of UCP1 in BAT of Ctrl- or MLN-treated chow- or HFD-fed mice. Equal protein loading

was confirmed by normalization to Actin expression. **(C)** Relative mRNA levels of the indicated genes in BAT normalized to Actin (n= 8-10 mice per group). Data are presented as mean ± SEM. Statistical significance is shown as ∗p ≤ 0.05, ∗∗∗p ≤ 0.001. Significance was determined by unpaired two-side t test.

Histological analysis of interscapular BAT demonstrated that MLN4924 administration resulted in smaller lipid droplets (Figure 65A). Going in line with this finding, BAT weight was decreased in HFD-fed mice under MLN4924 treatment (Figure 65B). Despite the fact that these observations would argue for an increased thermogenesis in BAT upon MLN4924 administration, we failed to detect a statistically significant increase in thermogenic markers. Thus, BAT thermogenesis is unlikely to account for the reduction in obesity and associated disorders in the MLN4924-treated mice.

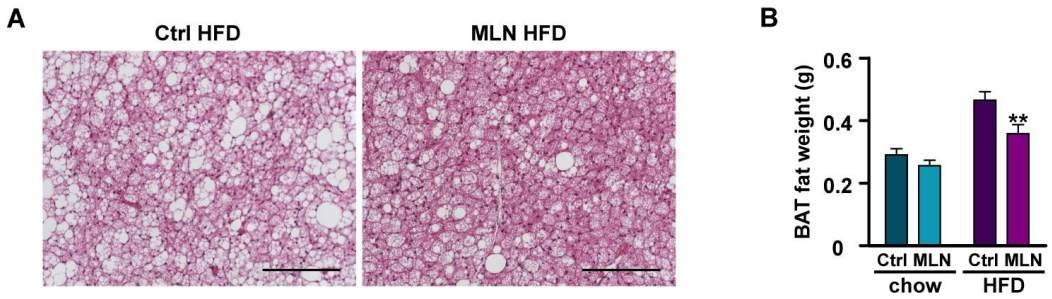

Figure 65: MLN4924 treatment reduces lipid content and weight of interscapular BAT. (A) Images showing HE staining of BAT sections. **(B)** BAT weights in Ctrl- and MLN-treated mice (n= 9-10 mice per group). Data are presented as mean ± SEM. Statistical significance is shown as ∗∗p ≤ 0.01. Significance was determined by two-way ANOVA with Bonferroni's multiple comparison test. Scale bars represent 175 µm (A).

As previously reported in the literature, the perirenal fat depot displayed a mix of BAT and WAT regions (de Jong et al., 2015; Zhang et al., 2018) (Figure 58E,66A). Next, we analyzed the effect of the pharmacological inhibitor on the histology and gene expression of perirenal AT. As already depicted above, MLN4924 administration decreased adipocyte size in the perirenal WAT depot of HFD-fed mice (Figure 58E). Histological analysis of perirenal BAT demonstrated reduced cell size, decreased lipid content and enhanced multilocularity in MLN4924-treated mice in comparison to Ctrl animals (Figure 66A). Confirming these histological findings, qRT-PCR and immunoblotting analyses revealed an increased expression of UCP1 mRNA and protein in perirenal fat of MLN4924-treated mice fed a HFD, whereas no difference was detected between chow-fed mice (Figure 66B-C). In accordance with these results, the expression of several genes related to thermogenesis, mitochondrial function and β-oxidation was upregulated in perirenal fat of HFD-fed MLN4924-treated mice respect to Ctrl animals (Figure 66B-D). Accordingly, expression of genes related to thermogenesis (Cidea, PGC-1β, Elovl3), mitochondrial function (Cox7a1, Cox8b (subunits of cytochrome c oxidase) and CytC) and β-oxidation (ACO, LCAD) was significantly upregulated in perirenal AT of HFD-fed MLN4924-treated mice compared to Ctrl mice (Figure

66B,D). We did not detect an elevation in thermogenesis and β-oxidation in chow-fed animals (Figure 66B-D), going in line with the observation that MLN4924 treatment in chow-fed mice did not alter AT mass and adipocyte size in the perirenal fat depot.

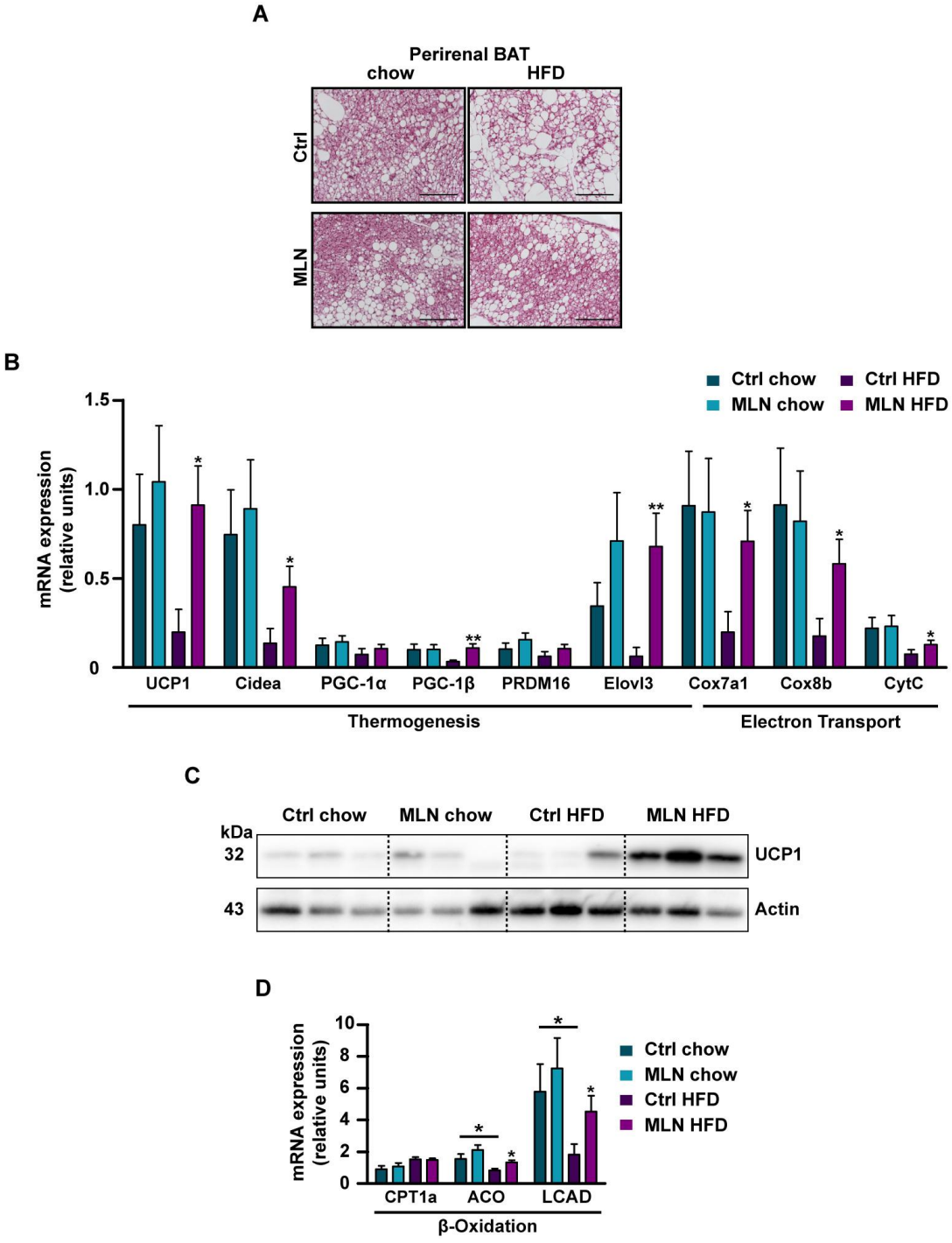

Figure 66: MLN4924 treatment in HFD-induced obese mice induces thermogenesis in perirenal adipose tissue. (A) Representative images showing HE staining of BAT areas in perirenal AT sections. **(B)** Relative mRNA levels of the indicated genes in perirenal AT normalized to Actin (n= 8-10 mice per group). **(C)** Immunoblot of UCP1 in perirenal AT of HFD-fed Ctrl- or MLN-treated mice. Equal protein loading was confirmed by normalization to Actin expression. **(D)** Relative mRNA levels of the indicated genes in perirenal AT normalized to Actin (n= 8-10 mice per group). Data are presented as mean ± SEM. Statistical significance is shown as $*p \leq 0.05$, $**p \leq 0.01$. Significance was determined by unpaired two-side t test.

Importantly, despite its high thermogenic capacity, we failed to detect UCP1 expression in inguinal fat upon MLN4924 administration. However, genes involved in β-oxidation were partially elevated in inguinal fat of chow-fed mice treated with the drug (Figure 67A). Analysis of the profiles of genes involved in β-oxidation by qRT-PCR revealed that β-oxidation was unaltered by MLN4924 treatment in muscle and liver and thus cannot explain the beneficial adaptations in these mice (Figure 67B-C). In fact, muscle expression of genes involved in lipogenesis, like SREBP1c and FAS, and β-oxidation, such as PPARα, CPT1b, ACO, MCAD and LCAD, were not affected by treatment with the drug (Figure 67B). Going in line, by performing qRT-PCR analysis of livers of MLN4924-injected mice, we observed that PPARα, CPT1, ACO and LCAD expression remained unchanged (Figure 67C). These observations together propose that inhibition of neddylation in the periphery by MLN4924 treatment results in a strong AT remodeling. Particularly, the drug is able to restore the whitening of perirenal BAT and thus reverts the devastating effects induced by HFD.

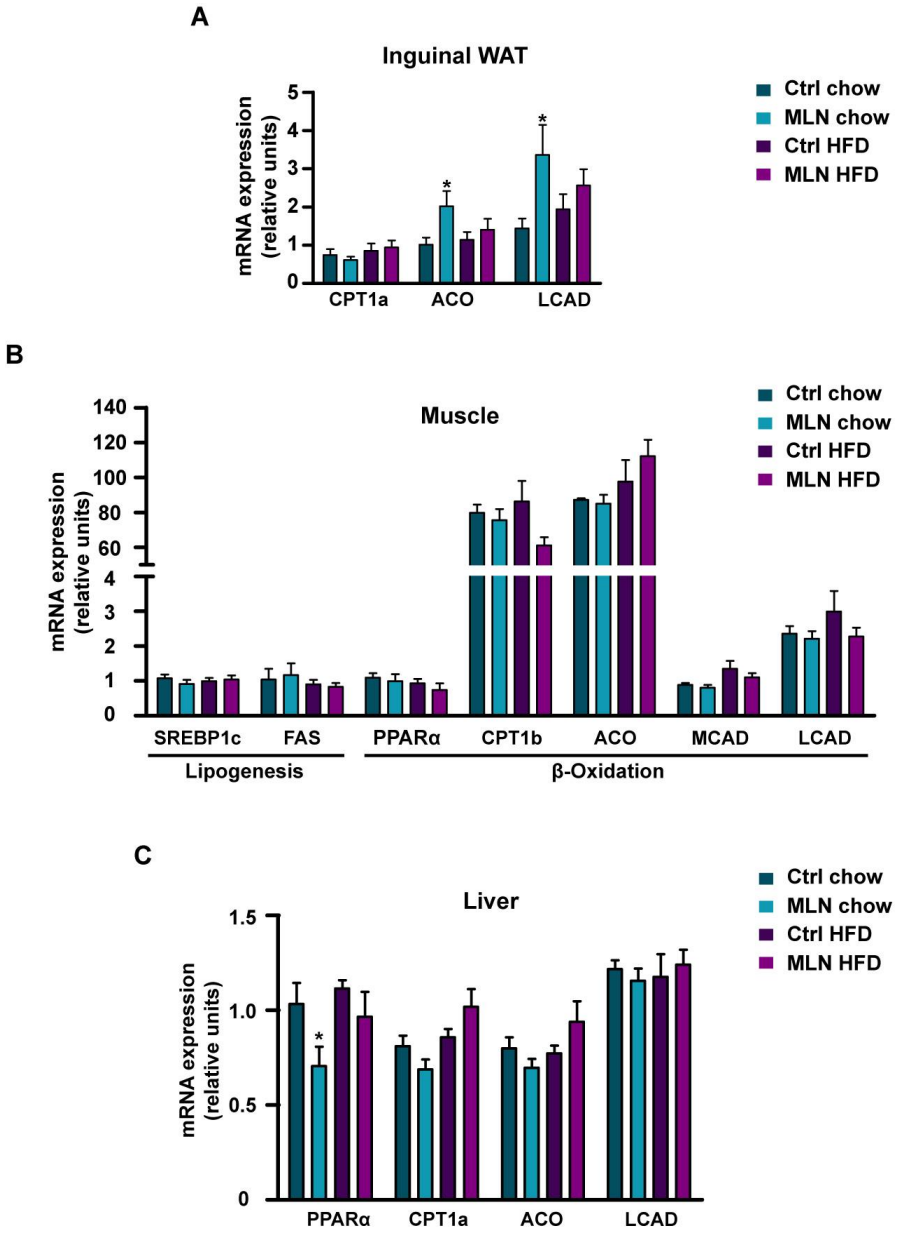

Figure 67: Effects of MLN4924 treatment on β-oxidation. (A) Relative mRNA levels of the indicated genes in inguinal AT normalized to Actin (n= 8-10 mice per group). **(B)** Relative mRNA levels of the indicated genes in muscle normalized to Actin (n= 4-5 mice per group). **(C)** Relative mRNA levels of the indicated genes in liver normalized to Actin (n= 9-10 mice per group). Data are presented as mean ± SEM. Statistical significance is shown as $*p \leq 0.05$. Significance was determined by unpaired two-side t test.

The increased expression of thermogenic markers and genes involved in β-oxidation could trigger enhanced energy dissipation. Accordingly, we found a moderate increase in oxygen consumption and energy expenditure by employing indirect calorimetry at ambient temperatures (Figure 68A-B). Neither food intake nor locomotor activity changed upon MLN4924 treatment (Figure 68C-D). Moreover, MLN4924 treatment did not result in an enhanced secretion of energy via feces, as assessed by bomb calorimetry (Figure 68E). As reflected by the RER, administration of the inhibitor did not impact metabolic flexibility of

treated mice (Figure 68F). Thus, the increase in energy expenditure in form of heat production might account for the MLN4924-induced body weight loss.

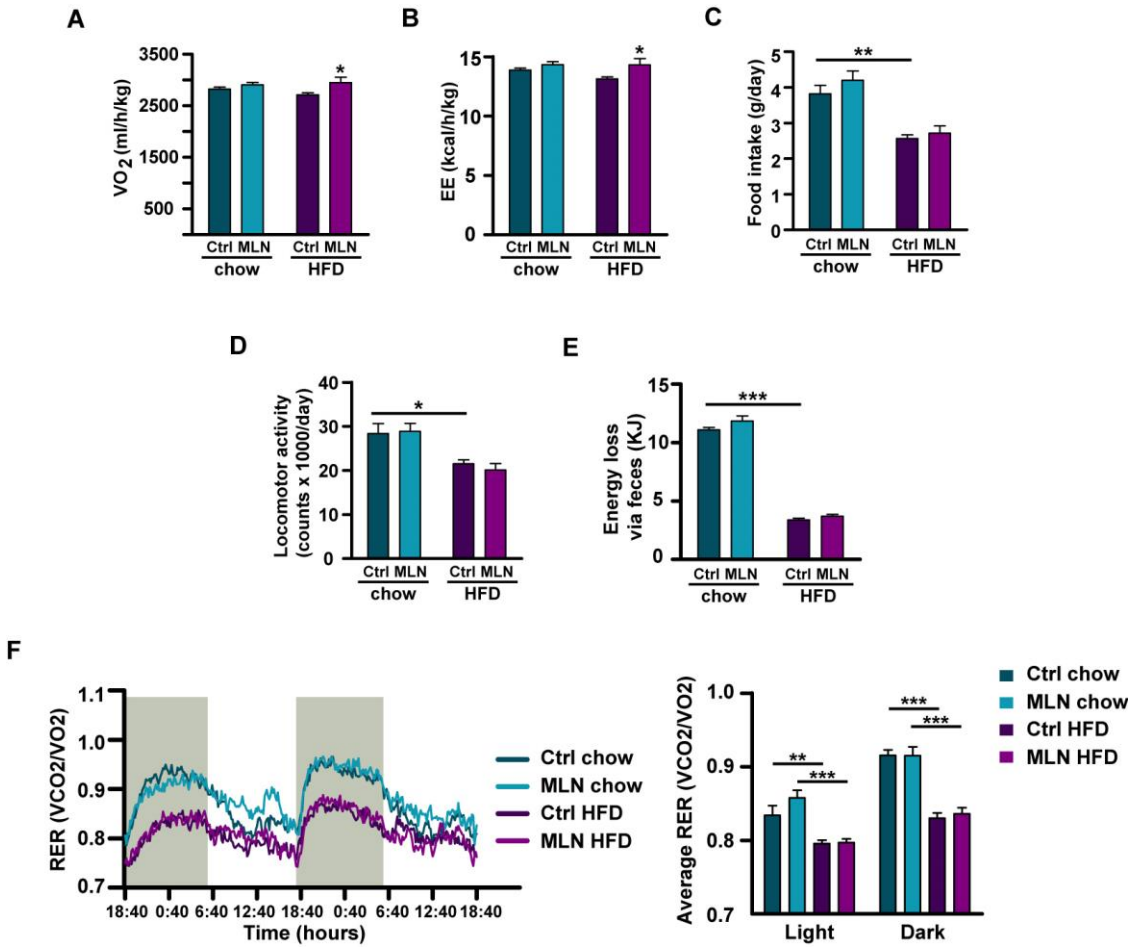

Figure 68: MLN4924-mediated increase in energy expenditure might account for weight loss in HFD-induced obese mice. (A-B) Oxygen consumption (VO_2) and energy expenditure (EE) in mice (n= 6-10 mice per group). **(C)** Food intake of mice (n= 7-8 mice per group). **(D)** Locomotor activity of mice (n= 8 mice per group). **(E)** Energy loss via feces per day in mice (n= 8-10 mice per group) assessed by bomb calorimetry. **(F)** RER and average RER measured during the light and dark cycle (shaded region) in Ctrl- and MLN-treated mice (n= 8 mice per group). Data are presented as mean ± SEM. Statistical significance is shown as $*p \leq 0.05$, $**p \leq 0.01$, $***p \leq 0.001$. Significance was determined by two-way ANOVA with Bonferroni's multiple comparison test in (A-B) and by one-way ANOVA with Bonferroni's multiple comparison test in (C-F Ctrl chow vs Ctrl HFD).

4.10.3 MLN4924 injection improves HFD-induced metabolic disorders

In contrast to our findings in the fat specific KO model of neddylation, global loss of AT resulted in beneficial metabolic effects in MLN4924-treated mice. Lower circulating glucose and insulin levels were observed in HFD-fed mice treated with MLN4924 (Figure 69), suggesting an improved insulin sensitivity in these animals.

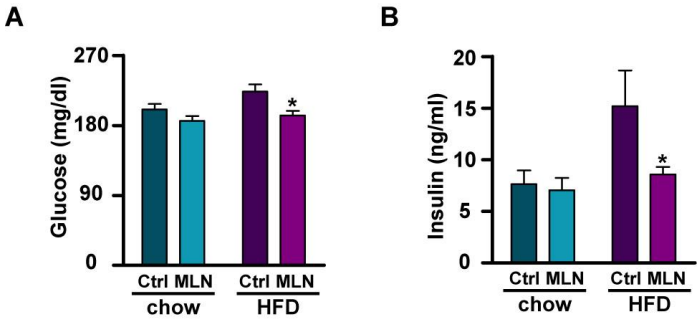

Figure 69: MLN4924 administration reverts HFD-induced hyperglycemia and hyperinsulinemia. (A-B) Plasma glucose and insulin levels (n= 8-10 mice per group). Data are presented as mean ± SEM. Statistical significance is shown as ∗p ≤ 0.05. Significance was determined by two-way ANOVA with Bonferroni's multiple comparison test.

This decrease might be secondary to reduced circulating FA levels in MLN4924-treated animals that were fed a HFD (Figure 70A). MLN4924 administration in HFD-fed mice resulted in decreased plasma leptin levels, possibly due to the reduction in fat mass (Figure 70B). Plasma TG levels remained in a normal range regardless of the diet (Figure 70C). Moreover, MLN4924 reverted HFD-induced liver steatosis, as evidenced by representative liver images, reduced liver weights and H&E staining of liver sections (Figure 70D-F). Altogether, MLN4924 treatment results in body weight loss, improved adipocyte function and restored metabolic homeostasis, most likely due to the induction of thermogenesis in perirenal fat tissue and following enhanced energy expenditure.

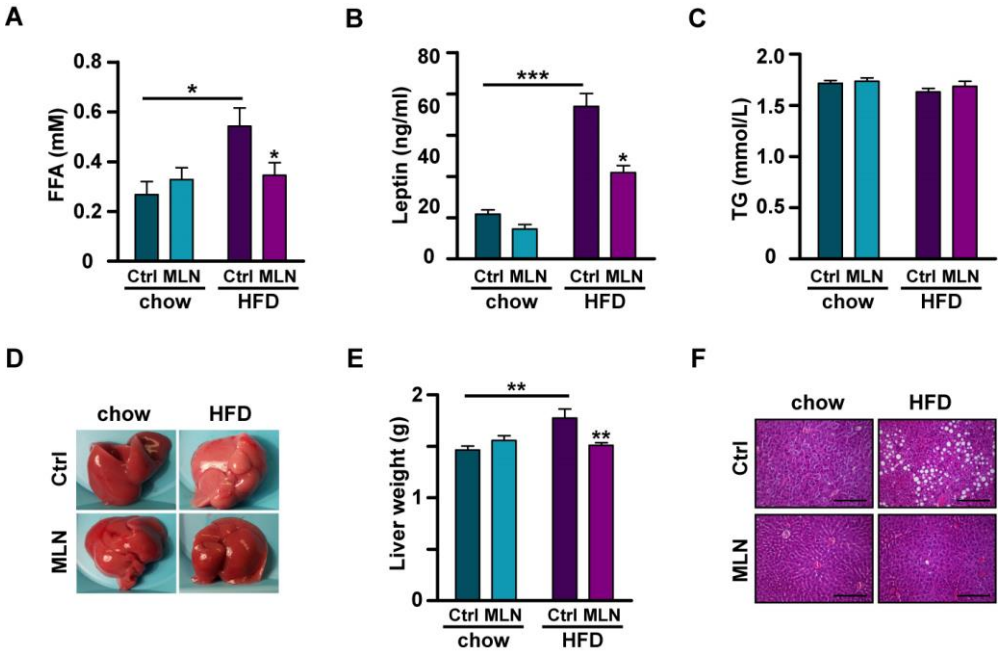

Figure 70: MLN4924 treatment reverts HFD-induced hepatic steatosis. (A-C) Plasma FA, leptin and TG levels (n= 8-10 mice per group). **(D-E)** Representative pictures of liver and liver weight in Ctrl- and MLN-treated mice (n= 6-10 mice per group). **(F)** Representative images showing HE staining of liver sections. Data are presented as mean ± SEM. Statistical significance is shown as ∗p ≤ 0.05, ∗∗p ≤ 0.01, ∗∗∗p ≤ 0.001. Significance was determined by two-way ANOVA with Bonferroni's multiple comparison test in (A-B, E) and by one-way ANOVA with Bonferroni's multiple comparison test in (A-B, E, ctrl chow vs ctrl HFD). Scale bars represent 200 µm (F).

5 Discussion

Obesity is a chronic metabolic disorder provoked by excessive energy intake and low energy expenditure which leads to a higher risk for the development of many human health problems like T2DM, dyslipidemia, hypertension and cardiovascular diseases (Kopelman, 2000). Reducing obesity and its associated comorbidities has become a research task worldwide because of the increasing medical costs for the treatment of obesity-related diseases (O'Neill and O'Driscoll, 2015). Therefore, understanding the mechanisms involved in adipogenesis and obesity and the discovery of new anti-obesity drugs is of high relevance.

So far, the research field has focused on the extensive study of the transcriptional regulation of adipogenesis. In this context, adipogenesis has been viewed as a cascade of sequential transcriptionally events as the main driver of adipocyte development. Nevertheless, this conceptual point of view that has strongly influenced the field, failed to include a very relevant aspect of differentiation programs: the many PTMs controlling stability, function, localization, partner interactions, etc. of the key players in fat development. Although in the last years the role of several PTMs, such as phosphorylation or acetylation, of transcription factors have been analysed, not much knowledge has been generated regarding the function of other PTMs. In particular, the role of neddylation in adipocyte development as well as function and obesity remained largely unknown.

5.1 Neddylation controls adipogenesis

In the present study we found that the expression profiles of members of the neddylation pathway during 3T3-L1 adipogenesis, like Nae1, the regulatory subunit of the first enzyme of the neddylation pathway, the neddylated form of the E2 enzyme Ubc12 and the pattern of neddylated proteins changed during 3T3-L1 differentiation. These results may indicate a regulatory role of neddylation during adipogenesis, going in line with previous observations that either described an upregulation of the Nedd8 protein during 3T3-L1 adipogenesis (Park et al., 2016) or an increase in neddylated Cul3 during adipocyte differentiation of LiSa-2 cells (Dubiel et al., 2017). The fact that immunoblotting yielded a pattern of neddylated proteins suggests that several Nedd8 targets might be involved in the regulation of adipogenesis.

Neddylation blockade inhibited adipogenesis reinforcing the notion that Nedd8 conjugation is essential for adipocyte differentiation. Blocking neddylation with the potent and selective Nae1 inhibitor MLN4924 (Soucy et al., 2009), repressed 3T3-L1 adipocyte differentiation. This result was further confirmed in PCC of inguinal fat tissue and MEFs. These observations

are in accordance with recent studies that described the inhibitory effects of MLN4924 treatment on adipogenesis in 3T3-L1 cells, human AT-derived stem cells and LiSa-2 cells (Dubiel et al., 2017; Park et al., 2016). Importantly, reversion experiments revealed that 3T3-L1 cells were able to differentiate into mature adipocytes to the same extend as control cells after washing out the inhibitor and re-stimulating cells for differentiation. Thus, we could rule out cytotoxic effects of the drug and propose that MLN4924-treated cells retained the commitment to become mature functional adipocytes. Experiments, in which the neddylation pathway was inhibited genetically, underscored the relevance of Nedd8 conjugation during adipogenesis. The dominant negative Ubc12 mutant Ubc12 C111S sequesters Nedd8 and thus prevents further conjugation to substrate proteins (Wada et al., 2000). Preventing neddylation by this mean also blocked 3T3-L1 adipocyte differentiation. Nevertheless, the limitation of this approach was the relatively low transfection efficiency in 3T3-L1 cells using electroporation. To circumvent this issue, we co-transfected the cells with a GFP overexpression plasmid that allowed us to include only the successful transfected cells expressing GFP into the quantitative analysis. In fact, lentiviral expression would be the method of choice for this approach which was unfortunately not applicable for us due to the lack of appropriate facilities.

The downregulation of the two adipocyte master genes PPARγ and C/EBPα accounts for the inhibition of adipogenesis. Adipogenesis is driven by a tightly controlled transcription factor cascade, ultimately resulting in the expression of the master regulators of adipogenesis PPARγ and C/EBPα that coordinate the expression of many adipocyte-specific metabolic genes (Cristancho and Lazar, 2011; Farmer, 2006; Rosen and MacDougald, 2006). Supporting our observations, it is well established that these adipogenic transcription factors are able to promote adipogenesis (Freytag and Geddes, 1992; Freytag et al., 1994; Lin and Lane, 1994; Tontonoz et al., 1994b) and their absence inhibits adipocyte differentiation (Lin and Lane, 1992; Rosen et al., 1999).

Altogether, we and others (Dubiel et al., 2017; Park et al., 2016) showed that Nedd8 conjugation plays essential roles in adipocyte differentiation. This idea is consistent with the general regulatory role for PTMs in cellular developmental processes and the observations that phosphorylation (Humphrey et al., 2013; Rabiee et al., 2017; Wu et al., 2009), acetylation (Xu et al., 2013), sumoylation (Chung et al., 2010; Liu et al., 2013; Mikkonen et al., 2013) and ubiquitination (Kim et al., 2014; Li et al., 2016; Watanabe et al., 2015), between others, control adipocyte development.

5.2 Neddylation promotes fat storage in mature adipocytes

In addition to its role in adipocyte differentiation, we demonstrated that neddylation also exhibits important functions in the maintenance of adipocyte cell identity. This notion was underpinned by the finding that MLN4924-mediated neddylation inhibition resulted in decreased TG content in developed 3T3-L1 and primary adipocytes. Notably, in respect to the effects on adipogenesis, in developed adipocytes the response to MLN4924-induced neddylation inhibition was milder as reflected by the higher MLN4924 concentrations required. Importantly, the lipid droplet loss in 3T3-L1 cells was reversible after washing out the drug. The recovery of beforehand treated cells was secondary to the addition of insulin, a hormone that was previously reported to promote lipogenesis (Knutson and Balba, 1997; Morales et al., 1992).

The MLN4924-mediated decrease in lipid droplet content was triggered by a dramatic downregulation of the adipocyte master gene PPARγ. PPARγ controls the maintenance of the mature adipocyte characteristics by regulating many adipocyte cellular functions, such as FA and glucose uptake, lipolysis, glyceroneogenesis, insulin signaling and lipogenesis (Tamori et al., 2002). It was demonstrated to govern the expression of many genes involved in these processes (Chawla and Lazar, 1994; Gustafson et al., 2003; Martin et al., 2000; Nagy et al., 1998; Schoonjans et al., 1996; Smith et al., 2001; Tontonoz et al., 1995; Tontonoz et al., 1994a). Accordingly, decreased PPARγ expression in MLN4924-treated 3T3-L1 cells resulted in the impairment of, both, lipolysis and lipogenesis leading to increased FA release from 3T3-L1 cells into the medium. Despite the decrease of lipolysis, a continuous cleavage of TG without a concomitant lipid synthesis resulted in a reduced cellular TG content. Notably, 3T3-L1 cells still conserved the isoproterenol-associated lipolytic capacity, suggesting that stimulated TG lipolysis is functionally conserved in these cells. Moreover, PPARγ is crucial for maintaining adipocyte insulin sensitivity by regulating genes involved in insulin signaling or glucose transport (Tamori et al., 2002). As a consequence, the MLN4924-mediated PPARγ downregulation might result in an insulin resistant state of 3T3-L1 adipocytes, although this was not examined. Thus, neddylation inhibition is resulting in dysfunctional adipocytes triggered by a downregulation of PPARγ. PPARγ is known to be fundamental for adipocyte survival (Imai et al., 2004). We showed by hematoxylin staining the presence of cell nuclei and demonstrated with reversion experiments (either by adding the pro-lipogenic hormone insulin or the PPARγ agonist rosiglitazone) that MLN4924-treated cells retain the ability to store TG, thereby ruling out cytotoxic effects. Nevertheless, this does not exclude that adipocyte cell death might occur at later time points when adipocyte dysfunction already proceeded. Dysfunctional adipocytes send signals, for instance chemoattractants like MCP1, in order to recruit immune cells to the

AT (Guilherme et al., 2008). 3T3-L1 cells have been shown to produce MCP-1 under certain conditions (Sartipy and Loskutoff, 2003). Adipocyte dysfunction triggered by neddylation inhibition resulted in an enhanced expression of MCP1. Altogether, these data implicate that neddylation plays important roles in promoting fat storage and in maintaining a functional adipocyte.

5.3 Neddylation regulates adipogenesis and fat storage by enhancing C/EBPβ transcriptional activity and DNA binding to the PPARγ promoter

Although a recent study showed that PPARγ neddylation stabilizes the protein and thus governs adipocyte differentiation (Park et al., 2016), we could not reproduce this result. First, neither pharmacological (MLN4924 treatment) nor genetic (Ubc12 C111S overexpression) neddylation inhibition did affect PPARγ protein stability in HEK293 cells in our study. Second, pull-down assays in HEK293 cells did not suggest that Nedd8 is covalently conjugated to PPARγ. Third, the dramatically decreased PPARγ mRNA levels observed in 3T3-L1 cells upon MLN4924 treatment would argue that Nedd8 is indeed targeting a factor upstream to PPARγ and C/EBPα that is controlling their expression during adipogenesis and in mature adipocytes. Along this line, the PPARγ agonist rosiglitazone was able to restore the MLN4924-mediated effects on lipid droplet loss, reinforcing that neddylation may target a protein upstream to PPARγ. Thus, we propose that the inhibitory effects of neddylation blockade on adipogenesis and developed adipocytes might be mediated by one or several factors upstream to PPARγ and C/EBPα. Indeed, pull-down assays revealed that Nedd8 is covalently conjugated to C/EBPβ and mutation of all lysines potentially targeted by Nedd8 prevented neddylation of the protein. The C/EBPβ protein consists of an N-terminal activation domain, a central regulatory domain and a C-terminal bZIP DNA binding domain (Tsukada et al., 2011). Identifying the specific lysine targeted by Nedd8 would help to define more precisely the effects of neddylation on the involved domain and ultimately on the function of the C/EBPβ protein. Mass spectrometry (MS)-based analysis in future studies will be needed to accomplish this task. However, identifying neddylated proteins by MS is not trivial. One limitation is the relatively low abundance of the neddylated forms of proteins (Jones et al., 2008). Moreover, neddylation is a dynamic process, reflected by constant neddylation and deneddylation of proteins (Rabut and Peter, 2008), even further resulting in a lower percentage of detectable neddylated proteins in certain states (Jones et al., 2008). In order to identify neddylated lysines in proteins, new MS approaches need to be developed to discriminate endogenous Nedd8 from other PTMs. A major limitation with current MS-based

methods is the inability to distinguish among modifications by ubiquitination, Nedd8 or ISG15, due to an identical di-glycine remnant generated by trypsin proteolysis of the modified proteins (Wagner et al., 2011). To overcome this limitation, our group previously created a C-terminal Nedd8 mutant that leads to larger overhangs after trypsination (Vogl et al., 2015). In addition to MS-based approaches the lysine residues in Nedd8 targets could be identified by mutation analysis. We created a C/EBPβ null mutant, in which all lysines were mutated to arginines, thereby preventing a possible neddylation. However, we failed to identify a single lysine mutant which could prevent Nedd8 conjugation to C/EBPβ (data not shown). The most plausible explanation is that neddylation on C/EBPβ does not require targeting a specific given lysine but rather acts as a domain-specific PTM, on which the first accessible lysine residue of a domain in a given time is enough for Nedd8 binding to exert its function. This has been already described for SUMO and is related to the enormous structural flexibility of its C-terminal binding domain (Hendriks and Vertegaal, 2016; Psakhye and Jentsch, 2012). Once a neddylated lysine or protein domain in C/EBPβ is identified, a lysine mutant could be created and subsequently validated in cell cultures and *in vivo*.

While C/EBPβ mRNA and protein levels remained unaffected by neddylation inhibition, MLN4924 treatment dramatically reduced C/EBPβ transcriptional activity on the PPARγ and C/EBPα promoters during adipogenesis and in developed adipocytes. The adipogenic transcription factor C/EBPβ is known to be involved in the coordinated regulation of PPARγ and C/EBPα expression during terminal differentiation (Hamm et al., 2001; Wu et al., 1996; Yeh et al., 1995). Moreover, C/EBPβ was described to act in the transcriptional network that maintains adipocyte cell identity by preserving the expression of adipocyte-specific metabolic genes (Lefterova et al., 2008). Therefore, it is likely that the prevention of C/EBPβ neddylation attenuates its transcriptional activity, which accounts for the downregulation of C/EBPα and PPARγ and the consequent inhibition of adipogenesis and loss of TG. The reduction in C/EBPβ transcriptional activity might be triggered by reduced binding of C/EBPβ to the PPARγ promoter under MLN4924 treatment. Previous studies demonstrated that C/EBPβ DNA binding and transcriptional activity is modified by various PTMs by changing either its protein confirmation, by regulating its exposure to DNA elements or by modifying its accessibility for other PTMs (Kowenz-Leutz et al., 1994; Lynch et al., 2011; Williams et al., 1995). How neddylation of C/EBPβ affects its DNA binding and transcriptional activity remains to be elucidated. Modification of C/EBPβ, involving the crosstalk of different types of PTMs, fine-tunes its function (Guo et al., 2015). These modifications comprise for instance acetylation, phosphorylation, sumoylation and ubiquitination (Cesena et al., 2007; Eaton and Sealy, 2003; Fu et al., 2015; Tang et al., 2005). Our discovery on the neddylation of C/EBPβ contributes to the elucidation of the function and roles of PTMs in adipogenesis and, importantly, also in developed adipocytes, a topic that has not been intensively studied so

far. Moreover, our finding represents a regulatory role of neddylation in adipocyte biology beyond its Cullin-dependent cross-talk with the ubiquitination cascade (Dubiel et al., 2017).

5.4 Neddylation is de-regulated in obesity

Assessing the pattern of neddylated proteins in distinct AT depots, we found that neddylation is de-regulated in subcutaneous but not in visceral AT of obese in respect to lean mice. One possible explanation could be the distinct nature of different fat depots. AT depots are known to differ in their localization, function and impact on metabolic regulation due to depot-specific features (Lee et al., 2013b). These characteristics might stem from different developmental processes of the respective depot (Gesta et al., 2006; Yamamoto et al., 2010) or distinct paracrine and endocrine signals driving their regulation (Girard and Lafontan, 2008). Going in line with the notion that distinct AT depots direct different metabolic outcomes, we observed depot-specific effects when mice were subcutaneously injected with MLN4924. In fact, global neddylation inhibition caused an increase in the thermogenic gene expression program in perirenal fat, whereas these thermogenic markers were not detectable in inguinal fat. Thus, neddylation could play distinct depot-specific roles. *Cre*-lines enabling depot-specific recombination in fat cells, which currently do not exist, would be of high value in order to investigate this hypothesis. Moreover, different protocols could have different outcomes on obesity. We were feeding mice for 8 weeks with an obesogenic HFD (45 kcal%), a protocol which is known to induce obesity (de Wilde et al., 2009). However, a variety of HFD protocols exist, differing in the time period of HFD feeding and the composition of the diets. Thus, it remains to be elucidated if a longer exposure to HFD or feeding a diet with a higher fat content would trigger changes in the pattern of neddylated proteins also in visceral fat. Moreover, it would be interesting to characterize if the changes in neddylated proteins in AT depend on the obese phenotype of mice or if HFD feeding triggers these effects. In this context, it would be of value to investigate the neddylation status of AT in other rodent models of obesity, such as the mouse model of leptin deficiency (ob/ob mouse) or the mouse model lacking the leptin receptor (db/db mouse) (Lutz and Woods, 2012). Going in line, it would be interesting to investigate the impacts of AT-specific and global neddylation inhibition on body weight and metabolic outcomes in other models of obesity, as well. Moreover, judging the change of neddylation in certain fat depots upon obesity induction is not a trivial task due to the low detection efficiency of the available α-Nedd8 antibodies. Furthermore, one would not expect a complete change in the neddylation pattern but rather modification of certain Nedd8 targets involved in adipogenesis and fat storage. Thus, the identification of Nedd8 target proteins *in vivo* would be required to further define how

neddylation of these specific factors change during the induction of obesity or in already obese versus lean animals.

5.5 Adipose tissue-specific ablation of the neddylation pathway results in a lipodystrophic phenotype accompanied with severe metabolic disturbances

We developed and characterized *Nae1Adipo*CreER^{T2} mice, a mouse model in which *Cre*-mediated recombination results in deletion of the floxed *Nae1* gene specifically in the AT (Lee et al., 2013a; Sassmann et al., 2010). Since adiponectin is exclusively expressed in mature adipocytes the *Adipo*CreER^{T2} mouse line allows the induction of recombination specifically in developed adipocytes in the AT without any observable recombination in other tissues (Lee et al., 2013a; Sassmann et al., 2010). To discard that tamoxifen itself may affect glucose and lipid metabolism parameters in mice (Hesselbarth et al., 2015), all mice received tamoxifen.

In a first set of experiments, we showed that loss of neddylation by ablating *Nae1* in mature adipocytes reduces HFD-induced obesity through a delayed but rapid loss of AT mass. The decrease in fat mass appears to be caused by a gradual death of adipose cells as revealed by perilipin-negative immunostaining on the lipid droplet membrane. A lack of perilipin staining can visualize lipid droplet degeneration, which is a sign of adipocyte death (Cinti et al., 2005; Wernstedt Asterholm et al., 2014). As a major regulator of many adipocyte-specific functions, PPARγ is crucial for maintaining mature adipocyte characteristics and survival (Imai et al., 2004; Tamori et al., 2002). Downregulation of PPARγ in AT of *Nae1Adipo*CreER^{T2} mice was probably triggered by a decreased binding of de-neddylated C/EBPβ to the PPARγ promoter, as observed in 3T3-L1 cells. Consequently, reduced PPARγ levels in *Nae1Adipo*CreER^{T2} resulted in decreased expression of many genes involved in glucose uptake and insulin signaling, FA uptake and lipogenesis, thereby strongly impairing adipocyte function and ultimately leading to adipocyte death. Histological analysis and evidence of rising inflammatory markers suggested an increase in AT inflammation, consistent with the observation that adipocyte death causes AT inflammation in mice with adipose-specific PPARγ deletion (He et al., 2003; Wang et al., 2013). Body weight decrease and AT loss in *Nae1Adipo*CreER^{T2} mice might also partially result from reduced food intake that could be triggered by potentially higher systemic inflammation. Although circulating inflammatory markers have not been analyzed in *Nae1Adipo*CreER^{T2} mice, support for this hypothesis could be provided by the fact that AT inflammation has been described to elicit chronic systemic inflammation (Bluher, 2016). Evidence for a role of cytokines in regulating

feeding behavior may be found in the observation that inflammation and infection induce interleukins, which centrally play a prominent role in anorexia (Wong and Pinkney, 2004). Many previous studies showed that liver steatosis frequently occurs in lipodystrophic mouse models (Asterholm et al., 2007). Accordingly, in HFD-fed *Nae1Adipo*CreER^{T2} mice the spillover of FA subsequently lead to lipid deposition in the liver and probably in other tissues, although the latter was not further tested. Increased FA levels are frequently associated with lipodystrophy (Asterholm et al., 2007). Compensatory effects of ectopic lipid accumulation could explain the unexpected lack in increased plasma FA in HFD-fed *Nae1* KO animals. Additionally, unchanged circulating FA levels could be secondary to a pronounced increase in FA oxidation as reflected by a lower RER during the dark phase. Since a RER close to 0.7 indicates that fat is the major fuel used (Speakman, 2013), this argues that fat is the preferred substrate for oxidation in HFD-fed *Nae1Adipo*CreER^{T2} mice. Also, impaired glucose uptake and utilization could account for the decrease in RER. *Nae1Adipo*CreER^{T2} mice displayed elevated glucose and insulin plasma levels, decreased adiponectin secretion and impaired glucose tolerance. This could explain the decrease in RER and might suggest an insulin resistant state. This hypothesis is supported by the fact, that ectopic lipid accumulation contributes to the development of insulin resistance (Shulman, 2014).

In a second *in vivo* experiment, in which the fat-specific *Nae1* KO was simultaneously induced with the initiation of HFD or chow feeding, we could confirm and complement our data obtained in the first model of *Nae1* KO in HFD-induced obese mice. As expected, fat specific ablation of the neddylation pathway in *Nae1Adipo*CreER^{T2} mice prevented HFD-induced body weight gain due to a decrease in WAT depot mass. Strikingly, although chow-fed *Nae1* KO mice displayed a decreased AT weight of perirenal, inguinal and epididymal depots and liver mass remained unchanged, their body weight was not significantly decreased compared to chow-fed Ctrl mice. A possible reason could be that the weight of other AT depots, which were not examined, remained unchanged and this prevented the significant decrease in the overall body weight. As the findings of our first KO experiment argue, AT loss of perirenal, inguinal and epididymal depots in *Nae1Adipo*CreER^{T2} mice probably resulted from a decreased food intake and might be caused by adipocyte death triggered by a reduction in PPARγ levels. Further confirming our previous observations, we detected hepatic steatosis in HFD-fed *Nae1Adipo*CreER^{T2} mice. Lipid accumulation in the liver might partially explain the reduced circulating FA levels in these animals. Besides, low FA plasma levels could be attributed to a higher fat oxidation, as reflected by a lower RER. The finding that HFD-fed *Nae1Adipo*CreER^{T2} mice display lower circulating FA levels is in contrast to our previous observation in obese *Nae1Adipo*CreER^{T2} mice on a HFD, in which the FA levels were similar to HFD-fed Ctrl mice. The discrepancy concerning FA levels between the two models might be due to a longer exposure time to HFD resulting in rising FA

levels in the first *Nae1* KO experiment. As expected, adiponectin secretion in *Nae1Adipo*CreER^{T2} mice was decreased, due to the loss of fat mass. Surprisingly, and in contrast to the HFD-induced obese *Nae1Adipo*CreER^{T2} mice, non-fasting plasma glucose levels were similar between the two genotypes. Meanwhile, insulin levels were elevated in HFD-fed *Nae1Adipo*CreER^{T2} animals. Insulin hypersecretion can occur in a normoglycemic state as a compensatory mechanism with beginning insulin resistance (Chen et al., 1994). Insulin resistance was shown to be a considerable factor underlying glucose intolerance (Nathan et al., 2007). In fact, *Nae1* KO mice displayed higher glucose intolerance respect to Ctrl mice under HFD, predicting an insulin resistant state. It is interesting that *Nae1Adipo*CreER^{T2} KO mice under chow conditions had, on one hand, a normal glucose tolerance, glycemia and insulinemia but on the other hand had less fat tissue weight and higher FA oxidation. Thus, the adverse metabolic consequences on glucose homeostasis were only observed in KO mice fed a HFD. Also going in a similar direction, it is striking that in comparison to the first KO experiment, in this second one, in which the KO was simultaneously induced with chow or HFD feeding, the effects on glucose levels were much milder in HFD-fed mice and the animals seem to compensate for a beginning insulin resistance. This raises the question if obesity potentiates the effects caused by AT-specific neddylation ablation or if lack of neddylation potentiates the consequences of obesity.

Collectively, AT-specific neddylation ablation protects against HFD-induced obesity and reduces an already established obesity triggered by HFD, but leads to a lipodystrophic phenotype accompanied with a metabolic dysfunction in mice. The metabolic alterations found in *Nae1Adipo*CreER^{T2} mice strongly resemble the phenotype of adipose-specific PPARγ KO mice (He et al., 2003; Wang et al., 2013). These studies revealed the significance of AT PPARγ in maintaining healthy AT. Consequently, deletion of PPARγ results in dysfunctional AT, AT inflammation, impaired adipokine secretion, ectopic lipid deposition and insulin resistance (He et al., 2003; Wang et al., 2013). We propose that C/EBPβ neddylation is pivotal for the regulation of PPARγ and consequently AT function and viability. Conditional C/EBPβ KO mice would be required to unambiguously address questions about the role of C/EBPβ in adipocytes *in vivo*, to assess physiological outcomes and to draw conclusions in comparison to *Nae1Adipo*CreER^{T2} mice. However, currently, only whole-body C/EBPβ KO mice exist. *Nae1Adipo*CreER^{T2} KO mice not only enable the study of the role of AT-specific roles of neddylation but also serve as a mouse model of inducible lipodystrophy. Obesity and lipodystrophy have similar devastating metabolic outcomes. Thus, lipodystrophic mouse models represent a valuable tool for investigating dysfunctional AT, which could potentially contribute to elucidating underlying mechanisms of, both, lipodystrophy and obesity (Asterholm et al., 2007). Nevertheless, one major limitation is the fact that the Adiponectin-driven *Cre* exclusively allows recombination in mature adipocytes. A

preadipocyte-selective *Cre*-line does not exist at the moment. Despite the discovery of more and more cell markers for adipocyte precursors, the expression of these markers is not exclusively restricted to these cells (Hepler et al., 2017). Therefore, so far, the role of AT neddylation *in vivo* could only be evaluated in developed adipocytes and not during adipogenesis.

5.6 Peripheral neddylation inhibition by MLN4924 administration reduces obesity and associated metabolic disorders by inducing thermogenesis in perirenal fat

The specific neddylation inhibitor MLN4924 (Pevonedistat) is currently tested in clinical trials in patients with Acute Myeloid Leukemia, Myelodysplastic Syndrome, Acute Lymphoblastic Leukemia and certain types of solid tumors (Sarantopoulos et al., 2016; Shah et al., 2016; Swords et al., 2018; Swords et al., 2017). MLN4924 exerts its effects on tumor cell apoptosis through deregulation of S-phase DNA synthesis (Soucy et al., 2009). Moreover, a recent study provided evidence that the inhibitor represents a possible pharmacological therapy for the treatment of liver fibrosis (Zubiete-Franco et al., 2017), pointing towards new avenues for the treatment of a large variety of diseases. Whether this drug could also be potentially used for the treatment of obesity and metabolic syndrome is just beginning to be explored.

Our study unexpectedly revealed that adipocyte-specific ablation or global inhibition of neddylation exhibit opposite effects on metabolism in response to HFD. Remarkably, MLN4924 treatment completely normalized HFD-induced hyperglycemia, hyperinsulinemia and hepatic steatosis. HFD-fed Ctrl mice showed a pre-diabetic state associated with increased glucose and insulin plasma levels and hepatosteatosis. The metabolic recovery was associated with a regeneration of both WAT and BAT. Although in chow-fed mice MLN4924 treatment partially decreased adipocyte size to levels below those seen in Ctrl mice, the underlying improvement was further emphasized by challenge with HFD. In HFD-fed mice MLN4924 treatment reverted not only HFD-induced alterations in WAT gene expression levels and structure but also restored the appropriate thermogenic response in perirenal BAT. Strikingly, also a partial increase in the expression of genes involved in FA uptake and lipolysis was observed in WAT of chow-fed mice under MLN4924 treatment. In fact, CD36, FATP1, LPL and HSL expression was found to be partially increased. These data suggest that the adipocyte gene expression of chow-fed mice, previously challenged with HFD for two months, might be already altered and that MLN4924 treatment restores these changes. The present study demonstrated that MLN4924 injection in HFD-fed mice reverses an already established inhibition of adipose PPARγ levels triggered by HFD

feeding. The reversion of PPARγ levels probably accounts for the restoration of adipocyte gene expression. C/EBPβ binding to the PPARγ promoter in the AT of MLN4924-treated mice was unaltered and thus cannot explain the increased PPARγ expression observed in this tissue. This surprising result may indicate that compensatory mechanisms, that prevent the direct inhibitory effects on C/EBPβ in the AT, are triggered by MLN4924 treatment *in vivo.* Moreover, higher C/EBPβ expression and/or an increase in transcriptional activity may impact PPARγ transcription in mice injected with the inhibitor. PPARγ expression in the mature adipocyte is regulated by several proteins, including C/EBPα, PPARγ itself, RXR and numerous co-activators (Lefterova et al., 2008). Thus, it cannot be excluded that these factors might be involved in restoring PPARγ levels upon MLN4924 treatment. PPARγ regulates its own expression via an auto-regulatory loop (Wu et al., 1999). Thus, MLN4924 treatment might boost the activity of PPARγ and thereby increases its protein expression. PPARγ is activated by several endogenous PPARγ ligands. Natural PPARγ ligands encompass 15-deoxy-$\Delta^{12,14}$ prostaglandin J2 (Forman et al., 1995; Kliewer et al., 1995), the oxidized lipid components 9- and 13-hydroxyoctadeca-9*Z*,11*E*-dienoic acids (9-and 13-HODE) of oxidized low density lipoprotein (Nagy et al., 1998), oxidized alkyl phospholipids (McIntyre et al., 2003), FA and eicosanoids (Forman et al., 1997; Kliewer et al., 1997). These PPARγ ligands could possibly be affected by MLN4924 treatment. It is striking that global neddylation inhibition by MLN4924 administration results in increased AT PPARγ levels, while AT-specific neddylation depletion but also treatment with the inhibitor in 3T3-L1 cells results in severe downregulation of this protein and consequently deleterious effects on adipocyte function. The reversion of HFD-triggered decrease in AT PPARγ expression could potentially be attributed to the combined effects in different tissues caused by global neddylation inhibition. PPARγ is required for adipocyte differentiation, regulation of insulin sensitivity, lipogenesis and adipocyte survival and function (Lefterova et al., 2014; Lehrke and Lazar, 2005; Siersbaek et al., 2010; Tontonoz and Spiegelman, 2008). Thus, PPARγ increases the capacity of the AT to buffer toxic lipid species by allowing the storage of harmless TGs. In this direction, PPARγ2 was reported to prevent lipotoxicity by controlling AT expandability and peripheral lipid metabolism (Medina-Gomez et al., 2007). Indeed, our data suggest that the restored expression of PPARγ in the AT of MLN4924-treated mice may have a protective role on systemic metabolism. When ectopically induced in liver and muscle PPARγ2 protects from accumulation of reactive lipid species, playing an important antilipotoxic role (Medina-Gomez et al., 2007). The relevance of liver and muscle PPARγ expression in MLN4924-treated mice remains to be elucidated. Although histological analysis did not reveal signs of macrophage infiltration, HFD per se increased the expression of MCP1, which was reverted by MLN4924 administration. This suggests that AT inflammation triggered by HFD is still in a preliminary stadium, in which the AT is secreting higher MCP1

levels but immune cells were not yet recruited to the AT. This preliminary state of inflammation could potentially progress with continuous HFD feeding. Importantly, MLN4924 was able to prevent a beginning AT inflammation in HFD-fed mice. Similar to the effects in WAT, the increased brown adipocyte function promoted by MLN4924 might positively contribute to the beneficial effects on metabolic health in obesity. Global neddylation inhibition resulted in the recovery of key genes involved in thermogenesis and mitochondrial biogenesis in perirenal AT, which contains a mixture of brown adipocytes and classical white adipocytes. Indeed, the HFD-induced thermogenic defects in this specific fat depot were reverted by MLN4924 treatment. These findings suggest that global neddylation inhibition induces a profound remodeling of the perirenal fat, particularly in response to nutritional stress. The mechanism underlying this positive activation of the thermogenic program in perirenal fat is not clear. Nevertheless, the anatomic localization of this AT could be determinant for its functionality. As the sympathetic nervous system controls adrenal catecholamine secretion (Perlman and Chalfie, 1977), it is plausible that MLN4924 acts directly on the catecholamine-signaling pathway, leading to browning of the perirenal WAT. Catecholamines induce brown fat activation and beige development (Wang and Seale, 2016). MLN4924 treatment may either result in a switch from white to beige fat or increase the activation or number of brown adipocytes, thereby probably inducing a discrete elevation of energy expenditure in these mice. In this regard, small but consistent changes in energy expenditure could ultimately determine body weight and metabolic health. Lasar et al. demonstrated that PPARγ is required to maintain the thermogenic capacity of mature brown adipocytes, which can be induced by activating β–adrenergic signaling (Lasar et al., 2018). Accordingly, we found that thermogenic capacity of perirenal fat is recovered when PPARγ mRNA levels are elevated in HFD-fed MLN4924-treated mice in respect to Ctrl mice. Strikingly, HFD did not substantially affect the expression of thermogenic, mitochondriogenic and β-oxidation genes in interscapular BAT. However, histology of interscapular BAT showed increased lipid droplet accumulation in HFD-fed mice that was dissipated upon peripheral neddylation depletion. This reinforced our hypothesis that loss of Nedd8 conjugation in the periphery results in restored BAT responsiveness. Dramatic changes in Elovl3 may reflect a high FA turnover rate, since Elovl3 is correlated with increased β-oxidation (Westerberg et al., 2006). These results additionally suggest an induction of BAT thermogenesis in MLN4924-treated mice fed a HFD. Nevertheless, we did not observe altered expression of other thermogenic markers in interscapular BAT. This is particularly surprising as the interscapular BAT represents the major site for thermogenesis in the body (Cypess and Kahn, 2010). Further studies under stimulated conditions (e.g. under cold exposure or β-adrenergic stimulation) would be of value to address this issue. Moreover, additional studies could contribute to delineating the effects of MLN4924 treatment on energy expenditure. We

found a small increase in energy expenditure in MLN4924-treated mice before a significant body weight difference was established. Thus, it could be of interest to evaluate the energy expenditure in later time points of the treatment after a significant body weight loss in MLN4924-treated mice has already been established.

Park et al. previously reported that general deletion of the neddylation pathway in mice protects from body weight gain and ameliorates glucose intolerance under HFD (Park et al., 2016). In our study, we present interesting similarities as well as striking discrepancies to their work. Moreover, certain aspects of the adipose biology were not discussed in that manuscript, such as the consequences of adipocyte-specific ablation of the neddylation pathway or global neddylation inhibition after obesity induction. Surprisingly, Park et al. showed that MLN4924 increased UCP1 but inhibited PPARγ expression in epididymal WAT of HFD-fed mice, while we actually did not detect UCP1 in this tissue and observed an increase in PPARγ expression in all adipose depots analyzed. The findings reported by Park et al. are especially surprising since PPARγ is required for the development of all types of fat cells (Nedergaard et al., 2005), to maintain the thermogenic capacity of mature brown adipocytes (Lasar et al., 2018) and the *UCP1* gene contains binding sites for PPARγ that mediates between others brown adipocyte cell fate (Kong et al., 2014). Contrastingly, our data indicate that MLN4924 treatment restores UCP1 levels in perirenal fat of HFD-fed mice. Thus, both studies described the positive effects of peripheral neddylation blockade on body weight, glucose intolerance and hepatic steatosis, but the underlying mechanisms are fundamentally different. Several possible explanations could account for these differences. The *in vivo* experiment differed largely from our study due to distinct MLN4924 doses used, a different MLN4924 provider, diverging kinetic pattern of injection and the HFD employed in the *in vivo* experiment. Importantly, another distinct feature of our study is that we assessed the curative role of MLN4924 in obese mice while Park et al. studied the protective role of the drug while obesity induction.

Our study unexpectedly revealed that adipocyte-specific ablation or global inhibition of neddylation exhibit opposite effects on metabolism in response to HFD. Nevertheless, comparing both of our models, *Nae1Adipo*CreER^{T2} mice and peripheral neddylation ablation, in quantitative terms on the neddylation inhibition in the AT, we cannot exclude differences between treatments. Whether the extend of neddylation inhibition in the AT may account for the distinct outcomes in the two models remains unclear.

In summary, the improvement of systemic metabolic parameters observed in mice injected with MLN4924 is consistent with the notion that the health and functionality of WAT and BAT determines systemic metabolic health (Senol-Cosar et al., 2016; Shao et al., 2018). Notably,

neddylation may be involved in the regulation of whole-body metabolism by playing distinct roles in different metabolism-related tissues like muscle, liver, pancreas and AT, with actions in one tissue presumably impacting actions in the other tissues. Thus, global neddylation inhibition by MLN4924 may contribute to overall improvement of metabolic outcomes by affecting different tissues. It still remains unclear what exact signals drive the recovery of AT in MLN4924-injected mice in the context of diet-induced obesity. Tissue-specific conditional Nedd8 KO mice would be of value to identify tissue-specific physiological outcomes and putative mediators of tissue crosstalk.

5.7 Conclusion and Outlook

This study provided a comprehensive assessment of the role of the PTM neddylation in adipogenesis and fat storage, as well as its physiological role in obesity and metabolic control *in vivo*. We found that neddylation has important functions during adipogenesis and in the adipocyte by controlling cell-specific regulatory transcriptional networks. More specifically, neddylation of the key transcription factor C/EBPβ controls its biochemical function as well as the biological outcomes that it regulates. Thus, C/EBPβ neddylation governs adipogenesis and adipocyte cell identity. Our study demonstrated that fat-specific neddylation ablation prevents and reduces obesity triggered by HFD feeding. Moreover, global neddylation inhibition reduces HFD-induced obesity. However, the underlying mechanisms differ significantly between the two distinct animal models. We demonstrated that AT-specific neddylation ablation triggers a lipodystrophic phenotype that is accompanied with severe metabolic disturbances. Additionally, we provided detailed evidence that only global neddylation depletion reversed key systemic features of an already established pre-diabetic and obese phenotype in HFD-fed mice by inducing thermogenesis in perirenal fat. Activation of brown fat and/or browning of white fat hold great promise in the treatment of obesity and related disorders, making this mouse attractive from a clinical perspective. This may be particularly important considering that MLN4924 (Pevonedistat) is a drug close to be on the market and already tested in several cancer clinical studies for hematological malignancies and certain types of solid tumors. Moreover, a recent study indicates the beneficial impact of MLN4924 treatment on liver fibrosis, suggesting neddylation as a potential and attractive therapeutic target in this human disease.

The present study provided an insight into new regulatory roles of neddylation in the context of adipocyte biology, however it also opened up a number of new questions that would be interesting to address in the future: Are there fat depot-specific differences in the regulatory role of AT neddylation? Which is the role of neddylation during adipogenesis *in vivo*? Which

are the underlying mechanisms improving metabolic homeostasis upon global neddylation inhibition? In this regard, which particular factors are involved in the governance of higher PPARγ levels and consequently improved AT function? Which are the driving forces triggering the thermogenic response in perirenal AT? Which are the tissue-specific roles of neddylation that are involved in tissue crosstalk in order to control metabolism? Which are the roles of neddylation in human obesity? Could the pharmacological neddylation inhibitor MLN4924 serve as potential anti-obesity drug in humans? Addressing these questions in future studies would highly contribute in elucidating the systems involved in the devastating disorder obesity.

In summary, our results demonstrate that neddylation represents a relevant posttranslational regulatory pathway controlling adipocyte differentiation and maintenance. Moreover, neddylation is a key regulator of obesity and metabolic homeostasis. Therefore, studying neddylation in the context of obesity could provide new potential therapeutic aspects.

6 Appendix

6.1 List of Abbreviations

9-and 13-HODE	9- and 13-hydroxyoctadeca-9*Z*,11*E*-dienoic acids
µg	Microgram
µl	Microlitre
ACC1	Acetyl-CoA carboxylase 1
ACO	Acyl-coenzyme A oxidase
ACS	Acyl-coenzyme A synthetase
AICD	APP intracellular domain
AMP	Adenosine 5'-monophosphate
APPBP1	NEDD8-activating enzyme E1 regulatory subunit
AT	Adipose tissue
ATGL	Adipose triglyceride lipase
ATP	Adenosine triphosphate
BAT	Brown adipose tissue
BCA3	Breast cancer-associated protein 3
BMP7	Bone morphogenetic protein 7
BRAP2	BRCA1-associated protein 2
BS	Bovine serum
BSA	Bovine serum albumin
bZIP	Basic leucine zipper
CACT	Carnitine acylcarnitine translocase
cAMP	Cyclic adenosine monophosphate
CD36	Fatty acid translocase
C/EBP	CCAAT/enhancer-binding protein
CGI-58	Comparative gene identification-58
ChIP	Chromatin Immunoprecipitation
CHX	Cycloheximide
Cidea	Cell death-inducing DNA fragmentation factor alpha-like effector A
COP9	Constitutive photomorphogenesis 9
CPT1	Carnitine palmitoyltransferase 1
CREB	cAMP regulatory element-binding protein
CRLs	Cullin RING ligases
CSN	COP9 signalosome

C-terminus	Carboxy-terminus
CytC	Cytochrome c
DG	Diacylglycerol
dH_2O	Distilled water
DMEM	Dulbecco’s modified Eagle medium
DMSO	Dimethyl sulfoxide
DNA	Deoxyribonucleic acid
DUBs	Deubiquitinating enzymes
EB2F	Early B cell factor 2
EGFR	Epidermal growth factor receptor
Elovl3	ELOVL fatty acid elongase 3
EN1	Engrailed 1
EWS	Ewing sarcoma
FA	Fatty acid
FABP4	Fatty acid-binding protein 4
FACS	Fluorescence-activated cell sorting
$FADH_2$	Flavin adenine dinucleotide
FAS	Fatty acid synthase
FATP1	Fatty acid transport protein 1
FCS	Fetal calf serum
g	Gram
G3P	Glycerol-3-phosphate
GLUT4	Glucose transporter type 4
Gly	Glycine
GR	Glucocorticoid receptor
GTT	Glucose tolerance test
h	Hours
H&E	Hematoxylin & eosin
HDAC1	Histone deacetylase 1
HECT	Homologous to E6-AP carboxyl terminus
HEK	Human embryonic kidney cells
HFD	High fat diet
HIV	Human immunodeficiency virus
HPBCD	2-Hydroxypropyl-beta-cyclodextrin
HSL	Hormone sensitive lipase
HuR	Hu antigen R
IBMX	3-isobutyl-1-methylxanthine
IGF1R	Insulin-like growth factor 1 receptor

IgG	Immunglobulin G
IR	Insulin receptor
K	Lysine
KLF11	Krüppel-like factor 11
KO	Knock out
LAP	Liver-enriched activator protein
LCAD	Long-chain acyl-CoA dehydrogenase
LIP	Liver-enriched inhibitory protein
LPL	Lipoprotein lipase
Lys	Lysine
MCAD	Medium-chain acyl-CoA dehydrogenase
MCE	Mitotic clonal expansion
MCP1	Monocyte chemoattractant protein 1
MDI	Methylisobutylxanthine, dexamethasone, insulin (adipogenic cocktail)
MDM2	Mouse double minute 2 homolog
MED1	Mediator complex subunit 1
MEFs	Mouse embryonic fibroblasts
mg	Milligram
MG	Monoacylglycerol
MGL	Monoacylglycerol lipase
min	Minutes
ml	Millilitre
MLN	MLN4924
MYF5	Myogenic factor 5
MYH11	Myosin heavy chain 11
NADH	Nicotinamide adenine dinucleotide
NAE	E1 Nedd8-activating enzyme
Nae1	NEDD8-activating enzyme E1 regulatory subunit
NAFLD	Non-alcoholic fatty liver disease
Nedd8	Neural precursor cell-expressed, developmentally downregulated 8
NEM	N-Ethylmaleimide
nm	Nanometer
N-terminus	Amino-terminus
O.N.	Overnight
OPT	1,10-orthophenathroline
ORO	Oil red O
PARP1	Poly ADP-ribose polymerase 1

PARylation	Poly(ADP-ribosyl)ation
PAX7	Paired-box protein 7
PBS	Phosphate buffered saline
PCC	Primary cell culture
PCR	Polymerase chain reaction
PD	Parkinson’s disease
PDGFRβ	Platelet-derived growth factor receptor β
PDL	Poly-(D)-Lysine
PEPCK	Phosphoenolpyruvate carboxykinase
PET	Fluorodeoxyglucose positron emission tomography
PGC1α	PPARγ coactivator 1
PHD	Plant homeodomain
PKA	Protein kinase A
PLIN1	Perilipin1
PPAR	Peroxisome proliferator-activated receptor
PPRE	Peroxisome proliferator response elements
PRDM16	PR domain containing 16
PTM	Posttranslational modification
PVDF	Polyvinylidene difluoride
Rbx	RING-box protein
RING	Really interesting new gene
RLU	Relative units
RNA	Ribonucleic acid
rpm	Rounds per minute
RT	Room temperature
RXR	Retinoid X receptor
Sca-1	Stem cells antigen 1
SDS-PAGE	Sodium dodecyl sulphate polyacrylamide gel electrophoresis
sec	Seconds
SEM	Standard error of the mean
SENP	SUMO-specific protease
Ser	Serine
SMURF	SMAD-specific E3 ubiquitin-protein ligase 1
SVF	Stromal vascular fraction
T2DM	Type 2 Diabetes Mellitus
TBS	Tris-buffered saline
TBST	TBS solution containing 0.1 % Tween 20
TG	Triacylglycerol/triglyceride

TGFβRII	Tyr kinase transforming growth factor-β type II receptor
Thr	Threonine
TNFα	Tumor necrosis factor α
TR	Thyroid receptor
TZD	Thiazolidinediones
Uba 3	Ubiquitin-activating enzyme 3
Ubc12	Nedd8 E2 conjugating enzyme
Ube2f	Nedd8 E2 conjugating enzyme
Ube2m	Nedd8 E2 conjugating enzyme
UBL	Ubiquitin-like protein
UCP1	Uncoupling protein 1
ULP	UBLs-specific protease
UPS	Ubiquitin-proteasome system
VEGF	Vascular endothelial growth factor
VHL	Von Hippel-Lindau tumor suppressor gene
WAT	White adipose tissue
YBX1	Y-box binding protein 1

6.2 List of Tables

6.3 List of Figures

7 References

Abdelmohsen, K., and Gorospe, M. (2010). Posttranscriptional regulation of cancer traits by HuR. Wiley Interdiscip Rev RNA *1*, 214-229.

Adams, M., Reginato, M.J., Shao, D., Lazar, M.A., and Chatterjee, V.K. (1997). Transcriptional activation by peroxisome proliferator-activated receptor gamma is inhibited by phosphorylation at a consensus mitogen-activated protein kinase site. J Biol Chem *272*, 5128-5132.

Adhikari, A., and Chen, Z.J. (2009). Diversity of polyubiquitin chains. Dev Cell *16*, 485-486.

Ahima, R.S., and Flier, J.S. (2000). Adipose tissue as an endocrine organ. Trends Endocrinol Metab *11*, 327-332.

Ahmadian, M., Suh, J.M., Hah, N., Liddle, C., Atkins, A.R., Downes, M., and Evans, R.M. (2013). PPARgamma signaling and metabolism: the good, the bad and the future. Nat Med *19*, 557-566.

Ahmed, K., Tunaru, S., Tang, C., Muller, M., Gille, A., Sassmann, A., Hanson, J., and Offermanns, S. (2010). An autocrine lactate loop mediates insulin-dependent inhibition of lipolysis through GPR81. Cell Metab *11*, 311-319.

Alessi, D.R., Andjelkovic, M., Caudwell, B., Cron, P., Morrice, N., Cohen, P., and Hemmings, B.A. (1996). Mechanism of activation of protein kinase B by insulin and IGF-1. EMBO J *15*, 6541-6551.

Amerik, A.Y., and Hochstrasser, M. (2004). Mechanism and function of deubiquitinating enzymes. Biochim Biophys Acta *1695*, 189-207.

Aoki, I., Higuchi, M., and Gotoh, Y. (2013). NEDDylation controls the target specificity of E2F1 and apoptosis induction. Oncogene *32*, 3954-3964.

Arner, E., Westermark, P.O., Spalding, K.L., Britton, T., Ryden, M., Frisen, J., Bernard, S., and Arner, P. (2010). Adipocyte turnover: relevance to human adipose tissue morphology. Diabetes *59*, 105-109.

Arner, P., Arner, E., Hammarstedt, A., and Smith, U. (2011). Genetic predisposition for Type 2 diabetes, but not for overweight/obesity, is associated with a restricted adipogenesis. PLoS One *6*, e18284.

Ashcroft, F.M., and Rorsman, P. (2012). Diabetes mellitus and the beta cell: the last ten years. Cell *148*, 1160-1171.

Asterholm, I.W., Halberg, N., and Scherer, P.E. (2007). Mouse Models of Lipodystrophy Key reagents for the understanding of the metabolic syndrome. Drug Discov Today Dis Models *4*, 17-24.

Atit, R., Sgaier, S.K., Mohamed, O.A., Taketo, M.M., Dufort, D., Joyner, A.L., Niswander, L., and Conlon, R.A. (2006). Beta-catenin activation is necessary and sufficient to specify the dorsal dermal fate in the mouse. Dev Biol *296*, 164-176.

Barbera, M.J., Schluter, A., Pedraza, N., Iglesias, R., Villarroya, F., and Giralt, M. (2001). Peroxisome proliferator-activated receptor alpha activates transcription of the brown fat

uncoupling protein-1 gene. A link between regulation of the thermogenic and lipid oxidation pathways in the brown fat cell. J Biol Chem *276*, 1486-1493.

Barbier-Torres, L., Delgado, T.C., Garcia-Rodriguez, J.L., Zubiete-Franco, I., Fernandez-Ramos, D., Buque, X., Cano, A., Gutierrez-de Juan, V., Fernandez-Dominguez, I., Lopitz-Otsoa, F., et al. (2015). Stabilization of LKB1 and Akt by neddylation regulates energy metabolism in liver cancer. Oncotarget *6*, 2509-2523.

Bartlett, K., and Eaton, S. (2004). Mitochondrial beta-oxidation. Eur J Biochem *271*, 462-469.

Bennett, P.H. (2018). Diabetes mortality in the USA: winning the battle but not the war? Lancet *391*, 2392-2393.

Berg, A.H., Combs, T.P., Du, X., Brownlee, M., and Scherer, P.E. (2001). The adipocyte-secreted protein Acrp30 enhances hepatic insulin action. Nat Med *7*, 947-953.

Berglund, E.D., Vianna, C.R., Donato, J., Jr., Kim, M.H., Chuang, J.C., Lee, C.E., Lauzon, D.A., Lin, P., Brule, L.J., Scott, M.M., et al. (2012). Direct leptin action on POMC neurons regulates glucose homeostasis and hepatic insulin sensitivity in mice. J Clin Invest *122*, 1000-1009.

Bernlohr, D.A., Bolanowski, M.A., Kelly, T.J., Jr., and Lane, M.D. (1985). Evidence for an increase in transcription of specific mRNAs during differentiation of 3T3-L1 preadipocytes. J Biol Chem *260*, 5563-5567.

Berry, R., Jeffery, E., and Rodeheffer, M.S. (2014). Weighing in on adipocyte precursors. Cell Metab *19*, 8-20.

Betz, M.J., and Enerback, S. (2015). Human Brown Adipose Tissue: What We Have Learned So Far. Diabetes *64*, 2352-2360.

Bjorndal, B., Burri, L., Staalesen, V., Skorve, J., and Berge, R.K. (2011). Different adipose depots: their role in the development of metabolic syndrome and mitochondrial response to hypolipidemic agents. J Obes *2011*, 490650.

Bjorntorp, P., Gustafson, A., and Persson, B. (1971). Adipose tissue fat cell size and number in relation to metabolism in endogenous hypertriglyceridemia. Acta Med Scand *190*, 363-367.

Bluher, M. (2009). Adipose tissue dysfunction in obesity. Exp Clin Endocrinol Diabetes *117*, 241-250.

Bluher, M. (2013). Adipose tissue dysfunction contributes to obesity related metabolic diseases. Best Pract Res Clin Endocrinol Metab *27*, 163-177.

Bluher, M. (2016). Adipose tissue inflammation: a cause or consequence of obesity-related insulin resistance? Clin Sci (Lond) *130*, 1603-1614.

Boh, B.K., Smith, P.G., and Hagen, T. (2011). Neddylation-induced conformational control regulates cullin RING ligase activity in vivo. J Mol Biol *409*, 136-145.

Bottger, A., Bottger, V., Sparks, A., Liu, W.L., Howard, S.F., and Lane, D.P. (1997). Design of a synthetic Mdm2-binding mini protein that activates the p53 response in vivo. Curr Biol *7*, 860-869.

Boucher, J., Tseng, Y.H., and Kahn, C.R. (2010). Insulin and insulin-like growth factor-1 receptors act as ligand-specific amplitude modulators of a common pathway regulating gene transcription. J Biol Chem *285*, 17235-17245.

Bradley, M.N., Zhou, L., and Smale, S.T. (2003). C/EBPbeta regulation in lipopolysaccharide-stimulated macrophages. Mol Cell Biol *23*, 4841-4858.

Braten, O., Livneh, I., Ziv, T., Admon, A., Kehat, I., Caspi, L.H., Gonen, H., Bercovich, B., Godzik, A., Jahandideh, S., et al. (2016). Numerous proteins with unique characteristics are degraded by the 26S proteasome following monoubiquitination. Proc Natl Acad Sci U S A *113*, E4639-4647.

Broemer, M., Tenev, T., Rigbolt, K.T., Hempel, S., Blagoev, B., Silke, J., Ditzel, M., and Meier, P. (2010). Systematic in vivo RNAi analysis identifies IAPs as NEDD8-E3 ligases. Mol Cell *40*, 810-822.

Brown, J.S., and Jackson, S.P. (2015). Ubiquitylation, neddylation and the DNA damage response. Open Biol *5*, 150018.

Brown, M.S., and Goldstein, J.L. (2008). Selective versus total insulin resistance: a pathogenic paradox. Cell Metab *7*, 95-96.

Brownell, J.E., Sintchak, M.D., Gavin, J.M., Liao, H., Bruzzese, F.J., Bump, N.J., Soucy, T.A., Milhollen, M.A., Yang, X., Burkhardt, A.L., et al. (2010). Substrate-assisted inhibition of ubiquitin-like protein-activating enzymes: the NEDD8 E1 inhibitor MLN4924 forms a NEDD8-AMP mimetic in situ. Mol Cell *37*, 102-111.

Browning, J.D., and Horton, J.D. (2004). Molecular mediators of hepatic steatosis and liver injury. J Clin Invest *114*, 147-152.

Camp, H.S., and Tafuri, S.R. (1997). Regulation of peroxisome proliferator-activated receptor gamma activity by mitogen-activated protein kinase. J Biol Chem *272*, 10811-10816.

Cancello, R., Henegar, C., Viguerie, N., Taleb, S., Poitou, C., Rouault, C., Coupaye, M., Pelloux, V., Hugol, D., Bouillot, J.L., et al. (2005). Reduction of macrophage infiltration and chemoattractant gene expression changes in white adipose tissue of morbidly obese subjects after surgery-induced weight loss. Diabetes *54*, 2277-2286.

Cannon, B., and Nedergaard, J. (2004). Brown adipose tissue: function and physiological significance. Physiol Rev *84*, 277-359.

Cao, W., Daniel, K.W., Robidoux, J., Puigserver, P., Medvedev, A.V., Bai, X., Floering, L.M., Spiegelman, B.M., and Collins, S. (2004). p38 mitogen-activated protein kinase is the central regulator of cyclic AMP-dependent transcription of the brown fat uncoupling protein 1 gene. Mol Cell Biol *24*, 3057-3067.

Cao, Z., Umek, R.M., and McKnight, S.L. (1991). Regulated expression of three C/EBP isoforms during adipose conversion of 3T3-L1 cells. Genes Dev *5*, 1538-1552.

Cappadocia, L., and Lima, C.D. (2018). Ubiquitin-like Protein Conjugation: Structures, Chemistry, and Mechanism. Chem Rev *118*, 889-918.

Ceddia, R.B., Somwar, R., Maida, A., Fang, X., Bikopoulos, G., and Sweeney, G. (2005). Globular adiponectin increases GLUT4 translocation and glucose uptake but reduces glycogen synthesis in rat skeletal muscle cells. Diabetologia *48*, 132-139.

Cesena, T.I., Cardinaux, J.R., Kwok, R., and Schwartz, J. (2007). CCAAT/enhancer-binding protein (C/EBP) beta is acetylated at multiple lysines: acetylation of C/EBPbeta at lysine 39 modulates its ability to activate transcription. J Biol Chem *282*, 956-967.

Cesena, T.I., Cui, T.X., Subramanian, L., Fulton, C.T., Iniguez-Lluhi, J.A., Kwok, R.P., and Schwartz, J. (2008). Acetylation and deacetylation regulate CCAAT/enhancer binding protein beta at K39 in mediating gene transcription. Mol Cell Endocrinol *289*, 94-101.

Cha, H.C., Oak, N.R., Kang, S., Tran, T.A., Kobayashi, S., Chiang, S.H., Tenen, D.G., and MacDougald, O.A. (2008). Phosphorylation of CCAAT/enhancer-binding protein alpha regulates GLUT4 expression and glucose transport in adipocytes. J Biol Chem *283*, 18002-18011.

Chan, N.L., and Hill, C.P. (2001). Defining polyubiquitin chain topology. Nat Struct Biol *8*, 650-652.

Chan, Y., Yoon, J., Wu, J.T., Kim, H.J., Pan, K.T., Yim, J., and Chien, C.T. (2008). DEN1 deneddylates non-cullin proteins in vivo. J Cell Sci *121*, 3218-3223.

Chang, S.H., Stoll, C.R., Song, J., Varela, J.E., Eagon, C.J., and Colditz, G.A. (2014). The effectiveness and risks of bariatric surgery: an updated systematic review and meta-analysis, 2003-2012. JAMA Surg *149*, 275-287.

Chatterjee, S., Khunti, K., and Davies, M.J. (2017). Type 2 diabetes. Lancet *389*, 2239-2251.

Chau, V., Tobias, J.W., Bachmair, A., Marriott, D., Ecker, D.J., Gonda, D.K., and Varshavsky, A. (1989). A multiubiquitin chain is confined to specific lysine in a targeted short-lived protein. Science *243*, 1576-1583.

Chau, Y.Y., Bandiera, R., Serrels, A., Martinez-Estrada, O.M., Qing, W., Lee, M., Slight, J., Thornburn, A., Berry, R., McHaffie, S., et al. (2014). Visceral and subcutaneous fat have different origins and evidence supports a mesothelial source. Nat Cell Biol *16*, 367-375.

Chawla, A., and Lazar, M.A. (1994). Peroxisome proliferator and retinoid signaling pathways co-regulate preadipocyte phenotype and survival. Proc Natl Acad Sci U S A *91*, 1786-1790.

Chen, C., Hosokawa, H., Bumbalo, L.M., and Leahy, J.L. (1994). Mechanism of compensatory hyperinsulinemia in normoglycemic insulin-resistant spontaneously hypertensive rats. Augmented enzymatic activity of glucokinase in beta-cells. J Clin Invest *94*, 399-404.

Chen, P., Hu, T., Liang, Y., Li, P., Chen, X., Zhang, J., Ma, Y., Hao, Q., Wang, J., Zhang, P., et al. (2016). Neddylation Inhibition Activates the Extrinsic Apoptosis Pathway through ATF4-CHOP-DR5 Axis in Human Esophageal Cancer Cells. Clin Cancer Res *22*, 4145-4157.

Chen, W., Yang, Q., and Roeder, R.G. (2009). Dynamic interactions and cooperative functions of PGC-1alpha and MED1 in TRalpha-mediated activation of the brown-fat-specific UCP-1 gene. Mol Cell *35*, 755-768.

Chen, Y.D., Liu, J.Y., Lu, Y.M., Zhu, H.T., Tang, W., Wang, Q.X., and Lu, H.Y. (2017). Functional roles of C/EBPalpha and SUMOmodification in lung development. Int J Mol Med *40*, 1037-1046.

Cho, Y.C., and Jefcoate, C.R. (2004). PPARgamma1 synthesis and adipogenesis in C3H10T1/2 cells depends on S-phase progression, but does not require mitotic clonal expansion. J Cell Biochem *91*, 336-353.

Choi, S.M., Tucker, D.F., Gross, D.N., Easton, R.M., DiPilato, L.M., Dean, A.S., Monks, B.R., and Birnbaum, M.J. (2010). Insulin regulates adipocyte lipolysis via an Akt-independent signaling pathway. Mol Cell Biol *30*, 5009-5020.

Choo, Y.S., Vogler, G., Wang, D., Kalvakuri, S., Iliuk, A., Tao, W.A., Bodmer, R., and Zhang, Z. (2012). Regulation of parkin and PINK1 by neddylation. Hum Mol Genet *21*, 2514-2523.

Christy, R.J., Kaestner, K.H., Geiman, D.E., and Lane, M.D. (1991). CCAAT/enhancer binding protein gene promoter: binding of nuclear factors during differentiation of 3T3-L1 preadipocytes. Proc Natl Acad Sci U S A *88*, 2593-2597.

Chung, S., Lapoint, K., Martinez, K., Kennedy, A., Boysen Sandberg, M., and McIntosh, M.K. (2006). Preadipocytes mediate lipopolysaccharide-induced inflammation and insulin resistance in primary cultures of newly differentiated human adipocytes. Endocrinology *147*, 5340-5351.

Chung, S.S., Ahn, B.Y., Kim, M., Choi, H.H., Park, H.S., Kang, S., Park, S.G., Kim, Y.B., Cho, Y.M., Lee, H.K., et al. (2010). Control of adipogenesis by the SUMO-specific protease SENP2. Mol Cell Biol *30*, 2135-2146.

Chung, S.S., Ahn, B.Y., Kim, M., Kho, J.H., Jung, H.S., and Park, K.S. (2011). SUMO modification selectively regulates transcriptional activity of peroxisome-proliferator-activated receptor gamma in C2C12 myotubes. Biochem J *433*, 155-161.

Cinti, S., Mitchell, G., Barbatelli, G., Murano, I., Ceresi, E., Faloia, E., Wang, S., Fortier, M., Greenberg, A.S., and Obin, M.S. (2005). Adipocyte death defines macrophage localization and function in adipose tissue of obese mice and humans. J Lipid Res *46*, 2347-2355.

Clarke, S.L., Robinson, C.E., and Gimble, J.M. (1997). CAAT/enhancer binding proteins directly modulate transcription from the peroxisome proliferator-activated receptor gamma 2 promoter. Biochem Biophys Res Commun *240*, 99-103.

Coburn, C.T., Knapp, F.F., Jr., Febbraio, M., Beets, A.L., Silverstein, R.L., and Abumrad, N.A. (2000). Defective uptake and utilization of long chain fatty acids in muscle and adipose tissues of CD36 knockout mice. J Biol Chem *275*, 32523-32529.

Collaborators, G.B.D.O., Afshin, A., Forouzanfar, M.H., Reitsma, M.B., Sur, P., Estep, K., Lee, A., Marczak, L., Mokdad, A.H., Moradi-Lakeh, M., et al. (2017). Health Effects of Overweight and Obesity in 195 Countries over 25 Years. N Engl J Med *377*, 13-27.

Collins, S. (2011). beta-Adrenoceptor Signaling Networks in Adipocytes for Recruiting Stored Fat and Energy Expenditure. Front Endocrinol (Lausanne) *2*, 102.

Cope, G.A., Suh, G.S., Aravind, L., Schwarz, S.E., Zipursky, S.L., Koonin, E.V., and Deshaies, R.J. (2002). Role of predicted metalloprotease motif of Jab1/Csn5 in cleavage of Nedd8 from Cul1. Science *298*, 608-611.

Covas, D.T., Panepucci, R.A., Fontes, A.M., Silva, W.A., Jr., Orellana, M.D., Freitas, M.C., Neder, L., Santos, A.R., Peres, L.C., Jamur, M.C., et al. (2008). Multipotent mesenchymal stromal cells obtained from diverse human tissues share functional properties and gene-expression profile with CD146+ perivascular cells and fibroblasts. Exp Hematol *36*, 642-654.

Cristancho, A.G., and Lazar, M.A. (2011). Forming functional fat: a growing understanding of adipocyte differentiation. Nat Rev Mol Cell Biol *12*, 722-734.

Cypess, A.M., and Kahn, C.R. (2010). The role and importance of brown adipose tissue in energy homeostasis. Curr Opin Pediatr *22*, 478-484.

Cypess, A.M., Lehman, S., Williams, G., Tal, I., Rodman, D., Goldfine, A.B., Kuo, F.C., Palmer, E.L., Tseng, Y.H., Doria, A., et al. (2009). Identification and importance of brown adipose tissue in adult humans. N Engl J Med *360*, 1509-1517.

Dalamaga, M., Chou, S.H., Shields, K., Papageorgiou, P., Polyzos, S.A., and Mantzoros, C.S. (2013). Leptin at the intersection of neuroendocrinology and metabolism: current evidence and therapeutic perspectives. Cell Metab *18*, 29-42.

Dalen, K.T., Schoonjans, K., Ulven, S.M., Weedon-Fekjaer, M.S., Bentzen, T.G., Koutnikova, H., Auwerx, J., and Nebb, H.I. (2004). Adipose tissue expression of the lipid droplet-associating proteins S3-12 and perilipin is controlled by peroxisome proliferator-activated receptor-gamma. Diabetes *53*, 1243-1252.

Dansinger, M.L., Gleason, J.A., Griffith, J.L., Selker, H.P., and Schaefer, E.J. (2005). Comparison of the Atkins, Ornish, Weight Watchers, and Zone diets for weight loss and heart disease risk reduction: a randomized trial. JAMA *293*, 43-53.

de Jong, J.M., Larsson, O., Cannon, B., and Nedergaard, J. (2015). A stringent validation of mouse adipose tissue identity markers. Am J Physiol Endocrinol Metab *308*, E1085-1105.

de Wilde, J., Smit, E., Mohren, R., Boekschoten, M.V., de Groot, P., van den Berg, S.A., Bijland, S., Voshol, P.J., van Dijk, K.W., de Wit, N.W., et al. (2009). An 8-week high-fat diet induces obesity and insulin resistance with small changes in the muscle transcriptome of C57BL/6J mice. J Nutrigenet Nutrigenomics *2*, 280-291.

Dempersmier, J., Sambeat, A., Gulyaeva, O., Paul, S.M., Hudak, C.S., Raposo, H.F., Kwan, H.Y., Kang, C., Wong, R.H., and Sul, H.S. (2015). Cold-inducible Zfp516 activates UCP1 transcription to promote browning of white fat and development of brown fat. Mol Cell *57*, 235-246.

Deng, T., Shan, S., Li, P.P., Shen, Z.F., Lu, X.P., Cheng, J., and Ning, Z.Q. (2006). Peroxisome proliferator-activated receptor-gamma transcriptionally up-regulates hormone-sensitive lipase via the involvement of specificity protein-1. Endocrinology *147*, 875-884.

Descombes, P., and Schibler, U. (1991). A liver-enriched transcriptional activator protein, LAP, and a transcriptional inhibitory protein, LIP, are translated from the same mRNA. Cell *67*, 569-579.

Di Dalmazi, G., Vicennati, V., Pasquali, R., and Pagotto, U. (2013). The unrelenting fall of the pharmacological treatment of obesity. Endocrine *44*, 598-609.

Dresner, A., Laurent, D., Marcucci, M., Griffin, M.E., Dufour, S., Cline, G.W., Slezak, L.A., Andersen, D.K., Hundal, R.S., Rothman, D.L., et al. (1999). Effects of free fatty acids on glucose transport and IRS-1-associated phosphatidylinositol 3-kinase activity. J Clin Invest *103*, 253-259.

Du, K., and Montminy, M. (1998). CREB is a regulatory target for the protein kinase Akt/PKB. J Biol Chem *273*, 32377-32379.

Dubiel, D., Bintig, W., Kahne, T., Dubiel, W., and Naumann, M. (2017). Cul3 neddylation is crucial for gradual lipid droplet formation during adipogenesis. Biochim Biophys Acta *1864*, 1405-1412.

Dubiel, D., Gierisch, M.E., Huang, X., Dubiel, W., and Naumann, M. (2013). CAND1-dependent control of cullin 1-RING Ub ligases is essential for adipogenesis. Biochim Biophys Acta *1833*, 1078-1084.

Dubiel, D., Ordemann, J., Pratschke, J., Dubiel, W., and Naumann, M. (2015). CAND1 exchange factor promotes Keap1 integration into cullin 3-RING ubiquitin ligase during adipogenesis. Int J Biochem Cell Biol *66*, 95-100.

Eckel, R.H. (1989). Lipoprotein lipase. A multifunctional enzyme relevant to common metabolic diseases. N Engl J Med *320*, 1060-1068.

Egan, J.J., Greenberg, A.S., Chang, M.K., Wek, S.A., Moos, M.C., Jr., and Londos, C. (1992). Mechanism of hormone-stimulated lipolysis in adipocytes: translocation of hormone-sensitive lipase to the lipid storage droplet. Proc Natl Acad Sci U S A *89*, 8537-8541.

Eletr, Z.M., Huang, D.T., Duda, D.M., Schulman, B.A., and Kuhlman, B. (2005). E2 conjugating enzymes must disengage from their E1 enzymes before E3-dependent ubiquitin and ubiquitin-like transfer. Nat Struct Mol Biol *12*, 933-934.

Elks, M.L., and Manganiello, V.C. (1985). A role for soluble cAMP phosphodiesterases in differentiation of 3T3-L1 adipocytes. J Cell Physiol *124*, 191-198.

Embade, N., Fernandez-Ramos, D., Varela-Rey, M., Beraza, N., Sini, M., Gutierrez de Juan, V., Woodhoo, A., Martinez-Lopez, N., Rodriguez-Iruretagoyena, B., Bustamante, F.J., et al. (2012). Murine double minute 2 regulates Hu antigen R stability in human liver and colon cancer through NEDDylation. Hepatology *55*, 1237-1248.

Enchev, R.I., Schulman, B.A., and Peter, M. (2015). Protein neddylation: beyond cullin-RING ligases. Nat Rev Mol Cell Biol *16*, 30-44.

Entenmann, G., and Hauner, H. (1996). Relationship between replication and differentiation in cultured human adipocyte precursor cells. Am J Physiol *270*, C1011-1016.

Fain, J.N., and Garcija-Sainz, J.A. (1983). Adrenergic regulation of adipocyte metabolism. J Lipid Res *24*, 945-966.

Farmer, S.R. (2006). Transcriptional control of adipocyte formation. Cell Metab *4*, 263-273.

Fasshauer, M., and Bluher, M. (2015). Adipokines in health and disease. Trends Pharmacol Sci *36*, 461-470.

Feingold, K.R., and Grunfeld, C. (2000). Introduction to Lipids and Lipoproteins. In Endotext. L.J. De Groot, G. Chrousos, K. Dungan, K.R. Feingold, A. Grossman, J.M. Hershman, C. Koch, M. Korbonits, R. McLachlan, M. New, et al., eds. (South Dartmouth (MA)).

Filtz, T.M., Vogel, W.K., and Leid, M. (2014). Regulation of transcription factor activity by interconnected post-translational modifications. Trends Pharmacol Sci *35*, 76-85.

Fiorenza, C.G., Chou, S.H., and Mantzoros, C.S. (2011). Lipodystrophy: pathophysiology and advances in treatment. Nat Rev Endocrinol *7*, 137-150.

Florant, G.L., Porst, H., Peiffer, A., Hudachek, S.F., Pittman, C., Summers, S.A., Rajala, M.W., and Scherer, P.E. (2004). Fat-cell mass, serum leptin and adiponectin changes during weight gain and loss in yellow-bellied marmots (Marmota flaviventris). J Comp Physiol B *174*, 633-639.

Floyd, Z.E., and Stephens, J.M. (2002). Interferon-gamma-mediated activation and ubiquitin-proteasome-dependent degradation of PPARgamma in adipocytes. J Biol Chem *277*, 4062-4068.

Forman, B.M., Chen, J., and Evans, R.M. (1997). Hypolipidemic drugs, polyunsaturated fatty acids, and eicosanoids are ligands for peroxisome proliferator-activated receptors alpha and delta. Proc Natl Acad Sci U S A *94*, 4312-4317.

Forman, B.M., Tontonoz, P., Chen, J., Brun, R.P., Spiegelman, B.M., and Evans, R.M. (1995). 15-Deoxy-delta 12, 14-prostaglandin J2 is a ligand for the adipocyte determination factor PPAR gamma. Cell *83*, 803-812.

Frayn, K.N., Arner, P., and Yki-Jarvinen, H. (2006). Fatty acid metabolism in adipose tissue, muscle and liver in health and disease. Essays Biochem *42*, 89-103.

Freytag, S.O., and Geddes, T.J. (1992). Reciprocal regulation of adipogenesis by Myc and C/EBP alpha. Science *256*, 379-382.

Freytag, S.O., Paielli, D.L., and Gilbert, J.D. (1994). Ectopic expression of the CCAAT/enhancer-binding protein alpha promotes the adipogenic program in a variety of mouse fibroblastic cells. Genes Dev *8*, 1654-1663.

Fruebis, J., Tsao, T.S., Javorschi, S., Ebbets-Reed, D., Erickson, M.R., Yen, F.T., Bihain, B.E., and Lodish, H.F. (2001). Proteolytic cleavage product of 30-kDa adipocyte complement-related protein increases fatty acid oxidation in muscle and causes weight loss in mice. Proc Natl Acad Sci U S A *98*, 2005-2010.

Fu, D., Lala-Tabbert, N., Lee, H., and Wiper-Bergeron, N. (2015). Mdm2 promotes myogenesis through the ubiquitination and degradation of CCAAT/enhancer-binding protein beta. J Biol Chem *290*, 10200-10207.

Fujisaka, S., Usui, I., Bukhari, A., Ikutani, M., Oya, T., Kanatani, Y., Tsuneyama, K., Nagai, Y., Takatsu, K., Urakaze, M., et al. (2009). Regulatory mechanisms for adipose tissue M1 and M2 macrophages in diet-induced obese mice. Diabetes *58*, 2574-2582.

Furtado, L.M., Somwar, R., Sweeney, G., Niu, W., and Klip, A. (2002). Activation of the glucose transporter GLUT4 by insulin. Biochem Cell Biol *80*, 569-578.

Galgani, J.E., Moro, C., and Ravussin, E. (2008). Metabolic flexibility and insulin resistance. Am J Physiol Endocrinol Metab *295*, E1009-1017.

Galic, S., Oakhill, J.S., and Steinberg, G.R. (2010). Adipose tissue as an endocrine organ. Mol Cell Endocrinol *316*, 129-139.

Gao, F., Cheng, J., Shi, T., and Yeh, E.T. (2006). Neddylation of a breast cancer-associated protein recruits a class III histone deacetylase that represses NFkappaB-dependent transcription. Nat Cell Biol *8*, 1171-1177.

Gao, Q., Yu, G.Y., Shi, J.Y., Li, L.H., Zhang, W.J., Wang, Z.C., Yang, L.X., Duan, M., Zhao, H., Wang, X.Y., et al. (2014). Neddylation pathway is up-regulated in human intrahepatic cholangiocarcinoma and serves as a potential therapeutic target. Oncotarget *5*, 7820-7832.

Gesta, S., Bluher, M., Yamamoto, Y., Norris, A.W., Berndt, J., Kralisch, S., Boucher, J., Lewis, C., and Kahn, C.R. (2006). Evidence for a role of developmental genes in the origin of obesity and body fat distribution. Proc Natl Acad Sci U S A *103*, 6676-6681.

Ginty, D.D., Bonni, A., and Greenberg, M.E. (1994). Nerve growth factor activates a Ras-dependent protein kinase that stimulates c-fos transcription via phosphorylation of CREB. Cell *77*, 713-725.

Girard, J., and Lafontan, M. (2008). Impact of visceral adipose tissue on liver metabolism and insulin resistance. Part II: Visceral adipose tissue production and liver metabolism. Diabetes Metab *34*, 439-445.

Glatz, J.F., Luiken, J.J., and Bonen, A. (2010). Membrane fatty acid transporters as regulators of lipid metabolism: implications for metabolic disease. Physiol Rev *90*, 367-417.

Gong, L., and Yeh, E.T. (1999). Identification of the activating and conjugating enzymes of the NEDD8 conjugation pathway. J Biol Chem *274*, 12036-12042.

Gonzalez, G.A., and Montminy, M.R. (1989). Cyclic AMP stimulates somatostatin gene transcription by phosphorylation of CREB at serine 133. Cell *59*, 675-680.

Granneman, J.G., Moore, H.P., Granneman, R.L., Greenberg, A.S., Obin, M.S., and Zhu, Z. (2007). Analysis of lipolytic protein trafficking and interactions in adipocytes. J Biol Chem *282*, 5726-5735.

Granneman, J.G., Moore, H.P., Krishnamoorthy, R., and Rathod, M. (2009). Perilipin controls lipolysis by regulating the interactions of AB-hydrolase containing 5 (Abhd5) and adipose triglyceride lipase (Atgl). J Biol Chem *284*, 34538-34544.

Grant, R.W., and Dixit, V.D. (2015). Adipose tissue as an immunological organ. Obesity (Silver Spring) *23*, 512-518.

Grarup, N., Sandholt, C.H., Hansen, T., and Pedersen, O. (2014). Genetic susceptibility to type 2 diabetes and obesity: from genome-wide association studies to rare variants and beyond. Diabetologia *57*, 1528-1541.

Green, H., and Kehinde, O. (1974). Sublines of Mouse 3T3 Cells That Accumulate Lipid. Cell *1*, 113-116.

Green, H., and Kehinde, O. (1975). An established preadipose cell line and its differentiation in culture. II. Factors affecting the adipose conversion. Cell *5*, 19-27.

Greenberg, A.S., Egan, J.J., Wek, S.A., Garty, N.B., Blanchette-Mackie, E.J., and Londos, C. (1991). Perilipin, a major hormonally regulated adipocyte-specific phosphoprotein associated with the periphery of lipid storage droplets. J Biol Chem *266*, 11341-11346.

Guilherme, A., Virbasius, J.V., Puri, V., and Czech, M.P. (2008). Adipocyte dysfunctions linking obesity to insulin resistance and type 2 diabetes. Nat Rev Mol Cell Biol *9*, 367-377.

Gumbau, V., Bruna, M., Canelles, E., Guaita, M., Mulas, C., Bases, C., Celma, I., Puche, J., Marcaida, G., Oviedo, M., et al. (2014). A prospective study on inflammatory parameters in obese patients after sleeve gastrectomy. Obes Surg *24*, 903-908.

Guo, L., Li, X., and Tang, Q.Q. (2015). Transcriptional regulation of adipocyte differentiation: a central role for CCAAT/enhancer-binding protein (C/EBP) beta. J Biol Chem *290*, 755-761.

Gustafson, B., Jack, M.M., Cushman, S.W., and Smith, U. (2003). Adiponectin gene activation by thiazolidinediones requires PPAR gamma 2, but not C/EBP alpha-evidence for differential regulation of the aP2 and adiponectin genes. Biochem Biophys Res Commun *308*, 933-939.

Haas, A.L., Warms, J.V., Hershko, A., and Rose, I.A. (1982). Ubiquitin-activating enzyme. Mechanism and role in protein-ubiquitin conjugation. J Biol Chem *257*, 2543-2548.

Haemmerle, G., Lass, A., Zimmermann, R., Gorkiewicz, G., Meyer, C., Rozman, J., Heldmaier, G., Maier, R., Theussl, C., Eder, S., et al. (2006). Defective lipolysis and altered energy metabolism in mice lacking adipose triglyceride lipase. Science *312*, 734-737.

Haffner, S., Temprosa, M., Crandall, J., Fowler, S., Goldberg, R., Horton, E., Marcovina, S., Mather, K., Orchard, T., Ratner, R., et al. (2005). Intensive lifestyle intervention or metformin on inflammation and coagulation in participants with impaired glucose tolerance. Diabetes *54*, 1566-1572.

Haglund, K., Di Fiore, P.P., and Dikic, I. (2003). Distinct monoubiquitin signals in receptor endocytosis. Trends Biochem Sci *28*, 598-603.

Halaas, J.L., Gajiwala, K.S., Maffei, M., Cohen, S.L., Chait, B.T., Rabinowitz, D., Lallone, R.L., Burley, S.K., and Friedman, J.M. (1995). Weight-reducing effects of the plasma protein encoded by the obese gene. Science *269*, 543-546.

Halban, P.A., Polonsky, K.S., Bowden, D.W., Hawkins, M.A., Ling, C., Mather, K.J., Powers, A.C., Rhodes, C.J., Sussel, L., and Weir, G.C. (2014). beta-cell failure in type 2 diabetes: postulated mechanisms and prospects for prevention and treatment. Diabetes Care *37*, 1751-1758.

Hamm, J.K., Park, B.H., and Farmer, S.R. (2001). A role for C/EBPbeta in regulating peroxisome proliferator-activated receptor gamma activity during adipogenesis in 3T3-L1 preadipocytes. J Biol Chem *276*, 18464-18471.

Haque, W.A., Shimomura, I., Matsuzawa, Y., and Garg, A. (2002). Serum adiponectin and leptin levels in patients with lipodystrophies. J Clin Endocrinol Metab *87*, 2395.

Hardy, O.T., Czech, M.P., and Corvera, S. (2012). What causes the insulin resistance underlying obesity? Curr Opin Endocrinol Diabetes Obes *19*, 81-87.

Hardy, O.T., Perugini, R.A., Nicoloro, S.M., Gallagher-Dorval, K., Puri, V., Straubhaar, J., and Czech, M.P. (2011). Body mass index-independent inflammation in omental adipose tissue associated with insulin resistance in morbid obesity. Surg Obes Relat Dis *7*, 60-67.

Harman-Boehm, I., Bluher, M., Redel, H., Sion-Vardy, N., Ovadia, S., Avinoach, E., Shai, I., Kloting, N., Stumvoll, M., Bashan, N., et al. (2007). Macrophage infiltration into omental versus subcutaneous fat across different populations: effect of regional adiposity and the comorbidities of obesity. J Clin Endocrinol Metab *92*, 2240-2247.

Harms, M., and Seale, P. (2013). Brown and beige fat: development, function and therapeutic potential. Nat Med *19*, 1252-1263.

Harms, M.J., Ishibashi, J., Wang, W., Lim, H.W., Goyama, S., Sato, T., Kurokawa, M., Won, K.J., and Seale, P. (2014). Prdm16 is required for the maintenance of brown adipocyte identity and function in adult mice. Cell Metab *19*, 593-604.

Haupt, Y., Maya, R., Kazaz, A., and Oren, M. (1997). Mdm2 promotes the rapid degradation of p53. Nature *387*, 296-299.

Hauser, S., Adelmant, G., Sarraf, P., Wright, H.M., Mueller, E., and Spiegelman, B.M. (2000). Degradation of the peroxisome proliferator-activated receptor gamma is linked to ligand-dependent activation. J Biol Chem *275*, 18527-18533.

He, W., Barak, Y., Hevener, A., Olson, P., Liao, D., Le, J., Nelson, M., Ong, E., Olefsky, J.M., and Evans, R.M. (2003). Adipose-specific peroxisome proliferator-activated receptor gamma knockout causes insulin resistance in fat and liver but not in muscle. Proc Natl Acad Sci U S A *100*, 15712-15717.

Hendriks, I.A., and Vertegaal, A.C. (2016). A comprehensive compilation of SUMO proteomics. Nat Rev Mol Cell Biol *17*, 581-595.

Hepler, C., Vishvanath, L., and Gupta, R.K. (2017). Sorting out adipocyte precursors and their role in physiology and disease. Genes Dev *31*, 127-140.

Herman, M.A., and Kahn, B.B. (2006). Glucose transport and sensing in the maintenance of glucose homeostasis and metabolic harmony. J Clin Invest *116*, 1767-1775.

Herrero, L., Shapiro, H., Nayer, A., Lee, J., and Shoelson, S.E. (2010). Inflammation and adipose tissue macrophages in lipodystrophic mice. Proc Natl Acad Sci U S A *107*, 240-245.

Hershko, A., and Ciechanover, A. (1998). The ubiquitin system. Annu Rev Biochem *67*, 425-479.

Hesselbarth, N., Pettinelli, C., Gericke, M., Berger, C., Kunath, A., Stumvoll, M., Bluher, M., and Kloting, N. (2015). Tamoxifen affects glucose and lipid metabolism parameters, causes browning of subcutaneous adipose tissue and transient body composition changes in C57BL/6NTac mice. Biochem Biophys Res Commun *464*, 724-729.

Hirsch, D., Stahl, A., and Lodish, H.F. (1998). A family of fatty acid transporters conserved from mycobacterium to man. Proc Natl Acad Sci U S A *95*, 8625-8629.

Hondares, E., Rosell, M., Diaz-Delfin, J., Olmos, Y., Monsalve, M., Iglesias, R., Villarroya, F., and Giralt, M. (2011). Peroxisome proliferator-activated receptor alpha (PPARalpha) induces PPARgamma coactivator 1alpha (PGC-1alpha) gene expression and contributes to thermogenic activation of brown fat: involvement of PRDM16. J Biol Chem *286*, 43112-43122.

Honnor, R.C., Dhillon, G.S., and Londos, C. (1985a). cAMP-dependent protein kinase and lipolysis in rat adipocytes. I. Cell preparation, manipulation, and predictability in behavior. J Biol Chem *260*, 15122-15129.

Honnor, R.C., Dhillon, G.S., and Londos, C. (1985b). cAMP-dependent protein kinase and lipolysis in rat adipocytes. II. Definition of steady-state relationship with lipolytic and antilipolytic modulators. J Biol Chem *260*, 15130-15138.

Hotamisligil, G.S. (2006). Inflammation and metabolic disorders. Nature *444*, 860-867.

Houten, S.M., and Wanders, R.J. (2010). A general introduction to the biochemistry of mitochondrial fatty acid beta-oxidation. J Inherit Metab Dis *33*, 469-477.

Hu, E., Kim, J.B., Sarraf, P., and Spiegelman, B.M. (1996). Inhibition of adipogenesis through MAP kinase-mediated phosphorylation of PPARgamma. Science *274*, 2100-2103.

Hua, W., Li, C., Yang, Z., Li, L., Jiang, Y., Yu, G., Zhu, W., Liu, Z., Duan, S., Chu, Y., et al. (2015). Suppression of glioblastoma by targeting the overactivated protein neddylation pathway. Neuro Oncol *17*, 1333-1343.

Huang-Doran, I., Sleigh, A., Rochford, J.J., O'Rahilly, S., and Savage, D.B. (2010). Lipodystrophy: metabolic insights from a rare disorder. J Endocrinol *207*, 245-255.

Huang, D.T., Ayrault, O., Hunt, H.W., Taherbhoy, A.M., Duda, D.M., Scott, D.C., Borg, L.A., Neale, G., Murray, P.J., Roussel, M.F., et al. (2009). E2-RING expansion of the NEDD8 cascade confers specificity to cullin modification. Mol Cell *33*, 483-495.

Huang, D.T., Paydar, A., Zhuang, M., Waddell, M.B., Holton, J.M., and Schulman, B.A. (2005). Structural basis for recruitment of Ubc12 by an E2 binding domain in NEDD8's E1. Mol Cell *17*, 341-350.

Huang, X., Ordemann, J., Muller, J.M., and Dubiel, W. (2012). The COP9 signalosome, cullin 3 and Keap1 supercomplex regulates CHOP stability and adipogenesis. Biol Open *1*, 705-710.

Humphrey, S.J., Yang, G., Yang, P., Fazakerley, D.J., Stockli, J., Yang, J.Y., and James, D.E. (2013). Dynamic adipocyte phosphoproteome reveals that Akt directly regulates mTORC2. Cell Metab *17*, 1009-1020.

Hunt, C.R., Ro, J.H., Dobson, D.E., Min, H.Y., and Spiegelman, B.M. (1986). Adipocyte P2 gene: developmental expression and homology of 5'-flanking sequences among fat cell-specific genes. Proc Natl Acad Sci U S A *83*, 3786-3790.

Hurley, J.H., Lee, S., and Prag, G. (2006). Ubiquitin-binding domains. Biochem J *399*, 361-372.

Iida, S., Chen, W., Nakadai, T., Ohkuma, Y., and Roeder, R.G. (2015). PRDM16 enhances nuclear receptor-dependent transcription of the brown fat-specific Ucp1 gene through interactions with Mediator subunit MED1. Genes Dev *29*, 308-321.

Ikeda, K., Maretich, P., and Kajimura, S. (2018). The Common and Distinct Features of Brown and Beige Adipocytes. Trends Endocrinol Metab *29*, 191-200.

Imai, T., Takakuwa, R., Marchand, S., Dentz, E., Bornert, J.M., Messaddeq, N., Wendling, O., Mark, M., Desvergne, B., Wahli, W., et al. (2004). Peroxisome proliferator-activated receptor gamma is required in mature white and brown adipocytes for their survival in the mouse. Proc Natl Acad Sci U S A *101*, 4543-4547.

Inagaki, T., Sakai, J., and Kajimura, S. (2017). Transcriptional and epigenetic control of brown and beige adipose cell fate and function. Nat Rev Mol Cell Biol *18*, 527.

Inzucchi, S.E., Bergenstal, R.M., Buse, J.B., Diamant, M., Ferrannini, E., Nauck, M., Peters, A.L., Tsapas, A., Wender, R., Matthews, D.R., et al. (2012). Management of hyperglycemia in type 2 diabetes: a patient-centered approach: position statement of the American Diabetes Association (ADA) and the European Association for the Study of Diabetes (EASD). Diabetes Care *35*, 1364-1379.

Jenkins, C.M., Mancuso, D.J., Yan, W., Sims, H.F., Gibson, B., and Gross, R.W. (2004). Identification, cloning, expression, and purification of three novel human calcium-independent phospholipase A2 family members possessing triacylglycerol lipase and acylglycerol transacylase activities. J Biol Chem *279*, 48968-48975.

Jeram, S.M., Srikumar, T., Zhang, X.D., Anne Eisenhauer, H., Rogers, R., Pedrioli, P.G., Matunis, M., and Raught, B. (2010). An improved SUMmOn-based methodology for the identification of ubiquitin and ubiquitin-like protein conjugation sites identifies novel ubiquitin-like protein chain linkages. Proteomics *10*, 254-265.

Jia, L., Li, H., and Sun, Y. (2011). Induction of p21-dependent senescence by an NAE inhibitor, MLN4924, as a mechanism of growth suppression. Neoplasia *13*, 561-569.

Johnson, A.M., and Olefsky, J.M. (2013). The origins and drivers of insulin resistance. Cell *152*, 673-684.

Johnson, J.A., Albu, J.B., Engelson, E.S., Fried, S.K., Inada, Y., Ionescu, G., and Kotler, D.P. (2004). Increased systemic and adipose tissue cytokines in patients with HIV-associated lipodystrophy. Am J Physiol Endocrinol Metab *286*, E261-271.

Jones, J., Wu, K., Yang, Y., Guerrero, C., Nillegoda, N., Pan, Z.Q., and Huang, L. (2008). A targeted proteomic analysis of the ubiquitin-like modifier nedd8 and associated proteins. J Proteome Res *7*, 1274-1287.

Kajimura, S. (2017). Adipose tissue in 2016: Advances in the understanding of adipose tissue biology. Nat Rev Endocrinol *13*, 69-70.

Kajimura, S., Seale, P., Kubota, K., Lunsford, E., Frangioni, J.V., Gygi, S.P., and Spiegelman, B.M. (2009). Initiation of myoblast to brown fat switch by a PRDM16-C/EBP-beta transcriptional complex. Nature *460*, 1154-1158.

Kajimura, S., Spiegelman, B.M., and Seale, P. (2015). Brown and Beige Fat: Physiological Roles beyond Heat Generation. Cell Metab *22*, 546-559.

Kamitani, T., Kito, K., Nguyen, H.P., and Yeh, E.T. (1997). Characterization of NEDD8, a developmentally down-regulated ubiquitin-like protein. J Biol Chem *272*, 28557-28562.

Kamura, T., Conrad, M.N., Yan, Q., Conaway, R.C., and Conaway, J.W. (1999). The Rbx1 subunit of SCF and VHL E3 ubiquitin ligase activates Rub1 modification of cullins Cdc53 and Cul2. Genes Dev *13*, 2928-2933.

Karamanlidis, G., Karamitri, A., Docherty, K., Hazlerigg, D.G., and Lomax, M.A. (2007). C/EBPbeta reprograms white 3T3-L1 preadipocytes to a Brown adipocyte pattern of gene expression. J Biol Chem *282*, 24660-24669.

Karamitri, A., Shore, A.M., Docherty, K., Speakman, J.R., and Lomax, M.A. (2009). Combinatorial transcription factor regulation of the cyclic AMP-response element on the Pgc-1alpha promoter in white 3T3-L1 and brown HIB-1B preadipocytes. J Biol Chem *284*, 20738-20752.

Kazak, L., Chouchani, E.T., Jedrychowski, M.P., Erickson, B.K., Shinoda, K., Cohen, P., Vetrivelan, R., Lu, G.Z., Laznik-Bogoslavski, D., Hasenfuss, S.C., et al. (2015). A creatine-driven substrate cycle enhances energy expenditure and thermogenesis in beige fat. Cell *163*, 643-655.

Kershaw, E.E., and Flier, J.S. (2004). Adipose tissue as an endocrine organ. J Clin Endocrinol Metab *89*, 2548-2556.

Kersten, S. (2001). Mechanisms of nutritional and hormonal regulation of lipogenesis. EMBO Rep *2*, 282-286.

Kilroy, G., Kirk-Ballard, H., Carter, L.E., and Floyd, Z.E. (2012). The ubiquitin ligase Siah2 regulates PPARgamma activity in adipocytes. Endocrinology *153*, 1206-1218.

Kilroy, G.E., Zhang, X., and Floyd, Z.E. (2009). PPAR-gamma AF-2 domain functions as a component of a ubiquitin-dependent degradation signal. Obesity (Silver Spring) *17*, 665-673.

Kim, J.H., Park, K.W., Lee, E.W., Jang, W.S., Seo, J., Shin, S., Hwang, K.A., and Song, J. (2014). Suppression of PPARgamma through MKRN1-mediated ubiquitination and degradation prevents adipocyte differentiation. Cell Death Differ *21*, 594-603.

Kim, J.W., Tang, Q.Q., Li, X., and Lane, M.D. (2007a). Effect of phosphorylation and S-S bond-induced dimerization on DNA binding and transcriptional activation by C/EBPbeta. Proc Natl Acad Sci U S A *104*, 1800-1804.

Kim, K.A., Kim, J.H., Wang, Y., and Sul, H.S. (2007b). Pref-1 (preadipocyte factor 1) activates the MEK/extracellular signal-regulated kinase pathway to inhibit adipocyte differentiation. Mol Cell Biol *27*, 2294-2308.

Kirkin, V., and Dikic, I. (2007). Role of ubiquitin- and Ubl-binding proteins in cell signaling. Curr Opin Cell Biol *19*, 199-205.

Klemm, D.J., Roesler, W.J., Boras, T., Colton, L.A., Felder, K., and Reusch, J.E. (1998). Insulin stimulates cAMP-response element binding protein activity in HepG2 and 3T3-L1 cell lines. J Biol Chem *273*, 917-923.

Kliewer, S.A., Lenhard, J.M., Willson, T.M., Patel, I., Morris, D.C., and Lehmann, J.M. (1995). A prostaglandin J2 metabolite binds peroxisome proliferator-activated receptor gamma and promotes adipocyte differentiation. Cell *83*, 813-819.

Kliewer, S.A., Sundseth, S.S., Jones, S.A., Brown, P.J., Wisely, G.B., Koble, C.S., Devchand, P., Wahli, W., Willson, T.M., Lenhard, J.M., et al. (1997). Fatty acids and eicosanoids regulate gene expression through direct interactions with peroxisome proliferator-activated receptors alpha and gamma. Proc Natl Acad Sci U S A *94*, 4318-4323.

Kliewer, S.A., Umesono, K., Noonan, D.J., Heyman, R.A., and Evans, R.M. (1992). Convergence of 9-cis retinoic acid and peroxisome proliferator signalling pathways through heterodimer formation of their receptors. Nature *358*, 771-774.

Kloting, N., Fasshauer, M., Dietrich, A., Kovacs, P., Schon, M.R., Kern, M., Stumvoll, M., and Bluher, M. (2010). Insulin-sensitive obesity. Am J Physiol Endocrinol Metab *299*, E506-515.

Knutson, V.P., and Balba, Y. (1997). 3T3-L1 adipocytes as a cell culture model of insulin resistance. In Vitro Cell Dev Biol Anim *33*, 77-81.

Kohn, A.D., Summers, S.A., Birnbaum, M.J., and Roth, R.A. (1996). Expression of a constitutively active Akt Ser/Thr kinase in 3T3-L1 adipocytes stimulates glucose uptake and glucose transporter 4 translocation. J Biol Chem *271*, 31372-31378.

Kolb, H., and Martin, S. (2017). Environmental/lifestyle factors in the pathogenesis and prevention of type 2 diabetes. BMC Med *15*, 131.

Kong, X., Banks, A., Liu, T., Kazak, L., Rao, R.R., Cohen, P., Wang, X., Yu, S., Lo, J.C., Tseng, Y.H., et al. (2014). IRF4 is a key thermogenic transcriptional partner of PGC-1alpha. Cell *158*, 69-83.

Kopelman, P.G. (2000). Obesity as a medical problem. Nature *404*, 635-643.

Koutkia, P., and Grinspoon, S. (2004). HIV-associated lipodystrophy: pathogenesis, prognosis, treatment, and controversies. Annu Rev Med *55*, 303-317.

Kowenz-Leutz, E., Twamley, G., Ansieau, S., and Leutz, A. (1994). Novel mechanism of C/EBP beta (NF-M) transcriptional control: activation through derepression. Genes Dev *8*, 2781-2791.

Krotkiewski, M., Bjorntorp, P., Sjostrom, L., and Smith, U. (1983). Impact of obesity on metabolism in men and women. Importance of regional adipose tissue distribution. J Clin Invest *72*, 1150-1162.

Kubbutat, M.H., Jones, S.N., and Vousden, K.H. (1997). Regulation of p53 stability by Mdm2. Nature *387*, 299-303.

Kumar, S., Tomooka, Y., and Noda, M. (1992). Identification of a set of genes with developmentally down-regulated expression in the mouse brain. Biochem Biophys Res Commun *185*, 1155-1161.

Kumar, S., Yoshida, Y., and Noda, M. (1993). Cloning of a cDNA which encodes a novel ubiquitin-like protein. Biochem Biophys Res Commun *195*, 393-399.

Kurz, T., Ozlu, N., Rudolf, F., O'Rourke, S.M., Luke, B., Hofmann, K., Hyman, A.A., Bowerman, B., and Peter, M. (2005). The conserved protein DCN-1/Dcn1p is required for cullin neddylation in C. elegans and S. cerevisiae. Nature *435*, 1257-1261.

Kwon, H., and Pessin, J.E. (2013). Adipokines mediate inflammation and insulin resistance. Front Endocrinol (Lausanne) *4*, 71.

Lagathu, C., Eustace, B., Prot, M., Frantz, D., Gu, Y., Bastard, J.P., Maachi, M., Azoulay, S., Briggs, M., Caron, M., et al. (2007). Some HIV antiretrovirals increase oxidative stress and alter chemokine, cytokine or adiponectin production in human adipocytes and macrophages. Antivir Ther *12*, 489-500.

Landschulz, W.H., Johnson, P.F., and McKnight, S.L. (1988). The leucine zipper: a hypothetical structure common to a new class of DNA binding proteins. Science *240*, 1759-1764.

Landschulz, W.H., Johnson, P.F., and McKnight, S.L. (1989). The DNA binding domain of the rat liver nuclear protein C/EBP is bipartite. Science *243*, 1681-1688.

Lasar, D., Rosenwald, M., Kiehlmann, E., Balaz, M., Tall, B., Opitz, L., Lidell, M.E., Zamboni, N., Krznar, P., Sun, W., et al. (2018). Peroxisome Proliferator Activated Receptor Gamma Controls Mature Brown Adipocyte Inducibility through Glycerol Kinase. Cell Rep *22*, 760-773.

Lass, A., Zimmermann, R., Haemmerle, G., Riederer, M., Schoiswohl, G., Schweiger, M., Kienesberger, P., Strauss, J.G., Gorkiewicz, G., and Zechner, R. (2006). Adipose triglyceride lipase-mediated lipolysis of cellular fat stores is activated by CGI-58 and defective in Chanarin-Dorfman Syndrome. Cell Metab *3*, 309-319.

Leblanc, E.S., O'Connor, E., Whitlock, E.P., Patnode, C.D., and Kapka, T. (2011). Effectiveness of primary care-relevant treatments for obesity in adults: a systematic evidence review for the U.S. Preventive Services Task Force. Ann Intern Med *155*, 434-447.

Lee, J., Ellis, J.M., and Wolfgang, M.J. (2015). Adipose fatty acid oxidation is required for thermogenesis and potentiates oxidative stress-induced inflammation. Cell Rep *10*, 266-279.

Lee, K.Y., Russell, S.J., Ussar, S., Boucher, J., Vernochet, C., Mori, M.A., Smyth, G., Rourk, M., Cederquist, C., Rosen, E.D., et al. (2013a). Lessons on conditional gene targeting in mouse adipose tissue. Diabetes *62*, 864-874.

Lee, M.J., Wu, Y., and Fried, S.K. (2013b). Adipose tissue heterogeneity: implication of depot differences in adipose tissue for obesity complications. Mol Aspects Med *34*, 1-11.

Lee, M.R., Lee, D., Shin, S.K., Kim, Y.H., and Choi, C.Y. (2008). Inhibition of APP intracellular domain (AICD) transcriptional activity via covalent conjugation with Nedd8. Biochem Biophys Res Commun *366*, 976-981.

Lefterova, M.I., Haakonsson, A.K., Lazar, M.A., and Mandrup, S. (2014). PPARgamma and the global map of adipogenesis and beyond. Trends Endocrinol Metab *25*, 293-302.

Lefterova, M.I., Zhang, Y., Steger, D.J., Schupp, M., Schug, J., Cristancho, A., Feng, D., Zhuo, D., Stoeckert, C.J., Jr., Liu, X.S., et al. (2008). PPARgamma and C/EBP factors orchestrate adipocyte biology via adjacent binding on a genome-wide scale. Genes Dev *22*, 2941-2952.

Lehr, S., Hartwig, S., and Sell, H. (2012). Adipokines: a treasure trove for the discovery of biomarkers for metabolic disorders. Proteomics Clin Appl *6*, 91-101.

Lehrke, M., and Lazar, M.A. (2005). The many faces of PPARgamma. Cell *123*, 993-999.

Lepper, C., and Fan, C.M. (2010). Inducible lineage tracing of Pax7-descendant cells reveals embryonic origin of adult satellite cells. Genesis *48*, 424-436.

Leto, D., and Saltiel, A.R. (2012). Regulation of glucose transport by insulin: traffic control of GLUT4. Nat Rev Mol Cell Biol *13*, 383-396.

Li, J.J., Wang, R., Lama, R., Wang, X., Floyd, Z.E., Park, E.A., and Liao, F.F. (2016). Ubiquitin Ligase NEDD4 Regulates PPARgamma Stability and Adipocyte Differentiation in 3T3-L1 Cells. Sci Rep *6*, 38550.

Li, L., Wang, M., Yu, G., Chen, P., Li, H., Wei, D., Zhu, J., Xie, L., Jia, H., Shi, J., et al. (2014). Overactivated neddylation pathway as a therapeutic target in lung cancer. J Natl Cancer Inst *106*, dju083.

Li, X., Kim, J.W., Gronborg, M., Urlaub, H., Lane, M.D., and Tang, Q.Q. (2007). Role of cdk2 in the sequential phosphorylation/activation of C/EBPbeta during adipocyte differentiation. Proc Natl Acad Sci U S A *104*, 11597-11602.

Liakopoulos, D., Doenges, G., Matuschewski, K., and Jentsch, S. (1998). A novel protein modification pathway related to the ubiquitin system. EMBO J *17*, 2208-2214.

Lin, F.T., and Lane, M.D. (1992). Antisense CCAAT/enhancer-binding protein RNA suppresses coordinate gene expression and triglyceride accumulation during differentiation of 3T3-L1 preadipocytes. Genes Dev *6*, 533-544.

Lin, F.T., and Lane, M.D. (1994). CCAAT/enhancer binding protein alpha is sufficient to initiate the 3T3-L1 adipocyte differentiation program. Proc Natl Acad Sci U S A *91*, 8757-8761.

Liu, Y., Zhang, Y.D., Guo, L., Huang, H.Y., Zhu, H., Huang, J.X., Liu, Y., Zhou, S.R., Dang, Y.J., Li, X., et al. (2013). Protein inhibitor of activated STAT 1 (PIAS1) is identified as the SUMO E3 ligase of CCAAT/enhancer-binding protein beta (C/EBPbeta) during adipogenesis. Mol Cell Biol *33*, 4606-4617.

Loft, A., Forss, I., Siersbaek, M.S., Schmidt, S.F., Larsen, A.S., Madsen, J.G., Pisani, D.F., Nielsen, R., Aagaard, M.M., Mathison, A., et al. (2015). Browning of human adipocytes requires KLF11 and reprogramming of PPARgamma superenhancers. Genes Dev *29*, 7-22.

Loftus, S.J., Liu, G., Carr, S.M., Munro, S., and La Thangue, N.B. (2012). NEDDylation regulates E2F-1-dependent transcription. EMBO Rep *13*, 811-818.

Longo, N., Amat di San Filippo, C., and Pasquali, M. (2006). Disorders of carnitine transport and the carnitine cycle. Am J Med Genet C Semin Med Genet *142C*, 77-85.

Lowell, B.B., V, S.S., Hamann, A., Lawitts, J.A., Himms-Hagen, J., Boyer, B.B., Kozak, L.P., and Flier, J.S. (1993). Development of obesity in transgenic mice after genetic ablation of brown adipose tissue. Nature *366*, 740-742.

Lumeng, C.N., Bodzin, J.L., and Saltiel, A.R. (2007). Obesity induces a phenotypic switch in adipose tissue macrophage polarization. J Clin Invest *117*, 175-184.

Luo, X., Ryu, K.W., Kim, D.S., Nandu, T., Medina, C.J., Gupte, R., Gibson, B.A., Soccio, R.E., Yu, Y., Gupta, R.K., et al. (2017). PARP-1 Controls the Adipogenic Transcriptional Program by PARylating C/EBPbeta and Modulating Its Transcriptional Activity. Mol Cell *65*, 260-271.

Luo, Z., Yu, G., Lee, H.W., Li, L., Wang, L., Yang, D., Pan, Y., Ding, C., Qian, J., Wu, L., et al. (2012). The Nedd8-activating enzyme inhibitor MLN4924 induces autophagy and apoptosis to suppress liver cancer cell growth. Cancer Res *72*, 3360-3371.

Lutz, T.A., and Woods, S.C. (2012). Overview of animal models of obesity. Curr Protoc Pharmacol *Chapter 5*, Unit5 61.

Lyapina, S., Cope, G., Shevchenko, A., Serino, G., Tsuge, T., Zhou, C., Wolf, D.A., Wei, N., Shevchenko, A., and Deshaies, R.J. (2001). Promotion of NEDD-CUL1 conjugate cleavage by COP9 signalosome. Science *292*, 1382-1385.

Lynch, V.J., May, G., and Wagner, G.P. (2011). Regulatory evolution through divergence of a phosphoswitch in the transcription factor CEBPB. Nature *480*, 383-386.

Ma, T., Chen, Y., Zhang, F., Yang, C.Y., Wang, S., and Yu, X. (2013). RNF111-dependent neddylation activates DNA damage-induced ubiquitination. Mol Cell *49*, 897-907.

MacDougald, O.A., Cornelius, P., Lin, F.T., Chen, S.S., and Lane, M.D. (1994). Glucocorticoids reciprocally regulate expression of the CCAAT/enhancer-binding protein alpha and delta genes in 3T3-L1 adipocytes and white adipose tissue. J Biol Chem *269*, 19041-19047.

MacDougald, O.A., Cornelius, P., Liu, R., and Lane, M.D. (1995). Insulin regulates transcription of the CCAAT/enhancer binding protein (C/EBP) alpha, beta, and delta genes in fully-differentiated 3T3-L1 adipocytes. J Biol Chem *270*, 647-654.

Magun, R., Burgering, B.M., Coffer, P.J., Pardasani, D., Lin, Y., Chabot, J., and Sorisky, A. (1996). Expression of a constitutively activated form of protein kinase B (c-Akt) in 3T3-L1 preadipose cells causes spontaneous differentiation. Endocrinology *137*, 3590-3593.

Marin-Penalver, J.J., Martin-Timon, I., Sevillano-Collantes, C., and Del Canizo-Gomez, F.J. (2016). Update on the treatment of type 2 diabetes mellitus. World J Diabetes *7*, 354-395.

Marmor, M.D., and Yarden, Y. (2004). Role of protein ubiquitylation in regulating endocytosis of receptor tyrosine kinases. Oncogene *23*, 2057-2070.

Martin, G., Poirier, H., Hennuyer, N., Crombie, D., Fruchart, J.C., Heyman, R.A., Besnard, P., and Auwerx, J. (2000). Induction of the fatty acid transport protein 1 and acyl-CoA synthase genes by dimer-selective rexinoids suggests that the peroxisome proliferator-activated receptor-retinoid X receptor heterodimer is their molecular target. J Biol Chem *275*, 12612-12618.

McIntyre, T.M., Pontsler, A.V., Silva, A.R., St Hilaire, A., Xu, Y., Hinshaw, J.C., Zimmerman, G.A., Hama, K., Aoki, J., Arai, H., et al. (2003). Identification of an intracellular receptor for lysophosphatidic acid (LPA): LPA is a transcellular PPARgamma agonist. Proc Natl Acad Sci U S A *100*, 131-136.

Medina-Gomez, G., Gray, S.L., Yetukuri, L., Shimomura, K., Virtue, S., Campbell, M., Curtis, R.K., Jimenez-Linan, M., Blount, M., Yeo, G.S., et al. (2007). PPAR gamma 2 prevents lipotoxicity by controlling adipose tissue expandability and peripheral lipid metabolism. PLoS Genet *3*, e64.

Mendoza, H.M., Shen, L.N., Botting, C., Lewis, A., Chen, J., Ink, B., and Hay, R.T. (2003). NEDP1, a highly conserved cysteine protease that deNEDDylates Cullins. J Biol Chem *278*, 25637-25643.

Mergner, J., Heinzlmeir, S., Kuster, B., and Schwechheimer, C. (2015). DENEDDYLASE1 deconjugates NEDD8 from non-cullin protein substrates in Arabidopsis thaliana. Plant Cell *27*, 741-753.

Merlet, J., Burger, J., Gomes, J.E., and Pintard, L. (2009). Regulation of cullin-RING E3 ubiquitin-ligases by neddylation and dimerization. Cell Mol Life Sci *66*, 1924-1938.

Mikkonen, L., Hirvonen, J., and Janne, O.A. (2013). SUMO-1 regulates body weight and adipogenesis via PPARgamma in male and female mice. Endocrinology *154*, 698-708.

Miyoshi, H., Souza, S.C., Zhang, H.H., Strissel, K.J., Christoffolete, M.A., Kovsan, J., Rudich, A., Kraemer, F.B., Bianco, A.C., Obin, M.S., et al. (2006). Perilipin promotes hormone-sensitive lipase-mediated adipocyte lipolysis via phosphorylation-dependent and -independent mechanisms. J Biol Chem *281*, 15837-15844.

Monteiro, M.P., and Batterham, R.L. (2017). The Importance of the Gastrointestinal Tract in Controlling Food Intake and Regulating Energy Balance. Gastroenterology *152*, 1707-1717 e1702.

Morales, L.M., Campos, G., Ryder, E., and Casanova, A. (1992). Insulin and lipogenesis in rat adipocytes. I. Effect of insulin incubation on lipid synthesis by isolated rat adipocytes. Biochem Biophys Res Commun *188*, 807-812.

Morimoto, M., Nishida, T., Nagayama, Y., and Yasuda, H. (2003). Nedd8-modification of Cul1 is promoted by Roc1 as a Nedd8-E3 ligase and regulates its stability. Biochem Biophys Res Commun *301*, 392-398.

Mueller, E., Drori, S., Aiyer, A., Yie, J., Sarraf, P., Chen, H., Hauser, S., Rosen, E.D., Ge, K., Roeder, R.G., et al. (2002). Genetic analysis of adipogenesis through peroxisome proliferator-activated receptor gamma isoforms. J Biol Chem *277*, 41925-41930.

Mukhopadhyay, D., and Riezman, H. (2007). Proteasome-independent functions of ubiquitin in endocytosis and signaling. Science *315*, 201-205.

Nagy, L., Tontonoz, P., Alvarez, J.G., Chen, H., and Evans, R.M. (1998). Oxidized LDL regulates macrophage gene expression through ligand activation of PPARgamma. Cell *93*, 229-240.

Nakayama, K.I., and Nakayama, K. (2006). Ubiquitin ligases: cell-cycle control and cancer. Nat Rev Cancer *6*, 369-381.

Nathan, D.M., Davidson, M.B., DeFronzo, R.A., Heine, R.J., Henry, R.R., Pratley, R., Zinman, B., and American Diabetes, A. (2007). Impaired fasting glucose and impaired glucose tolerance: implications for care. Diabetes Care *30*, 753-759.

Nedergaard, J., Petrovic, N., Lindgren, E.M., Jacobsson, A., and Cannon, B. (2005). PPARgamma in the control of brown adipocyte differentiation. Biochim Biophys Acta *1740*, 293-304.

Neuschwander-Tetri, B.A., and Caldwell, S.H. (2003). Nonalcoholic steatohepatitis: summary of an AASLD Single Topic Conference. Hepatology *37*, 1202-1219.

Niehof, M., Manns, M.P., and Trautwein, C. (1997). CREB controls LAP/C/EBP beta transcription. Mol Cell Biol *17*, 3600-3613.

Nielsen, R., Pedersen, T.A., Hagenbeek, D., Moulos, P., Siersbaek, R., Megens, E., Denissov, S., Borgesen, M., Francoijs, K.J., Mandrup, S., et al. (2008). Genome-wide profiling of PPARgamma:RXR and RNA polymerase II occupancy reveals temporal activation of distinct metabolic pathways and changes in RXR dimer composition during adipogenesis. Genes Dev *22*, 2953-2967.

Noguchi, K., Okumura, F., Takahashi, N., Kataoka, A., Kamiyama, T., Todo, S., and Hatakeyama, S. (2011). TRIM40 promotes neddylation of IKKgamma and is downregulated in gastrointestinal cancers. Carcinogenesis *32*, 995-1004.

O'Neill, S., and O'Driscoll, L. (2015). Metabolic syndrome: a closer look at the growing epidemic and its associated pathologies. Obes Rev *16*, 1-12.

Oberbach, A., Tonjes, A., Kloting, N., Fasshauer, M., Kratzsch, J., Busse, M.W., Paschke, R., Stumvoll, M., and Bluher, M. (2006). Effect of a 4 week physical training program on plasma concentrations of inflammatory markers in patients with abnormal glucose tolerance. Eur J Endocrinol *154*, 577-585.

Ohshima, T., Koga, H., and Shimotohno, K. (2004). Transcriptional activity of peroxisome proliferator-activated receptor gamma is modulated by SUMO-1 modification. J Biol Chem *279*, 29551-29557.

Olswang, Y., Cohen, H., Papo, O., Cassuto, H., Croniger, C.M., Hakimi, P., Tilghman, S.M., Hanson, R.W., and Reshef, L. (2002). A mutation in the peroxisome proliferator-activated receptor gamma-binding site in the gene for the cytosolic form of phosphoenolpyruvate carboxykinase reduces adipose tissue size and fat content in mice. Proc Natl Acad Sci U S A *99*, 625-630.

Osaka, F., Kawasaki, H., Aida, N., Saeki, M., Chiba, T., Kawashima, S., Tanaka, K., and Kato, S. (1998). A new NEDD8-ligating system for cullin-4A. Genes Dev *12*, 2263-2268.

Oved, S., Mosesson, Y., Zwang, Y., Santonico, E., Shtiegman, K., Marmor, M.D., Kochupurakkal, B.S., Katz, M., Lavi, S., Cesareni, G., et al. (2006). Conjugation to Nedd8 instigates ubiquitylation and down-regulation of activated receptor tyrosine kinases. J Biol Chem *281*, 21640-21651.

Pan, Y., Xu, H., Liu, R., and Jia, L. (2012). Induction of cell senescence by targeting to Cullin-RING Ligases (CRLs) for effective cancer therapy. Int J Biochem Mol Biol *3*, 273-281.

Pan, Z.Q., Kentsis, A., Dias, D.C., Yamoah, K., and Wu, K. (2004). Nedd8 on cullin: building an expressway to protein destruction. Oncogene *23*, 1985-1997.

Panzer, U., Schneider, A., Guan, Y., Reinking, R., Zahner, G., Harendza, S., Wolf, G., Thaiss, F., and Stahl, R.A. (2002). Effects of different PPARgamma-agonists on MCP-1 expression and monocyte recruitment in experimental glomerulonephritis. Kidney Int *62*, 455-464.

Park, H.S., Ju, U.I., Park, J.W., Song, J.Y., Shin, D.H., Lee, K.H., Jeong, L.S., Yu, J., Lee, H.W., Cho, J.Y., et al. (2016). PPARgamma neddylation essential for adipogenesis is a potential target for treating obesity. Cell Death Differ *23*, 1296-1311.

Park, J.H., Kang, H.J., Kang, S.I., Lee, J.E., Hur, J., Ge, K., Mueller, E., Li, H., Lee, B.C., and Lee, S.B. (2013). A multifunctional protein, EWS, is essential for early brown fat lineage determination. Dev Cell *26*, 393-404.

Perlman, R.L., and Chalfie, M. (1977). Catecholamine release from the adrenal medulla. Clin Endocrinol Metab *6*, 551-576.

Petersen, R.K., Madsen, L., Pedersen, L.M., Hallenborg, P., Hagland, H., Viste, K., Doskeland, S.O., and Kristiansen, K. (2008). Cyclic AMP (cAMP)-mediated stimulation of adipocyte differentiation requires the synergistic action of Epac- and cAMP-dependent protein kinase-dependent processes. Mol Cell Biol *28*, 3804-3816.

Petroski, M.D., and Deshaies, R.J. (2005). Function and regulation of cullin-RING ubiquitin ligases. Nat Rev Mol Cell Biol *6*, 9-20.

Psakhye, I., and Jentsch, S. (2012). Protein group modification and synergy in the SUMO pathway as exemplified in DNA repair. Cell *151*, 807-820.

Puigserver, P., Wu, Z., Park, C.W., Graves, R., Wright, M., and Spiegelman, B.M. (1998). A cold-inducible coactivator of nuclear receptors linked to adaptive thermogenesis. Cell *92*, 829-839.

Rabiee, A., Schwammle, V., Sidoli, S., Dai, J., Rogowska-Wrzesinska, A., Mandrup, S., and Jensen, O.N. (2017). Nuclear phosphoproteome analysis of 3T3-L1 preadipocyte differentiation reveals system-wide phosphorylation of transcriptional regulators. Proteomics *17*.

Rabut, G., and Peter, M. (2008). Function and regulation of protein neddylation. 'Protein modifications: beyond the usual suspects' review series. EMBO Rep *9*, 969-976.

Rajakumari, S., Wu, J., Ishibashi, J., Lim, H.W., Giang, A.H., Won, K.J., Reed, R.R., and Seale, P. (2013). EBF2 determines and maintains brown adipocyte identity. Cell Metab *17*, 562-574.

Rangwala, S.M., Rhoades, B., Shapiro, J.S., Rich, A.S., Kim, J.K., Shulman, G.I., Kaestner, K.H., and Lazar, M.A. (2003). Genetic modulation of PPARgamma phosphorylation regulates insulin sensitivity. Dev Cell *5*, 657-663.

Reaven, G.M. (1988). Banting lecture 1988. Role of insulin resistance in human disease. Diabetes *37*, 1595-1607.

Reilly, S.M., and Saltiel, A.R. (2017). Adapting to obesity with adipose tissue inflammation. Nat Rev Endocrinol *13*, 633-643.

Reusch, J.E., Colton, L.A., and Klemm, D.J. (2000). CREB activation induces adipogenesis in 3T3-L1 cells. Mol Cell Biol *20*, 1008-1020.

Rhee, S.D., Sung, Y.Y., Jung, W.H., and Cheon, H.G. (2008). Leptin inhibits rosiglitazone-induced adipogenesis in murine primary adipocytes. Mol Cell Endocrinol *294*, 61-69.

Roden, M., Price, T.B., Perseghin, G., Petersen, K.F., Rothman, D.L., Cline, G.W., and Shulman, G.I. (1996). Mechanism of free fatty acid-induced insulin resistance in humans. J Clin Invest *97*, 2859-2865.

Rodriguez, J.A., Ben Ali, Y., Abdelkafi, S., Mendoza, L.D., Leclaire, J., Fotiadu, F., Buono, G., Carriere, F., and Abousalham, A. (2010). In vitro stereoselective hydrolysis of diacylglycerols by hormone-sensitive lipase. Biochim Biophys Acta *1801*, 77-83.

Rosen, E.D., Hsu, C.H., Wang, X., Sakai, S., Freeman, M.W., Gonzalez, F.J., and Spiegelman, B.M. (2002). C/EBPalpha induces adipogenesis through PPARgamma: a unified pathway. Genes Dev *16*, 22-26.

Rosen, E.D., and MacDougald, O.A. (2006). Adipocyte differentiation from the inside out. Nat Rev Mol Cell Biol *7*, 885-896.

Rosen, E.D., Sarraf, P., Troy, A.E., Bradwin, G., Moore, K., Milstone, D.S., Spiegelman, B.M., and Mortensen, R.M. (1999). PPAR gamma is required for the differentiation of adipose tissue in vivo and in vitro. Mol Cell *4*, 611-617.

Rosen, E.D., and Spiegelman, B.M. (2006). Adipocytes as regulators of energy balance and glucose homeostasis. Nature *444*, 847-853.

Rosen, E.D., and Spiegelman, B.M. (2014). What we talk about when we talk about fat. Cell *156*, 20-44.

Rothwell, N.J., and Stock, M.J. (1979). A role for brown adipose tissue in diet-induced thermogenesis. Nature *281*, 31-35.

Rozman, J., Klingenspor, M., and Hrabe de Angelis, M. (2014). A review of standardized metabolic phenotyping of animal models. Mamm Genome *25*, 497-507.

Rubin, C.S., Hirsch, A., Fung, C., and Rosen, O.M. (1978). Development of hormone receptors and hormonal responsiveness in vitro. Insulin receptors and insulin sensitivity in the preadipocyte and adipocyte forms of 3T3-L1 cells. J Biol Chem *253*, 7570-7578.

Rufer, A.C., Thoma, R., and Hennig, M. (2009). Structural insight into function and regulation of carnitine palmitoyltransferase. Cell Mol Life Sci *66*, 2489-2501.

Russell, T.R., and Ho, R. (1976). Conversion of 3T3 fibroblasts into adipose cells: triggering of differentiation by prostaglandin F2alpha and 1-methyl-3-isobutyl xanthine. Proc Natl Acad Sci U S A *73*, 4516-4520.

Rutkowski, J.M., Stern, J.H., and Scherer, P.E. (2015). The cell biology of fat expansion. J Cell Biol *208*, 501-512.

Ruud, J., Steculorum, S.M., and Bruning, J.C. (2017). Neuronal control of peripheral insulin sensitivity and glucose metabolism. Nat Commun *8*, 15259.

Ryu, J.H., Li, S.H., Park, H.S., Park, J.W., Lee, B., and Chun, Y.S. (2011). Hypoxia-inducible factor alpha subunit stabilization by NEDD8 conjugation is reactive oxygen species-dependent. J Biol Chem *286*, 6963-6970.

Saha, A., and Deshaies, R.J. (2008). Multimodal activation of the ubiquitin ligase SCF by Nedd8 conjugation. Mol Cell *32*, 21-31.

Saltiel, A.R. (2012). Insulin resistance in the defense against obesity. Cell Metab *15*, 798-804.

Samuel, V.T., and Shulman, G.I. (2012). Mechanisms for insulin resistance: common threads and missing links. Cell *148*, 852-871.

Samuel, V.T., and Shulman, G.I. (2016). The pathogenesis of insulin resistance: integrating signaling pathways and substrate flux. J Clin Invest *126*, 12-22.

Sanchez-Gurmaches, J., and Guertin, D.A. (2014). Adipocytes arise from multiple lineages that are heterogeneously and dynamically distributed. Nat Commun *5*, 4099.

Saponaro, C., Gaggini, M., Carli, F., and Gastaldelli, A. (2015). The Subtle Balance between Lipolysis and Lipogenesis: A Critical Point in Metabolic Homeostasis. Nutrients *7*, 9453-9474.

Sarantopoulos, J., Shapiro, G.I., Cohen, R.B., Clark, J.W., Kauh, J.S., Weiss, G.J., Cleary, J.M., Mahalingam, D., Pickard, M.D., Faessel, H.M., et al. (2016). Phase I Study of the Investigational NEDD8-Activating Enzyme Inhibitor Pevonedistat (TAK-924/MLN4924) in Patients with Advanced Solid Tumors. Clin Cancer Res *22*, 847-857.

Sarikas, A., Hartmann, T., and Pan, Z.Q. (2011). The cullin protein family. Genome Biol *12*, 220.

Sartipy, P., and Loskutoff, D.J. (2003). Monocyte chemoattractant protein 1 in obesity and insulin resistance. Proc Natl Acad Sci U S A *100*, 7265-7270.

Sassmann, A., Offermanns, S., and Wettschureck, N. (2010). Tamoxifen-inducible Cre-mediated recombination in adipocytes. Genesis *48*, 618-625.

Sato, Y., Miyake, K., Kaneoka, H., and Iijima, S. (2006). Sumoylation of CCAAT/enhancer-binding protein alpha and its functional roles in hepatocyte differentiation. J Biol Chem *281*, 21629-21639.

Savage, D.B. (2009). Mouse models of inherited lipodystrophy. Dis Model Mech *2*, 554-562.

Scaglione, K.M., Basrur, V., Ashraf, N.S., Konen, J.R., Elenitoba-Johnson, K.S., Todi, S.V., and Paulson, H.L. (2013). The ubiquitin-conjugating enzyme (E2) Ube2w ubiquitinates the N terminus of substrates. J Biol Chem *288*, 18784-18788.

Schaffer, J.E., and Lodish, H.F. (1994). Expression cloning and characterization of a novel adipocyte long chain fatty acid transport protein. Cell *79*, 427-436.

Schoonjans, K., Peinado-Onsurbe, J., Lefebvre, A.M., Heyman, R.A., Briggs, M., Deeb, S., Staels, B., and Auwerx, J. (1996). PPARalpha and PPARgamma activators direct a distinct tissue-specific transcriptional response via a PPRE in the lipoprotein lipase gene. EMBO J *15*, 5336-5348.

Schwechheimer, C., Serino, G., Callis, J., Crosby, W.L., Lyapina, S., Deshaies, R.J., Gray, W.M., Estelle, M., and Deng, X.W. (2001). Interactions of the COP9 signalosome with the E3 ubiquitin ligase SCFTIRI in mediating auxin response. Science *292*, 1379-1382.

Seale, P. (2015). Transcriptional Regulatory Circuits Controlling Brown Fat Development and Activation. Diabetes *64*, 2369-2375.

Seale, P., Bjork, B., Yang, W., Kajimura, S., Chin, S., Kuang, S., Scime, A., Devarakonda, S., Conroe, H.M., Erdjument-Bromage, H., et al. (2008). PRDM16 controls a brown fat/skeletal muscle switch. Nature *454*, 961-967.

Seale, P., Conroe, H.M., Estall, J., Kajimura, S., Frontini, A., Ishibashi, J., Cohen, P., Cinti, S., and Spiegelman, B.M. (2011). Prdm16 determines the thermogenic program of subcutaneous white adipose tissue in mice. J Clin Invest *121*, 96-105.

Seale, P., Kajimura, S., Yang, W., Chin, S., Rohas, L.M., Uldry, M., Tavernier, G., Langin, D., and Spiegelman, B.M. (2007). Transcriptional control of brown fat determination by PRDM16. Cell Metab *6*, 38-54.

Sears, I.B., MacGinnitie, M.A., Kovacs, L.G., and Graves, R.A. (1996). Differentiation-dependent expression of the brown adipocyte uncoupling protein gene: regulation by peroxisome proliferator-activated receptor gamma. Mol Cell Biol *16*, 3410-3419.

Senol-Cosar, O., Flach, R.J., DiStefano, M., Chawla, A., Nicoloro, S., Straubhaar, J., Hardy, O.T., Noh, H.L., Kim, J.K., Wabitsch, M., et al. (2016). Tenomodulin promotes human adipocyte differentiation and beneficial visceral adipose tissue expansion. Nat Commun *7*, 10686.

Seuring, T., Archangelidi, O., and Suhrcke, M. (2015). The Economic Costs of Type 2 Diabetes: A Global Systematic Review. Pharmacoeconomics *33*, 811-831.

Shah, J.J., Jakubowiak, A.J., O'Connor, O.A., Orlowski, R.Z., Harvey, R.D., Smith, M.R., Lebovic, D., Diefenbach, C., Kelly, K., Hua, Z., et al. (2016). Phase I Study of the Novel Investigational NEDD8-Activating Enzyme Inhibitor Pevonedistat (MLN4924) in Patients with Relapsed/Refractory Multiple Myeloma or Lymphoma. Clin Cancer Res *22*, 34-43.

Shao, M., Vishvanath, L., Busbuso, N.C., Hepler, C., Shan, B., Sharma, A.X., Chen, S., Yu, X., An, Y.A., Zhu, Y., et al. (2018). De novo adipocyte differentiation from Pdgfrbeta(+) preadipocytes protects against pathologic visceral adipose expansion in obesity. Nat Commun *9*, 890.

Sharma, A.M., and Staels, B. (2007). Review: Peroxisome proliferator-activated receptor gamma and adipose tissue--understanding obesity-related changes in regulation of lipid and glucose metabolism. J Clin Endocrinol Metab *92*, 386-395.

Shimizu, H., Shimomura, Y., Hayashi, R., Ohtani, K., Sato, N., Futawatari, T., and Mori, M. (1997). Serum leptin concentration is associated with total body fat mass, but not abdominal fat distribution. Int J Obes Relat Metab Disord *21*, 536-541.

Shulman, G.I. (2014). Ectopic fat in insulin resistance, dyslipidemia, and cardiometabolic disease. N Engl J Med *371*, 2237-2238.

Sidossis, L., and Kajimura, S. (2015). Brown and beige fat in humans: thermogenic adipocytes that control energy and glucose homeostasis. J Clin Invest *125*, 478-486.

Siersbaek, R., Nielsen, R., and Mandrup, S. (2010). PPARgamma in adipocyte differentiation and metabolism--novel insights from genome-wide studies. FEBS Lett *584*, 3242-3249.

Singh, R.K., Zerath, S., Kleifeld, O., Scheffner, M., Glickman, M.H., and Fushman, D. (2012). Recognition and cleavage of related to ubiquitin 1 (Rub1) and Rub1-ubiquitin chains by components of the ubiquitin-proteasome system. Mol Cell Proteomics *11*, 1595-1611.

Skurk, T., Alberti-Huber, C., Herder, C., and Hauner, H. (2007). Relationship between adipocyte size and adipokine expression and secretion. J Clin Endocrinol Metab *92*, 1023-1033.

Smith, P.J., Wise, L.S., Berkowitz, R., Wan, C., and Rubin, C.S. (1988). Insulin-like growth factor-I is an essential regulator of the differentiation of 3T3-L1 adipocytes. J Biol Chem *263*, 9402-9408.

Smith, U., Gogg, S., Johansson, A., Olausson, T., Rotter, V., and Svalstedt, B. (2001). Thiazolidinediones (PPARgamma agonists) but not PPARalpha agonists increase IRS-2 gene expression in 3T3-L1 and human adipocytes. FASEB J *15*, 215-220.

Song, C.K., Schwartz, G.J., and Bartness, T.J. (2009). Anterograde transneuronal viral tract tracing reveals central sensory circuits from white adipose tissue. Am J Physiol Regul Integr Comp Physiol *296*, R501-511.

Soucy, T.A., Dick, L.R., Smith, P.G., Milhollen, M.A., and Brownell, J.E. (2010). The NEDD8 Conjugation Pathway and Its Relevance in Cancer Biology and Therapy. Genes Cancer *1*, 708-716.

Soucy, T.A., Smith, P.G., Milhollen, M.A., Berger, A.J., Gavin, J.M., Adhikari, S., Brownell, J.E., Burke, K.E., Cardin, D.P., Critchley, S., et al. (2009). An inhibitor of NEDD8-activating enzyme as a new approach to treat cancer. Nature *458*, 732-736.

Speakman, J.R. (2004). Obesity: the integrated roles of environment and genetics. J Nutr *134*, 2090S-2105S.

Speakman, J.R. (2013). Measuring energy metabolism in the mouse - theoretical, practical, and analytical considerations. Front Physiol *4*, 34.

Spiegelman, B.M., Frank, M., and Green, H. (1983). Molecular cloning of mRNA from 3T3 adipocytes. Regulation of mRNA content for glycerophosphate dehydrogenase and other differentiation-dependent proteins during adipocyte development. J Biol Chem *258*, 10083-10089.

Stern, J.H., Rutkowski, J.M., and Scherer, P.E. (2016). Adiponectin, Leptin, and Fatty Acids in the Maintenance of Metabolic Homeostasis through Adipose Tissue Crosstalk. Cell Metab *23*, 770-784.

Stickle, N.H., Chung, J., Klco, J.M., Hill, R.P., Kaelin, W.G., Jr., and Ohh, M. (2004). pVHL modification by NEDD8 is required for fibronectin matrix assembly and suppression of tumor development. Mol Cell Biol *24*, 3251-3261.

Stine, R.R., Shapira, S.N., Lim, H.W., Ishibashi, J., Harms, M., Won, K.J., and Seale, P. (2016). EBF2 promotes the recruitment of beige adipocytes in white adipose tissue. Mol Metab *5*, 57-65.

Stolarczyk, E. (2017). Adipose tissue inflammation in obesity: a metabolic or immune response? Curr Opin Pharmacol *37*, 35-40.

Subramanian, V., Rothenberg, A., Gomez, C., Cohen, A.W., Garcia, A., Bhattacharyya, S., Shapiro, L., Dolios, G., Wang, R., Lisanti, M.P., et al. (2004). Perilipin A mediates the

reversible binding of CGI-58 to lipid droplets in 3T3-L1 adipocytes. J Biol Chem *279*, 42062-42071.

Sundqvist, A., Liu, G., Mirsaliotis, A., and Xirodimas, D.P. (2009). Regulation of nucleolar signalling to p53 through NEDDylation of L11. EMBO Rep *10*, 1132-1139.

Swatek, K.N., and Komander, D. (2016). Ubiquitin modifications. Cell Res *26*, 399-422.

Swords, R.T., Coutre, S., Maris, M.B., Zeidner, J.F., Foran, J.M., Cruz, J., Erba, H.P., Berdeja, J.G., Tam, W., Vardhanabhuti, S., et al. (2018). Pevonedistat, a first-in-class NEDD8-activating enzyme inhibitor, combined with azacitidine in patients with AML. Blood *131*, 1415-1424.

Swords, R.T., Watts, J., Erba, H.P., Altman, J.K., Maris, M., Anwer, F., Hua, Z., Stein, H., Faessel, H., Sedarati, F., et al. (2017). Expanded safety analysis of pevonedistat, a first-in-class NEDD8-activating enzyme inhibitor, in patients with acute myeloid leukemia and myelodysplastic syndromes. Blood Cancer J *7*, e520.

Takashima, O., Tsuruta, F., Kigoshi, Y., Nakamura, S., Kim, J., Katoh, M.C., Fukuda, T., Irie, K., and Chiba, T. (2013). Brap2 regulates temporal control of NF-kappaB localization mediated by inflammatory response. PLoS One *8*, e58911.

Tamori, Y., Masugi, J., Nishino, N., and Kasuga, M. (2002). Role of peroxisome proliferator-activated receptor-gamma in maintenance of the characteristics of mature 3T3-L1 adipocytes. Diabetes *51*, 2045-2055.

Tang, Q.Q., Gronborg, M., Huang, H., Kim, J.W., Otto, T.C., Pandey, A., and Lane, M.D. (2005). Sequential phosphorylation of CCAAT enhancer-binding protein beta by MAPK and glycogen synthase kinase 3beta is required for adipogenesis. Proc Natl Acad Sci U S A *102*, 9766-9771.

Tang, Q.Q., and Lane, M.D. (2012). Adipogenesis: from stem cell to adipocyte. Annu Rev Biochem *81*, 715-736.

Tang, Q.Q., Otto, T.C., and Lane, M.D. (2003). Mitotic clonal expansion: a synchronous process required for adipogenesis. Proc Natl Acad Sci U S A *100*, 44-49.

Tatham, M.H., Plechanovova, A., Jaffray, E.G., Salmen, H., and Hay, R.T. (2013). Ube2W conjugates ubiquitin to alpha-amino groups of protein N-termini. Biochem J *453*, 137-145.

Thrower, J.S., Hoffman, L., Rechsteiner, M., and Pickart, C.M. (2000). Recognition of the polyubiquitin proteolytic signal. EMBO J *19*, 94-102.

Tiraby, C., Tavernier, G., Lefort, C., Larrouy, D., Bouillaud, F., Ricquier, D., and Langin, D. (2003). Acquirement of brown fat cell features by human white adipocytes. J Biol Chem *278*, 33370-33376.

Tirone, T.A., and Brunicardi, F.C. (2001). Overview of glucose regulation. World J Surg *25*, 461-467.

Tokunaga, F., Sakata, S., Saeki, Y., Satomi, Y., Kirisako, T., Kamei, K., Nakagawa, T., Kato, M., Murata, S., Yamaoka, S., et al. (2009). Involvement of linear polyubiquitylation of NEMO in NF-kappaB activation. Nat Cell Biol *11*, 123-132.

Tontonoz, P., Hu, E., Devine, J., Beale, E.G., and Spiegelman, B.M. (1995). PPAR gamma 2 regulates adipose expression of the phosphoenolpyruvate carboxykinase gene. Mol Cell Biol *15*, 351-357.

Tontonoz, P., Hu, E., Graves, R.A., Budavari, A.I., and Spiegelman, B.M. (1994a). mPPAR gamma 2: tissue-specific regulator of an adipocyte enhancer. Genes Dev *8*, 1224-1234.

Tontonoz, P., Hu, E., and Spiegelman, B.M. (1994b). Stimulation of adipogenesis in fibroblasts by PPAR gamma 2, a lipid-activated transcription factor. Cell *79*, 1147-1156.

Tontonoz, P., and Spiegelman, B.M. (2008). Fat and beyond: the diverse biology of PPARgamma. Annu Rev Biochem *77*, 289-312.

Tseng, Y.H., Kokkotou, E., Schulz, T.J., Huang, T.L., Winnay, J.N., Taniguchi, C.M., Tran, T.T., Suzuki, R., Espinoza, D.O., Yamamoto, Y., et al. (2008). New role of bone morphogenetic protein 7 in brown adipogenesis and energy expenditure. Nature *454*, 1000-1004.

Tsukada, J., Yoshida, Y., Kominato, Y., and Auron, P.E. (2011). The CCAAT/enhancer (C/EBP) family of basic-leucine zipper (bZIP) transcription factors is a multifaceted highly-regulated system for gene regulation. Cytokine *54*, 6-19.

van Marken Lichtenbelt, W.D., Vanhommerig, J.W., Smulders, N.M., Drossaerts, J.M., Kemerink, G.J., Bouvy, N.D., Schrauwen, P., and Teule, G.J. (2009). Cold-activated brown adipose tissue in healthy men. N Engl J Med *360*, 1500-1508.

Vaughan, M., Berger, J.E., and Steinberg, D. (1964). Hormone-Sensitive Lipase and Monoglyceride Lipase Activities in Adipose Tissue. J Biol Chem *239*, 401-409.

Vegiopoulos, A., Rohm, M., and Herzig, S. (2017). Adipose tissue: between the extremes. EMBO J *36*, 1999-2017.

Villena, J.A., Roy, S., Sarkadi-Nagy, E., Kim, K.H., and Sul, H.S. (2004). Desnutrin, an adipocyte gene encoding a novel patatin domain-containing protein, is induced by fasting and glucocorticoids: ectopic expression of desnutrin increases triglyceride hydrolysis. J Biol Chem *279*, 47066-47075.

Virtanen, K.A., Lidell, M.E., Orava, J., Heglind, M., Westergren, R., Niemi, T., Taittonen, M., Laine, J., Savisto, N.J., Enerback, S., et al. (2009). Functional brown adipose tissue in healthy adults. N Engl J Med *360*, 1518-1525.

Vogl, A.M., Brockmann, M.M., Giusti, S.A., Maccarrone, G., Vercelli, C.A., Bauder, C.A., Richter, J.S., Roselli, F., Hafner, A.S., Dedic, N., et al. (2015). Neddylation inhibition impairs spine development, destabilizes synapses and deteriorates cognition. Nat Neurosci *18*, 239-251.

Wada, H., Kito, K., Caskey, L.S., Yeh, E.T., and Kamitani, T. (1998). Cleavage of the C-terminus of NEDD8 by UCH-L3. Biochem Biophys Res Commun *251*, 688-692.

Wada, H., Yeh, E.T., and Kamitani, T. (2000). A dominant-negative UBC12 mutant sequesters NEDD8 and inhibits NEDD8 conjugation in vivo. J Biol Chem *275*, 17008-17015.

Wagner, S.A., Beli, P., Weinert, B.T., Nielsen, M.L., Cox, J., Mann, M., and Choudhary, C. (2011). A proteome-wide, quantitative survey of in vivo ubiquitylation sites reveals widespread regulatory roles. Mol Cell Proteomics *10*, M111 013284.

Wakil, S.J., and Abu-Elheiga, L.A. (2009). Fatty acid metabolism: target for metabolic syndrome. J Lipid Res *50 Suppl*, S138-143.

Wang, F., Mullican, S.E., DiSpirito, J.R., Peed, L.C., and Lazar, M.A. (2013). Lipoatrophy and severe metabolic disturbance in mice with fat-specific deletion of PPARgamma. Proc Natl Acad Sci U S A *110*, 18656-18661.

Wang, W., and Seale, P. (2016). Control of brown and beige fat development. Nat Rev Mol Cell Biol *17*, 691-702.

Watanabe, M., Takahashi, H., Saeki, Y., Ozaki, T., Itoh, S., Suzuki, M., Mizushima, W., Tanaka, K., and Hatakeyama, S. (2015). The E3 ubiquitin ligase TRIM23 regulates adipocyte differentiation via stabilization of the adipogenic activator PPARgamma. Elife *4*, e05615.

Watkins, P.A. (1997). Fatty acid activation. Prog Lipid Res *36*, 55-83.

Watson, I.R., Blanch, A., Lin, D.C., Ohh, M., and Irwin, M.S. (2006). Mdm2-mediated NEDD8 modification of TAp73 regulates its transactivation function. J Biol Chem *281*, 34096-34103.

Watson, I.R., Irwin, M.S., and Ohh, M. (2011). NEDD8 pathways in cancer, Sine Quibus Non. Cancer Cell *19*, 168-176.

Watson, I.R., Li, B.K., Roche, O., Blanch, A., Ohh, M., and Irwin, M.S. (2010). Chemotherapy induces NEDP1-mediated destabilization of MDM2. Oncogene *29*, 297-304.

Weisberg, S.P., McCann, D., Desai, M., Rosenbaum, M., Leibel, R.L., and Ferrante, A.W., Jr. (2003). Obesity is associated with macrophage accumulation in adipose tissue. J Clin Invest *112*, 1796-1808.

Welte, M.A. (2015). Expanding roles for lipid droplets. Curr Biol *25*, R470-481.

Wernstedt Asterholm, I., Tao, C., Morley, T.S., Wang, Q.A., Delgado-Lopez, F., Wang, Z.V., and Scherer, P.E. (2014). Adipocyte inflammation is essential for healthy adipose tissue expansion and remodeling. Cell Metab *20*, 103-118.

Westerberg, R., Mansson, J.E., Golozoubova, V., Shabalina, I.G., Backlund, E.C., Tvrdik, P., Retterstol, K., Capecchi, M.R., and Jacobsson, A. (2006). ELOVL3 is an important component for early onset of lipid recruitment in brown adipose tissue. J Biol Chem *281*, 4958-4968.

Williams, S.C., Baer, M., Dillner, A.J., and Johnson, P.F. (1995). CRP2 (C/EBP beta) contains a bipartite regulatory domain that controls transcriptional activation, DNA binding and cell specificity. EMBO J *14*, 3170-3183.

Williams, S.C., Cantwell, C.A., and Johnson, P.F. (1991). A family of C/EBP-related proteins capable of forming covalently linked leucine zipper dimers in vitro. Genes Dev *5*, 1553-1567.

Wiper-Bergeron, N., Salem, H.A., Tomlinson, J.J., Wu, D., and Hache, R.J. (2007). Glucocorticoid-stimulated preadipocyte differentiation is mediated through acetylation of C/EBPbeta by GCN5. Proc Natl Acad Sci U S A *104*, 2703-2708.

Wong, S., and Pinkney, J. (2004). Role of cytokines in regulating feeding behaviour. Curr Drug Targets *5*, 251-263.

Wu, J., Cohen, P., and Spiegelman, B.M. (2013). Adaptive thermogenesis in adipocytes: is beige the new brown? Genes Dev *27*, 234-250.

Wu, K., Yamoah, K., Dolios, G., Gan-Erdene, T., Tan, P., Chen, A., Lee, C.G., Wei, N., Wilkinson, K.D., Wang, R., et al. (2003). DEN1 is a dual function protease capable of processing the C terminus of Nedd8 and deconjugating hyper-neddylated CUL1. J Biol Chem *278*, 28882-28891.

Wu, Y.B., Dai, J., Yang, X.L., Li, S.J., Zhao, S.L., Sheng, Q.H., Tang, J.S., Zheng, G.Y., Li, Y.X., Wu, J.R., et al. (2009). Concurrent quantification of proteome and phosphoproteome to reveal system-wide association of protein phosphorylation and gene expression. Mol Cell Proteomics *8*, 2809-2826.

Wu, Z., Bucher, N.L., and Farmer, S.R. (1996). Induction of peroxisome proliferator-activated receptor gamma during the conversion of 3T3 fibroblasts into adipocytes is mediated by C/EBPbeta, C/EBPdelta, and glucocorticoids. Mol Cell Biol *16*, 4128-4136.

Wu, Z., Rosen, E.D., Brun, R., Hauser, S., Adelmant, G., Troy, A.E., McKeon, C., Darlington, G.J., and Spiegelman, B.M. (1999). Cross-regulation of C/EBP alpha and PPAR gamma controls the transcriptional pathway of adipogenesis and insulin sensitivity. Mol Cell *3*, 151-158.

Wu, Z., Xie, Y., Bucher, N.L., and Farmer, S.R. (1995). Conditional ectopic expression of C/EBP beta in NIH-3T3 cells induces PPAR gamma and stimulates adipogenesis. Genes Dev *9*, 2350-2363.

Wu, Z., Xie, Y., Morrison, R.F., Bucher, N.L., and Farmer, S.R. (1998). PPARgamma induces the insulin-dependent glucose transporter GLUT4 in the absence of C/EBPalpha during the conversion of 3T3 fibroblasts into adipocytes. J Clin Invest *101*, 22-32.

Xie, P., Yang, J.P., Cao, Y., Peng, L.X., Zheng, L.S., Sun, R., Meng, D.F., Wang, M.Y., Mei, Y., Qiang, Y.Y., et al. (2017). Promoting tumorigenesis in nasopharyngeal carcinoma, NEDD8 serves as a potential theranostic target. Cell Death Dis *8*, e2834.

Xie, P., Zhang, M., He, S., Lu, K., Chen, Y., Xing, G., Lu, Y., Liu, P., Li, Y., Wang, S., et al. (2014). The covalent modifier Nedd8 is critical for the activation of Smurf1 ubiquitin ligase in tumorigenesis. Nat Commun *5*, 3733.

Xirodimas, D.P. (2008). Novel substrates and functions for the ubiquitin-like molecule NEDD8. Biochem Soc Trans *36*, 802-806.

Xirodimas, D.P., Saville, M.K., Bourdon, J.C., Hay, R.T., and Lane, D.P. (2004). Mdm2-mediated NEDD8 conjugation of p53 inhibits its transcriptional activity. Cell *118*, 83-97.

Xirodimas, D.P., Sundqvist, A., Nakamura, A., Shen, L., Botting, C., and Hay, R.T. (2008). Ribosomal proteins are targets for the NEDD8 pathway. EMBO Rep *9*, 280-286.

Xu, A., Wang, Y., Keshaw, H., Xu, L.Y., Lam, K.S., and Cooper, G.J. (2003). The fat-derived hormone adiponectin alleviates alcoholic and nonalcoholic fatty liver diseases in mice. J Clin Invest *112*, 91-100.

Xu, J., and Liao, K. (2004). Protein kinase B/AKT 1 plays a pivotal role in insulin-like growth factor-1 receptor signaling induced 3T3-L1 adipocyte differentiation. J Biol Chem *279*, 35914-35922.

Xu, Z., Ande, S.R., and Mishra, S. (2013). Temporal analysis of protein lysine acetylation during adipocyte differentiation. Adipocyte *2*, 33-40.

Yamaguchi, T., Omatsu, N., Matsushita, S., and Osumi, T. (2004). CGI-58 interacts with perilipin and is localized to lipid droplets. Possible involvement of CGI-58 mislocalization in Chanarin-Dorfman syndrome. J Biol Chem *279*, 30490-30497.

Yamaguchi, T., Omatsu, N., Morimoto, E., Nakashima, H., Ueno, K., Tanaka, T., Satouchi, K., Hirose, F., and Osumi, T. (2007). CGI-58 facilitates lipolysis on lipid droplets but is not involved in the vesiculation of lipid droplets caused by hormonal stimulation. J Lipid Res *48*, 1078-1089.

Yamamoto, Y., Gesta, S., Lee, K.Y., Tran, T.T., Saadatirad, P., and Kahn, C.R. (2010). Adipose depots possess unique developmental gene signatures. Obesity (Silver Spring) *18*, 872-878.

Yamashita, D., Yamaguchi, T., Shimizu, M., Nakata, N., Hirose, F., and Osumi, T. (2004). The transactivating function of peroxisome proliferator-activated receptor gamma is negatively regulated by SUMO conjugation in the amino-terminal domain. Genes Cells *9*, 1017-1029.

Yamauchi, T., Kamon, J., Minokoshi, Y., Ito, Y., Waki, H., Uchida, S., Yamashita, S., Noda, M., Kita, S., Ueki, K., et al. (2002). Adiponectin stimulates glucose utilization and fatty-acid oxidation by activating AMP-activated protein kinase. Nat Med *8*, 1288-1295.

Yamauchi, T., Kamon, J., Waki, H., Terauchi, Y., Kubota, N., Hara, K., Mori, Y., Ide, T., Murakami, K., Tsuboyama-Kasaoka, N., et al. (2001). The fat-derived hormone adiponectin reverses insulin resistance associated with both lipoatrophy and obesity. Nat Med *7*, 941-946.

Ye, R., and Scherer, P.E. (2013). Adiponectin, driver or passenger on the road to insulin sensitivity? Mol Metab *2*, 133-141.

Ye, S., Xu, H., Jin, J., Yang, M., Wang, C., Yu, Y., and Cao, X. (2012). The E3 ubiquitin ligase neuregulin receptor degradation protein 1 (Nrdp1) promotes M2 macrophage polarization by ubiquitinating and activating transcription factor CCAAT/enhancer-binding Protein beta (C/EBPbeta). J Biol Chem *287*, 26740-26748.

Yeh, E.T., Gong, L., and Kamitani, T. (2000). Ubiquitin-like proteins: new wines in new bottles. Gene *248*, 1-14.

Yeh, W.C., Cao, Z., Classon, M., and McKnight, S.L. (1995). Cascade regulation of terminal adipocyte differentiation by three members of the C/EBP family of leucine zipper proteins. Genes Dev *9*, 168-181.

Yuan, H., Zhang, T., Liu, X., Deng, M., Zhang, W., Wen, Z., Chen, S., Chen, Z., de The, H., Zhou, J., et al. (2015). Sumoylation of CCAAT/enhancer-binding protein alpha is implicated in hematopoietic stem/progenitor cell development through regulating runx1 in zebrafish. Sci Rep *5*, 9011.

Zechner, R., Madeo, F., and Kratky, D. (2017). Cytosolic lipolysis and lipophagy: two sides of the same coin. Nat Rev Mol Cell Biol *18*, 671-684.

Zhang, F., Hao, G., Shao, M., Nham, K., An, Y., Wang, Q., Zhu, Y., Kusminski, C.M., Hassan, G., Gupta, R.K., et al. (2018). An Adipose Tissue Atlas: An Image-Guided Identification of Human-like BAT and Beige Depots in Rodents. Cell Metab *27*, 252-262 e253.

Zhang, J., Fu, M., Cui, T., Xiong, C., Xu, K., Zhong, W., Xiao, Y., Floyd, D., Liang, J., Li, E., et al. (2004a). Selective disruption of PPARgamma 2 impairs the development of adipose tissue and insulin sensitivity. Proc Natl Acad Sci U S A *101*, 10703-10708.

Zhang, J.W., Klemm, D.J., Vinson, C., and Lane, M.D. (2004b). Role of CREB in transcriptional regulation of CCAAT/enhancer-binding protein beta gene during adipogenesis. J Biol Chem *279*, 4471-4478.

Zhang, Y.Y., Li, S.F., Qian, S.W., Zhang, Y.Y., Liu, Y., Tang, Q.Q., and Li, X. (2012). Phosphorylation prevents C/EBPbeta from the calpain-dependent degradation. Biochem Biophys Res Commun *419*, 550-555.

Zhao, Y., Morgan, M.A., and Sun, Y. (2014). Targeting Neddylation pathways to inactivate cullin-RING ligases for anticancer therapy. Antioxid Redox Signal *21*, 2383-2400.

Zhou, L., Zhang, W., Sun, Y., and Jia, L. (2018). Protein neddylation and its alterations in human cancers for targeted therapy. Cell Signal *44*, 92-102.

Zhu, Y., Qi, C., Korenberg, J.R., Chen, X.N., Noya, D., Rao, M.S., and Reddy, J.K. (1995). Structural organization of mouse peroxisome proliferator-activated receptor gamma (mPPAR gamma) gene: alternative promoter use and different splicing yield two mPPAR gamma isoforms. Proc Natl Acad Sci U S A *92*, 7921-7925.

Zimmermann, R., Strauss, J.G., Haemmerle, G., Schoiswohl, G., Birner-Gruenberger, R., Riederer, M., Lass, A., Neuberger, G., Eisenhaber, F., Hermetter, A., et al. (2004). Fat mobilization in adipose tissue is promoted by adipose triglyceride lipase. Science *306*, 1383-1386.

Zubiete-Franco, I., Fernandez-Tussy, P., Barbier-Torres, L., Simon, J., Fernandez-Ramos, D., Lopitz-Otsoa, F., Gutierrez-de Juan, V., de Davalillo, S.L., Duce, A.M., Iruzubieta, P., et al. (2017). Deregulated neddylation in liver fibrosis. Hepatology *65*, 694-709.

Zuo, W., Huang, F., Chiang, Y.J., Li, M., Du, J., Ding, Y., Zhang, T., Lee, H.W., Jeong, L.S., Chen, Y., et al. (2013). c-Cbl-mediated neddylation antagonizes ubiquitination and degradation of the TGF-beta type II receptor. Mol Cell *49*, 499-510.

8 Acknowledgements

I have sincerely enjoyed the last years spent working in the collaboration project between the Max Planck Institute of Psychiatry and the IDG at the Helmholtz Zentrum München. I am grateful for all the relationships I have built and all the support I received during this time. Therefore, I would like to express my heartfelt gratitude.

Firstly, I would like to thank Prof. Dr. Wolfgang Wurst for welcoming me to his institute and for enabling and supporting this work as my thesis supervisor.

I am deeply grateful to my supervisor Dr. Damián Refojo for his constant support and guidance from close and far. I am truly thankful for your encouragement, your trust in me and I especially would like to thank you for sharing your passion for science with me.

I am especially grateful to Dr. Marta Labeur for her permanent support, advice and training. Thank you for all the inspiring work- and non-work-related discussions, for always caring and for enabling me to develop my own ideas. Simply, thank you for being a great mentor. It has been a lot of fun to work with you.

I would like to thank Prof. Dr. Günter Stalla for offering me the chance to work in his research group and his support for the project.

I would like to thank Dr. Annette Vogl for sharing with me her materials, experience and great moments also outside of the lab, like doing burpees in the snow with the other RG Refojo group members.

I am grateful to Barbara Wölfel for her technical support and for all the effort she put in this project, especially during Bad Nauheim nights. But mostly, I would like to thank you for your friendship and all the fun we had in and outside of the lab.

Thank you to Dr. Carola Meyer for introducing me to the PhenoMaster technique and for her support during my stay in Bad Nauheim.

I would like to thank Dr. Daniela Vogt-Weisenhorn for her help with all kind of organizational issues.

I would like to acknowledge my TAC member Dr. Paul Pfluger for his advice and for fruitful discussions.

I am grateful to all former and present members of the RG Stalla. Thank you for creating such a nice working environment, for the continuous help and support for each other and for many nice and memorable moments in and outside of the lab.

Thank you to everyone outside of the lab! Sonja, thank you for always listening and always caring. I am very grateful for all the fun times and memories and the friendship we share for almost our entire lives. Anna, I would like to thank you for your support and motivation, simply for being such a great friend. I am grateful for all the moments we shared-be it science slams or crazy midnight car rides. All these years of studying have been so much more fun together with you.

I dedicate this thesis to my family. Thank you to my parents, Manuela and Volker, for your ongoing support. And thanks to my sister, Daniela, who inspires me with her positive spirit.

9 Declaration

All experiments presented in this thesis were performed by me, unless otherwise stated. J. Stalla was measuring intracellular cAMP content by using the cAMP [^{125}I] Radioimmunoassay Kit. Bomb calorimetry to determine energy loss via feces was performed by R. Elvert.

The *Adipo*CreER^{T2} mouse line was created by Sassmann et al. (Sassmann et al., 2010). Nae1 knockout mice were developed by Vogl et al. (Vogl et al., 2015). By breeding the two lines together, A.M. Vogl created the *Nae1Adipo*CreER^{T2} mouse line.

Furthermore, I used the term "we" and not "I" throughout this work to write it similar to a publication.

Corinna Bauder